UNIVERSIDAD COMPLUTENSE DE MADRID

FACULTAD DE MEDICINA

Departamento de Anatomía Patológica

SEQUESTOSOME 1-P62 : A NEW PROMOTER OF MELANOMA PROGRESSION

SEQUESTOSOME 1-P62 : UN NUEVO PROMOTOR EN LA PROGRESIÓN DEL MELANOMA

MEMORIA PARA OPTAR AL GRADO DE DOCTOR
PRESENTADA POR

Erica Riveiro Meireles

Bajo la dirección de los doctores

José Luis Rodríguez Peralto
Pablo Luis Ortiz Romero

Madrid, 2013

UNIVERSIDAD COMPLUTENSE DE MADRID

FACULTAD DE MEDICINA

DEPARTAMENTO DE ANATOMÍA PATOLÓGICA

TESIS DOCTORAL

SEQUESTOSOME 1/P62: A NEW PROMOTER OF MELANOMA PROGRESSION

Sequestosome 1/p62: un nuevo promotor en la progresión del melanoma

ERICA RIVEIRO

Madrid, 2013

Hospital Universitario 12 de Octubre

SaludMadrid

i+12 Instituto de Investigación Hospital 12 de Octubre

D. José Luis Rodríguez Peralto, Profesor Titular del Departamento de Anatomía Patológica de la Universidad Complutense de Madrid.

D. Pablo Luis Ortiz Romero, Profesor Titular del Departamento de Medicina Interna de la Universidad Complutense de Madrid.

CERTIFICAN:

Que **Dña. Erica Riveiro** ha realizado bajo nuestra dirección el trabajo "**Sequestosome1/p62: a new promoter of melanoma progression (Sequestosome1/p62: un nuevo promotor en la progresión del melanoma)"** que a nuestro juicio reúne las condiciones para optar al Grado de Doctor. Para que así conste, firmamos el presente certificado en Madrid a 7 de Febrero del año dos mil y trece.

Vº Bº Directores de la Tesis Doctoral

Dr. José Luis Rodríguez Peralto
Profesor Titular
Departamento de Anatomía Patológica
Facultad de Medicina
Universidad Complutense de Madrid

Dr. Pablo Luis Ortiz Romero
Profesor Titular
Departamento de Medicina Interna
Facultad de Medicina
Universidad Complutense de Madrid

This thesis, submitted for the degree of Doctor in Philosophy at the Universidad Complutense de Madrid, has been performed in the Melanoma Laboratory, Molecular Pathology Program, at the Centro Nacional de Investigaciones Oncológicas, Madrid and in the Departments of Pathology and Dermatology at Hospital Universitario 12 de Octubre, Madrid. During the course of this thesis, a 3 months stay as Visiting Scientist was carried out in the Melanoma Laboratory of Dr. Meenhard Herlyn, at The Wistar Institute, Philadelphia, USA.

The present work was done under the guidance of Dr. José Luis Rodríguez Peralto (Head of the Department of Pathology, Hospital Universitario 12 de Octubre, Madrid), Dr. Pablo L. Ortiz Romero (Head of Section, Department of Dermatology, Hospital Universitario 12 de Octubre, Madrid) and Dr. María S. Soengas (Head of Melanoma Laboratory, Centro Nacional de Investigaciones Oncológicas, Madrid).

Supported by a grant from "Obra Social de Caja Navarra" (Post-residency training programme for translational research, 2008-2010) and National Institutes of Health (NIH 7R01CA125017-02, 2010-2012).

“No sabiendo que era imposible, fue y lo hizo”
Jean Cocteau

ACKNOWLEDGEMENTS/ AGRADECIMIENTOS:

"Tell me and I forget.
Teach me and I remember.
Involve me and I learn."
Benjamin Franklin

Me gustaría dedicar esta tesis a tres grandes mentores que tuve la suerte de encontrar en España: José Luis Rodríguez Peralto, Pablo Ortiz Romero y Marisol Soengas. Les agradezco no solo la oportunidad de hacer esta tesis, sino también su amistad y la acogida en España. Muchas gracias por abrirme las puertas de la investigación en España y por la oportunidad de aprender a su lado.

Muchas gracias a Beatriz Pérez Gómez del Centro Nacional de Epidemiología, Instituto de Salud Carlos III, por sus palabras de ánimo y toda su ayuda con los análisis de supervivencia.

A mis amigos y compañeros del grupo de Melanoma del Centro Nacional de Investigaciones Oncológicas que me han acompañado a lo largo de estos años de investigación. En especial a Lisa Osterloh, Agnieszka Checinska, Direna Alonso, David Olmeda, Panagiotis Karras, Estela Cañon, Tonan Calvo, Metehan Cifdaloz, Eva Perez, David Saenz, Damia Tormo, Lionel Larribere, Alícia Gonzalez, María Fernández y Angel Colmenar.

A todos los médicos, biólogos y técnicos de los servicios de Anatomía Patológica, de Dermatología y del Biobanco del Hospital Universitario 12 de Octubre de Madrid por toda su ayuda en la elaboración de este proyecto. En especial a Alicia Maroto, Rosa María García-Martín, Yolanda Ruano, Soledad Alonso, Alberto Muro, Magdalena Castaño, Susana Palacios, Susana Hernández, Juan Manuel de Tomas, Enrique Miranda, Santiago Macías, Ana Belén Enguita y María Garrido.

A Eva Andrés del Instituto de Investigación Sanitaria, Hospital Universitario 12 de Octubre, por su ayuda con los análisis estadísticos.

A todas las personas que también contribuyeron en la elaboración de este trabajo. En especial a José Ignacio Fernandez (CNIO), Lydia Sánchez y María Lozano (Unidad de Inmuohistoquímica, CNIO), María Jesús Artiga (Unidad de Banco de Tumores, CNIO), Diego Megías (Unidad de Microscopía Confocal, CNIO), Gonzalo Gómez (Unidad de Bioinformática, CNIO), Francesco Acquadro, Bibiana Ferreira y Juan Cigudosa (Grupo de Citogenética Molecular, CNIO), Esperanza Martín y Elena Rodríguez (Grupo de Linfoma, CNIO), Mª Isabel Ruppen y Maria Pilar Ximénez de Embún (Unidad de Proteómica, CNIO), Marta Cañamero (Unidad de Patología Comparada, CNIO), Grupo de Carcinogénesis Epitelial (CNIO), Isabel Colmenero (Hospital Niño Jesus), Carla Brohem (Universidade de São Paulo), Benilde Jiménez y Asunción Fernández (Instituto de Investigaciones Biomédicas, Madrid).

Special thanks to Meenhard Herlyn, Ling Li and Mizu Fukunaga-Kalabis for the warm reception and for the opportunity to work at The Wistar Institute. Special thanks to Ray Murta for all support and for giving me motivation.

Dedico esta tese também a minha mãe Sandra, meu pai Juan, meus queridos irmãos Raquel e Diego, que compreenderam e apoiaram minha decisão de vir à Espanha. Com eles percebi que a distancia não afasta, mas pelo contrário, consolida o amor, o carinho e a união entre as pessoas.

À minha segunda família, Tendresse, tia Sizuna, tio Airton e Pythagoras, que me acolheu e me encheu de carinho desde meus primeiros passos.

A mi gran amiga Pilar Sancho, que me acogió como hermana desde mis primeros instantes en España.

Aproveito a ocasião para agradecer aos professores que "me envolveram" ao longo de minha formação profissional. Agradeço ao Dr. Carlos Figueiredo por me ensinar com tanto carinho e dedicação o que é ser medica. Ao professor Gilberto Sachetto Martins por me iniciar de forma tão entusiástica no mundo da pesquisa. E aos professores Ednildo de Alcantara Machado (ETFQ-RJ), Denise Vigo Potsch (UFRJ), Maria de Fátima Alves (UERJ), Alexandre Gripp (UERJ) e Maria Auxiliadora Jeunon (UERJ), por suas excelentes classes ao longo de minha formação profissional.

Finalmente, esta tesis esta especialmente dedicada a todos los enfermos de melanoma y sus familias.

I. INDEX

II. SUMMARY/RESUMEN

II. SUMMARY/RESUMEN

Introduction

Melanoma is an extremely aggressive type of cancer, whose incidence continues to increase worldwide. Despite of new recently approved therapies, melanoma remains highly resistant to treatment and relapses are frequently seen in clinical practice. Thus, the identification of new mechanisms of melanoma progression and translation of this knowledge into the identification of potential therapeutic targets are still strictly necessary.

Aggressive cancers, and melanoma tumors are no exception, are characterized by an exacerbated cell metabolism, which frequently results in the production of misfolded proteins. In fact, tumor cells tend to be significantly more dependent on the continuous clearance of damaged proteins than their normal counterparts. Therefore, this intrinsic characteristic of cancer cells could represent a point of vulnerability for the development of improved therapies.

One of the least understood aspects in melanoma is the modulation of the proteasome and the autophagosome machineries, the main mediators of the degradation of damaged proteins and protein aggregates. This PhD Thesis focuses on Sequestosome 1/p62. Sequestosome 1/p62 is a multifunctional protein involved in proteasomal and autophagosomal degradation with key roles in other tumor types, but unknown in melanoma. Importantly, p62 has also been described as an adaptor protein activating multiple signaling cascades, again, virtually unexplored in melanoma. Therefore, p62 is an attractive candidate to be characterized in melanoma tumors.

Objectives

The main objectives of this study are: (1) to analyze the expression of Sequestosome1/p62 protein in benign melanocytic tumors and melanomas at different stages of progression; (2) to determine the function of Sequestosome 1/p62 protein in melanoma tumors using an *in vitro* approach with melanoma cell lines, and; (3) to establish the physiological impact of Sequestosome 1/p62 *in vivo* using mouse xenograft model and survival analyses of melanoma patients.

Results

Tissue microarrays revealed a notable overexpression of p62 in melanoma specimens, particularly at invasive stages. In contrast, melanocytic nevi were virtually negative for p62 expression. Comparative genomic hybridization and expression analyses in a large panel of melanoma cell lines support that p62 expression is regulated at transcriptional levels without amplification of its genomic locus. Moreover, *in vitro* studies with senescent melanocytes and *in vivo* analyses with melanoma mouse models support that p62 expression is induced during the malignant transformation of melanocytes.

Mechanistically, genetic depletion of p62 was found to inhibit cellular proliferation, leading to an invariable senescence-like phenotype in melanoma cells, but not in their normal melanocytic counterparts. Invasion assay and skin reconstruct experiments showed that p62 expression also contributes to melanoma invasion capacity. The lack of p62 expression in melanoma cells does not block autophagosome formation. Instead, transcriptomic analyses revealed new roles of p62 in multiple cellular pathways that modulate cell cycle, DNA replication and cellular invasion.

Corroborating the physiological impact of p62 in melanoma progression, the absence of p62 in melanoma cells inhibits tumor growth in mouse xenograft model. Furthermore, survival analyses performed in melanoma patients demonstrated that the expression of p62 in primary tumors is associated to an increased risk for the development of metastasis.

Conclusions

This multidisciplinary study supports for the first time that Sequestosome1/p62 protein is required for melanoma progression. Indeed, Sequestosome1/p62 protein represents a point of vulnerability for melanoma cells and, consequently, it may represent a potential target for melanoma treatment.

Introducción

Melanoma es un tipo muy agresivo de cáncer, cuya incidencia sigue aumentando en todo el mundo. A pesar de los tratamientos recientemente aprobados para pacientes con enfermedad metastásica, melanoma sigue siendo un tumor extremadamente resistente y recidivas son frecuentes en la práctica clínica. La identificación de nuevos mecanismos de progresión del melanoma y la implementación de esos conocimientos en la identificación de nuevas dianas terapéuticas sigue siendo estrictamente necesaria.

Melanoma, como otros tumores agresivos, se caracteriza por un metabolismo celular exacerbado que requiere la degradación continua de proteínas dañadas. De hecho, las células tumorales suelen ser significativamente más dependientes de la degradación de dichas proteínas que sus homólogas normales. Esa característica, intrínseca a células cancerosas, puede representar un punto de vulnerabilidad para el desarrollo de nuevas terapias.

Uno de los aspectos menos comprendidos del melanoma es la modulación del sistema proteasomal y autofagosomal, principales mediadores de la degradación de proteínas dañadas y agregadas. Esta tesis doctoral se centra en Sequestosome1/p62. Sequestosome1/p62 es una proteína multifuncional implicada en la degradación proteasomal y autofagosomal de proteínas, con funciones claves en otros tipos de tumores, pero todavía desconocidas en melanoma. Además, p62 funciona como una proteína adaptadora que activa distintas vías de señalización intracelulares implicadas en tumorigenesis. Por lo tanto, la propiedad multifuncional de Sequestosome1/p62 combinada con la necesidad de nuevas estrategias en el tratamiento del melanoma, señalizan p62 como un atractivo candidato para ser caracterizado en este tumor.

Objetivos

Los objetivos principales de este estudio son: (1) analizar la expresión de la proteína Sequestosome 1/p62 en tumores melanocíticos benignos y malignos en las diferentes etapas de progresión tumoral; (2) determinar la función de la proteína Sequestosome 1/p62 a través de estudios *in vitro* con líneas celulares de melanoma, y; (3) establecer el impacto fisiológico de Sequestosome1/p62 *in vivo* utilizando el modelo de xenoinjerto de ratón y análisis de supervivencia en pacientes con melanoma.

Resultados

Análisis inmunohistoquímicos en matrices tisulares de lesiones melanocíticas revelan que p62 está ausente en nevus intradérmicos, mientas que en los melanomas está significativamente sobreexpresada, particularmente en estadios tardíos (metástasis). Hibridación genómica comparativa y análisis de la expresión en un gran panel de líneas celulares de melanoma revelan que la expresión de p62 está regulada en niveles transcripcionales sin amplificación de su locus genómico. Además, estudios *in vitro* en melanocitos senescentes y en modelos de melanoma de ratones sugieren que la expresión de p62 es inducida durante la transformación maligna de melanocitos.

La inactivación dirigida de p62 mediante RNA interferente conduce a un bloqueo en la proliferación celular e inducción de senescencia prematura en células de melanoma, efectos que no se observaron en melanocitos normales. Ensayos de invasión celular *in vitro* y en piel artificial demuestran que p62 también contribuye a la capacidad invasiva de las células de melanoma. Curiosamente, la pérdida de expresión de p62 en células de melanoma no impide la formación de autofagosomas, sino que interfiere con una variedad de vías celulares que modulan el ciclo celular, la replicación del ADN y la invasión celular.

Corroborando el impacto fisiológico de p62 en la progresión del melanoma, la depleción de p62 se tradujo en un bloqueo significativo de la progresión tumoral en modelos de xenoinjertos. Por otra parte, los análisis de supervivencia en pacientes con melanoma han demostrado que la expresión de p62 en tumores primarios se asocia a un mayor riesgo de desarrollo de metástasis.

Conclusiones

El presente estudio de carácter multidisciplinario apoya por primera vez que la proteína Sequestosome1/p62 es necesaria para la progresión del melanoma. De hecho, Sequestosome1/p62 representa un punto de vulnerabilidad de las células de melanoma y, en consecuencia, podría representar una potencial diana terapéutica en el manejo de los pacientes con melanoma.

III. ABBREVIATIONS

III. ABBREVIATIONS

aa	Amino acid
AD	Alzheimer's disease
AJCC	American Joint Committee on Cancer
AKT	Serine/threonine protein kinase Akt
ALK	Anaplastic lymphoma receptor tyrosine kinase
aPKC	Atypical protein kinase
Atg7	Autophagy related 7
BAP1	Breast cancer 1-associated protein 1
BECN1	Beclin 1, autophagy relate
BRAF	v-raf murine sarcoma viral oncogene homolog B1
BSA	Bovine serum albumin
CDK1	Cyclin-dependent kinase 1
CDKN2A	Cyclin-dependent kinase inhibitor 2A
cDNA	Complementary DNA
CGH	Comparative Genomic Hybridization
CI	Confidence intervals
CNIO	Centro Nacional de Investigaciones Oncológicas
CO_2	Carbon Dioxide
CTLA-4	Cytotoxic T-lymphocyte antigen-4
DAPI	4,6-diamidino-2-phenylindole
DFS	Disease Free Survival
DMEM	Dulbecco's Modified Eagle's Medium
DNA	Deoxyribonucleic acid
dsRNA	Double-stranded RNA
EDTA	Ethylenediaminetetra-acetic acid
EGFP	Enhanced green fluorescent protein
EGFR	Epidermal growth factor receptor
ERK1	Extra-cellular signal-regulated kinase-1
FBS	Fetal Bovine Serum
FDA	Food and Drug Administration
FDR	False discovery rate
FGM	Fibroblast growth medium
GBM	Glioblastoma multiforme
GNAQ	Guanine nucleotide binding protein (G protein), q polypeptide
GSEA	Gene Set Enrichment Analysis
H&E	Hematoxylin and eosin
HD	Huntington's disease
HMGA2	High-Mobility Group A2
HR	Hazard ratio
IAP	Inhibitor of apoptosis protein
IF	Immunofluorescence

IHC	Immunohistochemistry
KEAP1	Kelch-like ECH-associated protein 1
KEGG	Kyoto Encyclopedia of Genes and Genomes
KGM	Keratinocyte growth medium
KIR	Keap-interacting region
KIT	Tyrosine-protein kinase Kit
LC3	Microtubule-associated protein 1 light chain 3
LIR	LC3-interacting region
MAPK	Mitogen-activated protein kinase
MC1R	Melanocortin receptor-1
MGM	Melanocyte growth medium
MITF	Microphthalmia-associated transcription factor
mRNA	Messenger RNA
mTOR	Mammalian target of rapamycin
NCCN	National Comprehensive Cancer Network
NF-kB	Nuclear factor of kappa light polypeptide gene enhancer in B-cells
NRAS	v-ras neuroblastoma RAS viral oncogene homolog
NRF2	Nuclear factor (erythroid-derived 2)-like 2
OCT	Optimal Cutting Temperature
OS	Overall Survival
P	Probability values
PB1	Phox and Bpem 1
PBS	Phosphate-Buffered Saline
PBS-T	Phosphate-Buffered Saline with Tween
PDB	Paget Disease of the Bone
PI3K	Phosphatidylinositol 3-kinase
pIC	Polyinosine-polycytidylic acid
PKC	Protein kinase C
PTEN	Phosphatase and tensin homolog
pUb	Polyubiquitin
RAC1	Ras-related C3 botulinum toxin substrate 1
RB	Retinoblastoma
RGP	Radial Growth Phase
RIP1	Receptor-interacting protein-1
RNA	Ribonucleic acid
RNAi	RNA interference
ROS	Reactive oxygen species
RT	Room Temperature
RT-qPCR	Real-time reverse transcription polymerase chain reaction
SA-β-Gal	Senescence-Associated β-Galactosidase
SD	Standard deviation
SEM	Standard error of estimate of mean value
shRNA	Short hairpin RNA
SQSTM1	Sequestosome1/p62

TMA	Tissue Microarrays
TNF	Tumor necrosis factor
TRAF6	TNF receptor-associated factor 6
TSC	Tuberosis sclerosis complex
Ub	Ubiquitin
UBA	Ubiquitin-associated domain
UPS	Ubiquitin-proteasome system
VGP	Vertical Growth Phase
WB	Western Blotting (Immunoblotting)
WHO	World Health Organization Classification
WT	Wild Type
ZIP	Zeta-interacting protein
ZZ	Zing finger
3D-SR	Three-Dimensional Human Skin Reconstruct

1. INTRODUCTION

1. INTRODUCTION

1.1. Melanoma

Melanocytes are dendritic cells derived from neural crest precursors. The neural crest cells give rise to unpigmented melanoblasts that home to specific destinations, where they ultimately form mature pigment-producing melanocytes. Mature melanocytes can be found in the skin, hair matrix, eye, inner ear, mucous membranes and central nervous system. In normal skin, these cells reside along the basal layer of the epidermis and in the hair bulb, with an approximated 1:10 ratio to basal keratinocytes (Dupin et al., 2003; Zabierowski et al., 2010).

The major function of melanocytes is to produce and transport melanin to surrounding keratinocytes. The pigment melanin confers protection of the mitotically active keratinocytes against the effects of ultraviolet light and is responsible for the visible pigmentation of the skin, hair, and eyes.

Defects in melanocytes can lead to numerous pigment disorders. Additionally, an abnormal proliferation of melanocytes can generate benign indolent neoplasias, known as melanocytic nevi, or a malignant tumor, melanoma.

Distinct categories of melanocytic neoplasms are distinguished by the current World Health Organization (WHO), which includes a list of lesions with different clinical and morphological profiles (LeBoit et al., 2006; Whiteman et al., 2011).

Common nevi are melanocytic lesions frequently found in population. This benign neoplasm originates as a focus of melanocytic proliferation within the lower layers of epidermis (junctional nevus) that progress to the presence of cells in both epidermis and dermis (compound nevus) and lately, it is confined to the dermis (dermal nevus). The likelihood of common nevi undergoing malignant transformation is quite remote. Their main relevance lies as a confounding factor in the diagnosis of melanomas or as a prognostic factor, since an increased number is correlating with a greater risk for melanoma development (Swerdlow et al., 1986; Holly et al., 1987).

Dysplastic nevi are junctional or compound melanocytic neoplasms characterized by architectural and cytological atypia. Clinically, dysplastic nevi may occur as sporadic lesions or associated to familial syndrome. Dysplastic nevus syndrome affects a group of patients with large numbers of atypical nevi, familial history of melanoma and an increased risk of

developing melanoma (Carey et al., 1994; Tucker et al., 1997). The malignant transformation of dysplastic nevi is quite controversial (Cook et al., 1985; Skender-Kalnenas et al., 1995). However, they may represent a confounding factor in the diagnosis of melanomas (Roth et al., 1991).

Malignant melanocytic tumors represent the most problematic group of skin cancers for patients and physicians. The first recorded description of melanoma in history appeared in the writings of Hippocrates in the 5th century, BC (Urteaga et al., 1966; Rebbeca et al, 2012). The original description of melanoma as an entity is attributed to René Laennec, who named this disease as 'melanose' in 1812 (Laennec, 1812). Later on, in 1838, the distinguished pathologist Robert Carswell was credited with the creation of the term 'melanoma', a word derived from the ancient Greek *melas*, 'dark' and *oma*, 'tumor' (Carswell, 1838; Rebbeca et al., 2012).

Since then, it has become clear that melanoma is a complex cancer, with an impressive aggressiveness and heterogeneity of its clinical, histological and genetic presentation. Although less common than basal or squamous cell carcinoma of the skin, melanomas are much more frequently fatal due to their intrinsic tendency to promote metastasis and extreme resistance to therapy. Already in 1840, the British surgeon Samuel Copper described that advanced stages of melanomas were untreatable, 'the only chance for benefit depends upon the early removal of the disease…' (Copper, 1840; Rebbeca et al., 2012). Unfortunately, this assertion is still largely true to this day.

1.1.1. Incidence and mortality of melanoma patients

Cancer is a major public health problem in many parts of the world. Melanoma is the fifth and sixth most incident cancer type in both males and females, respectively (Siegel et al., 2012). The incidence of melanoma continues to increase dramatically. It is increasing in men more rapidly than any other malignancy and, in woman more rapidly than any other malignancy except lung cancer (NCCN, 2013).

In the year 2012, an estimated 76,250 new cases of melanoma were diagnosed and about 9,180 patients died of melanoma in the United States (Siegel et al., 2012). The lifetime risk of developing the disease in the year 2005 for a person born in the United States was 1 in 55 (NCCN, 2013).

The levels of melanoma incidence vary considerably worldwide. Rates are higher in populations where Caucasians predominate (about 80% of the cases diagnosed in 2002 occurred in the predominantly white populations of Northern America, Australia, New Zealand and Europe), and lower in countries where inhabitants are of mainly Asian or African origin (LeBoit et al., 2006).

The median age of the patients at diagnosis of melanoma is 59 years (NCCN, 2013). It is one of the most aggressive types of cancer. In fact, melanoma ranks second to adult leukemia in terms of loss of years of potential life, per death (NCCN, 2013).

As with other malignancies, the outcome of melanoma initially depends on the stage at the time of diagnosis. The TNM classification and stage groupings for melanoma patients depend of histopathological and clinical aspects of the disease. Supplemental Tables 1 and 2 (page 131) summarize the recent revision of the staging system for cutaneous melanoma by the American Joint Committee on Cancer (AJCC) (Balch et al., 2009). The thickness of primary tumor, also named Breslow index (Breslow A, 1970), and the presence of ulceration and mitotic figures are the most relevant histological predictors for metastatic disease.

In general, the prognosis of melanoma patients is excellent for patients who present at the diagnosis with localized disease and primary tumors 1.0 mm or less in thickness, with 5-year and 10-year survival rates ranging from 97% to 93%, respectively. Unfortunately, this panorama changes with the increase of tumor thickness. In patients staged as T4bN0M0 (tumor thickness more than 4 mm with ulceration), 5-year and 10-year survival rates decrease to 53% and 39% respectively. Moreover, the likelihood of regional nodal involvement increases with increasing tumor thickness. When regional nodes or in transit metastases are present, 5-year survival decrease to 78%, 59%, and 40% for patients with stage IIIA, IIIB, and IIIC, respectively. When distant metastases are present, survival rates are extremely low. Thus, one-year survival rates among stage IV patients are 62% for M1a, 53% for M1b, and 33% for M1c melanomas (Balch et al., 2009).

1.1.2. Clinical, histological and genetic aspects of melanoma

Melanoma is a heterogeneous disease. It displays considerable variation at different levels: clinical presentation, histology, genetic alterations and patient outcome.

According to anatomical site, histopathology and degree of sun damage, there are four major types of cutaneous melanomas (Lentigo maligna, Superficial spreading, Nodular and Acral lentiginous) and two types of extracutaneous melanomas (Mucosal and Ocular).

Lentigo maligna melanoma appears mostly in head and neck region in elderly people and is related to chronic sun exposure. Superficial spreading melanoma is the most common type of melanoma in Caucasians patients. Legs and back are the anatomic sites most frequently involved and this type is related to intermittent exposition to sunlight. Nodular melanoma usually presents as a rapidly growing nodule on sites that are intermittently exposed to sunlight. This is the most aggressive type of cutaneous melanoma and is histologically characterized by the absence of radial growth phase. Acral lentiginous melanomas arise on sites protect from the sunlight, including the palm of the hand, sole of the foot or under the nails. It is the predominant type of melanoma in Afro-Caribbean and Oriental patients (LeBoit et al., 2006). Mucosal melanomas may originate in any mucosa, but mostly in nasal and oral cavity, anorectum, vulva and vagina. Compared with cutaneous and ocular melanoma, mucosal melanomas have the lowest percent of five-year survival (Mihajlovic et al., 2012). Melanoma can also originate from melanocytes of the uvea, encompassing intraocular structures such as the iris, ciliary body, and choroid (Laver et al., 2010; Whiteman et al., 2011).

Most cutaneous melanomas present as an initial intraepidermal proliferation that subsequently evolves to the invasion of basement membrane and dermal proliferation. The metastatic capacity of melanoma cells occurs when these cells reach the dermis and are able to invade lymph or blood vessels.

The first stage of skin melanoma progression is known as radial growth phase (RGP). In this phase, melanoma cells are confined to the epidermis (*in situ* melanoma) or involve papillary dermis as small nests composed of less than 15 cells without proliferative or metastatic capacity (Gimotty et al., 2005). The next step in melanoma progression is named vertical growth phase (VGP). In this phase, melanoma cells are located in the dermis and are able to proliferate and generate metastasis (Barnhill et al., 1993). Significant change in gene expression profile occurs in the transition from radial to vertical growth phase. Such alteration encourages proliferation, suppression of apoptotic programs, capacity for vascular invasion and metastatic spread (Alonso et al., 2004; Hoek, 2007).

Many studies performed over several years on benign nevi and melanoma tumors have tried to identify the mechanisms involved in malignant transformation of melanocytes.

Comparative genomic hybridization (CGH) of melanocytic neoplasms has identified multiple genomic regions with changes in DNA copy number in melanoma tumors and absence or a restricted set of chromosomal aberration in melanocytic nevi (Curtin et al., 2005; Bauer et al., 2006).

Numerous genes have been implicated in melanoma development and progression. The v-raf murine sarcoma viral oncogene homolog B1 (*BRAF*) and the v-ras neuroblastoma RAS viral oncogene homolog (*NRAS)* genes are the most common targets for somatic mutations in melanoma. A point mutation in the *BRAF* gene (predominantly V600E, where valine is substituted for glutamic acid at amino acid 600) is detected in around 40-60% of melanoma patients (Goel et al., 2006; Ribas et al., 2011). In the *RAS* family, *NRAS* is the most frequently affected gene. Its mutation occurs in approximately 10-20% of melanoma patients (Goel et al., 2006). Both *BRAF* and *NRAS* mutations seem to be mutually exclusive and lead to the constitutive activation of the mitogen-activated protein kinase (MAPK) pathway with the consequent induction of proliferative and survival programs (Mercer et al., 2003).

Although *BRAF* and *NRAS* mutations are a critical step in melanoma initiation, they are not exclusively expressed in malignant lesions of melanocytes. $BRAF^{V600E}$ mutation is found in 82% of common nevi (Pollock et al., 2003) and *NRAS* mutation in 56% of congenital nevi (Chin et al., 2006). In fact, the overexpression of such oncogenes in cultured melanocytes triggers a nonproliferative but viable state named senescence (Michaloglou et al., 2005; Denoyelle et al., 2006). Since the induction of senescence triggered by oncogenes is an intrinsic cellular mechanism against malignant transformation, the transformation of melanocytes must be invariably accompanied by additional deregulation, including the loss-of-function of tumor suppressors, as the inhibitor cyclin-dependent kinase 4 ($p16^{INK4a}$) and the phosphatase and tensin homolog (*PTEN*) (Tsao et al., 2004; Dankort et al., 2009).

The inactivation of $p16^{INK4a}$ protein, taken as whole, is detected in 30–70% of melanomas (Sharpless et al., 2003). $P16^{INK4a}$ is a tumor suppressor gene product involved in cell cycle regulation and induction of senescence (Hansson et al., 2010). Loss of $p16^{INK4a}$ function promotes retinoblastoma (RB) inactivation, resulting in unconstrained cell cycle progression (Serrano et al., 1993). This protein is coded by the cyclin-dependent kinase inhibitor 2A gene (*CDKN2A*) and approximately 20-40% of familial melanomas harbor germline mutations in this gene.

The allelic loss or altered expression of *PTEN* gene is observed in 20% and 40% of melanoma, respectively (Chin et al., 2006; Goel et al., 2006). *PTEN* inactivation leads to the

activation of the phosphatidylinositol 3-kinase/ serine/threonine protein kinase Akt (PI3K/AKT) pathway, which enhances melanoma cell survival and proliferation (Robertson et al., 2005).

Additional mutations have also been described in melanoma tumors. Mutations in the receptor tyrosine-protein kinase Kit (*cKIT*) gene occur more frequently in acral, mucosal and cutaneous melanomas with chronic sun-induced damage (Curtin et al., 2006). Somatic mutation in the heterotrimeric G protein α-subunit (*GNAQ*) gene has been found in 46% of uveal melanoma (Van Raamsdonk et al., 2009). Another study on uveal melanomas has identified an inactivating somatic mutation in the gene encoding the breast cancer 1-associated protein 1 (*BAP1*) (Harbour et al, 2010). Recently, the sequencing of 147 melanomas has demonstrated mutation in the ras-related C3 botulinum toxin substrate 1 (*RAC1*) gene in 9.2% of sun-exposed melanomas (Kraurhammer et al., 2012). RAC1 is a small G-protein in the Rho family that promotes cell-cell adhesion and regulates cell motility in response to extracellular signals (Kimura et al 2006; Sanz-Moreno et al., 2008; Leve et al., 2012). Interestingly, this mutation was the third most frequent in sun-exposed melanoma after *BRAF* and *NRAS* mutations (Kraurhammer et al., 2012).

Many other genetic aberrations, as microphthalmia-associated transcription factor (MITF) amplification (Garraway et al., 2005), genetic polymorphisms in the melanocortin receptor-1 (MC1R) and germline inactivation of the retinoblastoma 1 (*RB1*) gene (Fletcher et al., 2004), have been related to melanoma tumors and illustrate the extreme genetic heterogeneity of this disease.

1.1.3. The influence of autophagy in melanoma progression

Besides the aforementioned genetic alterations, melanoma progression also involves development of other events, such as adaptive responses to nutrient deprivation, hypoxia and anticancer drugs.

Macroautophagy (herein referred to as autophagy) is a lysosomal proteolytic process involved in the degradation of protein aggregates and cytoplasmic organelles. It can be stimulated by numerous forms of cellular stress, as nutrient deprivation, hypoxia, oxidative and endoplasmic reticulum stresses, protein aggregates and damaged organelles (Kroemer et al., 2010).

In autophagy, cytosolic substrates are engulfed by a double-layered membrane called autophagosome. The autophagosome microtubule-associated protein 1 light chain 3 (LC3) is an important constituent of autophagosomes. The cytosolic form LC3-I is cleaved by proteases to expose a C-terminal glycine residue, which is then conjugated to a phosphatidylethanolamine group to generate the isoform LC3-II that is tightly bound to the autophagosomal membrane. Subsequently, the autophagosome structure fuses with the lysosome, whereby the protein content is degraded by lysosomal proteases (Mehrpour et al., 2010).

Deregulation of autophagy has been described in different types of human cancers. Under biological stress, autophagy can promote survival of tumor cells by eliminating toxic substrates and supplying metabolic precursors. Paradoxically, autophagy can work as a tumor suppressor and promotes tumor cell death by induction of self-destroying programs (Levine et al, 2008).

In melanoma tumors, the activation of autophagy seems to be an adaptive mechanism for tumoral progression (Hersey et al., 2008; Checinska and Soengas, 2011). Immunohistochemical and electron microscopy studies of melanoma specimens have identified high levels of autophagy in the invasive front of primary melanomas (Lazova et al., 2010). The expression of LC3 protein in primary tumors was also strongly associated with the development of metastasis and shorter survival of melanoma patients (Han et al., 2011). Additionally, the inhibition of autophagy through RNA interference (RNAi) or drug treatment induced cellular death of aggressive melanoma cells (Ma et al., 2011). Autophagy can also protect cells against drug-induced stress, thus representing a mechanism of melanoma chemoresistance (Marino et al., 2010; Ma et al., 2011).

Nevertheless, as in other type of cancers, autophagy could work as a tumor suppressor and induces cellular death. Unlike the previously mentioned studies, another study has found that mRNA expression of two autophagy-related genes, beclin 1 (*BECN1*) and *LC3*, significantly decreases with tumor progression (Miracco et al., 2010). In addition, treatment of melanoma cells with dsRNA mimic polyinosine-polycytidylic acid (pIC) engendered hyperactivity of autophagy machinery with subsequent cell death through self-degradation (Tormo et al., 2009; Alonso-Curbelo et al., 2010).

1.1.4. The need for new melanoma treatment strategies

Melanoma is a very complex and heterogeneous disease, with multiple events involved in tumor initiation and progression. Despite all knowledge generated in last years, additional studies are still necessary for full comprehension of its pathogenesis (Soengas et al., 2003).

While melanoma can be curable when removed at early stages, the prognosis is grim in the context of metastatic disease. In fact, the overall long-term survival in patients with distant metastatic melanoma is less than 10% (NCCN, 2013). Metastases of melanoma may appear many years after the diagnosis, in different organs and usually, do not respond to treatment.

This type of cancer is characterized by the resistance to all forms of conventional treatments (radio-, immuno-and chemotherapy). During a long time, dacarbazine, which presents very disappointing response rates, was the unique single-agent approved by the Food and Drug Administration (FDA) for treating metastatic melanoma (Serrone et al., 2000). Other therapies used in clinical practice, as Interferon alfa-2b and Interleukin-2 also showed disappointing responses and failed to demonstrate prolonged overall survival (Atkins et al., 1999; Kirkwood et al., 2000).

After many years dedicated to the comprehension of genetic and immunologic alterations of melanoma tumors, recently, new strategies for melanoma treatment are emerging (Márquez-Rodas et al., 2011; Espinosa el at., 2012). Targeted therapies aimed to the frequently mutated oncogene *BRAF* (Chapman et al., 2011) and the cytotoxic T-lymphocyte antigen-4 (CTLA-4) (Hodi et al., 2010), were recently approved by the FDA. However, although both drugs have improved overall and disease free survival in phase III clinical trials, these are only effective on a fraction of affected patients. In addition, tumor resistance and relapses appear in most of patients treated with these drugs (Hodi et al., 2010; Chapman et al., 2011; Kudchadkar et al., 2012).

Many other clinical trials currently underway also demonstrate partial or unsatisfactory results. Therefore, unfortunately, melanoma remains highly resistant to current available treatments. This clinical picture, associated with an increasing incidence, justifies efforts for the discovery of new mechanisms of melanoma progression and translation of such insights into therapeutic strategies. The identification of new targets and generation of drugs,

used as single-therapy or in combination with the current ones, would be of great benefit for melanoma patients.

1.2. Sequestosome 1/p62 protein

In eukaryotic cells, large amounts of damaged/misfolded proteins are constantly produced. Furthermore, the exposure of cells to stress, principally oxidative stress, increases the production of misfolded proteins that need to be refolded or degraded.

Aggressive cancers, and melanoma is not an exception, are characterized by an exacerbated cellular metabolism. High metabolism associated to stressful microenvironment, such as nutrient deprivation, hypoxia and low pH, dramatically enhance the production of misfolded proteins in cancer cells (Schröder et al., 2005; Moenner et al., 2007; Kirkin et al., 2009). Thus, tumor cells appear to be significantly more dependent on the continuous clearance of damaged proteins than their normal counterparts. In fact, therapeutic drugs targeting systems of protein degradation, such as the ubiquitin-proteasome system (UPS) and autophagy, are a strategy used for the treatment of patients with cancer (Linder et al., 2005; Amaravadi et al., 2007; Mujtaba et al., 2011; Yang et al., 2011).

Since tumor cells present an intrinsic ability to overcome stressful conditions (Moenner et al., 2007), an understanding of the mechanisms by which tumor cells adapt to adverse environment is essential for developing a well-targeted therapy. Recently, the multifunctional protein Sequestosome 1/p62 has been emerging as a new promoter of tumor survival (Duran et al., 2008; Mathew et al., 2009; Duran et al., 2011). P62 protein is involved in proteasomal and autophagosomal degradation with key roles in other tumor types, but unknown in melanoma. Additionally, p62 works as an adaptor protein activating several intracellular signaling pathways involved in metabolism, antioxidative response, inflammation, and ultimately, tumorigenesis (Puissant et al., 2012).

One of the least understood aspects in melanoma is the modulation of protein degradation machineries. Therefore, the multifunctional property of Sequestosome1/p62 protein combined with the need for new melanoma treatment strategies turns p62 an attractive candidate to be characterized in melanoma tumors.

1.2.1. Structure and domains of Sequestosome 1/p62 protein

P62 was first described by Joung and collaborators in 1996 (Joung et al., 1996). It was cloned as a novel human cDNA encoding a 62 kDa protein able to bind to $p56^{lck}$, a T-cell-specific Src family tyrosine kinase. Independently, Puls and co-workers identified p62 as a cytosolic protein capable to interact with the atypical protein kinase C (PKC) member PKC-ζ (Puls et al., 1997). On this occasion, p62 was referred as zeta-interacting protein (ZIP). Currently, p62 is also named Sequestosome1 because of its ability to sequester aggregates of proteins inside the cytosol (Shin et al., 1998).

The Sequestosome1 human gene (*SQSTM1*) is located on the long (q) arm of chromosome 5 at position 35. More precisely, it is located from base pair 179,233,388 to base pair 179,265,078. It codes manly for two protein isoforms composed of 440 and 356 amino acids. Using protein immunoblot analysis, the main isoform identified presents around 62 kDa.

P62 mRNA is ubiquitously expressed in a variety of normal tissues (Joung et al., 1996). This protein is essentially located in the cytoplasm and can present different patterns of distribution: diffuse or forming small bodies or large aggregates of protein (Lamark et al., 2003; Bjørkøy et al., 2005). A minor number of publications have also referred the nuclear localization of p62 protein (Bjørkøy et al., 2005; Pankiv et al., 2009).

The functions of p62 are associated to two major processes: **protein degradation** and **activation of signaling pathways**. The structure and domains of p62 are illustrated in Figure1.

The N-terminal Phox and Bpem 1 domain (PB1, aa. 21-103) is responsible for the self-oligomerization of p62 and the interaction of p62 with the S5a proteasome subunit (Seibenhener et al., 2007). Through PB1 domain, p62 also interacts with atypical protein kinase (aPKC), regulating the nuclear factor of kappa light polypeptide gene enhancer in B-cells (NF-kB) pathway (Moscat et al., 2006; Saio et al., 2009) and with extra-cellular signal-regulated kinase-1 (ERK1), being involved in adipogenesis (Lee et al., 2010). The zing finger domain (ZZ, aa. 128-163) is responsible for p62 interaction with the receptor-interacting protein-1 (RIP1) and regulation of NF-kB pathway (Geetha et al., 2002; Moscat et al., 2006). The region between the ZZ and TRAF6-binding (TBS) domains (aa. 167-230) harbors the domain responsible for the association with Raptor protein, involved in the mammalian target of rapamycin (mTOR) pathway (Duran et al., 2011). Through TBS domain (TBS, aa. 225-

250), p62 interacts with TNF receptor-associated factor 6 (TRAF6) and activates NF-kB pathway (Sanz et al., 2000; Durán et al., 2004). The LC3-interacting region domain (LIR, aa. 321-345) is responsible for the interaction between p62 and the autophagy related protein LC3. Next, the Keap-interacting region (KIR, aa. 346-359) binds kelch-like ECH-associated protein 1 (Keap1) and activates the antioxidative response through nuclear factor (erythroid-derived 2)-like 2 (Nrf2) activation (Komatsu et al., 2010). Finally, through the C-terminal ubiquitin-associated domain (UBA, aa.386-440), p62 binds to ubiquitinated proteins and target them for proteasomal or autophagosomal degradation (Kirkin et al., 2009).

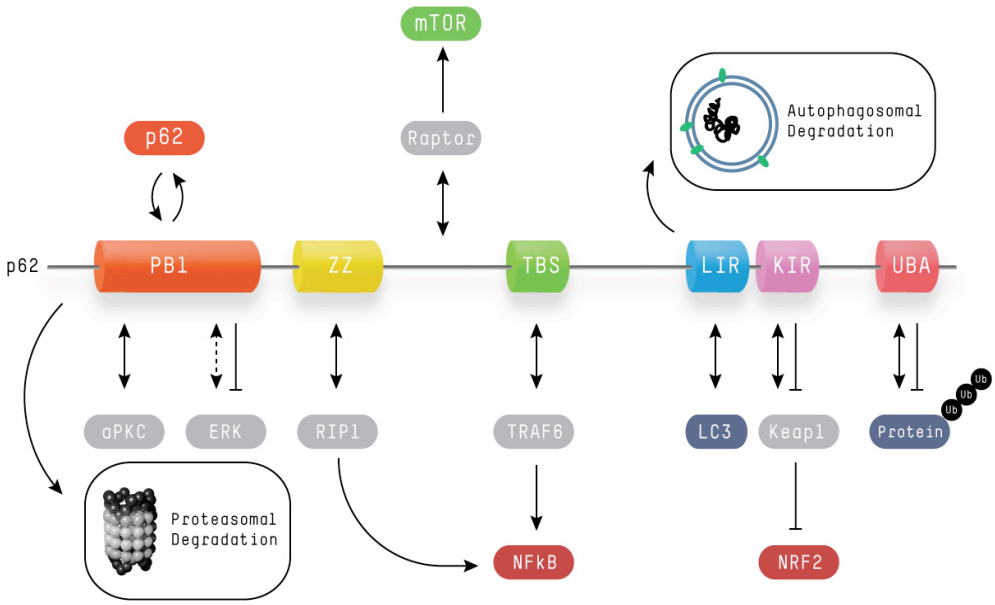

Figure 1. Schematic presentation of the domains and the main interactions/functions of p62 protein. Through diverse domains, p62 can interact with proteasomal and autophagosomal degradation systems and regulates different intracellular pathways (modified from Puissant et al., 2012).

1.2.2. Interaction of Sequestosome 1/p62 protein with protein degradation systems

The ubiquitin-proteasome system and autophagy process are the major routes for intracellular protein recycling. Both systems are essential for the maintenance of cellular homeostasis, especially under stressfull conditions.

Ubiquitination is a common type of posttranslational modification of proteins. It involves covalent attachment of the 76 amino acid peptide ubiquitin (Ub) to proteins, as mono or polyubiquitin (pUb) chains. Ubiquitination participates in different cellular processes, as

protein degradation, endocytosis, signal transduction and DNA repair (Kirkin et al., 2009). The addition of polyubiquitin chains, in which Ub is linked via lysine 48, targets the substrates for degradation by the proteasome system (Seibenhener et al., 2004).

The **ubiquitin-proteasome system** is responsible for the degradation of defective or misfolded proteins. Thus, the recognition of polyubiquitinated substrates by the proteasome complex plays an essential role in degradation of toxic proteins. Through the interaction with S5a proteasome subunit by PB1 domain and the interaction with pUb proteins by the UBA domain, p62 can bind ubiquitinated proteins and delivers them for proteasomal degradation.

As mentioned before, **autophagy** is a catabolic process involved in intracellular degradation of proteins aggregates and organelles through the lysosomal machinery. During a long time autophagy was considered an unspecific proteolytic system of cytoplasmic substrates. However, the discovery of p62 added new evidences of the specificity of autophagosomal degradation (Kirkin et al., 2009).

P62 can form ubiquitylated and non-ubiquitylated aggregates into the cytoplasm (Watanabe et al., 2011). Through LIR domains, p62 interacts with LC3 protein and transports protein aggregates (either ubiquitinated or not) to autophagosomal degradation, thereby being itself degraded by lysosomal proteases (Figure 2).

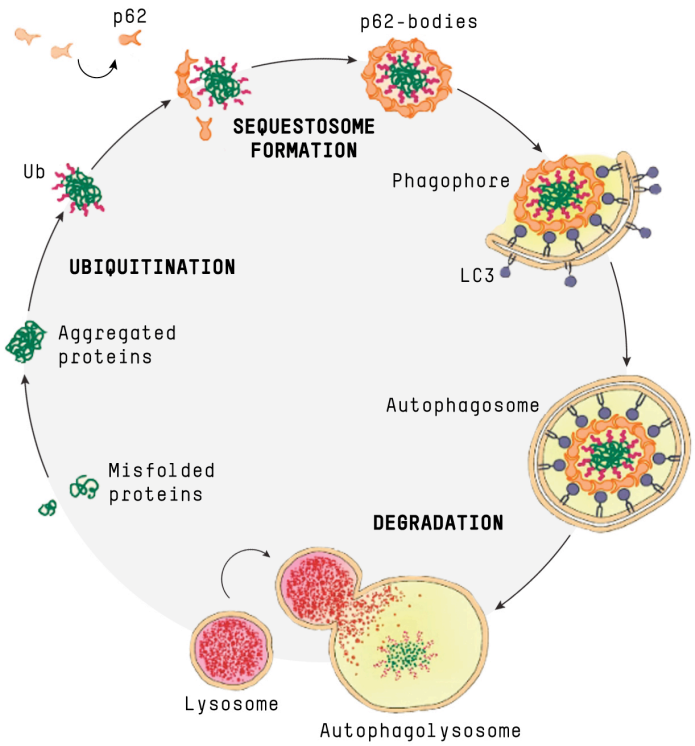

Figure 2. Schematic figure showing the function of p62 in sequestosome formation and autophagosome degradation. P62 binds and sequester aggregates of proteins in the cytosol (sequestosome formation). Through the interaction with LC3 protein located in the membrane of autophagosomes, p62 delivers aggregated proteins for lysosomal degradation (modified from Puissant et al., 2012).

In summary, p62 is able to interact with the two major proteolytic systems, UPS and autophagy. Because of its ability to form cytoplasmic bodies of proteins and interact with LC3 protein, p62 is considered the missing link between protein aggregation and autophagic clearance (Bjørkøy et al., 2005; Bjørkøy et al., 2006).

1.2.3. Implication of Sequestosome 1/p62 protein in cellular functions

Sequestosome1/p62 also works as an **adaptor protein**. The adaptor proteins are proteins without enzyme activity that act by forming complexes with other signaling molecules and are required for the efficient regulation of intracellular pathways.

The first signaling pathway related to p62 protein was the **NF-kB pathway**. NF-kB is a transcription factor governing the expression of genes involved in immuno response, inflammation, embryonic development, apoptosis, cell cycle, and oncogenesis (Hayedn et al., 2004). Through the interaction with different proteins of NF-kB pathway (as aPKC, RIP1 and TRAF6) p62 has been associated to the regulation of osteoclastogenesis (Duran et al., 2004), inflammation (Martin et al., 2006; Kim et al., 2009) and tumorigenesis (Duran et al., 2008; Ling et al., 2012).

P62 also works as an adaptor protein in **Keap1-Nrf2 signaling pathway**. The transcription factor Nrf2 plays a central role in the protection of cells against oxidative stress. It controls the expression of various detoxifying and antioxidant defence enzymes and proteins (Taguchi et al., 2011). Through a specific domain, p62 can bind Keap1 and competes with the interaction between Nrf2 and Keap1, resulting in the stabilization of Nrf2 and transcriptional activation of target genes. Therefore, the constitutive activation of Nrf2 by p62 confers resistance of tumor cells to oxidative stress and contributes to tumor progression (Komatsu et al., 2010; Copple et al., 2010; Lau et al., et al 2010).

The **mTOR signaling pathway**, a coordinator of cell growth and metabolism, is also regulated by P62. mTOR can be activated by different stimuli, like nutrients, hypoxia and growth factors, in order to control cell growth, proliferation and motility. The deregulation of mTOR pathway has been demonstrated in different types of cancer (Pópulo et al., 2012). Through the interaction with Raptor protein, p62 activates mTOR pathway in response to amino acids stimulation and contributes to tumorigenesis (Duran et al., 2011; Moscat et al., 2011).

Another critical function of p62, recently described, is its involvement in **cell cycle**. Linares and collaborators have shown that p62 is phosphorylated by the cyclin-dependent kinase 1 (CDK1) on threonine 269 and serine 272 during early mitosis phase (Linares et al, 2011). The phosphorylation of p62 permits the cells to properly continue through mitosis and is responsible for restraining cell growth and tumor progression On the other hand, the lack of CDK1-mediated phosphorylation of p62 promotes a faster exit from mitosis and enhances cell proliferation and tumorigenesis (Linares et al, 2011).

Recently, p62 has also been linked to **apoptosis**. The programmed cell death by apoptosis participates in various biological processes such as development, maintenance of tissue homeostasis and as a natural barrier to cancer progression. It initiates with the activation of normally latent proteases (caspase-8 and caspase-9), which promotes a cascade of proteolysis culminating in cellular death (Hanahan et al., 2011). Jin and colleagues have demonstrated the co-localization of p62 and caspase-8 into ubiquitinated cytoplasmic foci. Furthermore, the aggregation of caspase-8 promoted by p62 was responsible for the full activation of this protease and the consequent induction of apoptosis (Jin et al., 2009).

It has also been demonstrated the involvement of p62 in **energy homeostasis** and **adipogenesis** through the interaction with ERK1 protein. P62 antagonizes basal ERK activity and its loss conducts to the hyperactivation of ERK and adipogenesis. In fact, p62-deficient mice develop late-onset obesity that leads to insulin resistance and impaired glucose tolerance (Rodriguez et al., 2006; Lee et al., 2010).

In summary, in the last years, many works describing the function of p62 as an adaptor protein have been emerging in the literature. Through its different domains, p62 is able to interact and regulate diverse signaling pathways and, consequently, interfere with critical cellular functions.

1.2.4. Association of Sequestosome 1/p62 protein with human diseases

P62 has been associated to different human diseases. One of the most well described entities related to p62 is the **Paget Disease of the Bone** (PDB) (Layfield et al., 2004; Rhodes et al., 2008). PDB is a common skeletal disorder characterized by disorganized bone resorption due to increased osteoclastic activity. Mutations in the *SQSTM1* gene have been described in approximately 40% of familial and 8% of sporadic cases of Paget Disease. More than 20 different mutations have been identified and almost all of them affect the UBA

domain of p62 (Morissette et al., 2006; Najat et al., 2009; Michou et al., 2011). There are limited data about the functional consequence of *SQSTM1* mutations in PDB. Although it is not a consensus, *SQSTM1* mutations seem to interfere with osteoclastogenesis through deregulation of NF-kB signaling pathway (Durán et al., 2004; Layfield et al., 2004; Rea et al., 2006; Kurihara et al., 2007). Corroborating the influence of p62 in bone homeostasis, p62 knockout mice present increased bone density with defective osteoclastic function (Durán et al., 2004).

Abundant expression of p62 has also been identified in cytoplasmic inclusions of **neurodegenerative diseases** (Nagaoka et al., 2004; Bjørkøy et al., 2005).

Alzheimer's disease (AD) is the most common neurodegenerative disease characterized by progressive impairment in memory and cognition. Accumulation of polyubiquitinated tau protein in neuronal cells is one of the major histopathological features of AD. Immunohistological studies of parietal cortical samples of patients with AD showed that p62 co-localizes with tau-positive inclusions in neuronal cells (Kuusisto et al., 2002). Moreover, Babu and collaborators have described that p62 interacts with polyubiquitinated tau through its UBA domain (Babu et al., 2005). The study of p62 knockout mice performed by these authors also revealed a pathological accumulation of tau protein in neurons, associated to a massive neuronal degeneration, which suggests a protective role of p62 in Alzheimer's disease (Babu et al., 2005).

Huntington's disease (HD) is an inherited autosomal dominant neurodegenerative disorder characterized by late onset of motor dysfunctions, psychiatric disturbances and ultimately, death of patients. HD is caused by the expression of mutant forms of huntingtin protein that accumulates in the cytoplasm being deleterious to neuronal cells (Bano et al., 2011). Bjørkøy and collaborators have shown that p62 co-localizes with huntingtin protein aggregates in neurons (Bjørkøy et al., 2005). These authors have also demonstrated that p62 facilitates the clearance of huntingtin aggregates by the autophagy system, thus decreasing neuronal toxicity (Bjørkøy et al., 2005).

P62 was also identified in **Lewy bodies of Parkinson's disease** (Kuusisto et al., 2003; Braak et al., 2010) and ubiquitin-immunoreactive intraneuronal inclusions in **Amyotrophic lateral sclerosis** (Nakano et al., 2004; Mizuno et al., 2006).

In addition, p62 is related to protein aggregation entities other than neurodegenerative diseases. The co-expression of p62 was found within the Mallory body inclusions in **alcoholic hepatitis**; hepatocellular aggregates in **α1-antitrypsin deficiency**; intracytoplasmic hyaline

bodies in **hepatocellular carcinoma**; and Rosenthal fibers in **astrocytoma** (Stumptner et al., 2002; Zatloukal et al., 2002; Stumptner et al., 2007). In **sporadic inclusion-body myositis**, p62 is overexpressed at protein and mRNA levels and accumulates within p-tau containing inclusion bodies in muscle fibers (Nogalska et al., 2009).

Although the relevance of p62 aggregates in human diseases has not been fully elucidated, many studies indicate that it represents a protective mechanism developed by the cells. Through the ability of p62 to sequester toxic proteins and deliver misfolded proteins to proteasomal and autophagosomal degradation, p62 could prevent cell death and, consequently, contributes to cellular survival.

1.2.5. The role of Sequestosome 1/p62 in tumorigenesis

The overexpression and accumulation of p62 has been described in different types of human cancers (Thompson et al., 2003; Kitamura et al., 2006; Duran et al., 2008).

As already mentioned for other diseases, most of the studies indicate a **pro-survival role** of p62. The mechanisms whereby p62 contributes to tumorigenesis are diverse and are related to autophagy clearance or cell signaling activation functions. Moreover, the involvement of p62 in tumor progression appears to be tissue-specific and its mechanism dependent of the type of cancer cell studied.

Moscat's group described one of the first implications of p62 in cancer cells in 2008 (Duran et al., 2008). Using p62 knockout mice, these authors showed that the lack of p62 inhibits the induction of **lung adenocarcinoma** by RAS oncogene. They also demonstrated that Ras expression increases p62 mRNA levels through the activation of p62 promoter. In this context, the lack of p62 impaired NF-kB activation in Ras-transformed cells, which led to higher production of reactive oxygen species (ROS) and increased cell death (Duran et al., 2008). Confirming the involvement of p62 in lung cancer, other authors have performed immunohistochemical and survival analyses of p62 expression in 109 patients with non-small-cell lung cancer, including adenocarcinoma, squamous cell carcinoma, and large cell carcinoma, and found that the accumulation of p62 was particularly associated with poor prognosis in patients with lung adenocarcinoma (Inoue et al., 2012).

The group of Eileen White has also demonstrated the implication of p62 in tumorigenesis (Mathew et al., 2009). Taking in account that some human tumors can present mutations in autophagy genes leading to autophagy defects, these authors tried to elucidate

how the loss of such survival process could promote tumor growth. Using autophagy-defective tumor cells, they found that **p62 protein accumulates in response to metabolic stress.** Moreover, they found that the inability to clear p62 through autophagy and the consequent accumulation of p62 was responsible for increased DNA damaged response, cellular genomic instability and finally, tumor growth. Interestingly, opposite to Moscat's findings in lung carcinoma, these authors suggested that defective autophagy and p62 accumulation impaired NF-kB activation in hepatocellular carcinoma, demonstrating the tissue-specific mechanism of p62 function (Mathew et al., 2009).

Based on the fact that more than 25% of human hepatocellular carcinomas present cytosolic aggregates of p62, and that the induction of Nrf2 anti-oxidative pathway is recognized in most of these tumors, Komatsu's group has studied the link between autophagy deficiency, p62 and Nrf2 transcription factor (Inami et al., 2011). Using liver-specific autophagy related 7 (Atg7) knockout mice, these authors demonstrated the development of **hepatocellular tumors** in this model. Since *Atg7* is an essential gene for autophagy function, they found a marked accumulation of p62 in hepatocytes of Atg7-deficient cells. It was observed that most of the p62-containing aggregates were also positive for Keap1. The sequestration of Keap1 into p62 aggregate structures was responsible for the persistent activation of the Nrf2 transcriptional factor leading to an anti-oxidative response and tumor progression. Besides the transcriptional regulation proposed by Moscat's group (Duran et al., 2008), Jain and coworkers have also demonstrated that p62 is regulated by Nrf2 (Jain et al, 2010). Under oxidative stress stimulus, Nrf2 transcriptional factor binds to the antioxidant response element located in the p62 promoter and regulates the expression of p62 mRNA.

P62 was also linked to tumorigenesis through its ability to interact with the metabolic pathway mTOR. Duran and collaborators have shown that p62 is required for tumor proliferation of **prostate cancer** cells. In fact, the depletion of p62 affected the capacity of prostate cancer cells to form solid tumors in xenograft mice models. In this context, the inhibition of the survival pathway mTOR was the mechanism whereby the lack of p62 inhibits tumor growth (Duran et al., 2011).

The contribution of p62 in tumor growth was also described in **tuberosis sclerosis complex** (TSC). TSC is a genetic disorder characterized by mutations in the tuberous sclerosis complex 1 or 2 genes (TSC1 and TSC2). There are multiple clinical manifestations including neurologic disease and the formation of nonmalignant hamartomas in different organs. P62 was accumulated in angiomyoliomas and pulmonary lymphangioleiomyomatosis

of patients with TSC. Further, p62 was important for tumor growth in TSC since the depletion of p62 delayed TSC2-null tumor development in xenograft models (Parkhitko et al., 2011).

Recently, p62 was associated to **tumor invasion capacity**. Galavotti and coworkers have studied the influence of p62 in **glioblastoma multiforme** (GBM) progression. Using glioblastoma stem cells isolated from GBM surgical specimens, they found that the depletion of p62 expression inhibits the invasion and migration capacity of such cells. The mechanism underlying the role of p62 in invasion was not fully elucidated. However, it appears that p62 interferes with tumor invasion function through its involvement with autophagy and the regulation of energy metabolism (Galavotti et al., 2012).

P62 was also associated to cancer through the description of a **new gene translocation.** Takeuchi and collaborators reported the fusion of anaplastic lymphoma receptor tyrosine kinase (*ALK*) gene with Sequestosome1 gene in a patient with ALK-positive large B-cell lymphoma (Takeuchi et al., 2011). Additionally, 3T3 fibroblasts expressing *SQSTM1-ALK* were able to form solid tumors in nude mice model, demonstrating the transforming potential of such translocation. Although there is only one unique case referred in the literature, the new *SQSTM1-ALK* fusion is of great clinical interest since it presents oncogenic capacity.

In summary, the multifunctional protein p62 promotes tumorigenesis by activating pro-oncogenic signaling pathways and interfering with the autophagy system. As mentioned previously, the involvement of p62 in cancer is quite complex and dependent of the cell type. Although p62 has been linked to different types of human cancer, no data about its implication in melanoma are available in the literature. Altogether, the involvement of p62 in crucial cellular function, as degradation of misfolded proteins and protein aggregates, combined with the regulation of oncogenic pathways turn p62 an interesting candidate to be studied in melanoma tumors.

2. OBJECTIVES

2. OBJECTIVES

The increasing incidence of melanoma and the tendency for lethal metastasis and therapeutic resistance presented by such tumors justify the efforts for the identification of new mechanisms of melanoma progression and alternatives of treatment. Melanoma, like other aggressive tumors, is characterized by an exacerbated cellular metabolism, which requires continuous degradation of proteins. However, the molecular bases that mediate this process are poorly characterized and their understanding could provide a platform for the development of new drugs. Sequestosome 1/p62, a multifunctional protein involved mainly in protein degradation and activation of pro-oncogenic signaling pathways, is an attractive candidate to be investigated in aggressive tumors. This multidisciplinary study aims the characterization of the Sequestosome 1/p62 protein in melanoma, through the following main objectives:

2.1. To analyze the expression of Sequestosome 1/p62 in benign melanocytic tumors and melanomas at different stages of progression;

2.2. To determine the function of Sequestosome 1/p62 in melanoma tumors using an *in vitro* approach with melanoma cell lines;

2.3. To establish the physiological impact of Sequestosome 1/p62 *in vivo* using a xenograft model and correlating p62 expression with melanoma patient outcome.

3. MATERIALS AND METHODS

3. MATERIALS AND METHODS

3.1. *In vitro* experiments

3.1.1. Isolation of normal melanocytes, keratinocytes and fibroblasts

The sources of tissue for melanocytes, keratinocytes and fibroblasts isolation were human neonatal foreskins obtained from routine circumcision and donation by patients treated at Hospital Universitario 12 de Octubre and Hospital Niño Jesus, Madrid.

The skins were washed with 70% ethanol, cut into small pieces and digested by Dispase II (Invitrogen, Carlsbad, CA, USA) enzyme at 4°C overnight. The day after, epidermal sheets were detached from the dermis by sliding it off with a scalpel blade. Epidermal pieces were used for melanocytes and keratinocytes isolation. Dermal pieces were separated for fibroblasts isolation. The isolated epidermal sheets were then cut with a scalpel blade and digested by 0.25% Trypsin/EDTA (Invitrogen, Carlsbad, CA, USA) at 37°C during 3 minutes. The cell dispersal solution obtained was centrifuged. The pellet obtained from the epidermis was divided into two parts and resuspended with Melanocyte Growth Medium for melanocytes culture or Keratinocyte Growth Medium for keratinocytes culture (Table 1). The isolated dermis pieces were cut and digested by Collagenase IV (Invitrogen, Carlsbad, CA, USA) at room temperature (RT) during 24 hours. After centrifugation, the cells of the dermis were resuspended in Fibroblast Growth Medium for fibroblasts culture (Table 1). All cultures were incubated at 37°C/5% of CO_2.

Table 1. Culture mediums used for melanocytes, keratinocytes and fibroblasts isolation:

Melanocyte Growth Medium
500 mL 254CF Medium (Cascade Biologics, Portland, OR, USA)
500 µL of CaCl2 (0.2 mM)
5 mL of Cascade Biologics Human Melanocyte Growth Supplement (HMGS)
5 mL of Penicillin/Spreptomycin (100 µg/mL)
Keratinocyte Growth Medium
500 mL 154CF Medium (Cascade Biologics, Portland, OR, USA)
250 µL $CaCl_2$ (0.1 mM)
5 mL of Cascade Biologics Human Keratinocyte Growth Supplement (HKGS)
5 mL of Penicillin/Spreptomycin (100 µg/mL)
Fibroblast Growth Medium
500 mL DMEM with 4500 mg/L glucose (Nova-Tech Inc., Grand Island, NY, USA)
50 mL FBS (10%)
5 mL of Penicillin/Spreptomycin (100 µg/mL)

3.1.2. Melanoma cell lines

Human melanoma cell lines with different genetic backgrounds were kindly provided by two collaborators: Herlyn's laboratory, The Wistar Institute, Philadelphia and Memorial Sloan-Kettering Cancer Center, New York, USA (Table 2). Melanoma cells were cultured in Dulbecco's modified Eagle's medium (DMEM, Life Technologies, Rockville, MD, USA) supplemented with 10% fetal bovine serum (FBS) (Nova-Tech Inc., Grand Island, NY, USA) and 100 μg/mL of Penicillin/Streptomycin and incubated at 37°C/5% of CO_2. When cells were confluent, they were passaged to new plates using 0.05% Trypsin/EDTA solution (Invitrogen, Carlsbad, CA, USA).

Table 2. Human melanoma cell lines used in this study:

Melanoma cell line	*BRAF*	*NRAS*	*PTEN*	*p53*
G-361	wt/mutant (V600E)	wt	deletion	wt
SK-Mel-5	mutant (V600E)	wt	wt	wt
SK-Mel-19	mutant (V600E)	wt	deletion	wt
SK-Mel-28	mutant (V600E)	wt	mutant	mutant
SK-Mel-29	mutant (V600E)	wt	wt	wt
SK-Mel-94	mutant (V600E)	wt	ND	wt
SK-Mel-103	wt	mutant (Q61R)	wt	wt
SK-Mel-147	wt	mutant (Q61R)	wt	wt
SK-Mel-173	wt	mutant (Q61K)	wt	wt
UACC-62	mutant (V600E)	wt	deletion	wt
UACC-257	wt	wt	ND	wt
WM-35	mutant (V600E)	wt	mutant	wt
WM-115	mutant (V600E)	wt	deletion	wt
WM-164	mutant (V600E)	wt	wt	mutant
WM-852	wt	mutant (Q61R)	deletion	ND
WM-902B	mutant (V600E)	wt	ND	ND
WM-1158	mutant (V600E)	wt	deletion	ND
WM-1366	wt	mutant (Q61L)	wt	ND
980513	ND	ND	ND	ND

ND: Not determined

3.1.3. Protein cell lysates, extraction and protein immunoblots

Adherent cells were collected by trypsinization (0.05% Trypsin solution) and total cell lysates were obtained by Laemmli extraction. Pellets with $2x10^6$ cells were resuspended in 70-80 μl of Laemmli Buffer (0.0625 M Tris-HCl pH 6.8, 2% SDS, 10% Glycerol and 5% β-

mercaptoethanol) and boiled for 5 minutes at 95ºC. Protein concentrations were determined using the BCA Protein Assay (Pierce, Rockford, IL). The calibration curves were prepared with bovine serum albumin (0, 2, 4, 6, 8 and 10 µg/mL) of Bio-Rad Mix (Bio-Rad, Hercules, CA, USA, ref. 500-0001) and the absorbance was read at 595 nm.

Protein immunoblots were performed according to standard protocols; protein extracts were subjected to electrophoresis on sodium dodecyl sulfate polyacrylamide (SDS-PAGE) gels using the acrylamide concentration adequate for the size of the detected proteins (10-15%). Following electrophoresis, the proteins were transferred onto Immobilon®-P Transfer membrane (Millipore, Bedford, MA, USA) using Mini Trans-Blot Cell equipment (Bio-Rad, Hercules, CA, USA). Transference was performed at 100V during 1 hour at 4ºC. Membranes were blocked with 5% Milk in PBS-T (phosphate-buffered saline with 0.1% Tween-20) during 1 hour with shaking. Primary antibodies were diluted in 5% Milk PBS-T or 5% BSA PBS-T and added to the membrane overnight at 4ºC (Table 3). Membranes were washed and incubated with secondary antibody diluted in 5% Milk PBS-T during 2 hours at RT (Table 4). Protein bands were detected by the ECL system (GE, Healthcare, Buckinghamshire, UK) and quantified using the Java-based image processing program *ImageJ*.

Table 3. Primary antibodies used for protein immunoblots/Western blot (WB) and immunofluoresence (IF):

Common Name	Antibody	Catalog #	Company	Type	Dilution
Actin	β-Actin (AC-15)	A 5441	Sigma-Aldrich	mouse	WB 1:10.000
Aurora A	Aurora A/AIK (1G4)	4718	Cell Signaling Tech.	rabbit	WB 1:250
Aurora B	Aurora B/AIM1	3094	Cell Signaling Tech.	rabbit	WB 1:250
B-Raf	Raf-B (F-7)	sc-5284	Santa Cruz Biotech.	mouse	WB 1:1000
CDK1	CDK1	sc-54	Santa Cruz Biotech.	mouse	WB 1:250
Cyclin A2	Cyclin A2 (H-432)	sc-751	Santa Cruz Biotech.	rabbit	WB 1:250
Cyclin B1	Cyclin B1 (H-433)	sc-752	Santa Cruz Biotech.	rabbit	WB 1:1000
EGFR	EGFR	2232	Cell Signaling	rabbit	WB 1:1000
HMGA2	HMGA2	ab41878	Abcam	rabbit	WB 1:200
p62	p62 lck	610832	BD Biosciences	mouse	WB 1:1000 IF: 1:100
Pan-Ras	Pan-Ras (Ab-3) Mouse	OP40	Calbiochem	mouse	WB 1:1000
Survivin	Survivin	AF886	RD Systems	rabbit	WB 1:200
Tubulin	α-Tubulin	T 9026	Sigma-Aldrich	mouse	WB 1:10.000
Ubiquitin	Mono-polyubiquitinylated	SPA-205	Assay Designs	mouse	WB 1:1000

Table 4. Secondary antibodies used for protein immunoblots/Western blot (WB) and immunofluoresence (IF):

Common Name	Antibody	Catalog #	Company	Type	Dilution
Anti-mouse IgG	ECL Anti-mouse IgG	NA931V	Amersham	sheep	WB 1:2500
Anti-rabbit IgG	ECL Anti-rabbit IgG	NA934V	Amersham	donkey	WB 1:2500
Anti-mouse IgG (H+L)	Alexa Fluo 488 Green	A11017	Invitrogen	goat	IF 1:250
Anti-rabbit IgG (H+L)	Alexa Fluor 555 Red	A31572	Invitrogen	donkey	IF 1:250

3.1.4. Immunofluorescence analyses in cells lines

Melanocytes and melanoma cells were cultured on cover slips and fixed in 4% paraformaldehyde during 15 minutes. Cells were turn permeable with PBS-0.2%Triton-X for 5 minutes and blocked with PBS-1% BSA. Primary antibodies were added for 1 hour at room temperature (Table 3, page 47). After that, the cover slips were rinsed and incubated with fluorescent secondary antibodies for 1 hour at room temperature (Table 4). Counterstaining of nuclei with 4,6-diamidino-2-phenylindole (DAPI) and mounting of the cover slips were done with Prolong Gold 5µg/mL (Invitrogen, Carlsbad, CA, USA) 20 minutes before imaging. Negative controls were obtained by omitting the primary antibody. Fluorescence emission was imaged using a Leica DMI6000 B fluorescence microscope (Leica Microsystems, Wetzlar, Germany).

3.1.5. Lentiviral-mediated gene transfer

Lentiviral supernatants were generated using HEK 293T cells transfected via standard protocols of calcium phosphate precipitation: 500µL of HBS solution (280 mM NaCl, 10 mM KCl, 1.5 mM $Na_2HPO_4.2H_2O$, 12 mM dextrose and 50 mM HEPES), 250 nM of $CaCl_2$, 4 µg of vector plasmid, and 4 µg of each of the lentiviral packaging constructs (pRSV-REV, pMDLg/pRRE and the VSV-G expression plasmid pHCMVG). Media was changed 8 hours after transfection and the viral supernatants were collected 24–36 hours later. Cells were infected with 1:2-1:4 dilutions of the viral supernatants and 4 µg/mL of Polybreen (Sigma-Aldrich, Inc St Louis, MO, USA). Infected cells were selected with 1 µg/mL of Puromycin (Sigma-Aldrich Inc, St Louis, MO, USA).

For genetic depletion of p62, melanoma cells were first infected with 5 different p62 short hairpin RNA (p62 shRNA) purchased from Sigma-Aldrich (Sigma-Aldrich, Inc St Louis, MO, USA). After establishment of the conditions, melanoma cells, melanocytes and fibroblasts were infected with p62 shRNA number 1 or p62 shRNA number 5 (Table 5). Parallel infections with pLKO vector coding for scrambled shRNA (control shRNA) served as negative control (Sigma-Aldrich, Inc St Louis, MO, USA).

Table 5. Target sequences of shRNA used for genetic depletion of Sequestosome 1/p62:

	Hairpin sequence
p62shRNA1	CCGGGCCCTCCATTTGTAAGAACAACTCGAGTTGTTCTTACAAATGGAGGGCTTTTT
p62shRNA5	CCGGCCTCTGGGCATTGAAGTTGATCTCGAGATCAACTTCAATGCCCAGAGGTTTTT

Senescent melanocytes were generated infecting cells with FG12 vector expressing the oncogenic $BRAF^{V600E}$, $NRAS^{Q61R}$or $HRAS^{G12V}$mutants. Parallel infections with FG12 vector were used as negative control.

For p62 overexpression, melanoma cells and melanocytes were stably transfected with pLV-Cherry-p62 lentiviral vectors. Parallel infections with pLV-Cherry plasmid were used as negative control.

To monitor autophagy, melanoma cells were infected with pLV-puro-EGFP-LC3 and pLV-Cherry-p62 lentiviral vectors.

Fluorescence emission was imaged using a Leica DMI6000 B fluorescence microscope (Leica Microsystems, Wetzlar, Germany).

3.1.6. Cell proliferation, viability and colony formation assays

Total cell numbers infected with control shRNA and p62 shRNA vectors were estimated by manual counting at different time points.

For proliferation assay, 5.0 $x10^3$ UACC-62 cells were infected with control shRNA and p62 shRNA vectors. After 6 days of infection, cells were plated in 96-well optical bottom plates and, at the indicated time intervals cells were fixed with 4% paraformaldehyde and stained with DAPI. For each time point, the total number of cells was quantified by automated high-throughput confocal detection of DAPI-stained nuclei (Invitrogen; Carlsbad, CA, USA) using the OPERA HCS platform and the *Acapella* Analysis *Software* (Perkin Elmer).

For colony formation assays, $1.0x10^4$ UACC-62 cells infected with control shRNA and p62 shRNA vectors were seeded onto 6-well plates and were allowed to grow for 20 days. The colonies were then stained with crystal violet (0.4g/L), purchased from Sigma-Aldrich (Sigma-Aldrich, Inc St Louis, MO, USA).

3.1.7. Real-time reverse transcription polymerase chain reaction

Melanocytes infected with mutants $BRAF^{V600E}$, $NRAS^{Q61R}$, $HRAS^{G12V}$ and control FG12 were harvested at day 4 and day 6 post-infection and total RNA was extracted and purified using RNeasy Mini-Kit (QIAGEN, Valencia, CA, USA) following the manufacturer's instructions. The concentration of extracted RNA was determined by a NanoDrop Spectrophotometer ND-100 (NanoDrop Biotechnologies).

First-strand cDNA was synthesized from total RNA using the High Capacity cDNA Reverse Transcription kit (Applied Biosystems, Foster City, CA). 2µg of total RNA in 10 µl of Nuclease- free water were mixed with 10µl of RT Master Mix (2µl of 10x RT buffer and 10x Random Primers, 0.8 µl 25x dNTPs, 1 µl of 50U/µl MultiScribe RT, 3.2 µl of Nuclease-free water and 1 µl of RNAse inhibitor). The samples were processed in a thermocycler with the following program: 25 ºC for 10 min, 37 ºC for 120 min, 85 ºC for 5 min and 4 ºC O/N.

Real-time reverse transcription polymerase chain reaction (RT-qPCR) was done mixing 50 ng of total cDNA, 2X Power SYBR® Green PCR Master Mix (Applied Biosystems, Foster City, CA) and 10 uM of forward and reverse primers of p62 or 18S (Table 6). Triplicate samples of each condition were processed in 7500 fast Real-Time PCR System (Applied Biosystems, Foster City, CA) following the program: 50 ºC for 2 min, 95 ºC for 10 min and 30 cycles of 95 ºC for 15 sec and 60 ºC 1 min.

Table 6. Primers used for p62 and 18S amplification:

mRNA	Forward 5'- 3'	Reverse 5'- 3'
p62	CGCAGTCTCTGGCGGAGCAG	TGGCATCTGTAGGGACTGGAGTTCAC
18S	TTGGAGGGCAAGTCTGGTG	CCGCTCCCAAGATCCAACTA

3.1.8. Senescence-associated acidic β-galactosidase activity

Melanocytes, fibroblasts and melanoma cells infected with control shRNA and p62 shRNA on day 7 post-infection were washed twice with phosphate-buffered saline (PBS; pH

7.2), fixed with 0.5% glutaraldehyde in PBS and washed in PBS supplemented with 1 mM MgCl2. Cells were stained at 37°C in X-Gal solution (1 mg ml–1 X-Gal, 0.12 mM K3Fe[CN]6, 0.12 mM K4Fe[CN]6, 1 mM MgCl2 in PBS at pH 6.0). The staining was performed for 4–6 h to minimize the background signal.

3.1.9. Melanoma cells treatment

Melanoma cells were treated with 20 nM of Chloroquine, an autophagy inhibitor that blocks lysosome–autophagosome fusion (Solomon et al., 2009), during 7 hours.

Melanoma cells were treated with 25 nM of Rapamycin, an autophagy stimulator by the inhibition of mTOR pathway (Raught et al., 2001), during 7 hours.

3.1.10. Matrigel invasion assay

The invasive capacity of SK-Mel-103 melanoma cells was determined via matrigel transwell invasion assays according to manufacturer´s guidelines using boyden chambers (0.8µm BD BioCoat™ Matrigel™ Invasion Chambers; from BD Biosciences, San Jose, CA, USA). This method consists of a pore membrane with a thin layer of Matrigel substance, composed by a protein mixture extracted from the Engelbreth-Holm-Swarm mouse sarcoma, which include laminin, collagen IV, heparan sulfate proteoglycans, entactin/nidogen and different growth factors.

Melanoma cells infected with control shRNA and p62 shRNA were serum-starved overnight. 1 x 10^5 cells were harvested and seeded in serum-free DMEM onto the upper chamber. DMEM containing 10% FBS was placed in the lower chamber. After incubation during 20 hours, invading and non-invading cells were first fixed with 4% paraformaldehyde and then stained with DAPI. Single cells were visualized by confocal detection of DAPI-stained nuclei through the 20x objective of a TCS-SP5-WLL (AOBS-UV) spectral microscope (Leica Mycrosystems, Wetzlar, Germany) at Confocal Unit, CNIO. The transwell membrane was also visualized by laser reflection. LAS AF Matrix screening Software was used for an automated high-throughput acquisition across the total width of the matrigel membrane in 9 different fields per experimental condition. IMARIS 6.3 Software was used to quantify the percentage of invading cells (normalized to the total cell per field).

3.1.11. Three-dimensional human skin reconstruct model

The three-dimensional human skin reconstruct model (3D-SR) was developed during a 3 months stay as Visiting Scientist in the Melanoma laboratory of Dr. Meenhard Herlyn, at The Wistar Institute, Philadelphia, USA (Figure 3).

The 3D-SR consists of an artificial dermis with fibroblasts cells embedded in a collagen I matrix, an artificial epidermis, which is comprised of stratified and differentiated keratinocytes and a functional basement membrane. Skin reconstructs are a handful tool for the study of melanoma progression. It recapitulates the environment of melanoma cells and allows the study of cell-matrix, cell-cell interactions and melanoma invasion capacity in a more physiological system than 2D cultures (Li et al., 2011; Brohem et al., 2011). Due to the innovation and complexity of the 3D-SR protocol (Li et al., 2011), it will be described in detail.

Preparation of the dermis:

First, an acellular layer was prepared mixing the following reagents in a 50 mL tube on ice: 0.59 mL 10X EMEM, 50 µl 200mM L-glutamine, 0.6 mL FBS, 120 µl 7.5% sodium bicarbonate and 4.6 mL bovine collagen I. 1 mL of the mixture was added into each insert of tissue culture trays (Organogenesis, Canton, MA) and incubate for 30 min at room temperature for solidification. After that, a cellular layer ("dermis") was prepared mixing the following reagents in a 50 mL tube on ice: 1.65 mL 10X EMEM, 150 µl 200 mM L-glutamine, 1.85 mL FBS, 350 µl 7.5% Sodium bicarbonate, 14 mL bovine collagen I. Human fibroblasts were trypsinized from culture flasks with 0.25% trypsin/EDTA. 0.45 x 10^6 fibroblasts were resuspended in 1.5 mL DMEM with 10% FBS and added to the mix. 3 mL of the mixture were added to each acellular layer-coated insert.

The "dermis" was incubated for 45 min at 37 °C in a 5 % CO_2 tissue culture incubator. After that, DMEM containing 10% FBS was added to the inserts (2 mL inside and 10 mL outside of insert in each well of skin reconstruct trays) and it was incubated during 4 days for "dermis" contraction.

After 4 days, DMEM medium was aspirated from both inside and outside of each insert and washing medium (HBSS with 1% dialyzed FBS) was added in order to remove the regular serum. The "dermis" was incubated for 1 hour at 37 °C.

Preparation of the epidermis:

Human keratinocytes were trypsinized from culture flasks with 0.05% trypsin/EDTA. Trypsin was neutralized with soy bean trypsin inhibitor (250 mg/L in 1x phosphate buffered saline) and 4.17 x 10^6 cells/mL were resuspended in skin reconstruct Medium I (Table 7).

The non-invasive melanoma cell line WM-3211 was selected for the skin reconstruct invasion experiment. WM-3211 cells were infected with pLV-Cherry-p62 for p62 overexpression and pLV-Cherry as control. After infection, melanoma cells were trypsinized from culture flasks with 0.05% trypsin/EDTA. Trypsin was neutralized with soy bean trypsin inhibitor (250 mg/L in 1x phosphate buffered saline) and 0.83 x 10^6 cells/mL were resuspended in skin reconstruct Medium I.

Washing medium was removed from both inside and outside of each insert. Reconstruct Medium I was added (1.5 mL to the inside and 10 mL to the outside of each insert). Next, 600µl cell suspension of keratinocytes and 600 µl cell suspension of melanoma cells were mixed. 200 µl of the mixed cell suspension were dropped to the inside of each insert. The 3D-SR was incubated for 2 days at 37 °C.

After 2 days, the Skin Reconstruct Medium I was aspirated from both the inside and the outside of each insert. Skin reconstruct Medium II (Table 7) was added to the inserts (2 mL to the inside and 10 mL to the outside). The 3D-SR was incubated for another 2 days at 37 °C.

After 2 days, the Skin Reconstruct Medium II was aspirated from the inside and the outside of each insert and 7.5 mL Skin Reconstruct Medium III (Table 7) were added only the outside part of the insert. From this point, the surface of reconstructs was exposed to the air, favoring the differentiation of the keratinocytes. Medium III was changed every other day until day 18 (Figure 3).

At day 18, the 3D-SR was harvested and fixed in 4% formalin for 4 hours and stored in 70% ethanol at 4°C. The artificial skins were embedded in paraffin and cut for Hematoxylin and eosin (H&E) staining. 3D-SRs were also submitted to immunohistochemistry (IHC) analysis for p62 (antibody clone 3/P62 LCK LIGAND, BD Biosystem) and mCherry (antibody DsRED Goat Polyclonal, Santa Cruz Biotechnology, sc-33354) detection.

Table 7. Mediums used for three-dimensional human skin reconstruct:

	Medium I (100mL)	Medium II (100mL)	Medium III (300mL)
DMEM	72.5 mL	72.5 mL	142.5 mL
F12 (HAM's)	24 mL	24 mL	142.5 mL
L-glutamine (200 mM)	2 mL	2 mL	6 mL
Hydrocortisone (269 g/mL)	200 µl	200 µl	600 µl
ITES (500X)	200 µl	200 µl	600 µl
O-phosphorylethanolamine (0.05 M)	200 µl	200 µl	600 µl
Adenine (90 mM)	200 µl	200 µl	600 µl
Progesterone (2 nM)	200 µl	200 µl	600 µl
CaCl2 (1 M)	240 µl	240 µl	720 µl
Triiodothyronine (10 nM)	200 µl	200 µl	600 µl
Chelexed newborn calf serum	100 µl	0	0
Newborn calf serum	0	100 µl	6 mL

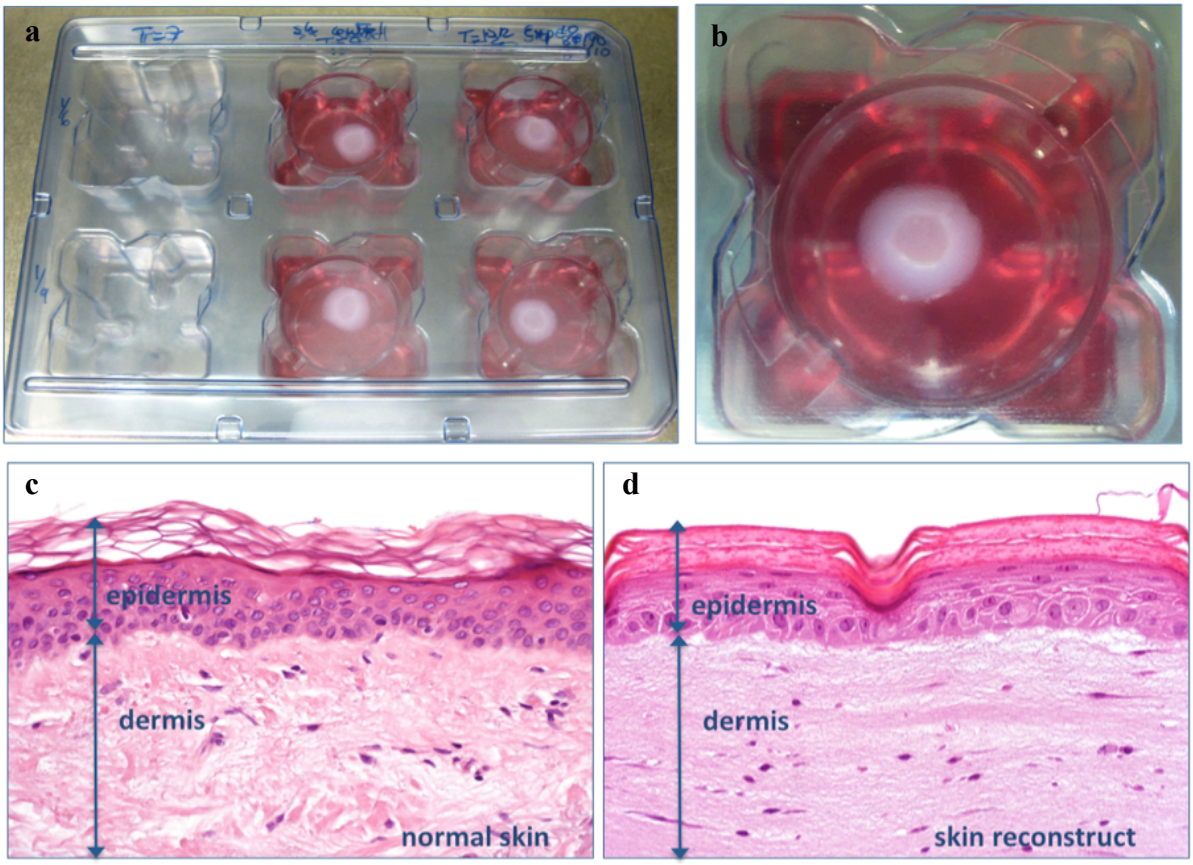

Figure 3. Three-dimensional human skin reconstruct model. (a, b) The gross appearance of the skin reconstructs. (c) H&E staining of normal human skin. (d) H&E staining of three-dimensional human skin reconstruct. The epidermis comprises oriented basal layer and differentiated stratified cell layers. The dermis contains fibroblasts embedded in a collagen type I matrix.

3.1.12. Array comparative genomic hybridization

Array comparative genomic hybridization was performed at the Cytogenetic Unit, CNIO. Genomic DNA from melanoma cell lines SK-Mel-28, SK-Mel-103, SK-Mel-173 and UACC-62 were extracted using DNeasy Blood & Tissue kit (QIAGEN, Valencia, CA, USA) and processed for analysis in Human Genome CGH 4x44k microarrays (Agilent Technologies, Palo Alto, CA, USA), as previously described (Barrett et al., 2004). Human Genomic female DNA (Promega) was used as the reference DNA for all hybridizations. Slides were scanned using an Agilent 2565AA DNA Microarray Scanner (Agilent Technologies) and the data were analyzed with Agilent Feature Extraction and CGH Analytic software 3.5.14.

3.1.13. Microarray hybridization and gene expression analysis

Melanoma cells (SK-Mel-103 and UACC-62) infected with control shRNA and p62 shRNA were harvested at day 3 and day 6 post-infection and total RNA was extracted with Trizol, precipitated with isopropanol and purified using RNeasy Mini-Kit (Qiagen, Valencia, CA) following the manufacturer's instructions. RNA quality was assessed in a 1% agarose-gel. Samples were hybridized onto 4 x 44K microarray slides (Whole Human Genome, Agilent Technologies, Inc., Santa Clara, CA), Universal Human Reference RNA (Stratagene, La Jolla, CA) and RNA from each sample were reverse-transcribed using a Low RNA Input Fluorescent Linear Amplification kit (Agilent Technologies, Inc.) for 2 h at 40 ºC. Equal amounts of Cy3- and Cy5-labeled amplified RNA were hybridized for 17 h at 65 ºC and 10 rpm. The slides were scanned using a G2565BA Microarray Scanner System (Agilent Technologies, Inc.). All experiments were done in triplicate. Data were obtained from scanned images using Feature Extraction v9.0 software (Agilent Technologies, Inc.) (Martín-Sánchez et al., 2011) (Figure 4).

In collaboration with Bioinformatics Unit of CNIO, data were normalized and preprocessed using the Gene Expression Pattern Analysis Suite (GEPAS v3.1, http://gepas3.bioinfo.cipf.es). Genes differentially expressed under each condition were identified using a method based on the Limma t-test (http://pomelo2.bioinfo.cnio.es). A false discovery rate (FDR) of < 0.25 was considered significant. These genes were hierarchically

clustered using Cluster/Treeview (http://rana.lbl.gov/EisenSoftware.htm). Functional analysis was carried out using Gene Set Enrichment Analysis (GSEA v2.0, http://www.broad.mit.edu/gsea) (Subramanian, *et al* 2005). A list of genes identified by the t-test was used in a preranked GSEA analysis to obtain pathways enriched in each class. Reactome (http://www.reactome.org/), Biocarta (http://www.biocarta.com/), KEGG (http://www.genome.ad.jp/kegg/) and GenMAPP were used to generate the gene set database.

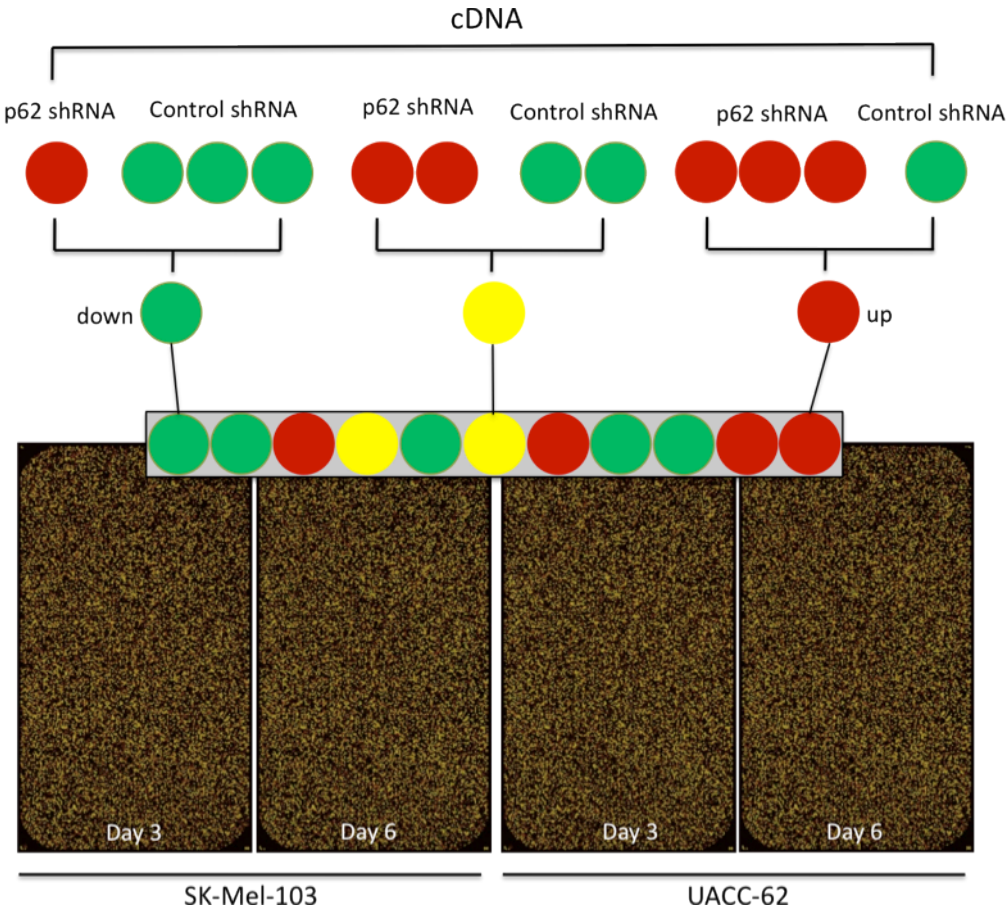

Figure 4. Experimental design for microarray sample labeling and hybridization. Indicated melanoma cells were collected 3 and 6 days after lentiviral infection with control and p62 shRNA. cDNA from control and p62 depleted cells were synthesized and labeled with Cy3 (green) or Cy5 (red), respectively. cDNA from control and p62 depleted cells were mixed and hybridized in microarrays slides. The slides correspond to different cell lines and time points. Green circles represent genes that are downregulated and red circles represent genes that are upregulated after p62 depletion.

SQSTM1 gene expression data from cDNA microarray hybridization of normal melanocytes and melanoma cell lines was performed and provided by Dr. Herlyn's laboratory, The Wistar Institute, Philadelphia, USA.

3.2. Animal models

3.2.1. Mouse xenograft model

UACC-62 melanoma cells infected with control shRNA and p62shRNA were harvested 72 hours after infection and subcutaneously injected ($2.0x10^6$ cells in 0.1 mL of PBS) into the flanks of 5 nude mice. SK-Mel-103 melanoma cells infected with control shRNA and p62shRNA were harvested 72 hours after infection and subcutaneously injected ($1.0x10^6$ cells in 0.1 mL of PBS plus 0.05 mL of Matrigel) bilaterally into the back region of 4 nude mice. Tumours growth was measured blinded to the experimental conditions. Every two days the two orthogonal external diameters was determinate using a calliper. Tumour volume was calculated by using the standard formula: $a \times b^2 \times 0.52$; where 'a' is the longest diameter and 'b' is the shortest diameter. When tumours reached a size of 1.5 cm^3 mice were sacrificed, tumours were surgically excised and processed for histopathological study.

H&E staining and p62 immunohistochemistry were performed in melanoma xenograft samples. Cell perimeters were quantified using an automated scanning microscope and computerized image analysis system (Ariol SL-50; Genetix) at the Immunhistochemistry Unit of CNIO.

All experiments with mice were performed at CNIO in accordance with protocols revised and approved by the Institutional Ethics Committee of the center.

3.2.2. Melanoma mouse model

Conditional melanocyte-specific $Braf^{V600E}$ and $Braf^{V600E}/Pten^{loxP/loxP}$ mouse models were generated as previously described (Dankort et al., 2009). Adult mice were treated with intraperitoneal injection of 4 mg of tamoxifen per 30 g of mouse 3 consecutive days for tumor induction. When tumors reached a diameter of 1cm they were surgically excised and processed for histopathological study. Conditional melanocyte-specific $Braf^{V600E}$ mice were able to develop benign melanocytic proliferation, meanwhile conditional melanocyte-specific $Braf^{V600E}/Pten^{loxP/loxP}$ mice developed malignant tumors with metastatic capacity. Melanocytic lesions were confirmed by histological analysis and by Trp2 immunohistochemical staining performed at Comparative Pathology Unit, CNIO. Trp2 (D-18, Santa Cruz Biotechnology) and p62 (clone 3/P62 LCK LIGAND, BD Biosystem) immunohistochemical staining were

performed with Alkaline phosphatase (in pink) due to the elevated amount of melanin presented by such tumours.

3.3. Analyses in human specimens

3.3.1. Tissue samples

A total of 213 paraffin embedded tissue samples including common melanocytic dermal nevi (n=47), dysplastic nevi (n=29), primary radial growth phase melanoma (n =16), primary vertical growth phase melanoma (n=26), skin (n=38), lymph node (n=35) and visceral (n=22) melanoma metastases were randomly selected from the files of Hospital Universitario 12 de Octubre for the construction of Tissue microarrays (TMA).

For survival analysis, 79 additional paraffin embedded cases of VGP melanomas randomly selected from the files of Hospital Universitario 12 de Octubre were analyzed on whole tissue-sections.

For RNA extraction and real time PCR, 10 frozen melanoma specimens, including 2 vertical growth phase, 4 skin metastatic melanomas and 4 lymph node metastatic melanomas were obtained from the Biobank of Hospital Universitario 12 de Octubre, Madrid.

H&E slides were available for review in all cases. The Breslow's index, the presence of ulceration and histological progression growth phase were defined according to standard criteria (Breslow A, 1970; Clark et al., 1989).

All patients included in this study were treated in the Dermatology Department of the Hospital Universitario 12 de Octubre according to standard National Comprehensive Cancer Network (NCCN) criteria and this study was performed following the Spanish biomedical law 14/2007.

3.3.2. Generation of tissue microarrays

For characterization of p62 and Ki67 expression, eight different tissue arrays (2 melanocytic dermal nevi, 1 dysplastic nevi, 1 RGP melanoma, 1 VGP melanoma, 1 skin metastatic melanoma, 1 lymph node metastatic melanoma and 1 visceral metastatic melanoma) containing the distinctive histological stages of melanocytic tumors were constructed.

Tissue microarray method was used because it allows the simultaneous analysis of multiple individual tissue samples on a single slide. Using this technology, the experimental conditions are more homogeneous and there is a minimal destruction of the original tissue. Indeed, the possibility of bias due to non-representative tissue sections is overcomed by the presence of duplicated samples and the elevated amount of tumors analyzed (Kononen et al., 1998; Kallioniemi et al., 2001).

TMAs were assembled as previously described (Kononen et al., 1998; Kallioniemi et al., 2001; Alonso et al., 2004). Two 1.5-mm-diameter cylinders of tissue were taken from representative areas of each paraffin block and arrayed into a new recipient paraffin block with a custom-built precision instrument (Beecher Instruments, Silver Spring, MD). Areas chosen for the cylinder core had high tumor cellularity. To evaluate the most adequate part of each primary tumor, the invasive border of the tumor in large lesions and all tumor cells in smaller samples were selected. In addition, normal tissues (skin, tonsil, and reactive lymphoid tissue) were placed adjacent to tumoral cylinders to serve as internal controls and to ensure the quality of staining slides. Initial sections were stained for hematoxylin and eosin to verify the quality of the TMAs (Figure 5).

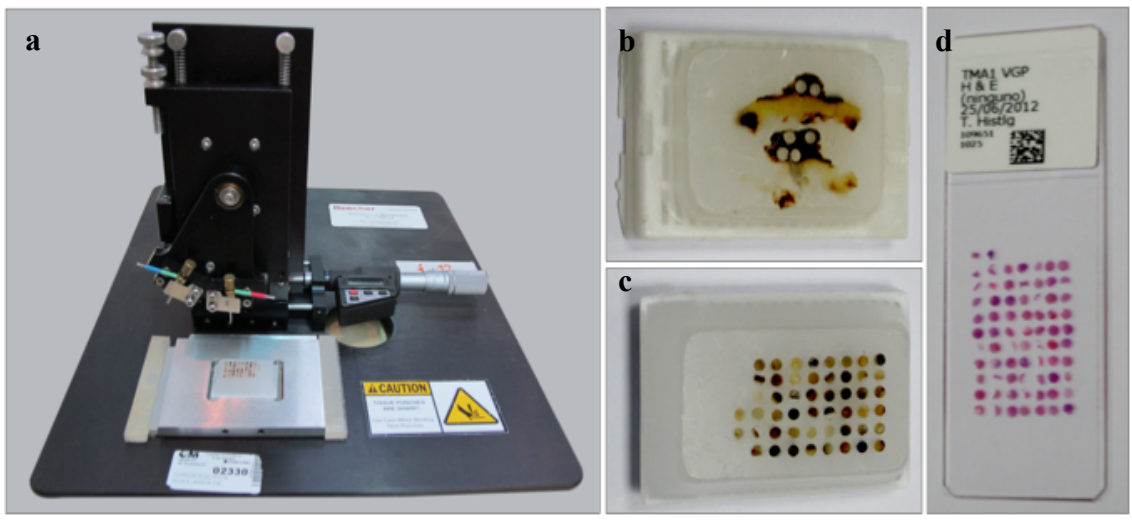

Figure 5. Generation of tissue microarrays of melanocytic lesions. (a) Tissue arrayer instrument used for array construction (b) Donor paraffin block with melanocytic lesion. (c) TMA paraffin block. (d) The gross appearance of TMA slide stained with H&E.

3.3.3. Immunohistochemistry

Three-micrometer tissue sections from the TMAs or paraffin blocks were sectioned and applied to special immunohistochemistry coated slides (DAKO, Glostrup, Denmark).

P62 immunohistochemical staining was performed using Bond™ Automated System (Leica Microsystems) at the Immunohistochemistry Unit of Hospital Universitario 12 de Octubre. After incubation with primary antibodies, immunodetection was performed with Bond™ Polymer Refine Detection (Leica Microsystems), according to the manufacturer's instructions. All sections were counterstained with hematoxylin. Sequestosome1/p62 antibody (clone 3/P62 LCK LIGAND, BD Biosystem), was diluted 1:100 and used with sodium citrate buffer (pH 6.5). Substantia nigra specimen from a patient with Parkinson disease was used as positive control (Layfield et al., 2008).

Ki 67 (clone MIB-1, Ready-to-use, DAKO) immunohistochemical staining was performed at Immunohistochemistry Unit, CNIO, using Dako Autostainer protocol and sodium citrate buffer (pH 6.5). Reactive lymphoid tissue was used as positive control.

P62 staining was blinded evaluated by Drs. José Luis Rodriguez Peralto and Erica Riveiro. Staining was considered positive for p62 taking into account both the percentage of positive cells and the intensity of its expression. The score system used was: 0 (no expression), 1 (week expression or less than 50% of the tumor presenting high intensity) or 2 (more than 50% of the tumor presenting high intensity). Ki67 percentage of expression was determined using an automated scanning microscope and computerized image analysis system (Ariol SL-50; Genetix) at the Immunhistochemistry Unit of CNIO.

3.3.4. Immunofluorescence analysis in tissues

For immunofluorescence analyses of human specimens, tissue sections were deparaffinized in xylene for 20 minutes, rehydrated through a graded ethanol series and washed with phosphate-buffered saline. Antigen retrieval was achieved by a 10-minutes heat treatment in a pressure cooker, containing 1 liter of 10 mmol/L sodium citrate buffer (pH 6.5). Tissue sections were incubated overnight with anti-S100 antibodies (dilution 1:400, DAKO, Z0311) or anti-p62 antibody (dilution 1:150, BD Biosciences, p62 lck) at 4°C in a humidified chamber. After that, the slides were rinsed with PBS and incubated with fluorescent secondary antibodies for 1 hour at room temperature. Secondary antibodies used were anti-

rabbit Alexa Fluor 555 (red) or anti-mouse Alexa Fluor 488 (green) (Invitrogen, Carlsbad, CA, USA). Counterstaining of nuclei and mounting of slides were done with Prolong Gold 5µg/mL (Invitrogen, Carlsbad, CA, USA) 20 minutes before imaging. Negative controls were obtained by omitting the primary antibody. Fluorescence emission was imaged using a Leica DMI6000 B fluorescence microscope (Leica Microsystems, Wetzlar, Germany).

3.3.5. RNA extraction from frozen melanoma specimens

Frozen melanoma biopsies were cut with a cryostat to get 10-20 slides with 10 µm. 1 ml of Trizol was added to the samples, homogenized with 23 G needles and incubated 5 min at room temperature. After that, 200 uL of chloroform was added, homogenized by vortexing and incubated at room temperature for 15 min. The tubes were centrifuged at 12000 rpm during 15 min at 4°C. Following centrifugation, the aqueous phases were transferred to clean tubes where 600 uL of 70% ethanol at -20 ° C were added to each sample. The product of the mixture was transferred to the columns of the kit RNeasy Mini Kit (QIAGEN, Valencia, CA, USA) and followed the manufacturer's instructions. The concentration of extracted RNA was determined by a NanoDrop Spectrophotometer ND-100 (NanoDrop Biotechnologies) and analyzed by 1% TAE agarose gel with DNA SYBERsafe Stain (Invitrogen, Carlsbad, CA, USA). First-strand cDNA and RT-qPCR were done as previously described.

3.4. Statistical and survival analyses

Differential expression of p62 among melanocytic tumors was analyzed by Chi-square test (Figure 7b, page 67). P62 mRNA and protein expression between melanocytes and melanoma cell lines was compared using Mann-Whitney *U* test (Figures 8 and 9b, pages 68-69). Differential expression of p62 mRNA among frozen melanoma speciemens was analyzed by one-way analysis of variance (Figure 13b, page 73). Statistical significance of SA-β-Gal activity in melanocytes, fibroblasts and melanoma cells depleted for p62 was analyzed by Student´s t test (Figure 20c, page 82). Difference on invasion capacity of melanoma cells after genetic depletion of p62 was analyzed by Student´s t test (Figure 21, page 83). Statistical differences between tumor volumes in xenograft mice model were analyzed by two-way analysis of variance (Figure 26a, page 90). The perimeters of melanoma cells in xenograft tumors were compared by Student´s t test (Figure 26c, page 90). Differences on Ki67

percentages across p62 expression categories were obtained by one-way analysis of variance (overall) and Student´s t test (negative versus low versus high) (Figure 27b, page 91).

For survival analysis, clinical data and immunohistochemical scoring were performed blind. P62 IHC staining was quantified by two independent investigators as negative (absence of expression) or positive (including low and high intensity of p62 expression). Clinical data were compiled only after all analyses were completed.

The distribution of 105 patients according to p62 expression was analyzed by Chi-square test (sex, ulceration and clinical staging) and Student´s t test (age and Breslow).

Five years of follow-up survival data were available in 104 patients with vertical growth phase melanoma. Disease Free Survival (DFS) and Overall Survival (OS) curves were estimated with Kaplan-Meier product-limit method and survival curves were compared using logrank test. The hazard ratio was calculated using Cox regression and adjusted with univariate and multivariate models adjusting by Breslow, Clinical Stage and T3 category. Distribution of patients into two T3 categories (T≤ T3a stage or T>T3a stage) was performed to include both thickness and ulceration status in multivariate analyses. These two subgroups were chosen because they present significant differences in survival rates (Balch et al., 2009).

- Disease Free Survival was defined as the time interval between diagnosis (made by histopathological study of primary melanoma) and the development of the first metastasis. It was considered censored for patients who did not present metastasis at last follow-up.

- Overall survival was defined as the time interval between diagnosis (made by histopathological study of primary melanoma) and death due to melanoma. It was considered censored for patients who were alive at last follow-up or who died from other causes.

Probability values (*P*) equal or less than 0.05 were considered statistically significant (*$P<0.05$, ** $P<0.01$, *** $P<0.001$, *** $P<0.0001$).

4. RESULTS

4. RESULTS

4.1. The expression of Sequestosome 1/p62 in melanocytic tumors

4.1.1. Benign and malignant melanocytic tumors express differential levels of p62 protein

The overexpression of p62 has been described in different types of human cancers (Thompson et al., 2003; Kitamura et al., 2006; Duran et al., 2008). However, no data about its expression in melanoma tumors are available in the literature.

First, to address whether p62 could have a role in melanoma, direct immunofluorescence for p62 was performed in 3 human benign intradermal nevi and 3 skin metastatic melanoma specimens. Representative pictures of co-staining with S100, a melanocytic marker, and p62 are shown in Figure 6. Interestingly, a strong expression of p62 was observed in metastatic melanoma samples while no expression was detected in benign nevi. S100 was clearly positive in both lesions, however.

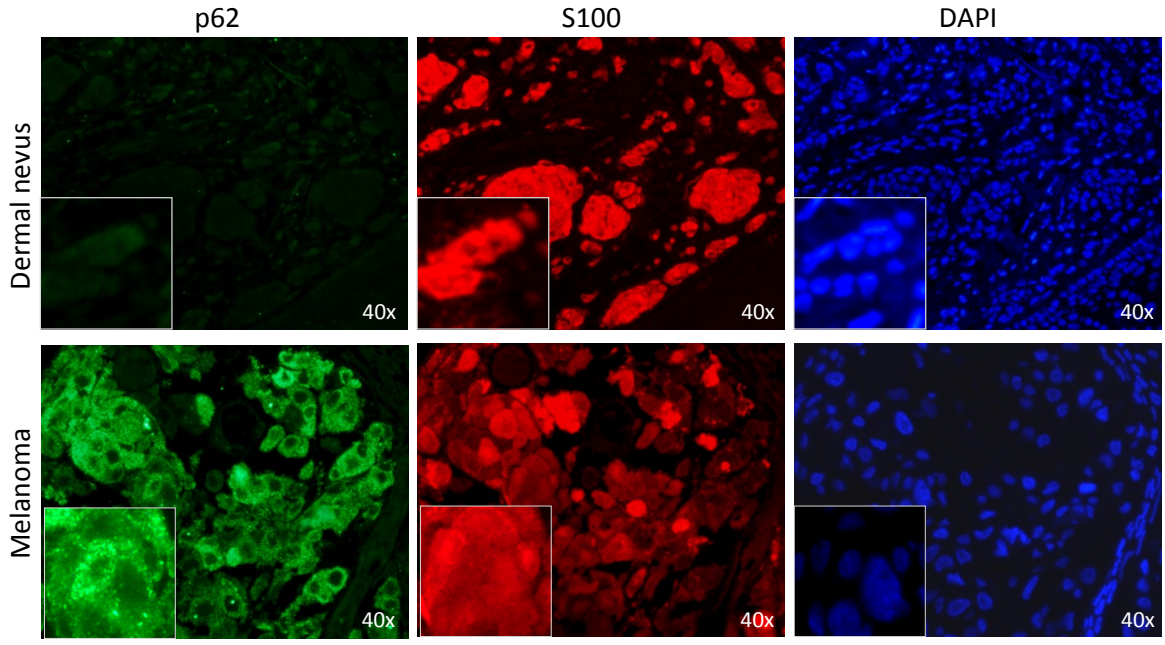

Figure 6. Differential expression of p62 protein in nevi and melanoma cells. Melanomas but not dermal nevi display enhanced p62 expression, as shown by immunofluorescence staining of human specimens (p62 in green, S100 in red and nuclei stained with DAPI in blue signal).

Next, to characterize p62 expression in melanoma progression, 8 tissue microarrays containing different stages of melanocytic tumors (common melanocytic dermal nevi (n=47), dysplastic nevi (n=29), primary radial growth phase melanoma (n =16), primary vertical growth phase melanoma (n=26), skin melanoma metastases (n=38), lymph node melanoma metastases (n=35) and visceral melanoma metastases (n=22)) were immunohistochemically analyzed for p62 by two independent investigators.

As shown in Table 8 and Figures 7a and 7b, all 47 common dermal nevi analyzed were negative for p62 staining. In 9 out of 29 dysplastic nevi (31%), a low expression of p62 was observed. Interestingly, an increase in frequency and intensity of p62 expression was observed in malignant melanocytic lesions ($P<0.0001$). The study of 16 radial growth phase melanomas, showed low expression of p62 in 10 specimens (62.5%) and high expression of p62 in 1 case out of 16 (6.25%). Moreover, the expression of p62 was increased with melanoma progression. The analysis of 26 vertical growth phase melanomas, an invasive form with metastatic capacity (Barnhill et al., 1993), showed low expression of p62 in 16 samples (61.54%) and high expression of p62 in 6 cases (23.08%). Skin metastatic and lymph node metastatic samples presented similar percentage of p62 expression. In skin metastases, 36.85% cases presented low expression (14/38) and 26.3% high expression of p62 (10/38). In lymph node metastases, 34.3% cases presented low expression (12/35) and 28.6% high expression of p62 (10/35). Metastatic melanomas to different organs (visceral metastasis) presented an increased expression of p62, with 36.4% with low expression (8/22) and 45.4% of the cases showing high expression of p62 (10/22).

Table 8. P62 protein expression in benign and malignant melanocytic tumors:

	p62 Negative		p62 Positive low		p62 Positive high	
Melanocytic Tumors	**N/total**	**%**	**N/total**	**%**	**N/total**	**%**
Dermal Nevi	47/47	100	0/47	0	0/47	0
Dysplastic Nevi	20/29	69	9/29	31	0/29	0
RGP Melanomas	5/16	31.25	10/16	62.5	1/16	6.25
VGP Melanomas	4/26	15.38	16/26	61.54	6/26	23.08
Skin Metastases	14/38	36.85	14/38	36.85	10/38	26.3
Node Metastases	13/35	37.1	12/35	34.3	10/35	28.6
Visceral Metastases	4/22	18.2	8/22	36.4	10/22	45.4

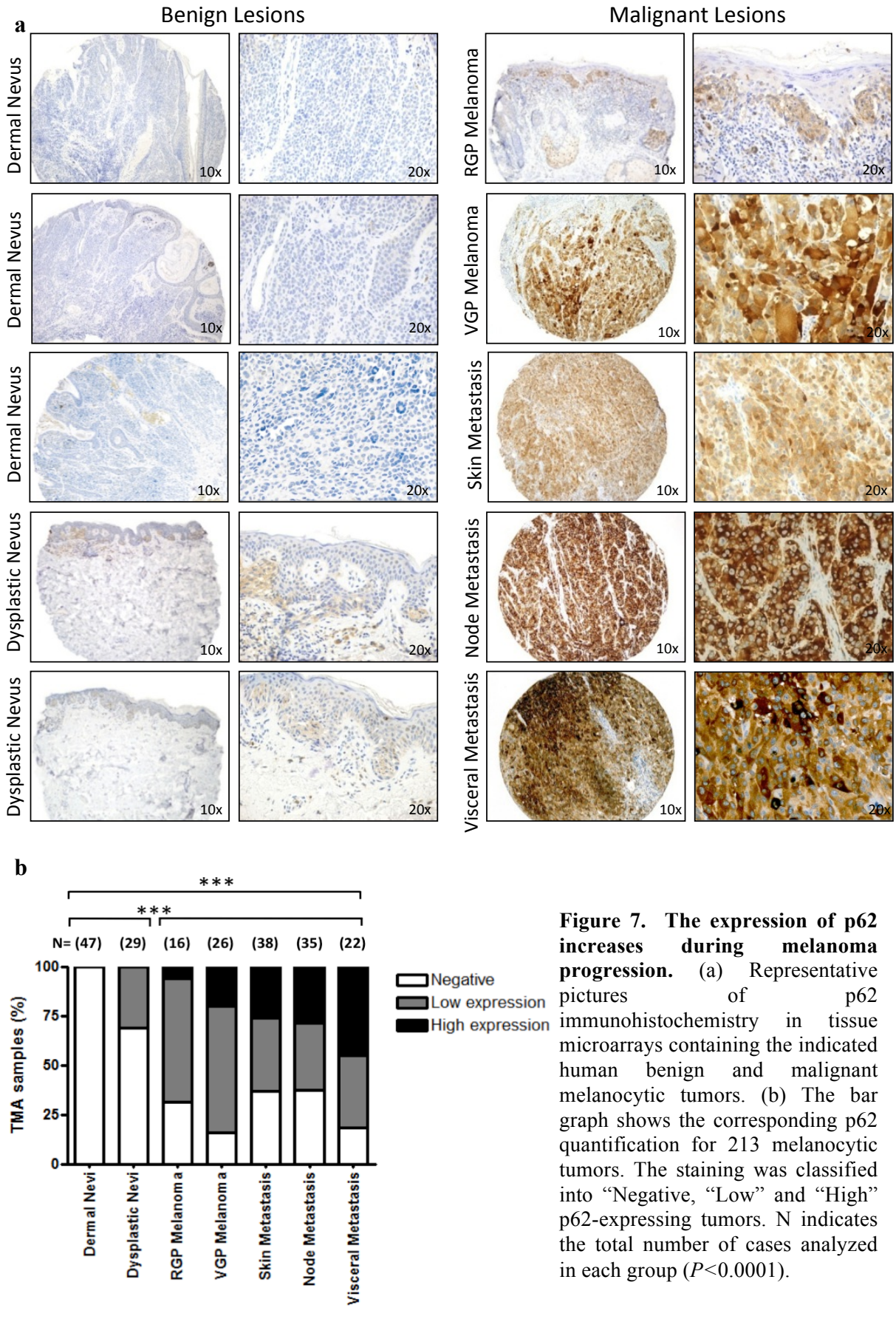

Figure 7. The expression of p62 increases during melanoma progression. (a) Representative pictures of p62 immunohistochemistry in tissue microarrays containing the indicated human benign and malignant melanocytic tumors. (b) The bar graph shows the corresponding p62 quantification for 213 melanocytic tumors. The staining was classified into "Negative, "Low" and "High" p62-expressing tumors. N indicates the total number of cases analyzed in each group (P<0.0001).

In summary, p62 protein expression was completely negative in common dermal nevi. Dysplastic nevi were positive for p62, however less frequently than malignant lesions. Additionally, an increased expression of p62 was observed in late stages of melanoma progression. Early phase of melanoma progression (radial growth phase) presented less expression of p62 comparing to invasive (vertical growth phase melanoma) and advanced stages of malignant melanoma (metastatic disease). Altogether, the immunohistochemical analysis of melanocytic tumors indicates that the expression of p62 is related to melanoma progression (P<0.0001).

4.1.2. Normal melanocytes and melanoma cell lines present differential levels and cellular distribution of p62 protein

To confirm the expression of p62 in melanoma cells and to establish an *in vitro* model for additional studies of p62 function, thirty-four melanoma cell lines and 4 normal melanocytes were cultured and collected for the detection of p62 RNA levels. Total mRNA was extracted and submitted to microarray hybridization and gene expression analysis. As shown in Figure 8, melanoma cell lines presented a statistically significant overexpression of p62 mRNA. In 32 out of 34 melanoma cell lines, a higher amount of p62 mRNA comparing to normal melanocytes was observed (P=0.007).

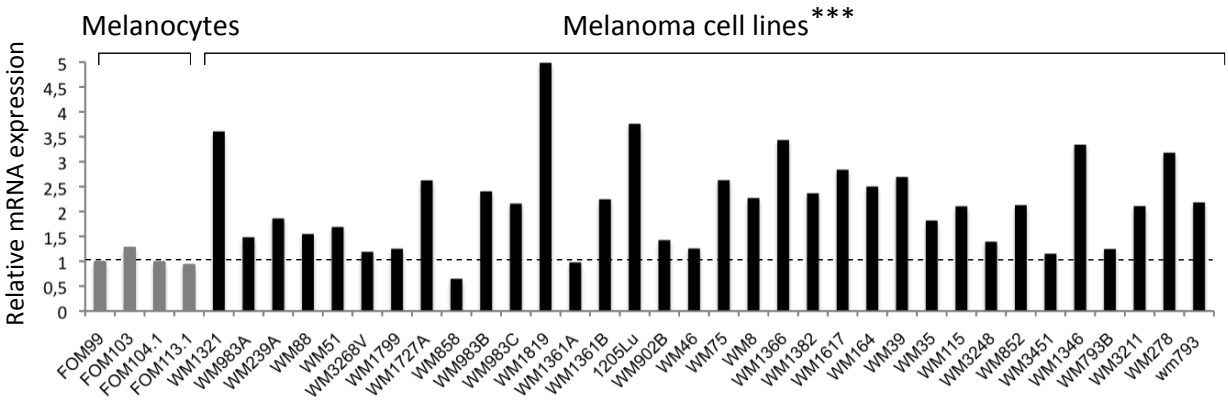

Figure 8. Overexpression of p62 at mRNA level in melanoma cells. Microarray hybridization of 4 normal melanocytes and 34 human melanoma cell lines showing an overall overexpression of p62 at mRNA level in melanoma cells (P = 0.007).

To analyze protein levels of p62 in cell lines, adherent melanoma and melanocytes cells were collected and total protein extracts were analyzed by protein immunoblots. Only one band of p62 protein with approximately 62 kDa was detected in melanocytes and melanoma cell lines. As shown in Figures 9a and 9b, p62 expression was clearly associated with a tumoral phenotype, with 12 out of 19 melanoma cell lines showing higher amounts of p62 protein comparing to normal melanocytes (*P*=0.007).

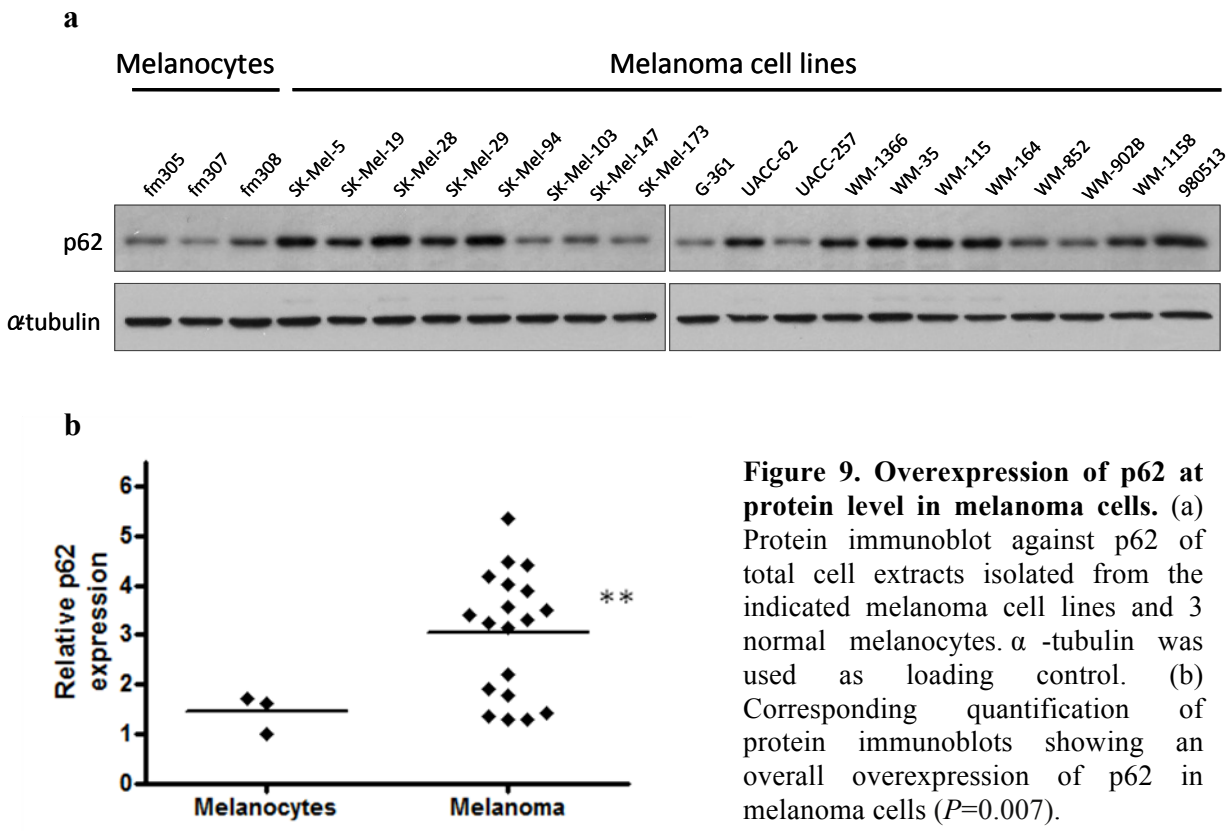

Figure 9. Overexpression of p62 at protein level in melanoma cells. (a) Protein immunoblot against p62 of total cell extracts isolated from the indicated melanoma cell lines and 3 normal melanocytes. α -tubulin was used as loading control. (b) Corresponding quantification of protein immunoblots showing an overall overexpression of p62 in melanoma cells (*P*=0.007).

Additionally, p62 localization and pattern of distribution in normal melanocytes and melanoma cells lines were assessed by direct immunofluorescence (Figure 10). Melanoma cells presented a punctuated pattern consistent with p62 being localized into cytosolic speckles or aggregates. In one out of seven melanoma cell lines (WM-1366), it was also observed nuclear expression of p62. As previously shown by protein immunoblots, direct immunofluorescence confirmed a higher expression of p62 in melanoma cells comparing to normal melanocytes. Moreover, normal melanocytes did not present aggregates of p62, but a weak and diffuse pattern of cytosolic p62 expression.

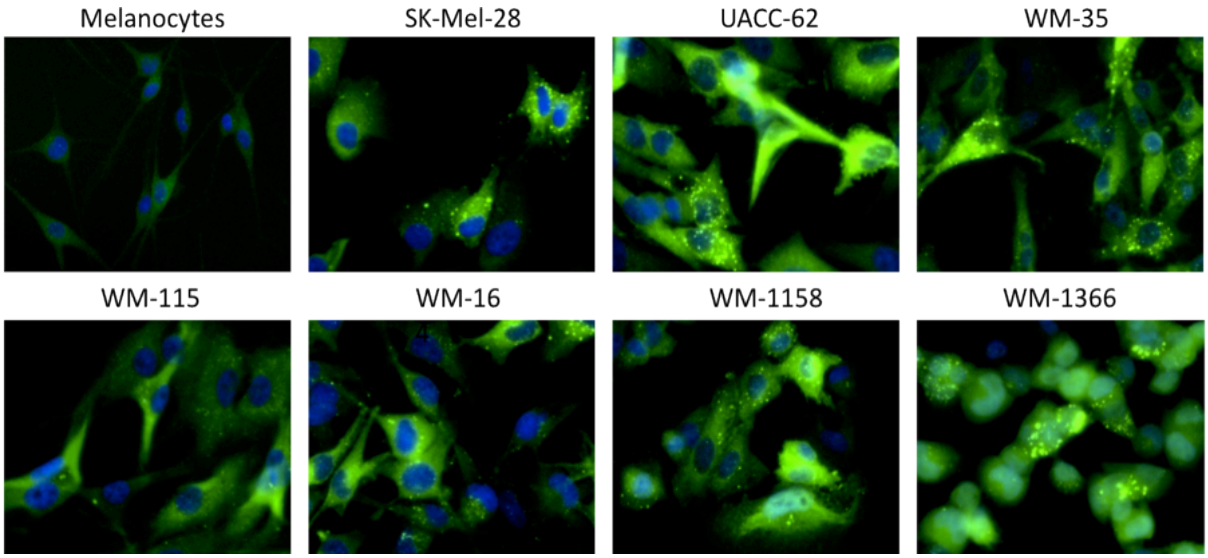

Figure 10. Differential basal expression and cytosolic distribution of p62 in melanoma and melanocytes. Immunofluorescence staining of endogenous p62 (green signal) revealing cytosolic aggresomes in melanoma cells.

The previous findings raised the question whether the differential pattern of p62 distribution was dependent to the amount of its expression. To answer this query, melanocytes and melanoma cells were stably transfected with pLV-Cherry-p62 lentiviral vector for p62 overexpression. This construct generates a cherry fluorescent protein fused to wild type form of human p62 protein. As demonstrated by protein immunoblots, the lentiviral infection conferred similar levels of ectopic p62 expression in both melanoma cells and melanocytes (Figure 11a). Unexpectedly, even a high expression of p62 in normal melanocytes did not change the diffuse pattern of p62 presented by these cells. On the other hand, the overexpression of p62 in metastatic melanoma cell line (SK-Mel-103) led to an increased number and size of protein aggregates (Figure 11b).

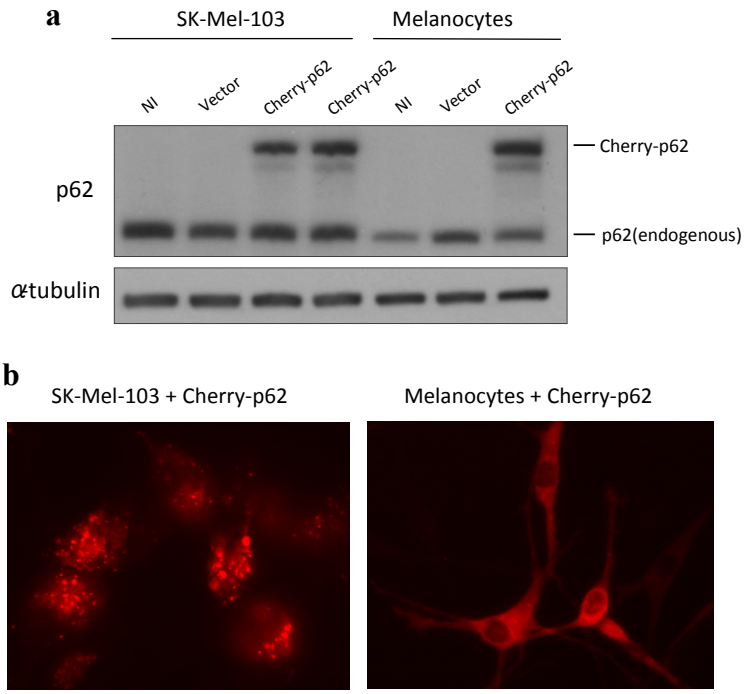

Figure 11. Ectopic overexpression of derivatives of p62 (fused to the fluorescent cherry protein) showing that even after overexpression the distribution of p62 differs in melanoma cells and melanocytes. (a) Protein immunoblots against p62 and α-tubulin showing similar levels of p62 expression in melanocytes and SK-Mel-103 melanoma cells after lentiviral transduction with the construct pLV-Cherry-p62. (b) Fluorescent microphotographs of indicated cells following ectopic overexpression of p62 demonstrating the accumulation of p62 aggregates only in melanoma cells.

Taken together, the increased levels and different cellular distribution of p62 in melanoma cells comparing to normal melanocytes suggest that p62 could play a relevant role in melanoma.

4.1.3. P62 is transcriptionally-regulated in melanoma tumors

Alteration in DNA copy number is a frequent reason of gene expression modification in cancer cells. In fact, DNA copy number variations are a common feature of melanoma tumors (Curtin et al., 2005).

As previously shown in this study, melanoma specimens and cell lines express high levels of p62. To address whether the overexpression of p62 was related to *SQSTM1* copy number variation, melanoma cell lines were submitted to high-resolution array comparative genomic hybridization (CGH). Genomic DNA of melanoma cells lines was extracted and hybridized against Human Genome CGH 44k microarrays. The cell lines chosen were SK-Mel-28, SK-Mel-103, SK-Mel-173 and UACC-62 which present different genetic background (Table 2, page 46) and levels of p62 expression (Figure 9, page 69).

The Sequestosome 1 gene (*SQSTM1*) is located on chromosome 5q35 (base pair 179,233,388 - 179,265,078). As shown in Figure 12, any of the cell lines studied by CGH presented amplification or gain of the *SQSTM1* locus that could justify p62 overexpression.

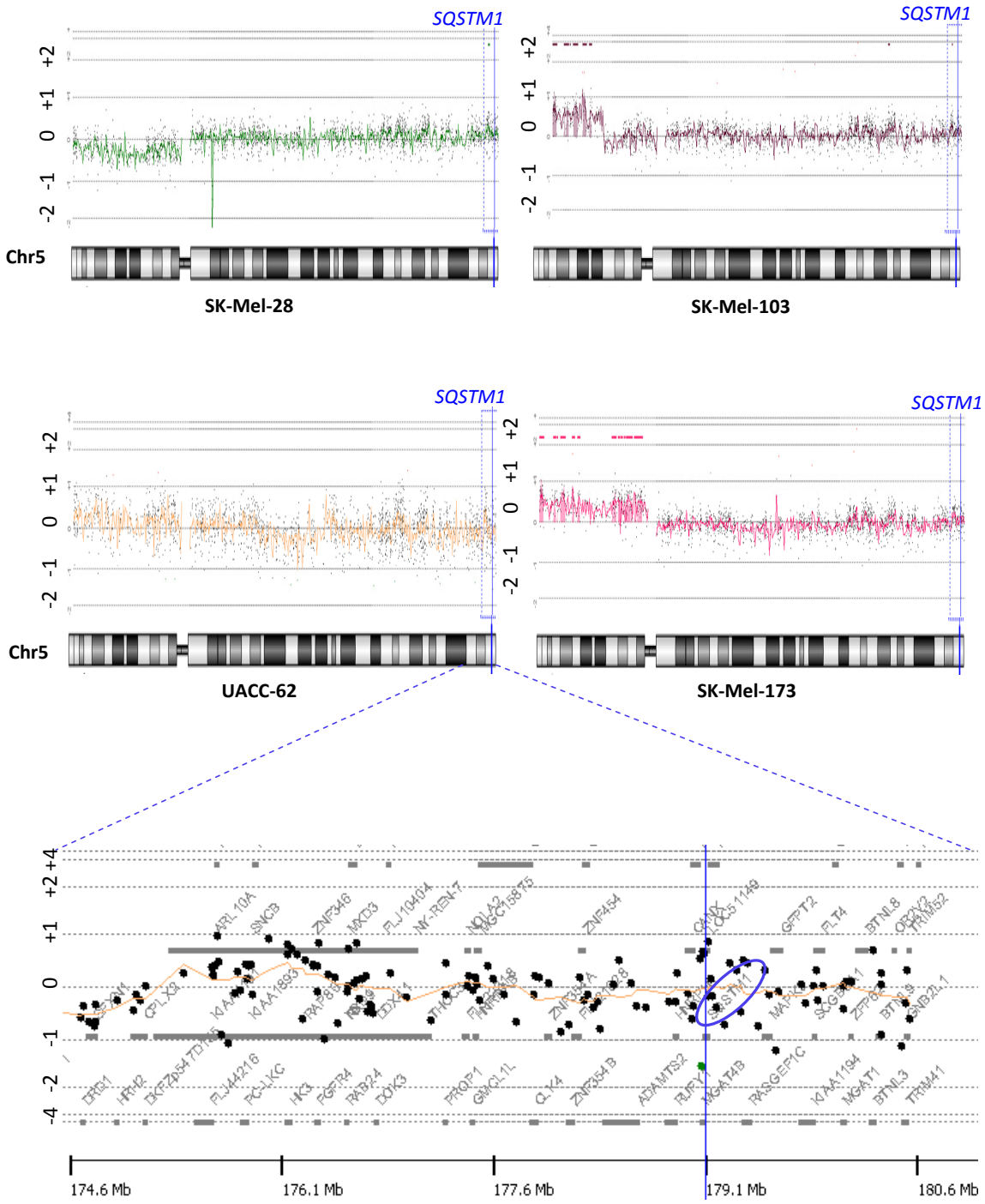

Figure 12. Absence of amplification of p62 genomic locus in melanoma cell lines. Comparative genomic hybridization analysis of 4 different melanoma cell lines demonstrated the absence of amplification of *SQSTM1* locus.

For further elucidation of p62 regulation in melanoma, the levels of p62 protein and mRNA were compared in 10 randomly chosen human melanoma samples. Paraffined-embedded sections of melanoma samples, including 2 VGP primary melanomas, 4 skin metastatic and 4 lymph node metastatic melanomas were submitted to p62 immunohistochemistry for protein level detection. After that, cryosections of the same cases were used for total RNA extraction and submitted to RT-qPCR for p62 mRNA level detection. As shown in Figures 13a and 13b, a positive association between p62 protein and mRNA levels suggests a transcriptional regulation of *SQSTM1* gene in melanoma.

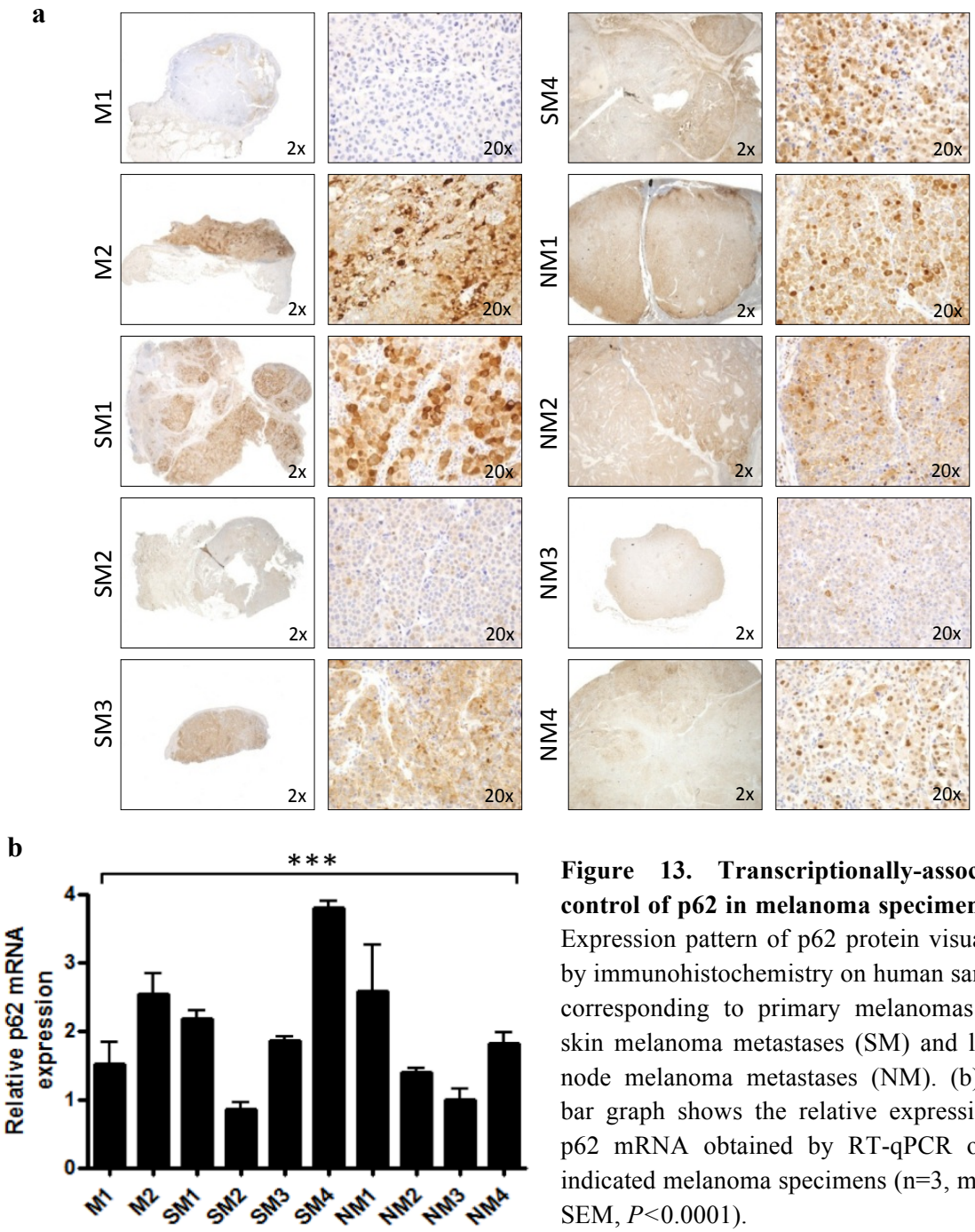

Figure 13. Transcriptionally-associated control of p62 in melanoma specimens. (a) Expression pattern of p62 protein visualized by immunohistochemistry on human samples corresponding to primary melanomas (M), skin melanoma metastases (SM) and lymph node melanoma metastases (NM). (b) The bar graph shows the relative expression of p62 mRNA obtained by RT-qPCR of the indicated melanoma specimens (n=3, mean ± SEM, $P<0.0001$).

Altogether, comparative genomic hybridization of melanoma cell lines and expression analyses of melanoma specimens support a transcriptional regulation of p62 without amplification of its genomic locus.

4.1.4. P62 expression is induced during malignant transformation of melanocytes

Several key genetic alterations governing melanoma initiation and progression have been identified. The most common proto-oncogenes involved in melanoma initiation are related to the activation of the mitogen-activated protein kinase pathway (MAPK). Mutations of RAS/MAPK pathway genes as *BRAF* and *NRAS* are detected in 40-60% and 10-20% of melanoma patients, respectively (Goel et al., 2006; Ribas et al., 2011). Moreover, Duran and coworkers have shown that the *RAS* oncogene leads to overexpression of p62 mRNA and protein levels in immortal embryo fibroblasts through the activation of the p62 promoter (Duran et al., 2008). Taking together, these observations presented in the literature address the question whether *BRAF* and *RAS* oncogenes could regulate p62 expression in melanocytic tumors.

To answer this question, freshly isolated normal melanocytes were submitted to lentiviral-driven transduction of $BRAF^{V600E}$, $NRAS^{Q61R}$ and $HRAS^{G12V}$ mutations. Non-infected, control melanocytes (infected with FG12 vector) and melanocytes infected with $BRAF^{V600E}$, $NRAS^{Q61R}$ or $HRAS^{G12V}$ were collected at days 4 and 6 post-infection for the detection of p62 mRNA and protein levels. As shown in Figure 14a, 4 to 6 days after infection, melanocytes expressing $BRAF^{V600E}$, $NRAS^{Q61R}$ and $HRAS^{G12V}$ mutations entered into a nonproliferative state and suffered morphological features of senescence, including enlarged cytoplasm, nuclear size and extensive cytosolic vacuolization.

Analyses by RT-qPCR (Figure 14b) and protein immunoblots (Figure 14c) did not show overexpression of p62 after infection with $BRAF^{V600E}$, $NRAS^{Q61R}$ or $HRAS^{G12V4}$ mutations (P>0.05). Interestingly enough, these finding corroborates the previous results obtained by IHC (Figure 6, page 65 and Figure 7, page 67), whereby the expression of p62 was negative in dermal nevi, benign lesions mostly composed by senescent melanocytes.

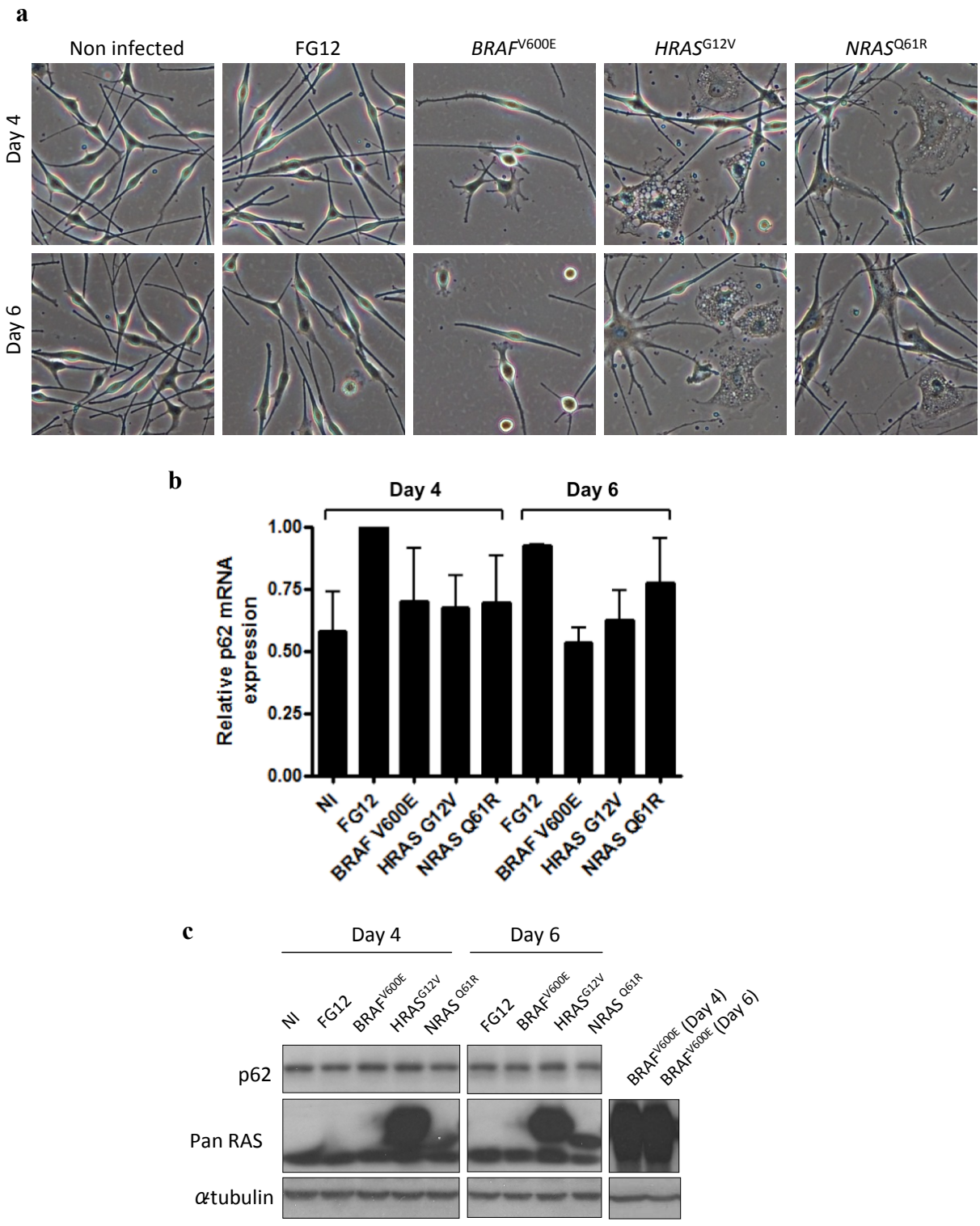

Figure 14. Absence of p62 upregulation in senescent melanocytes. (a) Microphotographs of non-infected (NI), control melanocytes (FG12) and melanocytes expressing *BRAF*^{V600E}, *NRAS*^{Q61R} or *HRAS*^{G12V} mutations after 4 and 6 days of lentiviral infection showing morphological features of senescent phenotype. (b) The bar graph shows the relative expression of p62 mRNA of the indicated melanocytes, obtained by qPCR (n=3, mean ± SEM, P>0.05) (c) Protein immunoblots against p62, Pan RAS and BRAF confirmed the overexpression of the indicated oncogenes but the absence of p62 upregulation in senescent melanocytes. α-tubulin was used as loading control.

Although *BRAF*^{V600E} or *NRAS*^{Q61R} mutations are present in most of the melanoma tumors, the malignant transformation of melanocytes is invariably accompanied by additional genetic alterations as the silencing of tumor suppressor genes (Curtin et al., 2005; Denoyelle et al., 2006). In this study, the absence of p62 upregulation in cultured senescent melanocytes and dermal nevi specimens opened the question whether p62 overexpression is induced during the malignant transformation of melanocytes.

To answer this query, conditional melanocyte-specific *Braf*^{V600E} and *Braf*^{V600E}/*Pten*$^{loxP/loxP}$ mice models were used for the analysis of p62 expression. Mice carrying *Braf*^{V600E} mutation are able to form melanocytic lesions without metastatic capacity (Dankfort et al., 2009). On the other hand, *Braf*^{V600E} mutation cooperates with *Pten* loss to induce malignant lesions and mice harboring such genetic alterations are able to form malignant melanomas with metastatic capacity (Dankfort et al., 2009).

Tumor samples from both mice models were surgically extracted and the expression of p62 was assessed by immunohistochemical staining. Interestingly, the expression of p62 was higher in malignant melanomas specimen of *Braf*^{V600E}/*Pten*$^{loxP/loxP}$ mice, than in benign melanocytic proliferation of the *Braf*^{V600} mice (Figure 15).

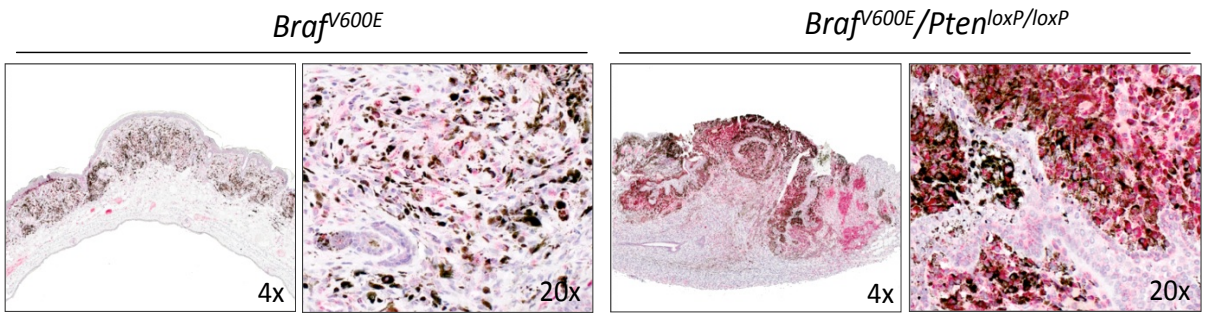

Figure 15. P62 overexpression is related to malignant transformation of melanocytes. Immunohistochemical staining for p62 (in pink) in melanocytic tumors of conditional melanocyte-specific mice models showing increased expression of p62 in malignant melanocytic tumors (*Braf*^{V600E}/*Pten*$^{loxP/loxP}$) when compared to benign melanocytic tumors (*Braf*^{V600E}).

In summary, the study of p62 expression in senescent melanocytes and in melanoma mice models suggest that p62 overexpression is a phenomenon associated to the malignant transformation of melanocytes.

4.2. The function of Sequestosome1/p62 in melanoma cells

4.2.1. Genetic inactivation of p62 triggers melanoma growth arrest

Sequestosome1/p62 has been related to tumorigenesis in different types of cancer as indicated above (Duran et al., 2008; Mathew et al., 2009; Inami et al., 2011). Taking in consideration that p62 is overexpressed in malignant tumors of melanocytes, it was hypothesized that p62 could play a relevant role in melanoma cells.

To address the function of p62 in melanoma, melanoma cell lines were submitted to genetic depletion of p62 by RNA interference (RNAi). First, to identify an adequate RNAi for p62 depletion, SK-Mel-103 melanoma cells were submitted to downregulation of endogenous p62 levels by lentiviral-driven transduction of 5 different p62 short harpirin RNA (p62 shRNA). The infection of SK-Mel-103 cells with a scramble short harpirin RNA was used as control (control shRNA). After 6 days of infection, melanoma cells were collected for protein immunoblot analysis. As shown in Figure 16a and 16b, an efficient downregulation of p62 protein was obtained with the shRNA constructs number 1, 3 and 5. The efficacy of p62 deletion was also checked by direct immunofluorescence and visualized as a decrease of fluorescent signal in p62 shRNA cells (Figure 16c). The constructs 1 or 5 were then selected for the following experiments.

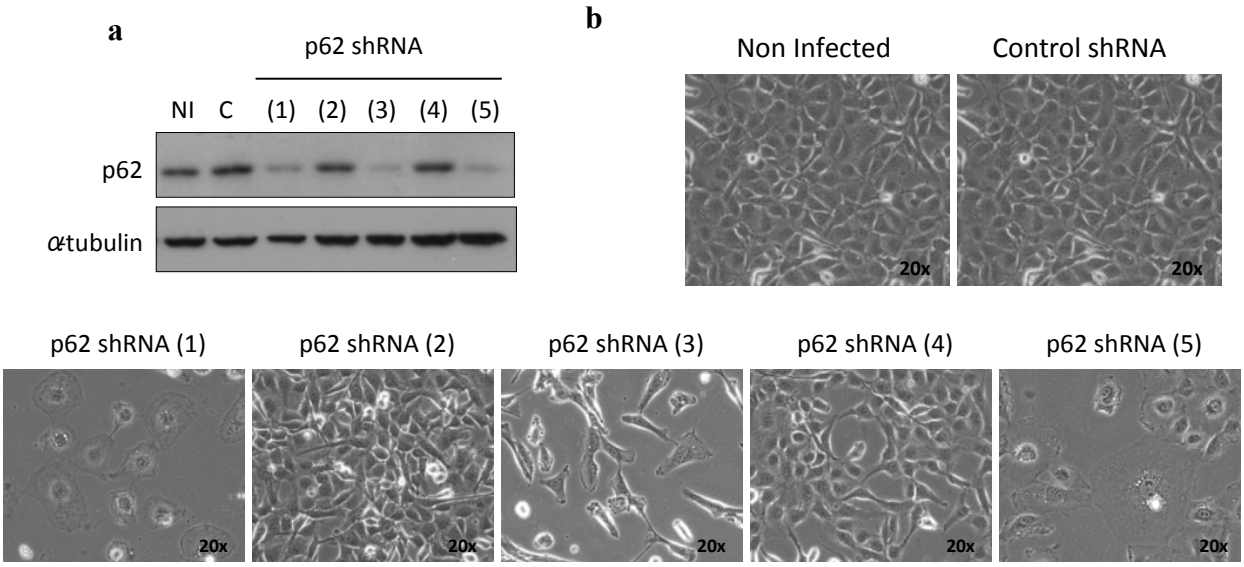

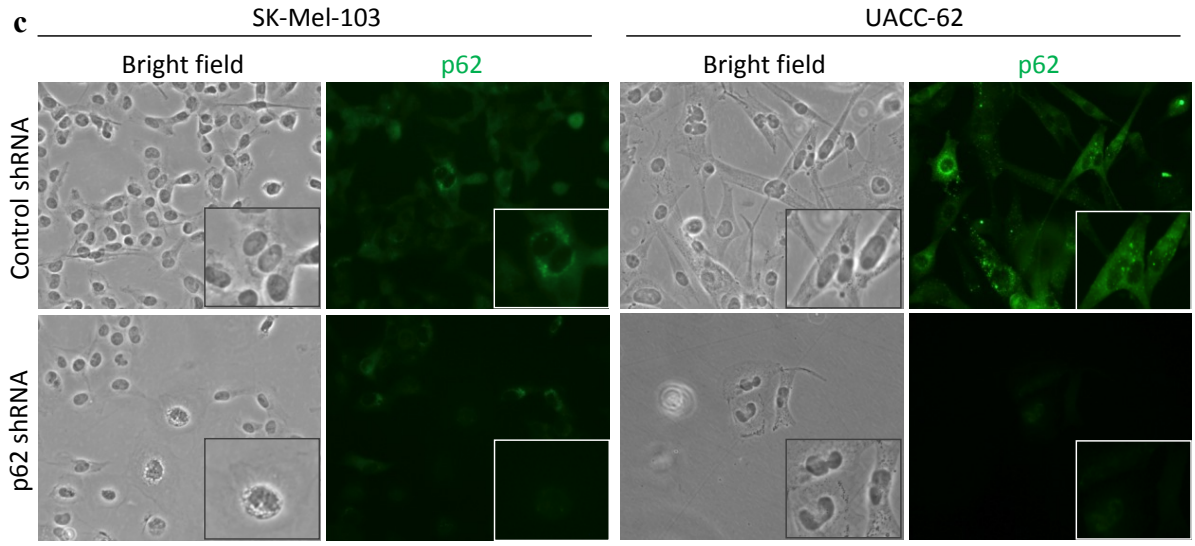

Figure 16. Genetic depletion of p62 using RNAi in melanoma cells. Downregulation of endogenous p62 levels by lentiviral-driven transduction of shRNAs in SK-Mel-103 melanoma cells. (a) Protein immunoblots against p62 and α-tubulin showing efficient downregulation of p62 in 3 out of 5 different p62 short harpirin RNA. (b) Microphotographs of melanoma cells 6 days after lentiviral infection with shRNA constructs. (c) Efficient depletion of p62 in SK-Mel-103 and UACC-62 melanoma cell lines confirmed by direct immunofluorescence 6 days after lentiviral infection.

Next, UACC-62 melanoma cells harboring the most common mutation found in melanoma patients ($BRAF^{V600E}$) were depleted for p62 using shRNA constructs (Figure 17a). Intriguingly, proliferation assay demonstrated that UACC-62 melanoma cells responded to p62 shRNA with a significant inhibition of cell growth (Figures 17b and 17c). Indeed, UACC-62 cells infected with control shRNA and p62 shRNA were plated at low confluence for the analysis of the capacity to form colonies. After 20 days, the plates were stained with crystal violet and it was observed that the depletion of p62 decreased the capacity of colony formation by melanoma cells (Figure 17d).

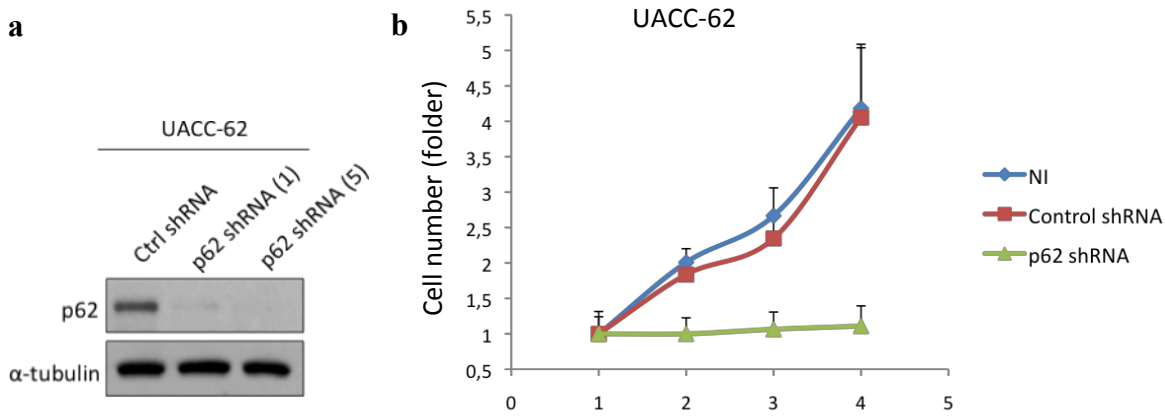

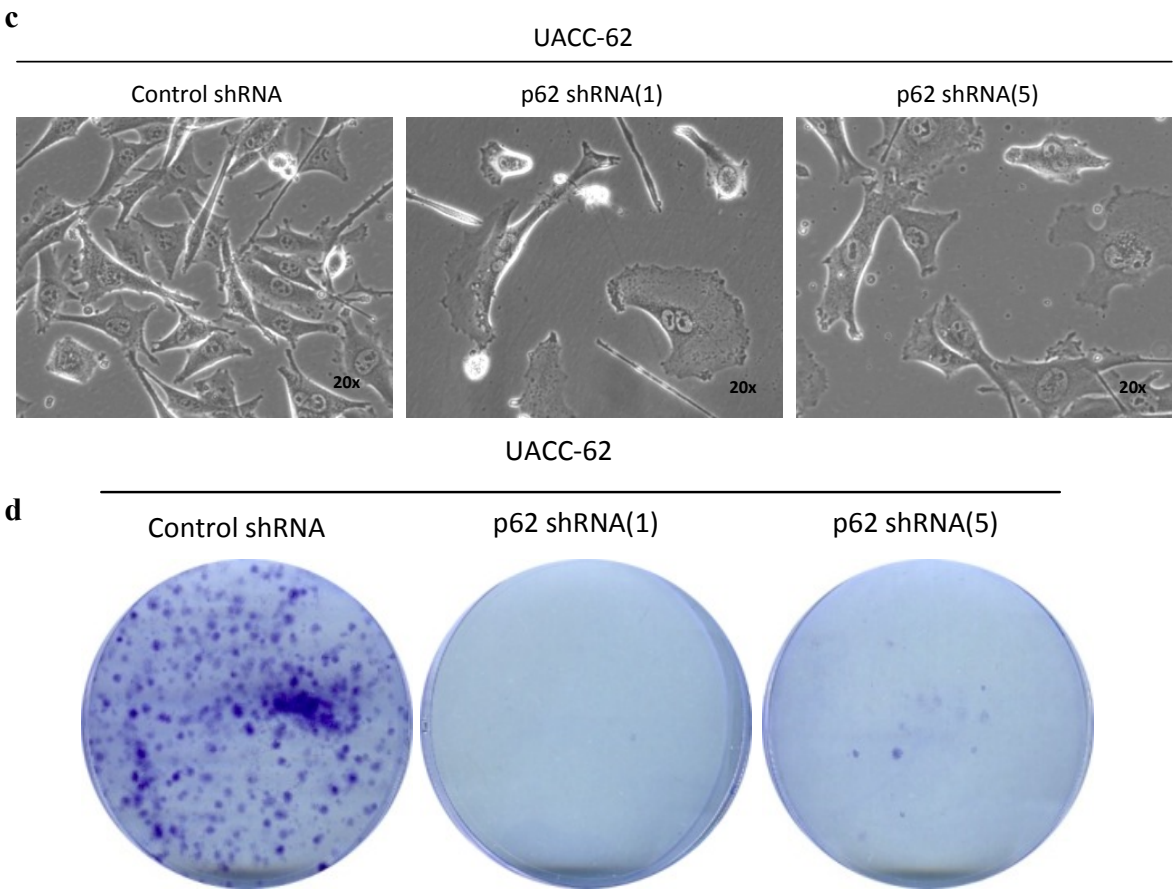

Figure 17. P62 genetic inactivation triggers melanoma growth arrest. (a) Protein immunoblots against p62 and α-tubulin showing an efficient downregulation of p62 in UACC-62 melanoma cells expressing p62 shRNA. (b) Corresponding proliferative curve of melanoma cells demonstrated an inhibition of cell growth after p62 depletion. Six days after lentiviral infection melanoma cells were seeded in 96-well optical bottom for quantification of total number of cells by automated high-throughput confocal detection of DAPI-stained nuclei (n=3, mean ± SEM, $P<0.05$). (c) Representative microphotographs of UACC-62 melanoma cells 6 days after lentiviral infection for p62 downregulation. (d) Colony formation ability of UACC-62 melanoma cell line after p62 downregulation. Cells were seeded at low density on day 6 after lentiviral transduction. Shown are representative scans of colonies visualized by crystal violet staining.

To confirm the influence of p62 in melanoma proliferation, 4 additional melanoma cell lines SK-Mel-28, SK-Mel-103, SK-Mel-173 and WM-164, harboring different mutational status (Table 2, page 46) were depleted for p62. The number of cells was quantified at day 0, 2, 4 and 6 after infection. As represented in Figure 18, the relative number of p62 shRNA cells, comparing to control, decreased with the time, validating the results obtained with UACC-62 cell line. Indeed, it demonstrates that the effect of p62 depletion in cellular proliferation is independent of the genetic background presented by melanoma cells.

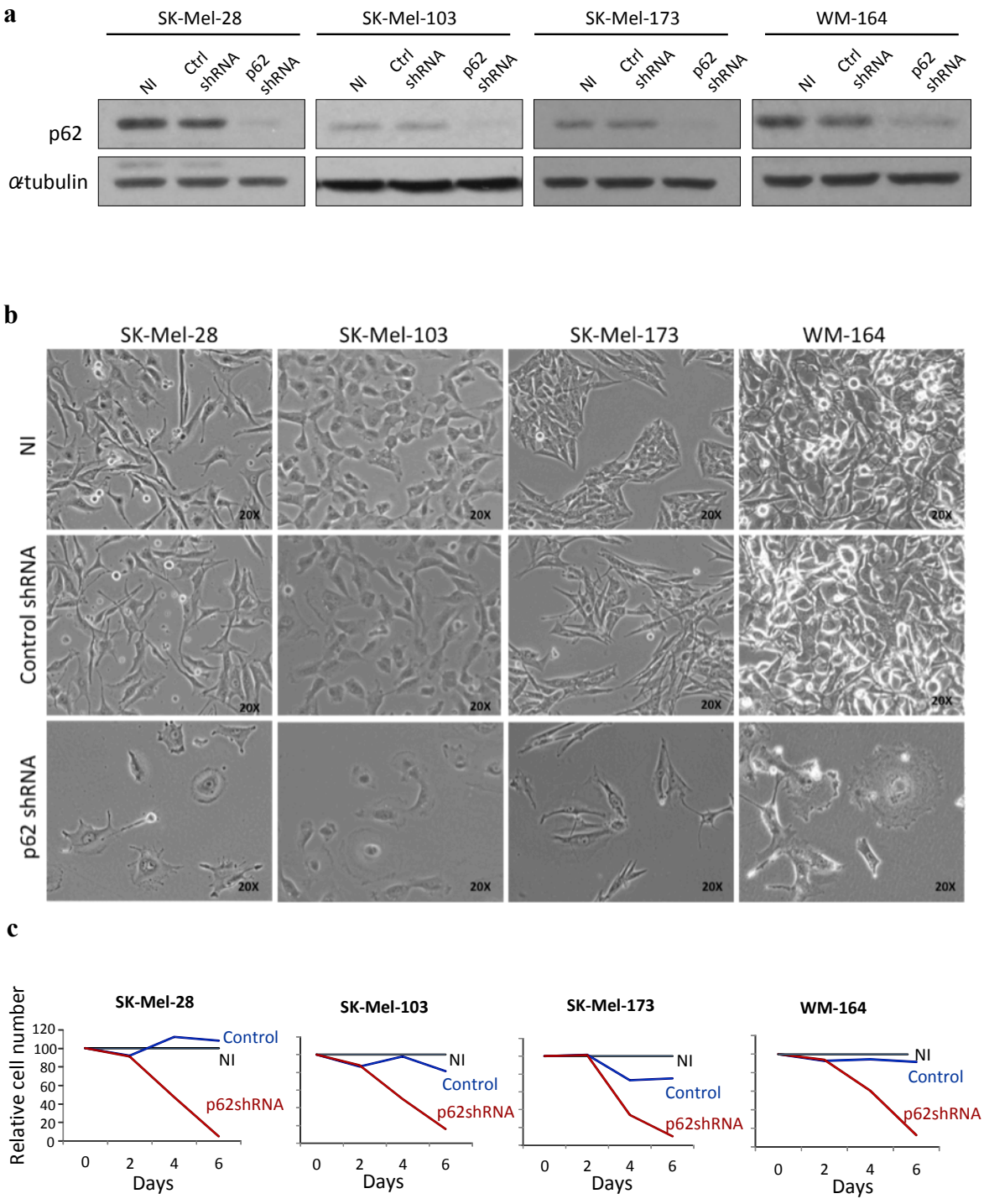

Figure 18. The interference of p62 in melanoma proliferation is independent of the genetic background of the cells. (a) Protein immunoblots against p62 and α-tubulin showing an efficient downregulation of p62 in melanoma cells expressing p62 shRNA. (b) Representative microphotographs of melanomas cells on day 6 after lentiviral transduction demonstrating cell growth arrest after the depletion of p62. (c) Growth curves on days 0, 2, 4 and 6 after lentiviral transduction showing a relative decrease in cell number of p62 depleted cells (p62 shRNA), when compared to non infected (NI) and control cells.

Moreover, as shown in Figure 19a, the depletion of p62 was accompanied by morphological changes evocative of classical senescent phenotype, as cell enlargement, vacuolization and flattening. The morphological changes suffered by p62-depleted cells were also suggestive of cytoskeleton alterations. To address whether the depletion of p62 triggers a senescent mechanism, the expression of the senescence-induced β -galactosidase enzyme (SA-β-Gal), a commonly used senescence marker (Michaloglou et al. 2005), was evaluated. UACC-62 and SK-Mel-103 melanoma cells were depleted for p62 using shRNA constructs and submitted to Xgal staining. The increased of SA-β-Gal activity in p62 depleted cells demonstrated the senescent state of these cells (Figure 19b).

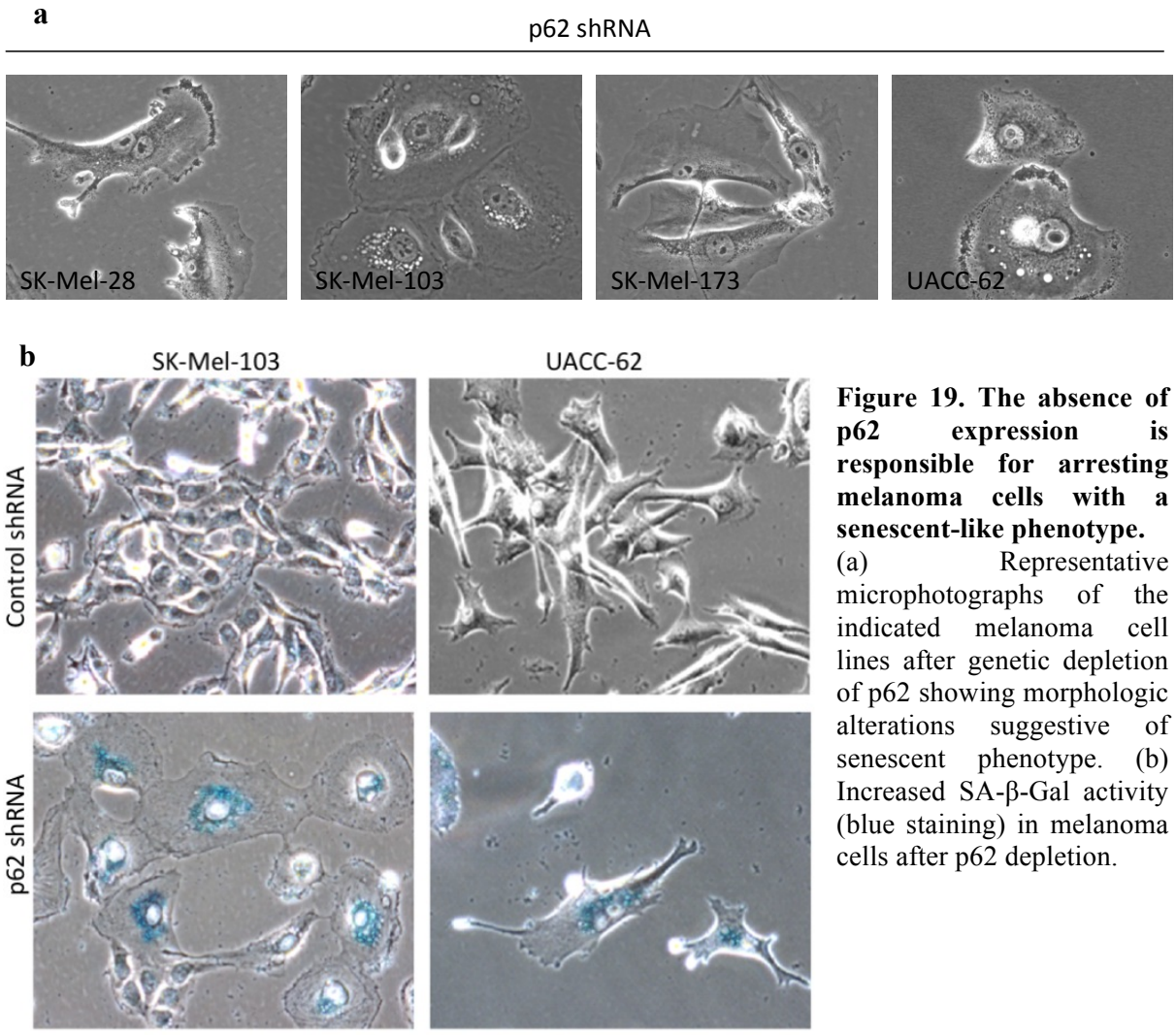

Figure 19. The absence of p62 expression is responsible for arresting melanoma cells with a senescent-like phenotype. (a) Representative microphotographs of the indicated melanoma cell lines after genetic depletion of p62 showing morphologic alterations suggestive of senescent phenotype. (b) Increased SA-β-Gal activity (blue staining) in melanoma cells after p62 depletion.

Taken together, the results obtained by RNA interference technique prove that p62 is essential for melanoma proliferation, and its absence is responsible for inducing a nonproliferative state with senescent-like phenotype.

4.2.2. The requirement of p62 is tumor cell selective

After addressing the relevance of p62 in melanoma cells, the next question was whether p62 could interfere with the proliferation of normal cells. Normal fibroblasts and melanocytes isolated from foreskin and UACC-62 melanoma cells were submitted to genetic depletion of p62 using RNA interference technique. As shown by protein immunoblots, an efficient downregulation of p62 was acquired in melanoma and normal cells after lentiviral-driven transduction of p62 shRNA (Figure 20a). Interestingly, after the depletion of p62, normal fibroblasts and melanocytes were still able to proliferate, meanwhile melanoma cells arrested. Unlike melanomas cells, normal fibroblasts and melanocytes did not suffer morphologic changes in the absence of p62 (Figure 20b). In fact, the senescence-associated β -galactosidase activity did not increase in normal cells depleted for p62 (P>0.05), but it increased in melanoma cells after p62 depletion (P=0.004) (Figures 20b and 20c).

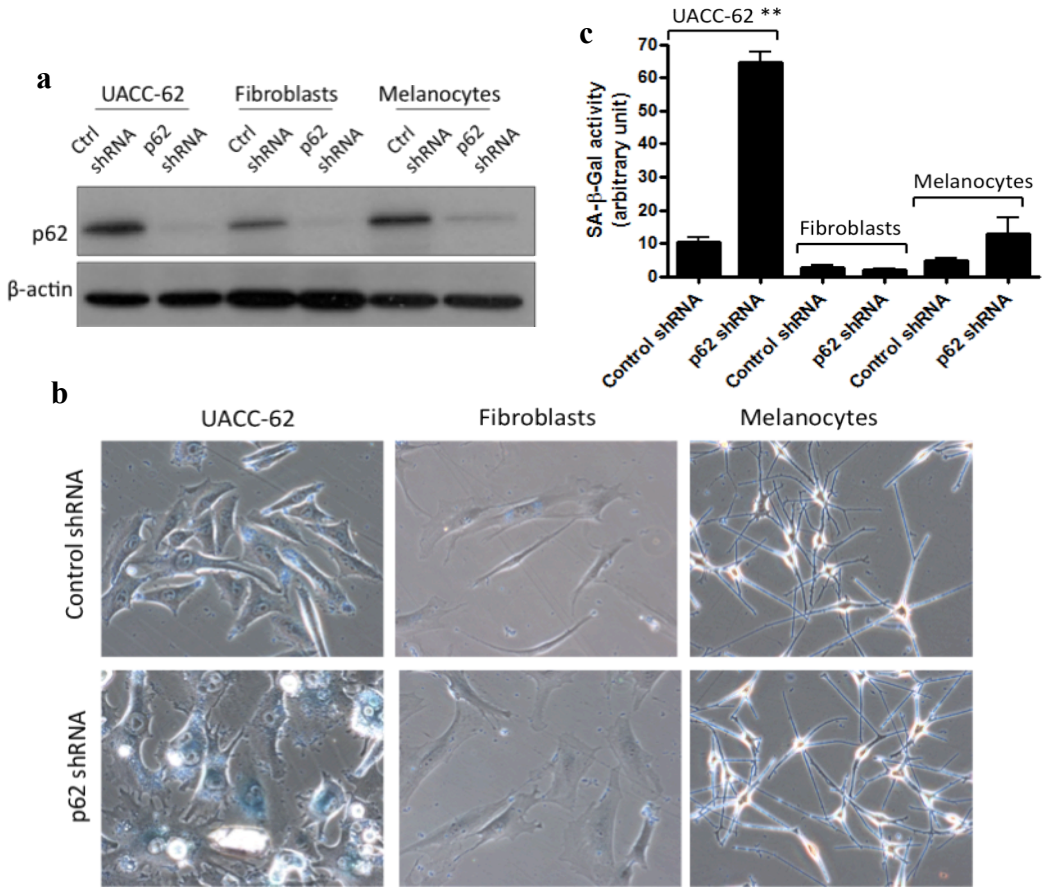

Figure 20. P62 depletion in normal melanocytes and fibroblats does not interfere with proliferative growth and morphologic changes. (a) Protein immunoblots against p62 and β-actin showing an efficient downregulation of p62 expression in melanoma cells, normal fibroblasts and melanocytes expressing p62 shRNA. (b) Representative microphotographics of cells on day 6 after lentiviral transduction showing increased SA-β-Gal activity (blue staining) in melanoma cells but not in normal cells after p62 depletion. (c) Corresponding quantification of SA-β-Gal activity after p62 depletion (n=3, mean ± SEM, P=0.004).

In summary, the depletion of p62 did not trigger a senescent phenotype in normal cells, indicating a tumor cell selective requirement of p62 protein.

4.2.3. P62 contributes to the invasive capacity of melanoma cells

Vertical growth phase melanomas, the invasive form of primary melanoma, showed elevated amount of p62 expression comparing to radial growth phase melanomas (Figure 7, page 67). Moreover, p62 depleted cells presented morphologic changes compatible with cytoskeleton remodeling (Figure 19, page 81). Since changes in cytoskeletal structure are involved in cellular adhesion and motility (Miyoshi et al., 2008), p62 could interfere with the invasive capacity of melanoma cells.

To address the influence of p62 in invasion function, a Matrigel Matrix Invasion assay (MMI) was performed. The MMI works as a reconstituted basement membrane *in vitro*, being a useful way to study the invasion capacity of malignant cells. The Matrigel layer occludes the pores of the membrane, blocking non-invasive cells from migrating through the membrane. On the other hand, invasive cells are capable to detach themselves and invade through the Matrigel Matrix and the membrane pores.

The extremely invasive melanoma cell line SK-Mel-103, isolated from metastatic melanoma, was submitted to lentiviral-driven transduction of control shRNA and p62 shRNA and plated in Matrigel transwell invasion chambers. Interestingly, after 24 hours of incubation, melanoma cells depleted to p62 lost invasion capacity. The quantification of melanoma cells above and below the membrane showed that p62 depleted cells invaded the reconstituted basement membrane 50% less than control cells (P<0.0001) (Figure 21).

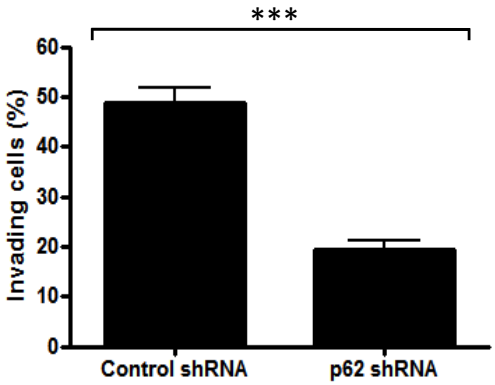

Figure 21. Matrigel invasion assay showing that p62 favors melanoma invasion capacity. Invasiveness of SK-Mel-28 melanoma cells infected with control shRNA or p62 shRNA lentiviral constructs. Cells were plated in BioCoat Matrigel™ Invasion Chambers. Samples were analyzed 24h after plating in invasion chambers by counting DAPI+ nuclei. The experiment shows a decreased melanoma invasion capacity after p62 depletion (n=3, mean ± SEM, P<0.0001).

Next, to test whether the overexpression of p62 could facilitate the invasion capacity of melanoma cells, a laborious skin reconstruct model was developed at Dr. Herlyn´s Laboratory, The Wistar Institute, Philadelphia. The skin reconstruct recapitulates the environment of melanoma cells and allows the study of melanoma invasion in a physiological system (Li et al., 2011; Brohem et al., 2011).

The non-invasive melanoma cell line WM3211, isolated from primary radial growth phase melanoma, was submitted to lentiviral-driven transduction of a cherry fluorescent protein fused to p62 (pLV-mCherry-p62) for p62 overexpression. WM3211 cells infected with the vector pLV-mCherry were used as control. The stable infected melanoma cells were added to the epidermal layer of the artificial skin. After 18 days, skins were harvested and processed for H&E and immunohistochemical analysis of p62 and mCherry. Interestingly, only melanoma cells expressing high levels of p62 were able to invade the dermis; meanwhile control melanoma cells were restricted to the epidermis (Figure 22).

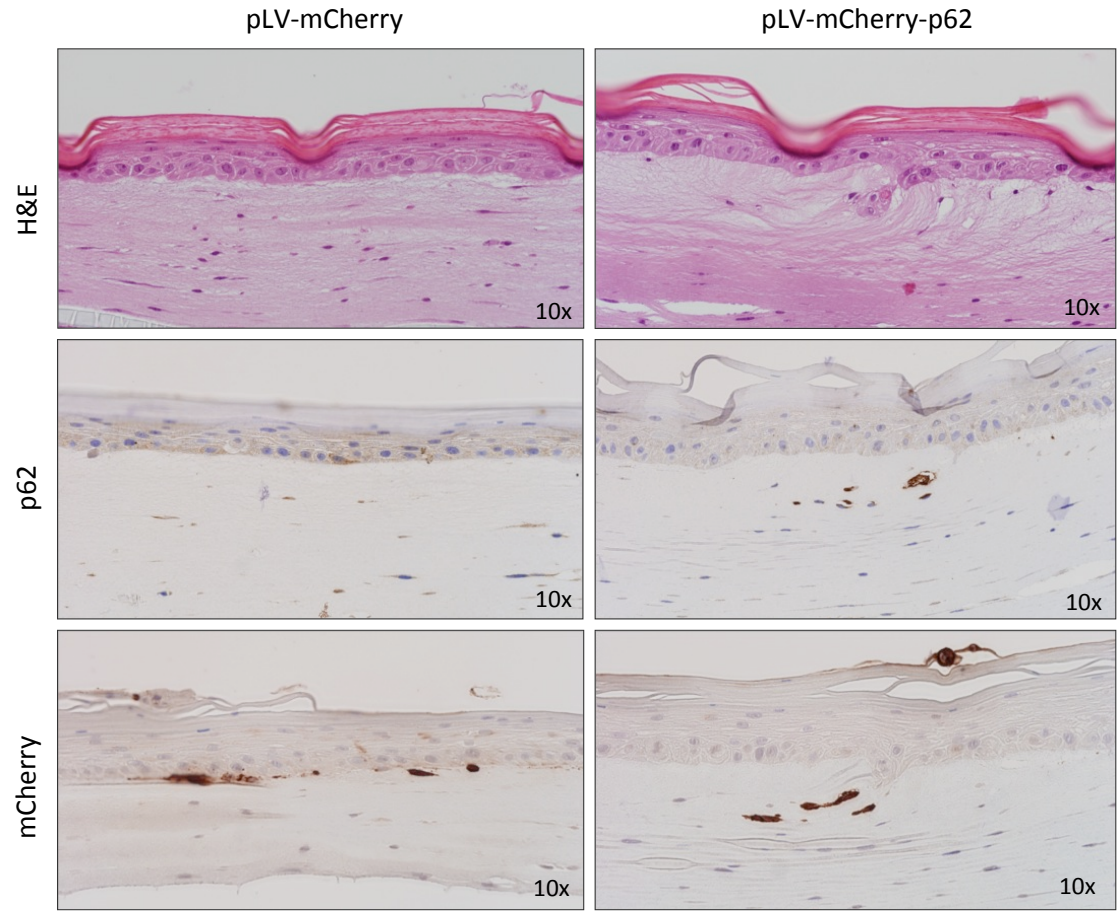

Figure 22. Skin Reconstruct model showing that p62 favors melanoma invasion capacity. Representative pictures of skin reconstruct model made with the non-invasive WM3211 melanoma cell line. Skins were harvested after 18 days, processed for H&E staining and immunohistochemically analyzed for p62 and mCherry. The experiment demonstrates an increased invasion capacity of melanoma cells after ectopic overexpression of p62 (pLV-mCherry-p62), when compared to control cells (pLV-mCherry).

Altogether, the downregulation of p62 leading to a reduced melanoma invasion capacity, combined to the overexpression of p62 leading to an increased melanoma invasion capacity corroborate to the relevance of p62 in melanoma progression.

4.2.4. P62 depletion does not impair the formation of autophagosomes in melanoma cells

After having verified the relevance of p62 in melanoma proliferation and invasion capacity, the next question was the mechanism underlying the p62 requirement in melanoma cells.

First of all, the involvement of p62 in autophagy was confirmed in melanoma cells. For that, SK-Mel-103 melanoma cells were stably transfected with the green fluorescent protein fused to wild type form of human LC3 (pLV-EGFP-LC3) and the cherry fluorescent protein fused to p62 (pLV-mCherry-p62). The cells generated were treated with Rapamycin, an autophagy stimulator by the inhibition of mTOR pathway (Raught et al., 2001) and with Chloroquine, an autophagy inhibitor that blocks lysosome–autophagosome fusion (Solomon et al., 2009). As represented in Figure 23a, after treatment with Rapamycin it could be observed few colocalization between p62 and LC3. Moreover, a strong colocalization of LC3 and p62 was seen after blocking lysosome-autophagosome fusion by Chloroquine, confirming that p62 is involved in autophagy in melanoma cells.

The posttranslational modification of LC3 form I (LC3-I) to form II (LC3-II) is an indicative of autophagosome formation (Mehrpour et al., 2010). To test if the depletion of p62 interferes with autophagosome formation, UACC-62 cells were depleted for p62, using shRNA constructs. After 3 and 6 days of infection, the levels of LC3-I and LC3-II were checked by protein immunoblots. As shown in Figures 23b and 23c, although there was a slight increase in total amount of LC3 protein, the downregulation of p62 did not interfere with the conversion of LC3-I to LC3-II.

To confirm the previous result, melanoma cells SK-Mel-104 expressing GFP-LC3 were submitted to lentiviral infection with control shRNA and p62 shRNA. After 7 days, the cells were treated with Rapamycin and Chloroquine during 7 hours. In fact, any difference of autophagosome formation, checked by green foci, was seen in melanoma cells after p62 depletion (Figure 23d).

Additionally, it was analyzed whether the absence of p62 could interfere with the accumulation of ubiquitinated (Ub) proteins. For that, SK-Mel-103 melanoma cells were

genetic depleted for p62 and ubiquitinaded proteins were checked by immunoblots. Surprisingly, the depletion of p62 was responsible for a decreasing of total Ub amount (Figure 23e).

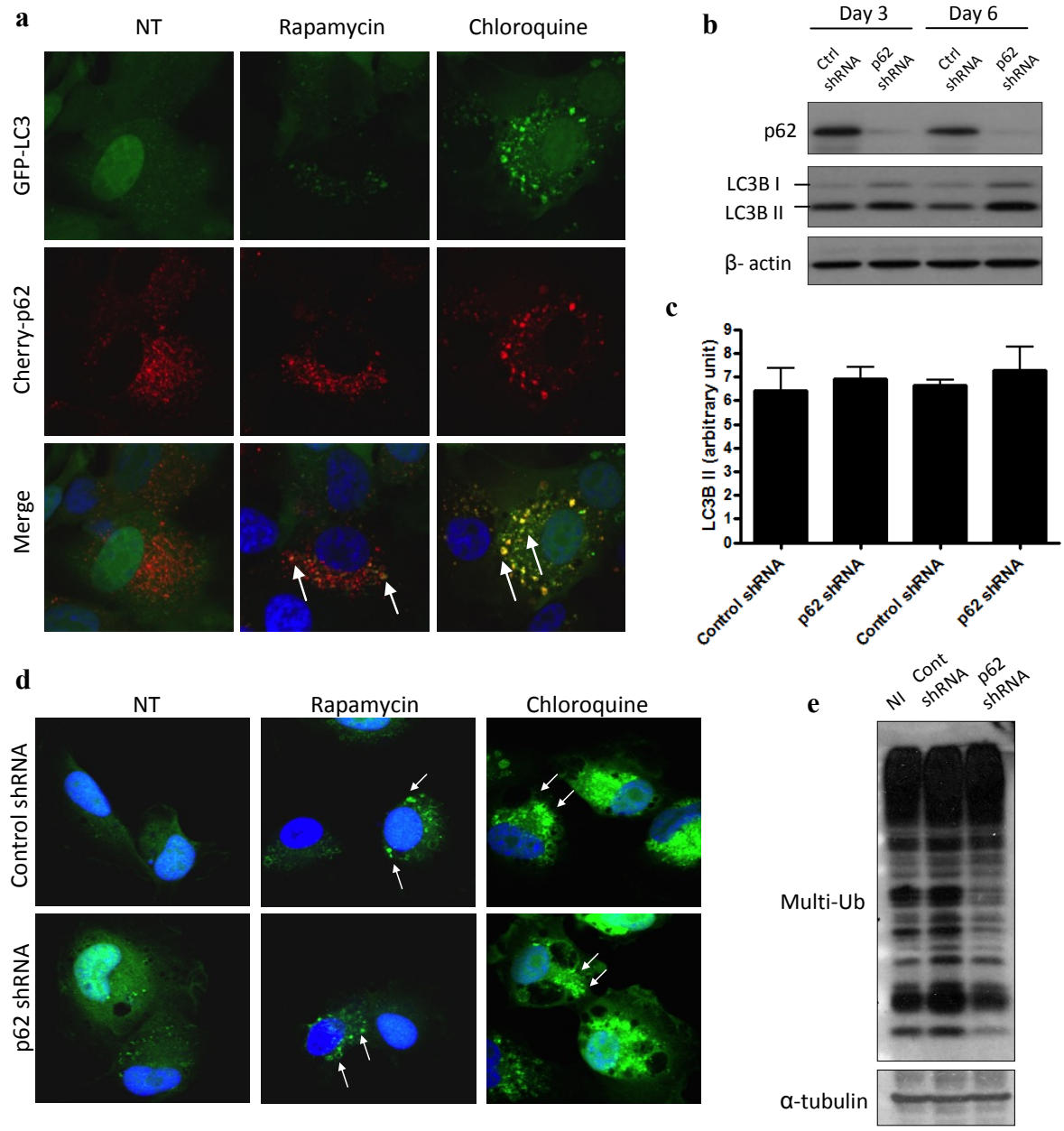

Figure 23. P62 depletion does not interfere with autophagosome formation in melanoma cells. (a) Representative fluorescent microphotographs of SK-Mel-103 melanoma cells expressing LC3 (in green) and p62 (in cherry), before treatment and 7 hours after treatment with Rapamycin and Cloroquine (NT= non treated). (b) Protein immunoblots against LC3 and β-actin in SK-Mel-103 melanoma cells expressing control shRNA and p62 shRNA. (c) Corresponding quantification of protein immunoblots showing that p62 downregulation did not interfere with the conversion of LC3-I to LC3-II (n=3, mean ± SEM, $P>0.05$). (d) Representative fluorescent microphotographs of SK-Mel-103 melanoma cells expressing EGFP-LC3 (in green) and treated with Rapamycin or Chloroquine showing no difference in autophagosome formation after p62 depletion (green foci). (e) Protein immunoblots against Ubiquitin and α-tubulin showing decreased Ub-proteins after p62 downregulation.

Altogether, these findings confirmed that p62 is involved in autophagy in melanoma cells however the depletion of p62 does not impair autophagosome formation.

4.2.5. P62 is required for proper expression of survival, cell cycle and invasion modulators

P62 protein is involved in protein degradation and activation of different cell signaling pathways (Puissant et al., 2012). Previous results of this study have shown that autophagy is still functional in the absence of p62. Thus, it was wondered whether specific targets or partners of p62 could not be shuttled to authopagosome degradation in the absence of p62. Moreover, the lack of p62 could interfere with different signaling pathways important for tumorigenesis in melanoma cells.

To identify the molecular pathways associated with the inhibition of proliferation and invasion in p62-deficient melanoma cells, transcriptomic studies were performed. Melanoma cells were depleted for p62 and examined by microarray hybridization and gene expression analysis. SK-Mel-103 and UACC-62 cells were infected with p62 shRNA and control shRNA and collected at day 3 (early time point) and day 6 (late time point) post-infection. Total RNA was extracted and processed for hybridization. Functional analysis was carried out using Gene Set Enrichment Analysis (GSEA). The list of enriched pathways found in p62 depleted UACC-62 and SK-Mel-103 melanoma cells is represented in Figure 24, Supplemental Figures 1 and 2 (pages 132-133).

Interestingly, after the depletion of p62 many pathways involved in cell cycle control, DNA repair and DNA replication process were downregulated at early time point. Indeed, pathways involved in cellular motility and invasion, as adherent junctions, regulation of actin-cytoskeleton, Rac-1 pathway and cell adhesion molecules were altered. Pathways related to cellular metabolism, proteosome degradation and membrane trafficking were also altered (Figure 24 and Supplemental Figures 1 and 2). Interestingly, NF-kB, mTOR and Keap1-Nrf2 signaling pathways did not present statistical significant deregulation in melanoma cells depleted for p62.

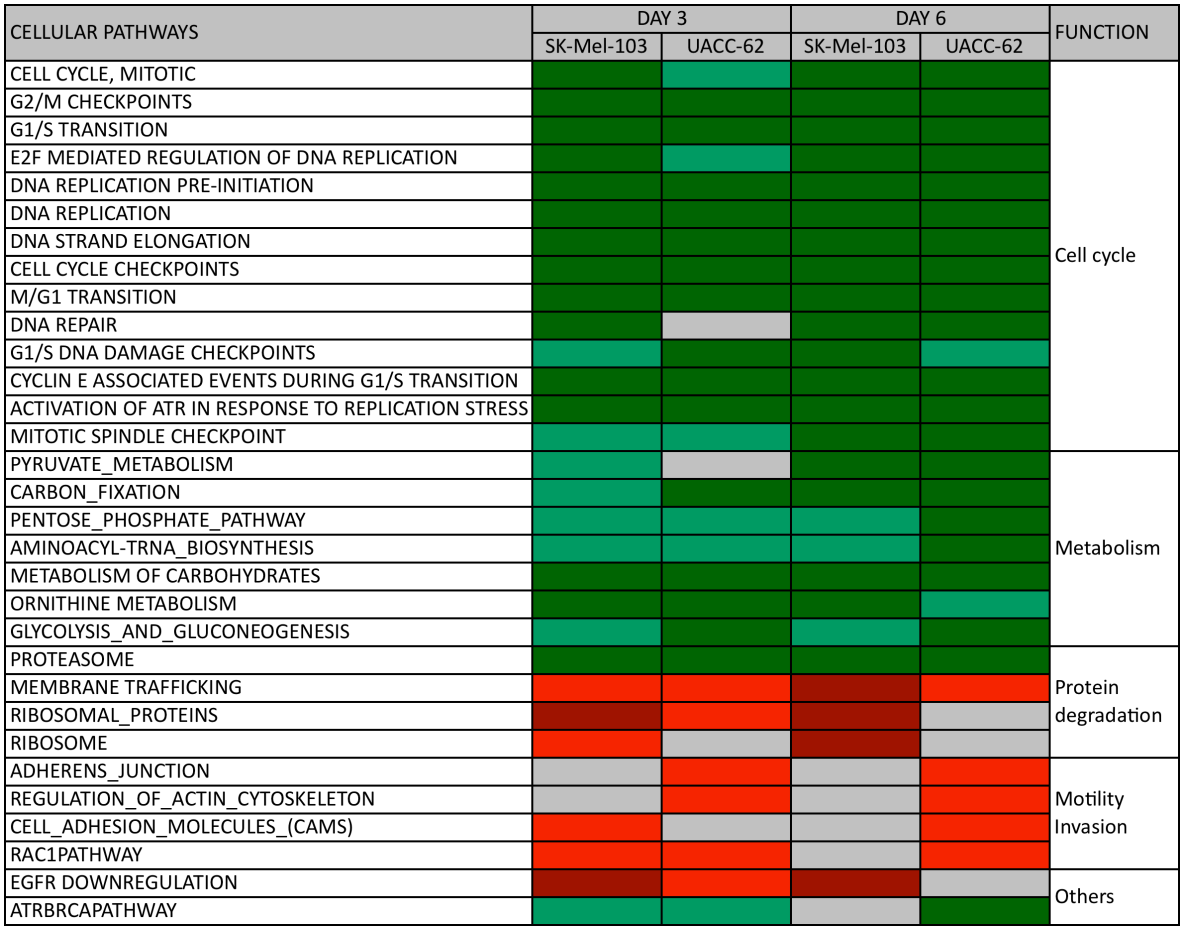

Figure 24. P62 depletion interferes with cell cycle and invasion functions. Altered pathways in SK-Mel-103 and UACC-62 cell lines at early (day 3) and late (day 6) time points after p62 depletion. Red, green and gray indicate upregulation, downregulation and no significant deregulation, respectively. Intensity of colors indicates the degree of significance (dark: FDR < 0.05; light: 0.05 < FDR < 0.25).

To validate the results obtained by cDNA arrays, some genes were selected for protein immunoblot analysis. As shown in Figure 25, after the depletion of p62, many proteins involved in cell cycle as Cyclins, Aurora proteins and Survivin were downregulated. Indeed, epidermal growth factor receptor (EGFR) and High-Mobility Group A2 (HMGA2) protein were upregulated after p62 depletion.

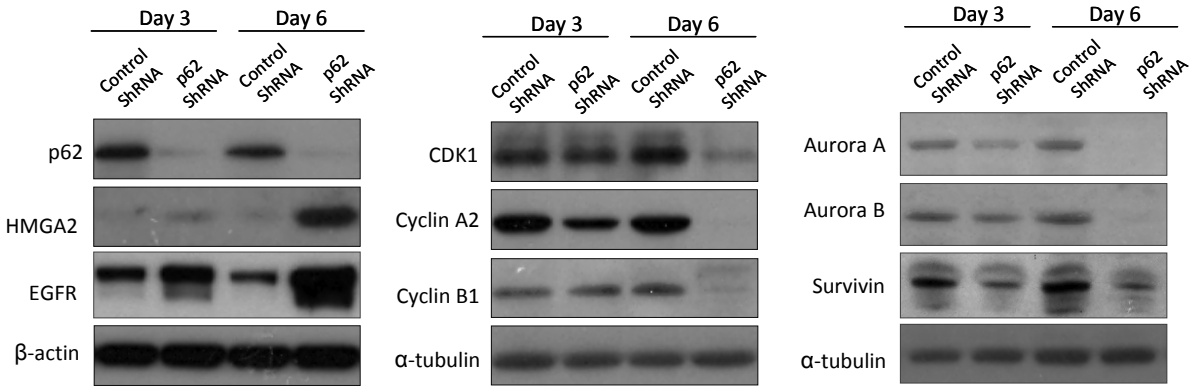

Figure 25. Validation of cDNA array data after p62 downregulation. Protein immunoblots against the indicated proteins on day 3 and 6 after lentiviral transduction with control and p62 shRNA in UACC-62 melanoma cells confirming the results found by cDNA arrays. α-tubulin or β-actin proteins were used as loading control.

In summary, transcriptomic analysis provides information that p62 is required for the proper expression of survival, cell cycle modulators and genes involved in cell migration and adhesion, justifying why the depletion of p62 interferes with melanoma proliferation and invasion.

4.3. The physiological relevance of Sequestosome 1/p62 in melanoma

4.3.1. The absence of p62 compromises melanoma tumor growth in mouse xenografts

The depletion of p62 blocks melanoma cell proliferation *in vitro.* To establish whether p62 depletion affects the ability of melanoma cells to form solid tumors *in vivo*, mouse xenograft models were generated.

SK-Mel-103 and UACC-62 melanoma cells were submitted to lentiviral-driven transduction of p62 shRNA and control shRNA. After 72 hours of lentiviral infection (before changes in cell morphology or proliferation), cells were collected and injected subcutaneously into the back region of athymic immunosuppressed mice (nude mice). A total of 9 nude mice were implanted with control cells (5 for UACC-62 and 4 for SK-Mel-103 cells) and 9 mice with p62-depleted cells (5 for UACC-62 and 4 for SK-Mel-103 cells). Growth of tumours was monitored for 4 weeks.

Importantly, melanoma control cells formed tumors that were visibly larger than the tumors formed by melanoma cells depleted for p62 (P<0.01) (Figure 26a). Immunohistochemical analysis of xenograft tumors confirmed the absence of p62 expression in the small tumors formed by p62-depleted cells (Figure 26b). Furthermore, cell flattening and morphological changes found in cultured p62-depleted cells were confirmed *in vivo* by an increase of cellular size of p62 shRNA tumor xenografts (P<0.0001) (Figure 26c).

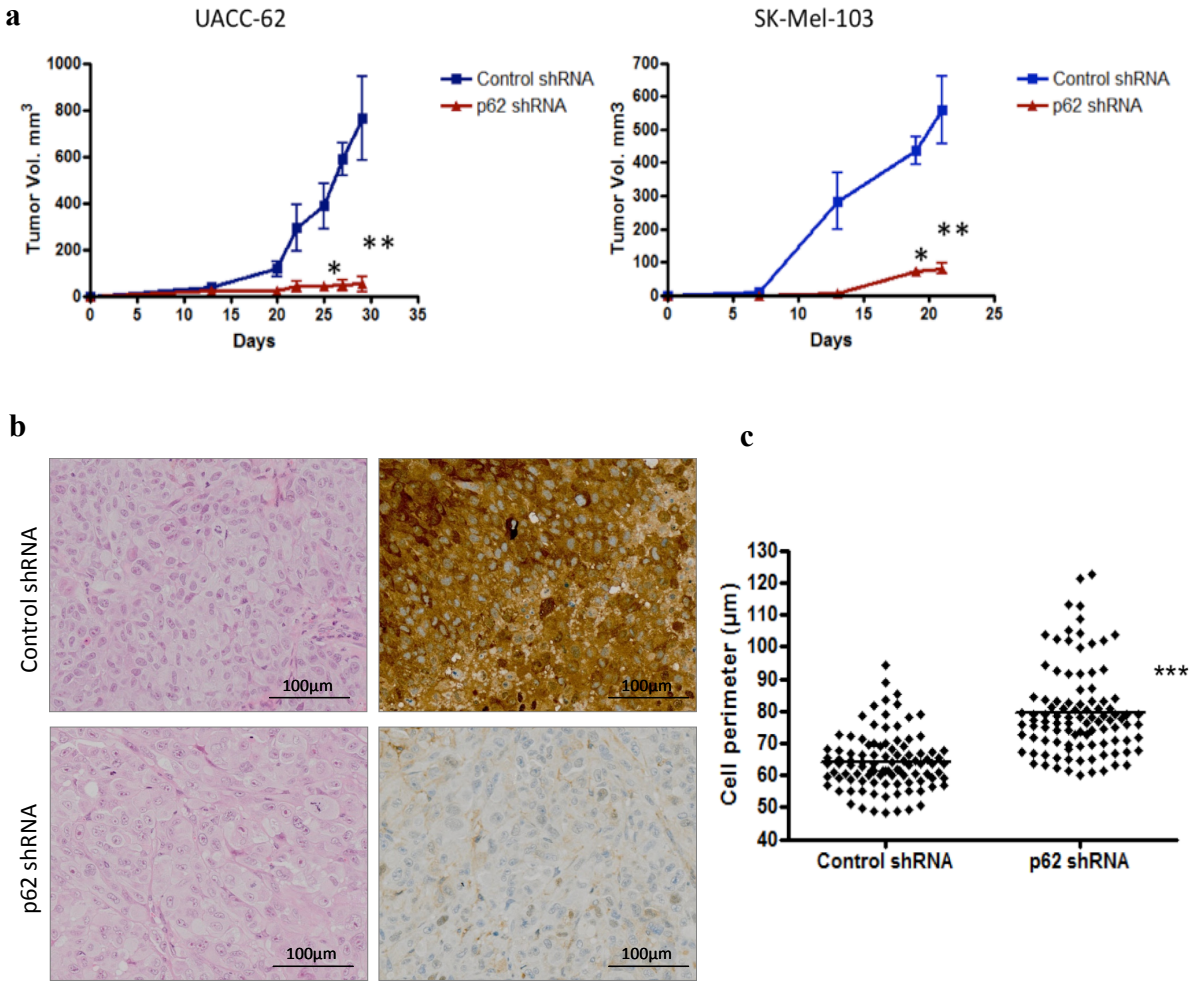

Figure 26. P62 depletion compromises tumor growth in mouse xenograft model. (a) Reduced tumorigenic potential of p62 depleted melanoma cells measured as a reduced growth of xenograft tumor ($1.0x10^6$ cells of the indicated cell lines) implanted subcutaneously in nude mice (P<0.01). (b) H&E and p62 immunohistochemical staining of xenograft tumors sections. (c) Quantification of cell perimeter of xenograft tumor sections showing increased size of p62 deficient melanoma cells *in vivo* (P<0.0001).

In summary, experiments performed with mouse xenograft model suggest that p62 is necessary for tumor proliferation *in vivo*.

4.3.2. P62 is associated with high proliferative index in human melanocytic tumors

The genetic depletion of p62 is responsible for melanoma cell arrest *in vitro* and in mouse xenograft model. To address the relation of p62 with a proliferative status in human melanoma specimens, the expression of p62 was compared to the expression of the proliferative marker Ki67. Consecutive sections of tissue microarrays of melanocytic tumors were submitted to p62 and Ki67 immunohistochemical staining. A total of 155 melanocytic tumors including 46 dermal nevi, 43 primary melanomas and 66 metastatic melanomas specimens were analyzed.

Interestingly, high expression of p62 in melanocytic tumors was related to an increased proliferative index (P<0.0001). On the other hand, negative expression of p62 was related to a low proliferative index (P<0.0001) (Figure 27). These results corroborate the hypothesis that p62 is related to cellular proliferation *in vivo*.

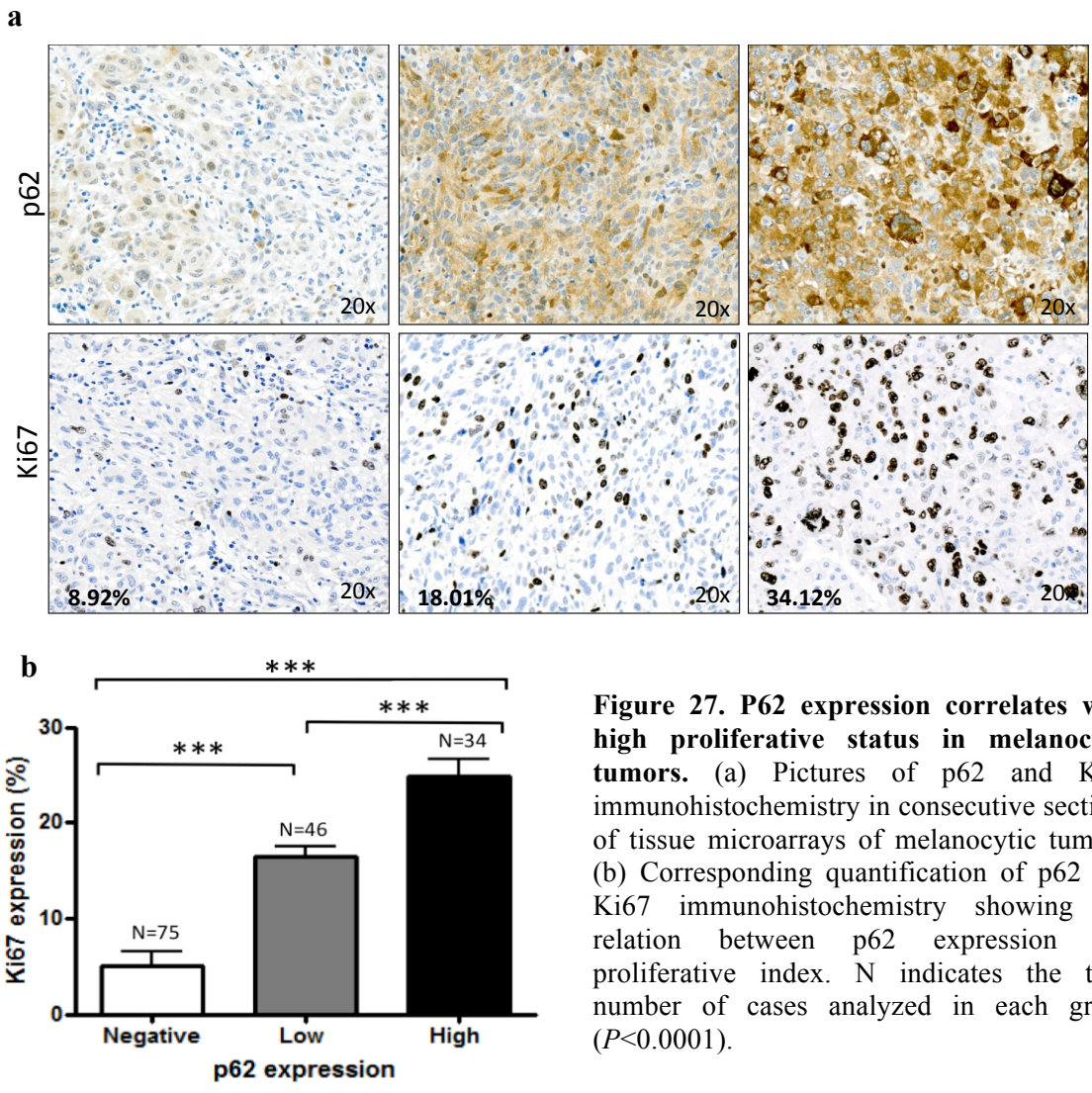

Figure 27. P62 expression correlates with high proliferative status in melanocytic tumors. (a) Pictures of p62 and Ki67 immunohistochemistry in consecutive sections of tissue microarrays of melanocytic tumors. (b) Corresponding quantification of p62 and Ki67 immunohistochemistry showing the relation between p62 expression and proliferative index. N indicates the total number of cases analyzed in each group (P<0.0001).

4.3.3. The expression of p62 increases the risk for metastatic disease in melanoma patients

For additional evaluation of the physiological relevance of p62, 105 specimens of vertical growth phase melanomas were randomly selected for survival analyses.

First, 105 melanoma samples were evaluated for the Breslow index and the presence of ulceration. P62 expression was evaluated by immunohistochemistry and classified as negative or positive. After the assessment of p62 expression, all clinical information was recompiled.

Results of immunohistochemical analyses showed that p62 stained positive in 76.2% (80/105) of primary melanoma specimens. P62 expression in melanomas was heterogeneous with an inter- and intratumor variability. In the cases of melanomas associated to dermal nevi, a clear positive expression of p62 in melanoma cells in contrast with the absence of p62 expression in nevi cells was observed. Surprisingly, nuclear expression of p62 was observed in 44.8% (47/105) of the VGP primary melanomas, some of them presenting the formation of big aggregates inside the nucleus (Figure 28).

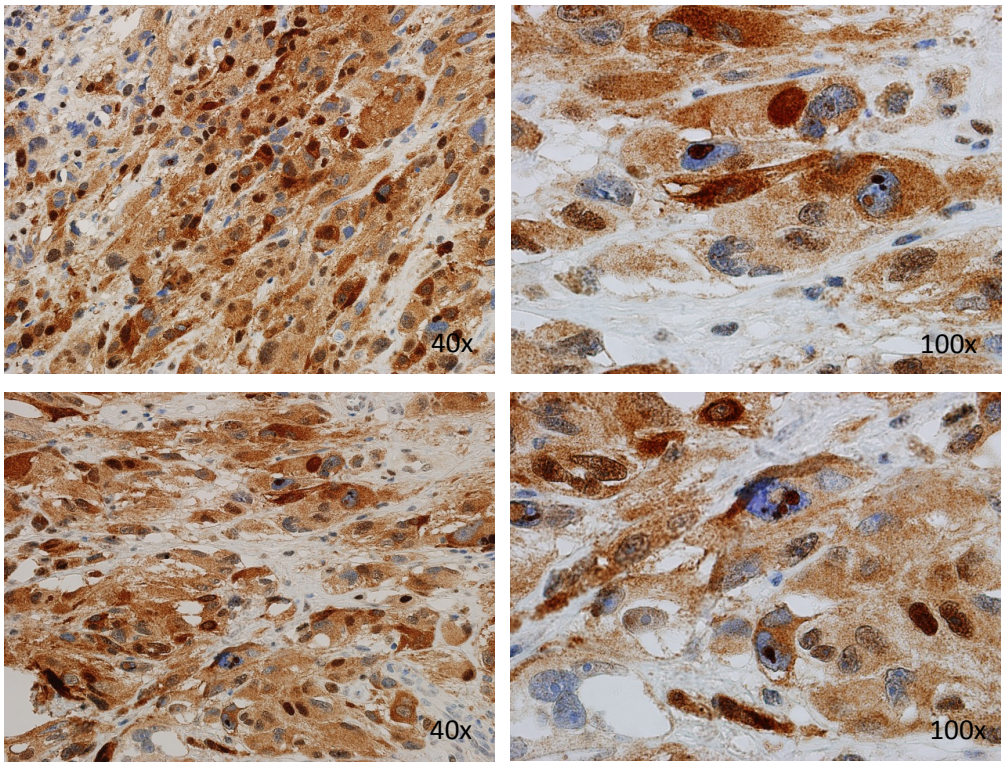

Figure 28. Nuclear expression of p62 protein in melanoma cells. Pictures of p62 immunohistochemistry in VGP melanoma specimen showing nuclear expression of p62 and the formation of p62 bodies inside the nucleus.

Clinical and histopathologic characteristics of the selected cases were analyzed. The age of the patients at diagnosis ranged from 25 to 99 years old (mean 58.51 years). Fifty-six patients were female and 49 male. All cases were confirmed as vertical growth phase melanomas, with Breslow ranging from 0.4 to x 19 mm (mean 3.66 mm) and 42% of the melanomas showing ulceration. Regarding the clinical staging at the moment of the diagnosis, 25 patients were classified as stage I, 28 patients as stage IIA, 39 patients as stage IIB and 13 patients as stage IIC.

The distribution of patients according to p62 expression is summarized in Table 9. Interestingly, the expression of p62 was related to greater tumor thickness. The mean of Breslow for p62 positive specimens was 3.99 mm, while 2.64 mm for p62 negative samples (P=0.05). The expression of p62 was also associated to a higher clinical stage (P=0.04). Most of the patients with undetectable p62 expression were classified at stage I (44%), while the majority of patients with detectable p62 expression were classified at stage IIB (40%). A superior prevalence of ulceration was found within melanomas expressing p62, however this difference was not statistical significant (44% versus 28%, P>0.05). Differences between distribution of sex and age were not significant.

Table 9. Distribution of 105 patients according to p62 expression:

Expression of p62 **Number of patients**		**Negative** N=25		**Positive** N=80		***P* value**
Women	N; %	13	52%	43	54%	0.878
Age (years)	Mean; SD	54.86	18.54	59.65	16.57	0.223
With Ulceration	N; %	7	28%	35	44%	0.161
Breslow (mm)	Mean; SD	2.64	2.23	3.99	3.17	**0.050**
Clinical Staging	N; %					**0.040**
	I	11	44%	14	18%	
	IIA	6	24%	22	28%	
	IIB	7	28%	32	40%	
	IIC	1	4%	12	15%	

The relation between p62 expression in primary melanomas and patient outcome was evaluated using Kaplan–Meier survival curves and COX analysis.

For survival curves, 105 patients were analysed. Four patients had to be excluded because of incomplete clinical information. Regarding disease free survival, from the total of 101 patients, 57 had developed metastasis within five years of melanoma diagnosis. Interestingly, Kaplan–Meier survival curves and COX analysis showed that patients with positive p62 expression presented an increased risk for development of metastasis, with a

hazard ratio (HR) of 2.96 (*P*=0.022). Remarkable, adjusting by Breslow and T3 category (T≤ T3a stage or T>T3a stage) the expression of p62 was an independent prognostic factor for the development of metastasis in melanoma patients (*P*=0.034 and *P*=0.044, respectively) (Figure 29 and Table 10).

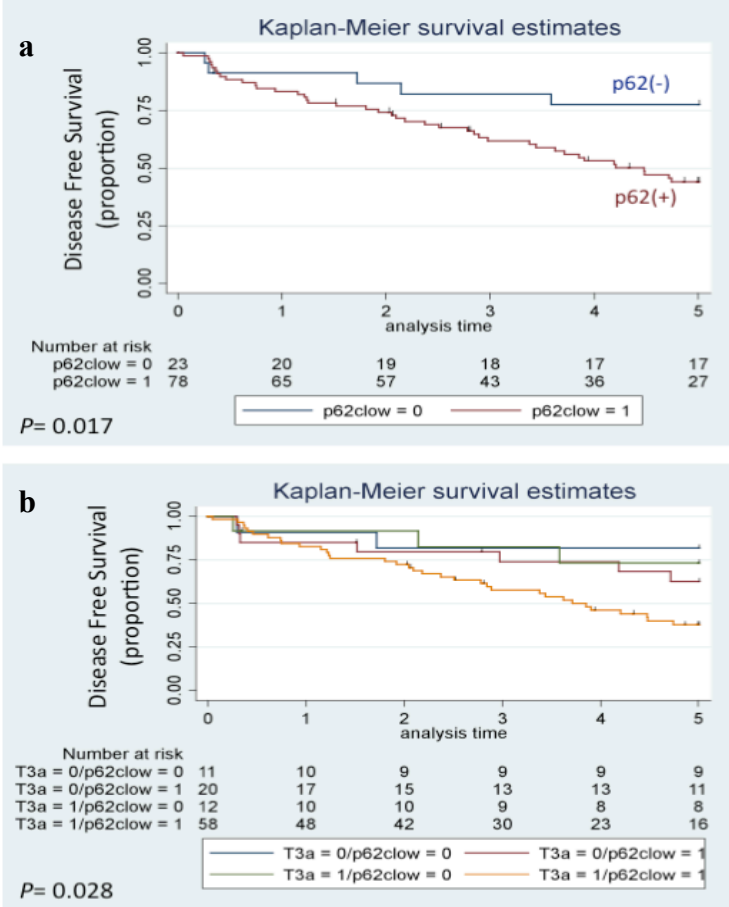

Figure 29. Disease Free Survival curves of 101 melanoma patients subgrouped by p62 expression. (a) Disease free survival curves subgrouped by p62 expression (p62clow0 = negative and p62clow1 = positive). (b) Disease free survival curves subgrouped by T3 category (T3a0 ≤ T3a stage and T3a1 > T3a stage) and p62 expression (p62clow0 = negative and p62clow1 = positive). Analysis time represents years of follow-up. The corresponding hazard ratios (HR) and 95% confidence intervals (95%CI) according to Cox regression analyses are shown in Table 10.

Table 10. Multivariated Cox regression analysis of pathological and clinical factors:

Disease Free Survival				
		HR	**95%CI**	***P***
p62		2.96	1.17 - 7.5	**0.022**
Adjusting by	**Breslow**	2.75	1.08 - 7.02	**0.034**
	Clinical staging	2.51	0.97 - 6.53	0.058
	T3 category	2.62	1.03 - 6.71	**0.044**

Regarding overall survival, from the total of 101 patients, 39 had died from melanoma in the first 5 years of diagnostic. Kaplan–Meier survival curves and COX analysis showed that patients with negative p62 expression had a higher median overall survival than patients with p62 expression, however the log-rank section test was not significant (HR=1.69, *P*=0.289) (Figure 30 and Table 11).

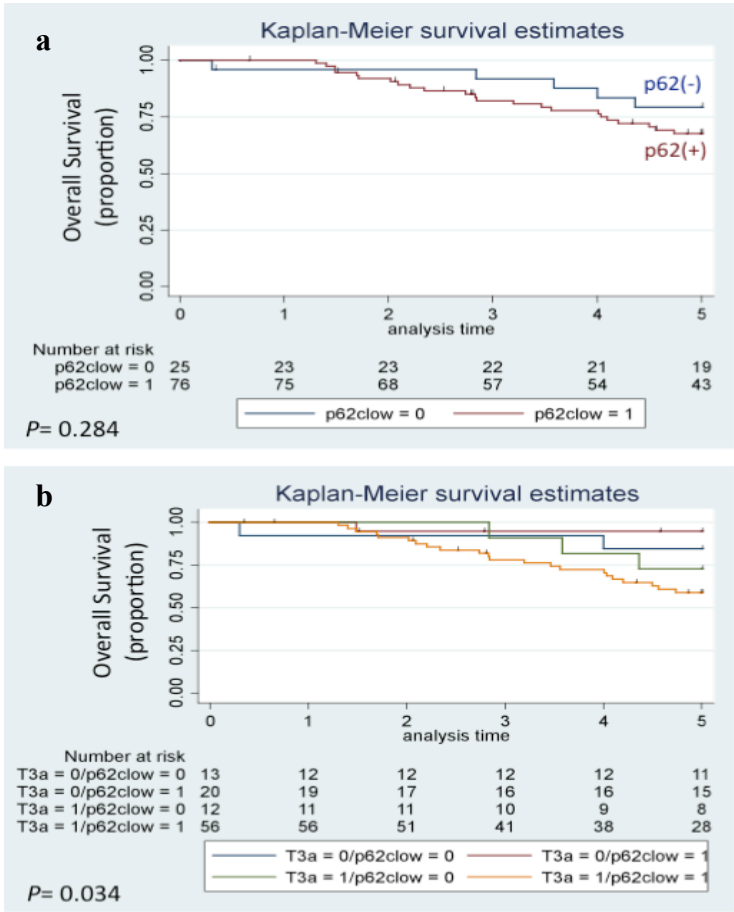

Figure 30. Overall Survival curves of 101 melanoma patients subgrouped by p62 expression. (a) Overall survival curves subgrouped by p62 expression (p62clow0 = negative and p62clow1 = positive). (b) Overall survival curves subgrouped by T3 category (T3a0 ≤ T3a stage and T3a1 > T3a stage) and p62 expression (p62clow0 = negative and p62clow1 = positive). Analysis time represents years of follow-up. The corresponding hazard ratios (HR) and 95% confidence intervals (95%CI) according to Cox regression analyses are shown in Table 11.

Table 11. Multivariated Cox regression analysis of pathological and clinical factors:

		Overall Survival		
		HR	**95%CI**	***P***
p62		1.69	0.64 - 4.44	0.289
Adjusting by	**Breslow**	1.5	0.56 - 4.0	0.416
	Clinical staging	0.96	0.36 - 2.6	0.939
	T3 category	1.26	0.47 - 3.37	0.641

In summary, clinical, pathological and survival analyses demonstrate that p62 expression is involved in melanoma patient follow-up and corroborate previous findings that p62 is implicated in melanoma tumor progression.

5. DISCUSSION

5. DISCUSSION

Melanoma is a complex cancer, which is aggressive and has a strong resistance to current available treatments. Despite all the studies generated in recent years, the mechanisms of melanoma progression remain not well understood. Sequestosome1/p62 is a multifunctional protein that promotes tumorigenesis by interfering with protein degradation machineries and activating pro-oncogenic signaling pathways (Duran et al., 2008; Mathew et al., 2009; Inami et al., 2011). Since one of the least understood aspects in melanoma is the modulation of protein degradation systems, p62 is an attractive candidate to be characterized in melanoma tumors.

5.1. The expression of Sequestosome 1/p62 in melanocytic tumors

During the last few years, some studies have identified the overexpression and accumulation of p62 in different human tumors (Thompson et al., 2003; Kitamura et al., 2006; Duran et al., 2008). Nevertheless, no data about the expression of p62 in melanoma tumors are available in the literature.

To address the expression of p62 in melanoma, tissue microarrays containing melanocytic lesions were immunohistochemically analyzed in this study. Surprisingly, p62 was undetectable in any of the benign dermal nevi analyzed. Dysplastic nevi, a controversial lesion considered by some authors as a melanoma precursor and by others as a malignant neoplasm (Ackerman, 1988; Roth et al., 1991; Skender-Kalnenas et al., 1995), showed low expression of p62 in one-third of samples. Interestingly, the expression of p62 increases in malignant lesions of melanocytes. Primary melanoma samples (radial and vertical growth phase melanomas) express p62 more frequently than dysplastic nevi. Moreover, the frequency and intensity of p62 expression increase with the progression of melanoma. Vertical growth phase melanomas, which are primary tumors with metastatic capacity (Barnhill et al., 1993), and metastatic lesions, considered the last stage in tumor progression, show higher expression of p62 than early stage of melanoma tumors (RGP). Hence, analysis of p62 expression in melanocytic tumors suggests that its expression is related to melanoma progression.

In addition, the comparison of p62 mRNA and protein levels between normal melanocytes and melanoma cell lines confirmed an overall upregulation of p62 in malignant cells. Interestingly, not only the amount of p62 protein expression but also the pattern of its

distribution was different in normal melanocytes and melanoma cells. In this study, immunofluorescence analyses confirmed the presence of p62 cytoplasmic aggregates in melanoma cells. In fact, p62 positive bodies were found both in cultured melanoma cells and melanoma tissue specimens stained by immunofluorescence. On the other hand, normal melanocytes showed a weak and diffuse pattern of p62 expression into the cytoplasm. Moreover, the aggregate pattern of p62 presented by melanoma cells was independent of p62 levels. Even increasing the expression of p62 in melanocytes to similar levels of those presented in melanoma, normal melanocytes cells were not able to form p62 cytosolic aggregates.

The presence of p62 cytoplasmic aggregates has been identified in different types of human cells and diseases, as neurodegenerative diseases, hepatitis, myositis and cancer (Lamark et al., 2003; Nagaoka et al., 2004; Bjørkøy et al., 2005). Although the relevance of p62 in such cellular inclusions is not clear, latest studies indicate that p62 presents a protective effect against cell death (Babu et al., 2005; Bjørkøy et al., 2005). The differential levels and pattern of p62 distribution in normal melanocytes and melanoma cells demonstrated in this study could be a consequence of differential metabolism and oxidative stress presented by such cells. Elevated metabolism of melanoma cells might be responsible for an increased production of damaged/misfolded proteins that needed to be degraded (Moenner et al., 2007; Kirkin et al., 2009). Consequently, through the ability of p62 to sequester aggregated proteins and shuttle proteins for proteasomal or autophagosomal degradation, p62 accumulation may represent a melanoma cell's attempt to rid itself of toxic substrates.

In an attempt to understand the regulation of p62 intracellular levels, melanoma cell lines were submitted to comparative genomic hybridization. Although alterations in the number of gene copies are a common feature of melanoma tumors (Curtin et al., 2005), CGH analyses performed in this study failed to identify amplification or gain of *SQSTM1* gene locus that could justify the upregulation of p62 in melanoma.

The increased p62 mRNA levels in melanoma cells compared to normal melanocytes led the hypothesis that p62 is transcriptionally regulated in melanoma tumors. In fact, the strong correlation between p62 mRNA and protein levels found in human melanoma specimens corroborates this hypothesis.

The transcriptional regulation of p62 was also described in others type of human tumors (Duran et al., 2008; Thompson et al., 2003). Nevertheless, a post-translational

regulation of p62 cannot be excluded in melanoma cells. As mentioned before, p62 protein is itself degraded by the autophagic machinery (Komatsu et al., 2007). Consequently, interferences in autophagy process could be a post-translational way to regulate the levels of p62 in melanoma. In fact, the deregulation of autophagy has been described in melanoma tumors (Checinska et al., 2011). While most authors support that autophagy is activated and necessary for melanoma progression (Hersey et al., 2008; Lazova et al., 2010; Han et al., 2011; Ma et al., 2011), others believe that autophagy represent a tumor suppressor mechanism and its activity decreases with melanoma progression (Miracco et al., 2010). The observation made in this study that melanoma cells accumulate p62 aggregates after treatment with chloroquine, an inhibitor of lysosome–autophagosome fusion (Solomon et al., 2009), suggests that p62 could also be post-translationally regulated in melanoma tumors.

Certain mechanisms of p62 regulation have been described in the literature. Duran and collaborators have shown that oncogenic RAS expression increases p62 mRNA levels through the activation of p62 promoter (Duran et al., 2008). Moreover, Galavotti and coworkers have demonstrated increased levels of p62 in $HRAS^{G12V}$ transformed cells (Galavotti et al., 2012).

Taking into account that the activation of the RAS/MEK/ERK pathway is a common feature of benign and malignant melanocytic tumors (Curtin et al., 2005), it was hypothesized in this study that *BRAF* or *RAS* mutations could regulate the expression of p62. Through lentiviral infection, normal melanocytes were transduced with the most frequently *BRAF*, *NRAS* and *HRAS* mutations found in melanocytic lesions. As already known, forced expression of such oncogenes in normal melanocytes led to a nonproliferative stage of the cells called senescence (Michaloglou et al., 2005; Denoyelle et al., 2006). Interestingly, the analyses of senescent melanocytes expressing $BRAF^{V600E}$, $NRAS^{Q61R}$ and $HRAS^{G12V}$ mutations performed in this work failed to show upregulation of p62 mRNA and protein levels.

In fact, the absence of p62 induction in senescent melanocytes corroborates the results obtained by IHC analysis of dermal nevi, which are benign lesions mostly composed by senescent melanocytes harboring $BRAF^{V600E}$ mutation (Pollock et al., 2003; Michaloglou et al., 2005). As mentioned before, all dermal nevi studied were negative for p62 expression.

Although $BRAF^{V600E}$ mutation is one of the most important triggers for melanoma initiation, genetic alterations, as PTEN or $p16^{INK4a}$ loss of function, are needed for the malignant transformation of melanocytes (Tsao et al., 2004; Denoyelle et al., 2006; Dankort et al., 2009). The absence of p62 overexpression in cultured senescent melanocytes and dermal

nevi specimens open the question of whether p62 upregulation is related to the malignant transformation of melanocytes. To answer this question, established melanoma mice models (Dankfort et al., 2009) were used for the analysis of p62 expression in lesions harboring $Braf^{V600E}$ mutation and $Braf^{V600E}$ mutation associated to *Pten* loss. Interestingly, p62 was overexpressed in malignant tumors formed by $Braf^{V600E}/Pten^{loxP/loxP}$ mice, meanwhile its expression was very low in benign lesions formed by $Braf^{V600E}$ mice.

Taken together, the study of senescent melanocytes and melanoma mice model performed in this study propose that p62 upregulation is related to the malignant transformation of melanocytes. Corroborating the transforming potential of p62 protein, Duran and coworkers have shown that the downregulation of p62 reduces the capacity of prostate cancer cells to form colonies in soft agar, a marker of cellular transformation (Duran et al., 2011). Moreover, Takeuchi and collaborators have demonstrated that 3T3 fibroblasts expressing *SQSTM1-ALK* translocation were able to form solid tumors when injected in immunodeficient mice (Takeuchi et al., 2011). Although results herein suggest the transforming potential of p62, additional analyses are necessary to fully elucidate the role of p62 in malignant transformation of melanocytes.

In summary, the upregulation of p62 in malignant cells, the presence of p62 cytoplasmic aggregates in melanoma cells but not in normal melanocytes and the increased expression of p62 in late stages of melanoma progression indicate that p62 plays a relevant role in melanoma survival and progression.

5.2. The function of Sequestosome 1/p62 in melanoma cells

The different levels and distribution of p62 in normal melanocytes and melanoma cells shown here, together with its exclusive overexpression in malignant lesions, suggest a relevant function of p62 in melanoma tumors. To study the function of p62, melanoma cell lines were submitted to genetic depletion of p62 by RNA interference technique.

The RNAi is a common technique used to determine the function of genes. For that, double-stranded RNAs are synthesized with sequences complementary to a target mRNA and introduced into the cells, promoting the degradation of mRNA. Consequently, RNAi promotes the posttranscriptional interruption of the expression of the target gene. The study of

effects and phenotypes obtained by RNAi introduction can thus elucidate the cellular role of the gene of interest (Shan et al., 2010).

In total, five different melanoma cell lines were depleted for p62. Fascinatingly, the genetic depletion of p62 was responsible for the inhibition of melanoma proliferation in all cell lines studied. After 5 to 6 days without p62 expression, melanoma cells arrested and changed the morphology, adopting a senescent-like phenotype. In fact, melanoma cells depleted for p62 presented an increase senescence-induced β-galactosidase activity (SA-β-Gal), a well-described marker for senescence (Michaloglou et al., 2005). Moreover, the effect of p62 depletion in cellular proliferation was independent of the genetic background presented by melanoma cells.

Interestinlgy, the dependence of p62 seems to occur only in melamoma cells. Normal melanocytes and fibroblasts depleted for p62 were still able to proliferate in culture and did not change their morphology or SA-β-Gal activity. The tumor cell selective requirement of p62 shown in this study could be justified by a differential metabolism and proliferative rate presented by normal and tumor cells.

Other studies have also described the influence of p62 in tumor growth. Many of them agree with results herein presented, that p62 is required for cellular proliferation (Mathew et al., 2009; Parkhitko et al., 2011; Duran et al., 2011). In fact, Duran and collaborators have shown that genetic depletion of p62 through RNAi reduces the proliferation of prostate cancer cells (Duran et al., 2011). However, other authors support that p62 restrain cellular proliferation (Linares et al, 2011; Galavotti et al., 2012). Opposite to Duran´s study, Galavotti and collaborators have described that the downregulation of p62 in glioblastoma stem cells promotes cell growth (Galavotti et al., 2012). Such contradictory results found in the literature suggest that the involvement of p62 in tumor proliferation might be tissue-specific.

After establishing the requirement of p62 in melanoma proliferation, the next question of this study was the influence of p62 in melanoma invasion capacity. Since invasive forms of melanoma specimens (vertical growth phase melanomas) express higher levels of p62 protein than non-invasive primary melanomas (radial growth phase melanomas), p62 may be required for cellular invasion capacity. Furthermore, melanoma cells depleted for p62 present morphologic changes compatible with cytoskeleton remodeling that could promote alterations in cellular adhesion and motility.

Fascinatingly, using Matrigel Matrix Invasion assay, this study demonstrated that the absence of p62 expression impairs the invasive capacity of highly metastatic melanoma cells

in vitro. Moreover, through a sophisticated artificial skin, which physiologically recapitulates the environment of melanoma cells (Li et al., 2011; Brohem et al., 2010), the overexpression of p62 turned non-invasive melanoma cells able to cross the basement membrane and invade the artificial dermis. These findings shown here confirm the recently published study of Galavotti and collaborators, where p62 contributes to the invasion capacity of glioblastoma multiforme cells (Galavotti et al., 2012).

One of the most well described functions of p62 is its involvement in protein degradation (Bjørkøy et al., 2005; Bjørkøy et al., 2006; Kirkin et al., 2009). Since the absence of p62 interferes with the proliferative and invasion capacity of melanoma cells, to understand the mechanism underlying such phenotypic changes, proteolytic systems were analyzed in p62 depleted cells.

Melanoma cells expressing green fluorescent protein fused to LC3 protein and cherry fluorescent protein fused to p62 were treated with an inductor (Rapamycin) or inhibitor (chloroquine) of autophagy.

As described before, through the LIR domain p62 binds to LC3 protein located in the membrane of autophagosomes and shuttles ubiquitinated and/or aggregates of proteins to autophagosomal degradation (Watanabe et al., 2011). The co-localization of p62 with LC3 protein after induction of autophagy, associated to an increased foci formation after inhibition of lysosome–autophagosome fusion (treatment with chloroquine) confirmed that p62 is involved in autophagy in melanoma cells.

Melanoma cells were then depleted for p62 and the autophagosome formation capacity was checked through the formation of LC3 foci and the quantification of the isoform LC3-II (tightly bound to the autophagosomal membrane). In both approaches, the depletion of p62 did not interfere with the autophagosome formation.

Through its UBA domain, p62 is able to bind ubiquitinated proteins and delivers them to proteasomal or autophagosomal degradation (Seibenhener et al., 2007; Kirkin et al., 2009). Unexpectedly, immunoblots of p62 depleted cells performed in this study failed to show an accumulation of ubiquitinaded proteins.

These results described above reveal that p62 is involved in autophagic degradation, however it is not required for the proper function of autophagy system. In fact, this result corroborates the study of Komatsu, which previously suggested that p62 knockout did not affect basal or starvation-induced autophagy (Komatsu et al., 2007).

Despite the fact that proteolytic systems are still functional in p62 depleted cells, the phenotypic changes found in such cells could be justified by a deficient delivery and degradation of specific partners of p62. Moreover, disturbance of proliferation and invasion capacity of melanoma cells could be justified by deregulation of intracellular signaling pathways, since p62 also works as an adaptor protein.

To comprehend the mechanism whereby p62 interferes with melanoma progression, two different cell lines were submitted to transcriptomic analysis. Melanoma cells were submitted to p62 depletion through RNAi and changes in gene expression profile were analyzed at early and late time points.

Transcriptomic analysis revealed broad changes in the expression profile of p62 depleted cells and the consequent deregulation of different cellular pathways. Several pathways involved in cell cycle regulation, DNA replication and DNA repair were downregulated at early time point after p62 depletion. This finding not only supports the involvement of p62 in cell cycle (Linares et al, 2011) but also adds new information about its implication in DNA repair and replication processes. Moreover, it also justifies why melanoma cells arrest in the absence of p62.

Recently, Galavotti and colleagues have published the unique study that describes the influence of p62 in tumoral invasion (Galavotti et al., 2012). However, these authors have not fully elucidated the mechanism underlying such involvement. Tanscriptomic analyses herein performed demonstrate for the first time that p62 is involved in cellular motility and invasion through deregulation of actin-cytoskeleton and adherent junction pathways. Moreover, the RAC1 pathway that promotes cell-cell adhesion and regulates cell motility (Kimura et al 2006; Sanz-Moreno et al., 2008) was also altered in p62 depleted cells. Interestingly, mutations in *RAC1* gene were recently described in 9.2% of sun-exposed melanomas. Indeed, it was the third most frequent mutation, after *BRAF* and *NRAS*, in this type of cutaneous melanoma (Kraurhammer et al., 2012).

Trancriptomic analyses performed in this study also demonstrated that p62 depletion alters metabolic and proteolytic pathways in melanoma cells, confirming previous published data (Seibenhener et al., 2007; Kirkin et al., 2009; Galavotti et al., 2012).

The depletion of p62 in melanoma cells in the present study also led to downregulation of Survivin mRNA and protein levels. Survivin is a member of the inhibitor of apoptosis protein (IAP) family. Survivin protein is clearly associated with cancer and its expression is related to drug resistance and poor prognosis. When located in the nucleus, it is involved in

mitosis regulation. In the cytoplasm, Survivin inhibits apoptosis through the interaction with Caspase-9 (Zangemeister-Wittke et al., 2004). The overexpression of Survivin has been described in melanoma tumors (Alonso et al., 2004) and is associated with reduced survival in melanoma patients (Gradilone et al., 2003; Takeuchi et al., 2005). Recently, it was described that Survivin enhances the migration and invasion ability of melanocytic cells (McKenzie et al., 2010). Transcriptomic analyses performed in this work demonstrated for the first time a relation between p62 and Survivin expression. In fact, downregulation of Survivin protein may justify p62 interference with proliferation and invasion capacity of melanoma cells.

The interruption of p62 expression was also responsible for the upregulation of HMGA2 protein. The HMGA family of proteins are architectural transcription factors that regulate the expression of numerous genes involved in cell growth, differentiation and cell death. This family of proteins consists of two members: HMGA1 and HMGA2. Usually, HMGAs are considered pro-oncogenic proteins. They can promote tumorigenesis and are upregulated in different tumors (Reeves, 2001; Young et al., 2007). Paradoxically, Narita and coworkers have described a novel role of HMGA proteins in cellular senescence. These authors found that HMGA accumulate on chromatin in senescent cells and promote proliferative arrest, thus acting as a tumor suppressor (Narita et al, 2006). Curiously, experiments performed in this study have shown that the depletion of p62 induces a senescence-like state of melanoma cells and produces overexpression of HMGA2 protein, corroborating the tumor suppressor role of HMGA2 proposed by Narita's group.

Surprisingly, the main signaling pathways regulated by p62 protein, NF-kB (Duran et al., 2008), mTOR (Duran et al., 2011) and Keap1-Nrf2 (Inami et al., 2011), were not altered in the transcriptomic experiment performed in this study. As mentioned before, the involvement of p62 in cancer is quite complex and its mechanism appears to be tissue-specific. In fact, Moscat's and Eileen White's groups have found divergent data concerning NF-kB regulation by p62 (Duran et al., 2008; Mathew et al., 2009). In consequence, further analyses are required to fully dissect the relation between p62 and those signaling pathways in melanoma progression.

In summary, alterations in cell cycle, metabolism and adhesion/motility pathways justify the inhibition of cellular proliferation, reduction of invasion capacity and morphologic changes suffered by p62 depleted melanoma cells. Thus, RNA interference and transcriptomic analyses confirm the relevance of p62 in melanoma progression.

5.3. The physiological relevance of Sequestosome 1/p62 in melanoma

After having established the implication of p62 in melanoma progression using an *in vitro* approach, the next step of this work was to identify the physiological relevance of p62.

To analyze if p62 interferes with tumor progression *in vivo,* mouse xenograft models were generated. Two different cell lines, harboring the $BRAF^{V600E}$ mutation or the $NRAS^{Q61R}$ mutation respectively, were genetically depleted for p62 expression and subcutaneously introduced in immunodeficient mice. Confirming *in vitro* results, the depletion of p62 inhibited tumor formation in these mice. Moreover, small tumors formed by p62 depleted cells showed an increased cell area, supporting the morphological changes observed *in vitro*.

Despite its limitations, xenograft models are still an useful tool to determine clinical application of potential targets identified in basic research. Moreover, it has been used in preclinical drug development for the past 30 years (Kelland, 2004; Céspedes et al., 2006). In this study, the significant blockage of tumor progression in a xenograft model suggests that the inhibition of p62 is a promising strategy for melanoma treatment. Furthermore, the tumor cell-selective interference with proliferation, independent of the genetic background of melanoma cells, supports the use of p62 as therapeutic target.

The relation of p62 with a proliferative status was also confirmed *in vivo* by a significant association between p62 expression and the proliferative marker Ki67 in human melanocytic tumors.

For further characterization of the physiological relevance of p62 in melanoma patients, 105 primary vertical growth phase tumors were randomly selected for survival analyses. Immunohistochemical study of these 105 primary melanomas demonstrated a quite heterogeneous pattern of p62 expression, with a vast inter- and intratumoral variability. Whether this heterogeneity could reflect cellular subpopulations with different biological features, is an open question to be answered in the future. In addition, although nuclear localization of p62 has been only sporadically reported in the literature (Bjørkøy et al., 2005; Pankiv et al., 2009), herein, nearly half of melanoma specimens showed nuclear expression.

Interestingly, classification of 105 patients according to p62 expression demonstrated that p62 expression is associated to melanoma thickness, which is the most important histopathological prognostic factor in melanoma tumors (Balch et al., 2009). Furthermore, categorizing patients by TNM stages, high expression of p62 is related to an increased stage of disease. Correlation of p62 expression with ulceration, age and sex was not statistical

significant. Altogether, these data indicate that p62 expression may predict an unfavorable outcome of melanoma patients.

In fact, survival analyses performed in this study revealed that positive expression of p62 in primary melanoma is a predictive factor for the development of metastasis in the first five years after diagnosis. Patients with positive expression of p62 in primary lesions presented an increased risk for metastatic disease. The multivariated analysis for Breslow index showed that p62 is an independent prognostic factor. Additionally, a multivariable analysis including both tumor thickness and ulceration was performed categorizing patients by p62 expression and clinical staging less or more than T3a. Interestingly, p62 positive staining was an independent prognostic factor for the development of metastasis in these two categories of patients. The expression of p62 also increases the risk of death in melanoma patients, however overall survival analyses were not statistical significant. Since most of melanoma patients relapse within 5 years after diagnosis, disease free survival results support the biological function of p62 in tumor progression.

In summary, by combining *in vitro* experiments with tissue specimens and survival analyses, p62 was characterized as a new biomarker of the development and regulation of melanoma progression. Since melanoma is noted for its propensity for lethal metastasis and therapeutic resistance, the characterization of p62 as a promising target for melanoma treatment has broad clinical relevance. In addition, results herein generated through a multidisciplinary approach highlight the importance of translational research for the identification of new therapeutic strategies.

6. CONCLUSIONS

6. CONCLUSIONS

Tissue expression patterns, *in vitro* experiments and survival analyses performed in this study support for the first time that Sequestosome1/p62 protein is required for melanoma progression. The results herein presented reveal Sequestosome1/p62 as a novel point of vulnerability for melanoma cells, thus representing a potential target for therapeutic intervention in melanoma patients. The main conclusions of this multidisciplinary study are listed below:

1. **P62 is overexpressed in melanoma cell lines and human melanoma specimens, particularly at invasive stages.** In contrast, normal melanocytes express low levels of p62 and dermal melanocytic nevi are virtually negative for p62 expression. The expression of p62 in melanoma tumors seems to be transcriptionally regulated without amplification of its genomic locus. In addition, increased levels of p62 observed in transformed cells but not in senescent melanocytes suggest that p62 expression is upregulated during malignant transformation of melanocytes.

2. **Genetic depletion of p62 invariably leads to a senescence-like phenotype, inhibition of cell proliferation and loss of invasion capacity of melanoma cells.** The requirement of p62 appears to be tumor cell selective since normal melanocytes and fibroblasts do not suffer phenotypic changes after p62 depletion. Moreover, cDNA array analysis points to various cellular pathways related to cellular growth and invasion capacity as new targets of p62 in melanoma cells.

3. The inhibition of cellular proliferation in **p62 depleted melanoma cells translates into a significant blockage of tumor growth in mouse xenograft model**. Furthermore, survival analysis corroborates the physiological relevance of p62 in melanoma progression, since **the expression of p62 in primary tumors identifies an at-risk group of patients for the subsequent development of metastasis.**

7. REFERENCES

7. REFERENCES

Ackerman AB. What naevus is dysplastic, a syndrome and the commonest precursor of malignant melanoma? A riddle and an answer. Histopathology. 1988 Sep;13(3):241-56.

Alonso SR, Ortiz P, Pollán M, Pérez-Gómez B, Sánchez L, Acuña MJ, Pajares R, Martínez-Tello FJ, Hortelano CM, Piris MA, Rodríguez-Peralto JL. Progression in cutaneous malignant melanoma is associated with distinct expression profiles: a tissue microarray-based study. Am J Pathol. 2004 Jan;164(1):193-203.

Alonso-Curbelo D, Soengas MS. Self-killing of melanoma cells by cytosolic delivery of dsRNA: wiring innate immunity for a coordinated mobilization of endosomes, autophagosomes and the apoptotic machinery in tumor cells. Autophagy. 2010 Jan;6(1):148-50.

Amaravadi RK, Yu D, Lum JJ, Bui T, Christophorou MA, Evan GI, Thomas-Tikhonenko A, Thompson CB. Autophagy inhibition enhances therapy-induced apoptosis in a Myc-induced model of lymphoma. J Clin Invest. 2007 Feb;117(2):326-36.

Atkins MB, Lotze MT, Dutcher JP, Fisher RI, Weiss G, Margolin K, Abrams J, Sznol M, Parkinson D, Hawkins M, Paradise C, Kunkel L, Rosenberg SA. High-dose recombinant interleukin 2 therapy for patients with metastatic melanoma: analysis of 270 patients treated between 1985 and 1993. J Clin Oncol. 1999 Jul;17(7):2105-16.

Babu JR, Geetha T, Wooten MW. Sequestosome 1/p62 shuttles polyubiquitinated tau for proteasomal degradation. J Neurochem. 2005 Jul;94(1):192-203.

Balch CM, Gershenwald JE, Soong SJ, Thompson JF, Atkins MB, Byrd DR, Buzaid AC, Cochran AJ, Coit DG, Ding S, Eggermont AM, Flaherty KT, Gimotty PA, Kirkwood JM, McMasters KM, Mihm MC Jr, Morton DL, Ross MI, Sober AJ, Sondak VK. Final version of 2009 AJCC melanoma staging and classification. J Clin Oncol. 2009 Dec 20;27(36):6199-206.

Bano D, Zanetti F, Mende Y, Nicotera P. Neurodegenerative processes in Huntington's disease. Cell Death Dis. 2011 Nov 10;2:e228.

Barnhill RL, Mihm MC Jr. The histopathology of cutaneous malignant melanoma. Semin Diagn Pathol. 1993 Feb;10(1):47-75.

Barrett MT, Scheffer A, Ben-Dor A, Sampas N, Lipson D, Kincaid R, et al. Comparative genomic hybridization using oligonucleotide microarrays and total genomic DNA. Proc NatlAcad Sci USA 2004;101:17765-70

Bauer J, Bastian BC. Distinguishing melanocytic nevi from melanoma by DNA copy number changes: comparative genomic hybridization as a research and diagnostic tool. Dermatol Ther. 2006 Jan-Feb;19(1):40-9.

Beaumont KA, Wong SS, Ainger SA, Liu YY, Patel MP, Millhauser GL, Smith JJ, Alewood PF, Leonard JH, Sturm RA. Melanocortin MC1 receptor in human genetics and model systems. Eur J Pharmacol. 2011 Jun 11;660(1):103-10.

Bjørkøy G, Lamark T, Brech A, Outzen H, Perander M, Overvatn A, Stenmark H, Johansen T. p62/SQSTM1 forms protein aggregates degraded by autophagy and has a protective effect on huntingtin-induced cell death. J Cell Biol. 2005 Nov 21;171(4):603-14.

Bjørkøy G, Lamark T, Johansen T. p62/SQSTM1: a missing link between protein aggregates and the autophagy machinery. Autophagy. 2006 Apr-Jun;2(2):138-9.

Braak H, Thal DR, Del Tredici K. Nerve cells immunoreactive for p62 in select hypothalamic and brainstem nuclei of controls and Parkinson's disease cases. J Neural Transm. 2011 May;118(5):809-19.

Breslow A: Thickness, cross-sectional areas, and depth of invasion inthe prognosis of cutaneous melanoma. Ann Surg 1970, 172:902–908.

Brohem CA, Cardeal LB, Tiago M, Soengas MS, Barros SB, Maria-Engler SS. Artificial skin in perspective: concepts and applications.Pigment Cell Melanoma Res. 2011 Feb;24(1):35-50.

Carey WP Jr, Thompson CJ, Synnestvedt M, Guerry D 4th, Halpern A, Schultz D, Elder DE. Dysplastic nevi as a melanoma risk factor in patients with familial melanoma. Cancer. 1994 Dec 15;74(12):3118-25.

Carswell R. Illustrations of the elementary forms of disease. London: Longman, Orme, Brown, Greene and Longman; 1838.

Céspedes MV, Casanova I, Parreño M, Mangues R. Mouse models in oncogenesis and cancer therapy. Clin Transl Oncol. 2006 May;8(5):318-29.

Chapman PB, Hauschild A, Robert C, Haanen JB, Ascierto P, Larkin J, Dummer R, Garbe C, Testori A, Maio M, Hogg D, Lorigan P, Lebbe C, Jouary T, Schadendorf D, Ribas A, O'Day SJ, Sosman JA, Kirkwood JM, Eggermont AM, Dreno B, Nolop K, Li J, Nelson B, Hou J, Lee RJ, Flaherty KT, McArthur GA; BRIM-3 Study Group. Improved survival with vemurafenib in melanoma with BRAF V600E mutation. N Engl J Med. 2011 Jun 30;364(26):2507-16.

Checinska A, Soengas MS. The gluttonous side of malignant melanoma: basic and clinical implications of macroautophagy. Pigment Cell Melanoma Res. 2011 Dec;24(6):1116-32.

Chin L, Garraway LA, Fisher DE. Malignant melanoma: genetics and therapeutics in the genomic era. Genes Dev. 2006 Aug 15;20(16):2149-82.

Cook MG, Robertson I. Melanocytic dysplasia and melanoma. Histopathology. 1985 Jun;9(6):647-58.

Cooper S. The first lines of the theory and practice of surgery. London: Longman; 1840.

Copple IM, Lister A, Obeng AD, Kitteringham NR, Jenkins RE, Layfield R, Foster BJ, Goldring CE, Park BK. Physical and functional interaction of sequestosome 1 with Keap1 regulates the Keap1-Nrf2 cell defense pathway. J Biol Chem. 2010 May 28;285(22):16782-8.

Curtin JA, Busam K, Pinkel D, Bastian BC. Somatic activation of KIT in distinct subtypes of melanoma. J Clin Oncol. 2006 Sep 10;24(26):4340-6.

Curtin JA, Fridlyand J, Kageshita T, Patel HN, Busam KJ, Kutzner H, Cho KH, Aiba S, Bröcker EB, LeBoit PE, Pinkel D, Bastian BC. Distinct sets of genetic alterations in melanoma. N Engl J Med. 2005 Nov 17;353(20):2135-47.

Dankort D, Curley DP, Cartlidge RA, Nelson B, Karnezis AN, Damsky WE Jr, You MJ, DePinho RA, McMahon M, Bosenberg M. Braf(V600E) cooperates with Pten loss to induce metastatic melanoma. Nat Genet. 2009 May;41(5):544-52.

Denoyelle C, Abou-Rjaily G, Bezrookove V, Verhaegen M, Johnson TM, Fullen DR, Pointer JN, Gruber SB, Su LD, Nikiforov MA, Kaufman RJ, Bastian BC, Soengas MS. Anti-oncogenic role of the endoplasmic reticulum differentially activated by mutations in the MAPK pathway. Nat Cell Biol. 2006 Oct;8(10):1053-63.

Duran A, Amanchy R, Linares JF, Joshi J, Abu-Baker S, Porollo A, Hansen M, Moscat J, Diaz-Meco MT.. p62 is a key regulator of nutrient sensing in the mTORC1 pathway. Mol Cell. 2011 Oct 7;44(1):134-46. doi: 10.1016/j.molcel.2011.06.038.

Duran A, Linares JF, Galvez AS, Wikenheiser K, Flores JM, Diaz-Meco MT, Moscat J. The signaling adaptor p62 is an important NF-kappaB mediator in tumorigenesis. Cancer Cell. 2008 Apr;13(4):343-54.

Durán A, Serrano M, Leitges M, Flores JM, Picard S, Brown JP, Moscat J, Diaz-Meco MT. The atypical PKC-interacting protein p62 is an important mediator of RANK-activated osteoclastogenesis. Dev Cell. 2004 Feb;6(2):303-9.

Espinosa E, Berrocal A, López Martín JA, González Cao M, Cerezuela P, Mayordomo JI, Martín Algarra S; Grupo Español de Melanoma (GEM). Advances in cutaneous melanoma. Clin Transl Oncol. 2012 May;14(5):325-32.

Fletcher O, Easton D, Anderson K, Gilham C, Jay M, Peto J. Lifetime risks of common cancers among retinoblastoma survivors. J Natl Cancer Inst. 2004 Mar 3;96(5):357-63.

Galavotti S, Bartesaghi S, Faccenda D, Shaked-Rabi M, Sanzone S, McEvoy A, Dinsdale D, Condorelli F, Brandner S, Campanella M, Grose R, Jones C, Salomoni P. The autophagy-associated factors DRAM1 and p62 regulate cell migration and invasion in glioblastoma stem cells. Oncogene. 2012 Apr 23.

Garraway LA, Widlund HR, Rubin MA, Getz G, Berger AJ, Ramaswamy S, Beroukhim R, Milner DA, Granter SR, Du J, Lee C, Wagner SN, Li C, Golub TR, Rimm DL, Meyerson ML, Fisher DE, Sellers WR. Integrative genomic analyses identify MITF as a lineage survival oncogene amplified in malignant melanoma. Nature. 2005 Jul 7;436(7047):117-22.

Geetha T, Wooten MW. Structure and functional properties of the ubiquitin binding protein p62. FEBS Lett. 2002 Feb 13;512(1-3):19-24.

Gimotty PA, Van Belle P, Elder DE, Murry T, Montone KT, Xu X, Hotz S, Raines S, Ming ME, Wahl P, Guerry D. Biologic and prognostic significance of dermal Ki67 expression, mitoses, and tumorigenicity in thin invasive cutaneous melanoma. J Clin Oncol. 2005 Nov 1;23(31):8048-56.

Goel VK, Lazar AJ, Warneke CL, Redston MS, Haluska FG. Examination of mutations in BRAF, NRAS, and PTEN in primary cutaneous melanoma. J Invest Dermatol. 2006 Jan;126(1):154-60.

Gradilone A, Gazzaniga P, Ribuffo D, Scarpa S, Cigna E, Vasaturo F, Bottoni U, Innocenzi D, Calvieri S, Scuderi N, Frati L, Agliano AM. Survivin, bcl-2, bax, and bcl-X gene expression in sentinel lymph nodes from melanoma patients. J Clin Oncol 2003;21:306–312.

Han C, Sun B, Wang W, Cai W, Lou D, Sun Y, Zhao X. Overexpression of microtubule-associated protein-1 light chain 3 is associated with melanoma metastasis and vasculogenic mimicry. Tohoku J Exp Med. 2011;223(4):243-51.

Hanahan D, Weinberg RA. Hallmarks of cancer: the next generation. Cell. 2011 Mar 4;144(5):646-74.

Hansson J. Familial cutaneous melanoma. Adv Exp Med Biol. 2010;685:134-45.

Harbour JW, Onken MD, Roberson ED, Duan S, Cao L, Worley LA, Council ML, Matatall KA, Helms C, Bowcock AM. Frequent mutation of BAP1 in metastasizing uveal melanomas. Science. 2010 Dec 3;330(6009):1410-3.

Hayden MS, Ghosh S. Signaling to NF-kappaB. Genes Dev. 2004 Sep 15;18(18):2195-224.

Hodi FS, O'Day SJ, McDermott DF, Weber RW, Sosman JA, Haanen JB, Gonzalez R, Robert C, Schadendorf D, Hassel JC, Akerley W, van den Eertwegh AJ, Lutzky J, Lorigan P, Vaubel JM, Linette GP, Hogg D, Ottensmeier CH, Lebbé C, Peschel C, Quirt I, Clark JI, Wolchok JD, Weber JS, Tian J, Yellin MJ, Nichol GM, Hoos A, Urba WJ. Improved survival with ipilimumab in patients with metastatic melanoma. N Engl J Med. 2010 Aug 19;363(8):711-23.

Hoek KS. DNA microarray analyses of melanoma gene expression: a decade in the mines. Pigment Cell Res. 2007 Dec;20(6):466-84.

Inami Y, Waguri S, Sakamoto A, Kouno T, Nakada K, Hino O, Watanabe S, Ando J, Iwadate M, Yamamoto M, Lee MS, Tanaka K, Komatsu M. Persistent activation of Nrf2 through p62 in hepatocellular carcinoma cells. J Cell Biol. 2011 Apr 18;193(2):275-84.

Inoue D, Suzuki T, Mitsuishi Y, Miki Y, Suzuki S, Sugawara S, Watanabe M, Sakurada A, Endo C, Uruno A, Sasano H, Nakagawa T, Satoh K, Tanaka N, Kubo H, Motohashi H, Yamamoto M. Accumulation of p62/SQSTM1 is associated with poor prognosis in patients with lung adenocarcinoma. Cancer Sci. 2012 Apr;103(4):760-6.

Jain A, Lamark T, Sjøttem E, Larsen KB, Awuh JA, Øvervatn A, McMahon M, Hayes JD, Johansen T. p62/SQSTM1 is a target gene for transcription factor NRF2 and creates a positive feedback loop by inducing antioxidant response element-driven gene transcription. J Biol Chem. 2010 Jul 16;285(29):22576-91

Jin Z, Li Y, Pitti R, Lawrence D, Pham VC, Lill JR, Ashkenazi A. Cullin3-based polyubiquitination and p62-dependent aggregation of caspase-8 mediate extrinsic apoptosis signaling. Cell. 2009 May 15;137(4):721-35.

Joung I, Strominger JL, Shin J. Molecular cloning of a phosphotyrosine-independent ligand of the p56lck SH2 domain. Proc Natl Acad Sci U S A. 1996 Jun 11;93(12):5991-5.

Kallioniemi OP, Wagner U, Kononen J, Sauter G. Tissue microarray technology for high-throughput molecular profiling of cancer. Hum Mol Genet. 2001 Apr;10(7):657-62.

Kelland LR. Of mice and men: values and liabilities of the athymic nude mouse model in anticancer drug development. Eur J Cancer. 2004 Apr;40(6):827-36.

Kim JY, Ozato K. The sequestosome 1/p62 attenuates cytokine gene expression in activated macrophages by inhibiting IFN regulatory factor 8 and TNF receptor-associated factor 6/NF-kappaB activity. J Immunol. 2009 Feb 15;182(4):2131-40.

Kimura K, Kawamoto K, Teranishi S, Nishida T. Role of Rac1 in fibronectin-induced adhesion and motility of human corneal epithelial cells. Invest Ophthalmol Vis Sci. 2006 Oct;47(10):4323-9.

Kirkin V, McEwan DG, Novak I, Dikic I. A role for ubiquitin in selective autophagy. Mol Cell. 2009 May 15;34(3):259-69.

Kirkwood JM, Ibrahim JG, Sondak VK, Richards J, Flaherty LE, Ernstoff MS, Smith TJ, Rao U, Steele M, Blum RH. High- and low-dose interferon alfa-2b in high-risk melanoma: first analysis of intergroup trial E1690/S9111/C9190. J Clin Oncol. 2000 Jun;18(12):2444-58.

Kitamura H, Torigoe T, Asanuma H, Hisasue SI, Suzuki K, Tsukamoto T, Satoh M, Sato N. Cytosolic overexpression of p62 sequestosome 1 in neoplastic prostate tissue. Histopathology. 2006 Jan;48(2):157-61.

Komatsu M, Kurokawa H, Waguri S, Taguchi K, Kobayashi A, Ichimura Y, Sou YS, Ueno I, Sakamoto A, Tong KI, Kim M, Nishito Y, Iemura S, Natsume T, Ueno T, Kominami E, Motohashi H, Tanaka K, Yamamoto M. The selective autophagy substrate p62 activates the stress responsive transcription factor Nrf2 through inactivation of Keap1. Nat Cell Biol. 2010 Mar;12(3):213-23.

Komatsu M, Waguri S, Koike M, Sou YS, Ueno T, Hara T, Mizushima N, Iwata J, Ezaki J, Murata S, Hamazaki J, Nishito Y, Iemura S, Natsume T, Yanagawa T, Uwayama J, Warabi E, Yoshida H, Ishii T, Kobayashi A, Yamamoto M, Yue Z, Uchiyama Y, Kominami E, Tanaka K. Homeostatic levels of p62 control cytoplasmic inclusion body formation in autophagy-deficient mice. Cell. 2007 Dec 14;131(6):1149-63.

Kononen J, Bubendorf L, Kallioniemi A, Bärlund M, Schraml P, Leighton S, Torhorst J, Mihatsch MJ, Sauter G, Kallioniemi OP. Tissue microarrays for high-throughput molecular profiling of tumor specimens. Nat Med. 1998 Jul;4(7):844-7.

Krauthammer M, Kong Y, Ha BH, Evans P, Bacchiocchi A, McCusker JP, Cheng E, Davis MJ, Goh G, Choi M, Ariyan S, Narayan D, Dutton-Regester K, Capatana A, Holman EC, Bosenberg M, Sznol M, Kluger HM, Brash DE, Stern DF, Materin MA, Lo RS, Mane S, Ma S, Kidd KK, Hayward NK, Lifton RP, Schlessinger J, Boggon TJ, Halaban R. Exome sequencing identifies recurrent somatic RAC1 mutations in melanoma. Nat Genet. 2012 Sep;44(9):1006-14.

Kroemer G, Mariño G, Levine B. Autophagy and the integrated stress response. Mol Cell. 2010 Oct 22;40(2):280-93.

Kudchadkar R, Paraiso KH, Smalley KS. Targeting mutant BRAF in melanoma: current status and future development of combination therapy strategies. Cancer J. 2012 Mar-Apr;18(2):124-31.

Kurihara N, Hiruma Y, Zhou H, Subler MA, Dempster DW, Singer FR, Reddy SV, Gruber HE, Windle JJ, Roodman GD. Mutation of the sequestosome 1 (p62) gene increases osteoclastogenesis but does not induce Paget disease. J Clin Invest. 2007 Jan;117(1):133-42.

Kuusisto E, Parkkinen L, Alafuzoff I. Morphogenesis of Lewy bodies: dissimilar incorporation of alpha-synuclein, ubiquitin, and p62. J Neuropathol Exp Neurol. 2003 Dec;62(12):1241-53.

Kuusisto E, Salminen A, Alafuzoff I. Early accumulation of p62 in neurofibrillary tangles in Alzheimer's disease: possible role in tangle formation. Neuropathol Appl Neurobiol. 2002 Jun;28(3):228-37.

Laennec RTH. Extrait au memoire de M Laennec, sur les melanoses.
Bull Ecole Soc Med Paris. 1812;1:24.

Lamark T, Perander M, Outzen H, Kristiansen K, Øvervatn A, Michaelsen E, Bjørkøy G, Johansen T. Interaction codes within the family of mammalian Phox and Bem1p domain-containing proteins. J Biol Chem. 2003 Sep 5;278(36):34568-81.

Lau A, Wang XJ, Zhao F, Villeneuve NF, Wu T, Jiang T, Sun Z, White E, Zhang DD. A noncanonical mechanism of Nrf2 activation by autophagy deficiency: direct interaction between Keap1 and p62. Mol Cell Biol. 2010 Jul;30(13):3275-85.

Laver NV, McLaughlin ME, Duker JS. Ocular melanoma. Arch Pathol Lab Med. 2010 Dec;134(12):1778-84.

Layfield R, Ciani B, Ralston SH, Hocking LJ, Sheppard PW, Searle MS, Cavey JR. Structural and functional studies of mutations affecting the UBA domain of SQSTM1 (p62) which cause Paget's disease of bone.Biochem Soc Trans. 2004 Nov;32(Pt 5):728-30.

Layfield R, Searle MS.Disruption of ubiquitin-mediated processes in diseases of the brain and bone. Biochem Soc Trans. 2008 Jun;36(Pt 3):469-71.

Lazova R, Klump V, Pawelek J. Autophagy in cutaneous malignant melanoma.J Cutan Pathol. 2010 Feb;37(2):256-68.

LeBoit, P., Burg, G., Weedon, D., and Sarasain, A.. Pathology and Genetics of Skin Tumours. World Health Organization Classification of Tumours. 2006 (Lyon: IARC Press).

Lee SJ, Pfluger PT, Kim JY, Nogueiras R, Duran A, Pagès G, Pouysségur J, Tschöp MH, Diaz-Meco MT, Moscat J. A functional role for the p62-ERK1 axis in the control of energy homeostasis and adipogenesis. EMBO Rep. 2010 Mar;11(3):226-32.

Leve F, Morgado-Díaz JA. Rho GTPase signaling in the development of colorectal cancer. J Cell Biochem. 2012 Aug;113(8):2549-59.

Levine B, Kroemer G. Autophagy in the pathogenesis of disease. Cell. 2008 Jan 11;132(1):27-42.

Li L, Fukunaga-Kalabis M, Herlyn M. The three-dimensional human skin reconstruct model: a tool to study normal skin and melanoma progression. J Vis Exp. 2011 Aug 3;(54). pii: 2937. doi: 10.3791/2937.

Linares JF, Amanchy R, Greis K, Diaz-Meco MT, Moscat J. Phosphorylation of p62 by cdk1 controls the timely transit of cells through mitosis and tumor cell proliferation. Mol Cell Biol. 2011 Jan;31(1):105-17.

Ling J, Kang Y, Zhao R, Xia Q, Lee DF, Chang Z, Li J, Peng B, Fleming JB, Wang H, Liu J, Lemischka IR, Hung MC, Chiao PJ. KrasG12D-induced IKK2/β/NF-κB activation by IL-1α and p62 feedforward loops is required for development of pancreatic ductal adenocarcinoma. Cancer Cell. 2012 Jan 17;21(1):105-20.

Marino ML, Fais S, Djavaheri-Mergny M, Villa A, Meschini S, Lozupone F, Venturi G, Della Mina P, Pattingre S, Rivoltini L, Codogno P, De Milito A. Proton pump inhibition induces autophagy as a survival mechanism following oxidative stress in human melanoma cells. Cell Death Dis. 2010 Oct 21;1:e87.

Márquez-Rodas I, Martín Algarra S, Avilés Izquierdo JA, Custodio Cabello S, Martín M. A new era in the treatment of melanoma: from biology to clinical practice. Clin Transl Oncol. 2011 Nov;13(11):787-92.

Martin P, Diaz-Meco MT, Moscat J. The signaling adapter p62 is an important mediator of T helper 2 cell function and allergic airway inflammation. EMBO J. 2006 Aug 9;25(15):3524-33.

Martín-Sánchez E, Sánchez-Beato M, Rodríguez ME, Sánchez-Espiridión B, Gómez-Abad C, Bischoff JR, Piris MA, García-Orad A, García JF. HDAC inhibitors induce cell cycle arrest, activate the apoptotic extrinsic pathway and synergize with a novel PIM inhibitor in Hodgkin lymphoma-derived cell lines. Br J Haematol. 2011 Feb;152(3):352-6.

Mathew R, Karp CM, Beaudoin B, Vuong N, Chen G, Chen HY, Bray K, Reddy A, Bhanot G, Gelinas C, Dipaola RS, Karantza-Wadsworth V, White E. Autophagy suppresses tumorigenesis through elimination of p62. Cell. 2009 Jun 12;137(6):1062-75.

McKenzie JA, Grossman D. Role of the apoptotic and mitotic regulator survivin in melanoma. Anticancer Res. 2012 Feb;32(2):397-404.

McKenzie JA, Liu T, Goodson AG, Grossman D. Survivin enhances motility of melanoma cells by supporting Akt activation and {alpha}5 integrin upregulation. Cancer Res. 2010 Oct 15;70(20):7927-37.

Mehrpour M, Esclatine A, Beau I, Codogno P. Overview of macroautophagy regulation in mammalian cells. Cell Res. 2010 Jul;20(7):748-62.

Mercer KE, Pritchard CA. Raf proteins and cancer: B-Raf is identified as a mutational target. Biochim Biophys Acta. 2003 Jun 5;1653(1):25-40.

Michaloglou C, Vredeveld LC, Soengas MS, Denoyelle C, Kuilman T, van der Horst CM, Majoor DM, Shay JW, Mooi WJ, Peeper DS. BRAFE600-associated senescence-like cell cycle arrest of human naevi. Nature. 2005 Aug 4;436(7051):720-4.

Michou L, Morissette J, Gagnon ER, Marquis A, Dellabadia M, Brown JP, Siris ES. Novel SQSTM1 mutations in patients with Paget's disease of bone in an unrelated multiethnic American population.Bone. 2011 Mar 1;48(3):456-60.

Miracco C, Cevenini G, Franchi A, Luzi P, Cosci E, Mourmouras V, Monciatti I, Mannucci S, Biagioli M, Toscano M, Moretti D, Lio R, Massi D. Beclin 1 and LC3 autophagic gene expression in cutaneous melanocytic lesions. Hum Pathol. 2010 Apr;41(4):503-12.

Miyoshi J, Takai Y. Structural and functional associations of apical junctions with cytoskeleton. Biochim Biophys Acta. 2008 Mar;1778(3):670-91.

Mizuno Y, Amari M, Takatama M, Aizawa H, Mihara B, Okamoto K. Immunoreactivities of p62, an ubiqutin-binding protein, in the spinal anterior horn cells of patients with amyotrophic lateral sclerosis. J Neurol Sci. 2006 Nov 1;249(1):13-8.

Moenner M, Pluquet O, Bouchecareilh M, Chevet E. Integrated endoplasmic reticulum stress responses in cancer. Cancer Res. 2007 Nov 15;67(22):10631-4.

Morissette J, Laurin N, Brown JP. Sequestosome 1: mutation frequencies, haplotypes, and phenotypes in familial Paget's disease of bone. J Bone Miner Res. 2006 Dec;21 Suppl 2:P38-44.

Moscat J, Diaz-Meco MT, Albert A, Campuzano S.Cell signaling and function organized by PB1 domain interactions. Mol Cell. 2006 Sep 1;23(5):631-40.

Moscat J, Diaz-Meco MT. Feedback on fat: p62-mTORC1-autophagy connections. Cell. 2011 Nov 11;147(4):724-7.

Mujtaba T, Dou QP. Advances in the understanding of mechanisms and therapeutic use of bortezomib. Discov Med. 2011 Dec;12(67):471-80.

Nagaoka U, Kim K, Jana NR, Doi H, Maruyama M, Mitsui K, Oyama F, Nukina N. Increased expression of p62 in expanded polyglutamine-expressing cells and its association with polyglutamine inclusions. J Neurochem. 2004 Oct;91(1):57-68.

Najat D, Garner T, Hagen T, Shaw B, Sheppard PW, Falchetti A, Marini F, Brandi ML, Long JE, Cavey JR, Searle MS, Layfield R. Characterization of a non-UBA domain missense mutation of sequestosome 1 (SQSTM1) in Paget's disease of bone. J Bone Miner Res. 2009 Apr;24(4):632-42.

Nakano T, Nakaso K, Nakashima K, Ohama E. Expression of ubiquitin-binding protein p62 in ubiquitin-immunoreactive intraneuronal inclusions in amyotrophic lateral sclerosis with dementia: analysis of five autopsy cases with broad clinicopathological spectrum. Acta Neuropathol. 2004 Apr;107(4):359-64.

Narita M, Narita M, Krizhanovsky V, Nuñez S, Chicas A, Hearn SA, Myers MP, Lowe SW. A novel role for high-mobility group a proteins in cellular senescence and heterochromatin formation. Cell. 2006 Aug 11;126(3):503-14.

NCCN Clinical Practice Guidelines in Oncology (NCCN Guidelines TM). Melanoma v2.2013. www.nccn.org.

Nogalska A, Terracciano C, D'Agostino C, King Engel W, Askanas V. p62/SQSTM1 is overexpressed and prominently accumulated in inclusions of sporadic inclusion-body myositis muscle fibers, and can help differentiating it from polymyositis and dermatomyositis. Acta Neuropathol. 2009 Sep;118(3):407-13.

Pankiv S, Lamark T, Bruun JA, Øvervatn A, Bjørkøy G, Johansen T. Nucleocytoplasmic shuttling of p62/SQSTM1 and its role in recruitment of nuclear polyubiquitinated proteins to promyelocytic leukemia bodies.J Biol Chem. 2010 Feb 19;285(8):5941-53.

Parkhitko A, Myachina F, Morrison TA, Hindi KM, Auricchio N, Karbowniczek M, Wu JJ, Finkel T, Kwiatkowski DJ, Yu JJ, Henske EP. Tumorigenesis in tuberous sclerosis complex is autophagy and p62/sequestosome 1 (SQSTM1)-dependent.Proc Natl Acad Sci U S A. 2011 Jul 26;108(30):12455-60.

Pollock PM, Harper UL, Hansen KS, Yudt LM, Stark M, Robbins CM, Moses TY, Hostetter G, Wagner U, Kakareka J, Salem G, Pohida T, Heenan P, Duray P, Kallioniemi O, Hayward NK, Trent JM, Meltzer PS. High frequency of BRAF mutations in nevi. Nat Genet. 2003 Jan;33(1):19-20.

Pópulo H, Lopes JM, Soares P. The mTOR Signalling Pathway in Human Cancer. Int J Mol Sci. 2012;13(2):1886-918.

Puissant A, Fenouille N, Auberger P. When autophagy meets cancer through p62/SQSTM1. Am J Cancer Res. 2012;2(4):397-413.

Puls A, Schmidt S, Grawe F, Stabel S. Interaction of protein kinase C zeta with ZIP, a novel protein kinase C-binding protein. Proc Natl Acad Sci U S A. 1997 Jun 10;94(12):6191-6.

Raught B, Gingras AC, Sonenberg N. The target of rapamycin (TOR) proteins. Proc Natl Acad Sci U S A. 2001 Jun 19;98(13):7037-44.

Rea SL, Walsh JP, Ward L, Yip K, Ward BK, Kent GN, Steer JH, Xu J, Ratajczak T. A novel mutation (K378X) in the sequestosome 1 gene associated with increased NF-kappaB signaling and Paget's disease of bone with a severe phenotype. J Bone Miner Res. 2006 Jul;21(7):1136-45.

Rebecca VW, Sondak VK, Smalley KS. A brief history of melanoma: from mummies to mutations.Melanoma Res. 2012 Apr;22(2):114-22.

Reeves R. Molecular biology of HMGA proteins: hubs of nuclear function. Gene. 2001 Oct 17;277(1-2):63-81.

Rhodes EC, Johnson-Pais TL, Singer FR, Ankerst DP, Bruder JM, Wisdom J, Hoon DS, Lin E, Bone HG, Simcic KJ, Leach RJ. Sequestosome 1 (SQSTM1) mutations in Paget's disease of bone from the United States. Calcif Tissue Int. 2008 Apr;82(4):271-7.

Ribas A, Flaherty KT. BRAF targeted therapy changes the treatment paradigm in melanoma.Nat Rev Clin Oncol. 2011 May 24;8(7):426-33.

Robertson GP. Functional and therapeutic significance of Akt deregulation in malignant melanoma. Cancer Metastasis Rev. 2005 Jun;24(2):273-85.

Rodriguez A, Durán A, Selloum M, Champy MF, Diez-Guerra FJ, Flores JM, Serrano M, Auwerx J, Diaz-Meco MT, Moscat J. Mature-onset obesity and insulin resistance in mice deficient in the signaling adapter p62. Cell Metab. 2006 Mar;3(3):211-22.

Roth ME, Grant-Kels JM, Ackerman AB, Elder DE, Friedman RJ, Heilman ER, Maize JC, Sagebiel RW. The histopathology of dysplastic nevi. Continued controversy. Am J Dermatopathol. 1991 Feb;13(1):38-51.

Saio T, Yokochi M, Inagaki F. The NMR structure of the p62 PB1 domain, a key protein in autophagy and NF-kappaB signaling pathway. J Biomol NMR. 2009 Nov;45(3):335-41.

Sanz L, Diaz-Meco MT, Nakano H, Moscat J. The atypical PKC-interacting protein p62 channels NF-kappaB activation by the IL-1-TRAF6 pathway. EMBO J. 2000 Apr 3;19(7):1576-86.

Sanz-Moreno V, Gadea G, Ahn J, Paterson H, Marra P, Pinner S, Sahai E, Marshall CJ. Rac activation and inactivation control plasticity of tumor cell movement. Cell. 2008 Oct 31;135(3):510-23.

Schröder M, Kaufman RJ. The mammalian unfolded protein response. Annu Rev Biochem. 2005;74:739-89.

Seibenhener ML, Babu JR, Geetha T, Wong HC, Krishna NR, Wooten MW. Sequestosome 1/p62 is a polyubiquitin chain binding protein involved in ubiquitin proteasome degradation. Mol Cell Biol. 2004 Sep;24(18):8055-68.

Seibenhener ML, Geetha T, Wooten MW. Sequestosome 1/p62--more than just a scaffold. FEBS Lett. 2007 Jan 23;581(2):175-9.

Serrano M, Hannon GJ, Beach D. A new regulatory motif in cell-cycle control causing specific inhibition of cyclin D/CDK4. Nature. 1993 Dec 16;366(6456):704-7.

Serrone L, Zeuli M, Sega FM, Cognetti F. Dacarbazine-based chemotherapy for metastatic melanoma: thirty-year experience overview. J Exp Clin Cancer Res. 2000 Mar;19(1):21-34.

Shan G.RNA interference as a gene knockdown technique. Int J Biochem Cell Biol. 2010 Aug;42(8):1243-51.

Sharpless E, Chin L. The INK4a/ARF locus and melanoma. Oncogene. 2003 May 19;22(20):3092-8.

Siegel R, Naishadham D, Jemal A. Cancer statistics, 2012. CA Cancer J Clin. 2012 Jan-Feb;62(1):10-29.

Soengas MS, Lowe SW. Apoptosis and melanoma chemoresistance. Oncogene. 2003 May 19;22(20):3138-51.

Solomon VR, Lee H. Chloroquine and its analogs: a new promise of an old drug for effective and safe cancer therapies. Eur J Pharmacol. 2009 Dec 25;625(1-3):220-33.

Stumptner C, Fuchsbichler A, Heid H, Zatloukal K, Denk H. Mallory body--a disease-associated type of sequestosome. Hepatology. 2002 May;35(5):1053-62.

Stumptner C, Fuchsbichler A, Zatloukal K, Denk H. In vitro production of Mallory bodies and intracellular hyaline bodies: the central role of sequestosome 1/p62. Hepatology. 2007 Sep;46(3):851-60.

Swerdlow AJ, English J, MacKie RM, O'Doherty CJ, Hunter JA, Clark J, Hole DJ. Benign melanocytic naevi as a risk factor for malignant melanoma. Br Med J (Clin Res Ed). 1986 Jun 14;292(6535):1555-9.

Taguchi K, Motohashi H, Yamamoto M. Molecular mechanisms of the Keap1–Nrf2 pathway in stress response and cancer evolution. Genes Cells. 2011 Feb;16(2):123-40.

Takeuchi H, Morton DL, Elashoff D, Hoon DS. Survivin expression by metastatic melanoma predicts poor disease outcome in patients receiving adjuvant polyvalent vaccine. Int J Cancer 2005;117:1032– 1038.

Takeuchi K, Soda M, Togashi Y, Ota Y, Sekiguchi Y, Hatano S, Asaka R, Noguchi M, Mano H. Identification of a novel fusion, SQSTM1-ALK, in ALK-positive large B-cell lymphoma. Haematologica. 2011 Mar;96(3):464-7.

Thompson HG, Harris JW, Wold BJ, Lin F, Brody JP. p62 overexpression in breast tumors and regulation by prostate-derived Ets factor in breast cancer cells. Oncogene. 2003 Apr 17;22(15):2322-33.

Tormo D, Checińska A, Alonso-Curbelo D, Pérez-Guijarro E, Cañón E, Riveiro-Falkenbach E, Calvo TG, Larribere L, Megías D, Mulero F, Piris MA, Dash R, Barral PM, Rodríguez-Peralto JL, Ortiz-Romero P, Tüting T, Fisher PB, Soengas MS. Targeted activation of innate immunity for therapeutic induction of autophagy and apoptosis in melanoma cells. Cancer Cell. 2009 Aug 4;16(2):103-14.

Tsao H, Goel V, Wu H, Yang G, Haluska FG. Genetic interaction between NRAS and BRAF mutations and PTEN/MMAC1 inactivation in melanoma. J Invest Dermatol. 2004 Feb;122(2):337-41.

Tucker MA, Halpern A, Holly EA, Hartge P, Elder DE, Sagebiel RW, Guerry D 4th, Clark WH Jr. Clinically recognized dysplastic nevi. A central risk factor for cutaneous melanoma. JAMA. 1997 May 14;277(18):1439-44.

Urteaga O, Pack GT. On the antiquity of melanoma. Cancer. 1966 May;19(5):607-10.

Van Raamsdonk CD, Bezrookove V, Green G, Bauer J, Gaugler L, O'Brien JM, Simpson EM, Barsh GS, Bastian BC. Frequent somatic mutations of GNAQ in uveal melanoma and blue naevi. Nature. 2009 Jan 29;457(7229):599-602.

Watanabe Y, Tanaka M. p62/SQSTM1 in autophagic clearance of a non-ubiquitylated substrate. J Cell Sci. 2011 Aug 15;124(Pt 16):2692-701.

Whiteman DC, Pavan WJ, Bastian BC. The melanomas: a synthesis of epidemiological, clinical, histopathological, genetic, and biological aspects, supporting distinct subtypes, causal pathways, and cells of origin. Pigment Cell Melanoma Res. 2011 Oct;24(5):879-97.

Yang ZJ, Chee CE, Huang S, Sinicrope FA. The role of autophagy in cancer: therapeutic implications. Mol Cancer Ther. 2011 Sep;10(9):1533-41.

Young AR, Narita M. Oncogenic HMGA2: short or small? Genes Dev. 2007 May 1;21(9):1005-9.

Zabierowski SE, Herlyn M. Embryonic stem cells as a model for studying melanocyte development.Methods Mol Biol. 2010;584:301-16.

Zangemeister-Wittke U, Simon HU. An IAP in action: the multiple roles of survivin in differentiation, immunity and malignancy. Cell Cycle. 2004 Sep;3(9):1121-3.

Zatloukal K, Stumptner C, Fuchsbichler A, Heid H, Schnoelzer M, Kenner L, Kleinert R, Prinz M, Aguzzi A, Denk H. p62 Is a common component of cytoplasmic inclusions in protein aggregation diseases. Am J Pathol. 2002 Jan;160(1):255-63.

8. APPENDIX

8.1. Supplemental tables and figures

Clinical Staging				Pathologic Staging			
	T	N	M		T	N	M
0	Tis	N0	M0	0	Tis	N0	M0
IA	T1a	N0	M0	IA	T1a	N0	M0
IB	T1b	N0	M0	IB	T1b	N0	M0
	T2a	N0	M0		T2a	N0	M0
IIA	T2b	N0	M0	IIA	T2b	N0	M0
	T3a	N0	M0		T3a	N0	M0
IIB	T3b	N0	M0	IIB	T3b	N0	M0
	T4a	N0	M0		T4a	N0	M0
IIC	T4b	N0	M0	IIC	T4b	N0	M0
III	Any T	N>N0	M0	IIIA	T1-4a	N1a or N2a	M0
				IIIB	T1-4b	N1a or N2a	M0
					T1-4a	N1b or N2b or N2c	M0
				IIIC	T1-4b	N1b or N2b or N2c	M0
					Any T	N3	M0
IV	Any T	Any N	M1	IV	Any T	Any N	M1

Supplemental Table 1. TNM Staging Categories for Cutaneous Melanoma. AJCC Melanoma Staging and Classification (adapted from Balch et al., 2009).

T	Thickness (mm)	Ulceration Status/Mitoses
Tis	in situ	Not applicable
T1	≤ 1.00	a: Without ulceration and mitosis < 1/mm^2
		b: With ulceration or mitosis ≥ 1/mm^2
T2	1.01-2.00	a: Without ulceration
		b: With ulceration
T3	2.01-4.00	a: Without ulceration
		b: With ulceration
T4	>4.00	a: Without ulceration
		b: With ulceration
N	**No. of Metastatic Nodes**	**Nodal Metastatic**
N0	0	Not applicable
N1	1	a: Micrometastasis
		b: Macrometastasis
N2	2	a: Micrometastasis
		b: Macrometastasis
		c: In transit metastases/satellites without metastatic nodes
N3	4 + metastatic nodes, or matted nodes, or in transit metastases/satellites with metastatic nodes	
M	**Site**	**Serum LDH**
M0	No distant metastases	Not applicable
M1a	Distant skin, subcutaneous, or nodal metastases	Normal
M1b	Lung metastases	Normal
M1c	All other visceral metastases	Normal
	Any distant metastasis	Elevated

Supplemental Table 2. Anatomic Stage Grouping for Cutaneous Melanoma. AJCC Melanoma Staging and Classification (adapted from Balch et al., 2009).

	Day3		Day 6	
CELLULAR PATHWAY	**SK-Mel-103**	**UACC-62**	**SK-Mel-103**	**UACC-62**
CELL CYCLE, MITOTIC				
ACTIVATION OF ATR IN RESPONSE TO REPLICATION STRESS				
G2/M CHECKPOINTS				
G1/S TRANSITION				
ACTIVATION OF THE PRE-REPLICATIVE COMPLEX				
E2F MEDIATED REGULATION OF DNA REPLICATION				
M PHASE				
DNA REPLICATION PRE-INITIATION				
DNA REPLICATION				
DNA STRAND ELONGATION				
CELL CYCLE CHECKPOINTS				
MITOTIC PROMETAPHASE				
M/G1 TRANSITION				
CHOLESTEROL BIOSYNTHESIS				
ASSEMBLY OF THE PRE-REPLICATIVE COMPLEX				
EXTENSION OF TELOMERES				
LAGGING STRAND SYNTHESIS				
CDT1 ASSOCIATION WITH THE CDC6:ORC:ORIGIN COMPLEX				
GAP-FILLING DNA REPAIR SYNTHESIS AND LIGATION IN TC-NER				
GAP-FILLING DNA REPAIR SYNTHESIS AND LIGATION IN GG-NER				
ORC1 REMOVAL FROM CHROMATIN				
COOPERATION OF PREFOLDIN AND TRIC/CCT IN ACTIN AND TUBULIN FOLDING				
APC/C:CDC20 MEDIATED DEGRADATION OF MITOTIC PROTEINS				
ACTIVATION OF APC/C AND APC/C:CDC20 MEDIATED DEGRADATION OF MITOTIC PROTEINS				
APC/C-MEDIATED DEGRADATION OF CELL CYCLE PROTEINS				
CDC20:PHOSPHO-APC/C MEDIATED DEGRADATION OF CYCLIN A				
CHAPERONIN-MEDIATED PROTEIN FOLDING				
DNA REPAIR				
G2/M TRANSITION				
METABOLISM OF CARBOHYDRATES				
ORNITHINE METABOLISM				
GLOBAL GENOMIC NER (GG-NER)				
CYCLIN E ASSOCIATED EVENTS DURING G1/S TRANSITION				
CDK-MEDIATED PHOSPHORYLATION AND REMOVAL OF CDC6				
APC/C:CDC20 MEDIATED DEGRADATION OF SECURIN				
DOUBLE-STRAND BREAK REPAIR				
ORNITHINE AND PROLINE METABOLISM				
APC/C:CDH1 MEDIATED DEGRADATION OF CDC20 AND OTHER APC/C:CDH1 TARGETED PROTEINS IN LATE MITOSIS/EARLY G1				
MEMBRANE TRAFFICKING				
FORMATION OF THE TERNARY COMPLEX, AND SUBSEQUENTLY, THE 43S COMPLEX				
ACTIVATION OF THE MRNA UPON BINDING OF THE CAP-BINDING COMPLEX AND EIFS, AND SUBSEQUENT BINDING TO 43S				
ABORTIVE ELONGATION OF HIV-1 TRANSCRIPT IN THE ABSENCE OF TAT				
CYTOCHROME P450 - ARRANGED BY SUBSTRATE TYPE				
ATRBRCAPATHWAY				
NKTPATHWAY				
G1_TO_S_CELL_CYCLE_REACTOME				
CHOLESTEROL_BIOSYNTHESIS				
KREBS_TCA_CYCLE				
CITRATE_CYCLE_TCA_CYCLE				
GLYCOLYSIS_AND_GLUCONEOGENESIS				
PYRIMIDINE_METABOLISM				
VALINE_LEUCINE_AND_ISOLEUCINE_DEGRADATION				
PENTOSE_PHOSPHATE_PATHWAY				
UREA_CYCLE_AND_METABOLISM_OF_AMINO_GROUPS				
ARGININE_AND_PROLINE_METABOLISM				

Supplemental Figure 1. Altered pathways in SK-Mel-103 and UACC-62 cell lines at early (day 3) and late (day 6) time points after p62 downregulation. Red, green and gray indicate upregulation, downregulation and no significant deregulation, respectively (FDR < 0.05).

	Day3		Day 6	
CELLULAR PATHWAY	**SK-Mel-103**	**UACC-62**	**SK-Mel-103**	**UACC-62**
PROPANOATE_METABOLISM				
RIBOSOMAL_PROTEINS				
GLYCOSPHINGOLIPID_METABOLISM				
PHOTOSYNTHESIS				
TYPE_III_SECRETION_SYSTEM				
FLAGELLAR_ASSEMBLY				
ATP_SYNTHESIS				
GAMMA_HEXACHLOROCYCLOHEXANE_DEGRADATION				
PROTEASOME_-_HOMO_SAPIENS_(HUMAN)				
BIOSYNTHESIS_OF_STEROIDS_-_HOMO_SAPIENS_(HUMAN)				
PYRUVATE_METABOLISM_-_HOMO_SAPIENS_(HUMAN)				
CARBON_FIXATION_-_HOMO_SAPIENS_(HUMAN)				
PENTOSE_PHOSPHATE_PATHWAY_-_HOMO_SAPIENS_(HUMAN)				
POLYUNSATURATED_FATTY_ACID_BIOSYNTHESIS_-_HOMO_SAPIENS_(HUMAN)				
PORPHYRIN_AND_CHLOROPHYLL_METABOLISM_-_HOMO_SAPIENS_(HUMAN)				
AMINOACYL-TRNA_BIOSYNTHESIS_-_HOMO_SAPIENS_(HUMAN)				
RIBOSOME_-_HOMO_SAPIENS_(HUMAN)				
SPHINGOLIPID_METABOLISM_-_HOMO_SAPIENS_(HUMAN)				
CYTOKINE-CYTOKINE_RECEPTOR_INTERACTION_-_HOMO_SAPIENS_(HUMAN)				
LINOLEIC_ACID_METABOLISM_-_HOMO_SAPIENS_(HUMAN)				
CYTOSOLIC TRNA AMINOACYLATION				
INHIBITION OF THE PROTEOLYTIC ACTIVITY OF APC/C REQUIRED FOR THE ONSET OF ANAPHASE BY MITOTIC SPINDLE CHECKPOINT COMPONENTS				
CYCLIN A:CDK2-ASSOCIATED EVENTS AT S PHASE ENTRY				
APC-CDC20 MEDIATED DEGRADATION OF NEK2A				
G1/S DNA DAMAGE CHECKPOINTS				
CENTROSOME MATURATION				
PACKAGING OF TELOMERE ENDS				
CITRIC ACID CYCLE (TCA CYCLE)				
NUCLEOTIDE EXCISION REPAIR				
LOSS OF NLP FROM MITOTIC CENTROSOMES				
LOSS OF PROTEINS REQUIRED FOR INTERPHASE MICROTUBULE ORGANIZATION FROM THE CENTROSOME				
DEGRADATION OF BETA-CATENIN BY THE DESTRUCTION COMPLEX				
INACTIVATION OF APC/C VIA DIRECT INHIBITION OF THE APC/C COMPLEX				
AUTODEGRADATION OF CDH1 BY CDH1:APC/C				
MITOTIC SPINDLE CHECKPOINT				
FORMATION OF INCISION COMPLEX IN GG-NER				
DUAL INCISION REACTION IN GG-NER				
METABLISM OF NUCLEOTIDES				
METABOLISM OF NON-CODING RNA				
EUKARYOTIC TRANSLATION ELONGATION				
PEPTIDE CHAIN ELONGATION				
EUKARYOTIC TRANSLATION TERMINATION				
FORMATION OF A POOL OF FREE 40S SUBUNITS				
GTP HYDROLYSIS AND JOINING OF THE 60S RIBOSOMAL SUBUNIT				
L13A-MEDIATED TRANSLATIONAL SILENCING OF CERULOPLASMIN EXPRESSION				
3 -UTR-MEDIATED TRANSLATIONAL REGULATION				
EUKARYOTIC TRANSLATION INITIATION				
CAP-DEPENDENT TRANSLATION INITIATION				
INFLUENZA VIRAL RNA TRANSCRIPTION AND REPLICATION				
INFLUENZA INFECTION				
INFLUENZA LIFE CYCLE				
INTEGRIN CELL SURFACE INTERACTIONS				
AXON GUIDANCE				
NCAM SIGNALING FOR NEURITE OUT-GROWTH				
IMMUNOREGULATORY INTERACTIONS BETWEEN A LYMPHOID AND A NON-LYMPHOID CELL				
EGFR DOWNREGULATION				

Supplemental Figure 2. Altered pathways in SK-Mel-103 and UACC-62 cell lines at early (day 3) and late (day 6) time points after p62 downregulation. Red, green and gray indicate upregulation, downregulation and no significant deregulation, respectively (FDR < 0.05).

8.2. Presentations and awards related to this study

Erica Riveiro-Falkenbach, J.L. Rodriguez-Peralto, P. Ortiz-Romero, B. Pérez-Gomez and M.S. Soengas. P62/Sequestosome 1, nuevo oncogén y diana terapéutica en el melanoma. III Simposio en Melanoma GEM - Post Asco 2012, Grupo Español Multidisciplinar de Melanoma. Madrid, Spain, 2012 **– awarded as best oral communication**

E. Riveiro-Falkenbach, P. Ortiz-Romero, J.L. Rodriguez-Peralto, B. Pérez-Gomez and M.S. Soengas. P62/Sequestosome 1, nuevo oncogén y diana terapéutica en el melanoma. Congreso Nacional de Dermatología y Venereología. Oviedo, Spain, 2012 - oral presentation

E. Riveiro-Falkenbach, D. Alonso-Curbelo, D. Olmeda, M. Cifdoloz, P. Ortiz-Romero, J.L. Rodriguez-Peralto and M.S. Soengas. Oncogenic addiction of melanoma cells to the p62/sequestosome 1 protein. 8th International Melanoma Congress of the Society for Melanoma Research. Tampa, USA, 2011 – **awarded as best poster**

E. Riveiro-Falkenbach, D. Alonso-Curbelo, D. Olmeda, M. Cifdoloz, P. Ortiz-Romero, J.L. Rodriguez-Peralto and M.S. Soengas. Oncogenic addiction of melanoma cells to the p62/sequestosome 1 protein. EORTC Melanoma Group, Barcelona, Spain, 2011 – oral presentation

E. Riveiro-Falkenbach and M.S. Soengas. Joining forces to control melanoma cell proliferation: the case of p62 (Sequestosome1). Progress Report, Centro Nacional de Investigaciones Oncológicas. Madrid, Spain, 2011 – oral presentation

8.3. Publications related to melanoma field

Erica Riveiro-Falkenbach and María S. Soengas. The Role of Dek in Tumorigenesis and Chemoresistance. **Clin Cancer Res. 2010** Jun 1;16(11):2932-8.

Khodadoust MS, Verhaegen M, Kappes F, **Riveiro-Falkenbach E**, Cigudosa JC, Kim DS, Chinnaiyan AM, Markovitz DM, Soengas MS. Melanoma proliferation and chemoresistance controlled by the DEK oncogene. **Cancer Res. 2009** Aug 15;69(16):6405-13.

Tormo D, Checińska A, Alonso-Curbelo D, Pérez-Guijarro E, Cañón E, **Riveiro-Falkenbach E**, Calvo TG, Larribere L, Megías D, Mulero F, Piris MA, Dash R, Barral PM, Rodríguez-Peralto JL, Ortiz-Romero P, Tüting T, Fisher PB, Soengas MS.Targeted Activation of Innate Immunity for Therapeutic Induction of Autophagy and Apoptosis in Melanoma Cells. **Cancer Cell. 2009** Aug 4;16(2):103-14.

GEM
Grupo Español
Multidisciplinar de Melanoma

III SIMPOSIO GEM

Madrid, 15 de Junio, 2012

El Comité Científico del Grupo Español Multidisciplinar de Melanoma otorga el primer premio de Comunicaciones Orales a

Dra. Erica Riveiro - Falkenbach

por su comunicación

P62/Sequestosome 1, Nuevo Oncogén y Diana Terapéutica en el Melanoma

2011 International Melanoma Congress

Advancement Through Collaboration

November 9-13, 2011
Tampa, Florida, USA - Marriott Waterside Hotel

Best Poster on prevention, diagnosis, translational research or treatment of melanoma

Oncogenic addiction of melanoma cells to the p62/ sequestosome1 protein

Lead Author: Erica Riveiro-Falkenbach

Boris C. Bastian, MD

President, Society for Melanoma Research

SMR
Society for Melanoma Research

THE WISTAR INSTITUTE

January 15, 2013

To Whom It May Concern:

The letter provided, is to verify that Dr. Erica Riveiro, M.D. has completed her appointment as Visiting Scientist within the laboratory of Dr. Meenhard Herlyn at The Wistar Institute, but was not funded by our organization. Dr. Riveiro's dates of appointment were from April 1, 2010 to June 30, 2010.

Please let me know if you have any questions or require additional information.

Sincerely,

Jennifer Hunter
Human Resources Coordinator

Cc: Meenhard Herlyn
Personnel File

Molecular Pathways

Clinical Cancer Research

Control of Tumorigenesis and Chemoresistance by the DEK Oncogene

Erica Riveiro-Falkenbach and María S. Soengas

Abstract

Slight modifications of chromatin dynamics can translate into small- and large-scale changes in DNA replication and DNA repair. Similarly, promoter usage and accessibility are tightly dependent on chromatin architecture. Consequently, it is perhaps not surprising that factors controlling chromatin organization are frequently deregulated (directly or indirectly) in cancer cells. DEK is emerging as a novel class of DNA topology modulators that can be both targets and effectors of protumorigenic events. The locus containing DEK at chromosome 6p22.3 is amplified or reorganized in multiple cancer types. In addition, DEK can be subject to a variety of tumor-associated transcriptional and post-translational modifications. In turn, DEK can favor cell transformation, at least in part by inhibiting cell differentiation and premature senescence. More recently, DEK has also been linked to the resistance of malignant cells to apoptotic inducers. Interestingly, a fraction of DEK can also bind RNA and affect alternative splicing, further illustrating the pleiotropic roles that this protein may exert in cancer cells. Here we will summarize the current literature about the regulation and function(s) of DEK as a proto-oncogene. In addition, the translational relevance of DEK as a putative diagnostic marker and candidate for drug development will be discussed.

Clin Cancer Res; 16(11); 2932–8. ©2010 AACR.

Background

DEK, a highly conserved nuclear factor and the only member of its protein class, is preferentially expressed in actively proliferating and malignant cells, where it can reach up to 4 to 6 million copies per nucleus (1). DEK was initially described as the target of a recurrent t(6;9) translocation in a subset of acute myeloid leukemia (AML) patients (2, 3). Subsequently, DEK has been shown to promote tumorigenesis in a variety of cancer cell types, at least in part by its ability to interfere with cell division or DNA repair, inhibit cell differentiation, senescence and apoptosis, and cooperate with transforming oncogenes (Leave as such).

The bulk of DEK is bound to chromatin (1, 4, 5), preferentially to euchromatic regions (6). However, DEK can also be found within the nuclear matrix (7), or in interchromatin granule clusters (8). The precise determinants that DEK recognizes in the DNA are still under investigation. Although DEK exhibits some sequence-specific DNA binding, it primarily seems to recognize structural features (cruciform and supercoiled DNA; ref. 9). Two main domains in DEK are responsible for its interaction with DNA (see Fig. 1; ref. 10). Residues 87 to 187 are homologous to the scaffold attachment factor-box (SAF-box) domain (11, 12) found in multiple nuclear proteins (13). A second domain comprises residues 270 to 350 in the carboxyl-terminal region of the DEK protein, which is also responsible for multimerization (10).

Although the best known protumorigenic features of DEK are related to DNA binding, a fraction of DEK (approximately 10%) is associated with RNA (1) and can modulate RNA processing. Thus, DEK can affect 3′ splice site discrimination by the splicing factor U2AF (14). In addition, DEK can interact with serine-arginine-rich (SR) proteins (15) and other factors involved in exon-exon junction complexes (16), although the functional relevance of these interactions in cancer still needs to be defined. Finally, DEK can also be secreted, particularly by dying cells, and lead to the generation of autoimmune antigens that might play a key role in juvenile rheumatoid arthritis and other inflammatory diseases (17, 18).

The impact of DEK on mRNA splicing and autoimmunity has been addressed by other reports (14, 17, 18). Here we will focus primarily on the regulation and pro-oncogenic roles of DEK that are dependent on its DNA-associated functions.

Molecular Mechanisms of DEK Regulation

DEK has been shown to be upregulated in AML (2, 19, 20); retinoblastoma (21–23); glioblastoma (24);

Authors' Affiliation: Centro Nacional de Investigaciones Oncológicas (Spanish National Cancer Research Centre), Madrid, Spain

Note: E. R-F. is the recipient of a postresidency training program from "Obra Social de Caja Navarra."

Corresponding Author: María S. Soengas, Centro Nacional de Investigaciones Oncológicas, Melchor Fernández Almagro 3, Madrid 28049, Spain. Phone: 34-91-732-8000; Fax: 34-91-732-8000; E-mail: msoengas@cnio.es.

doi: 10.1158/1078-0432.CCR-09-2330

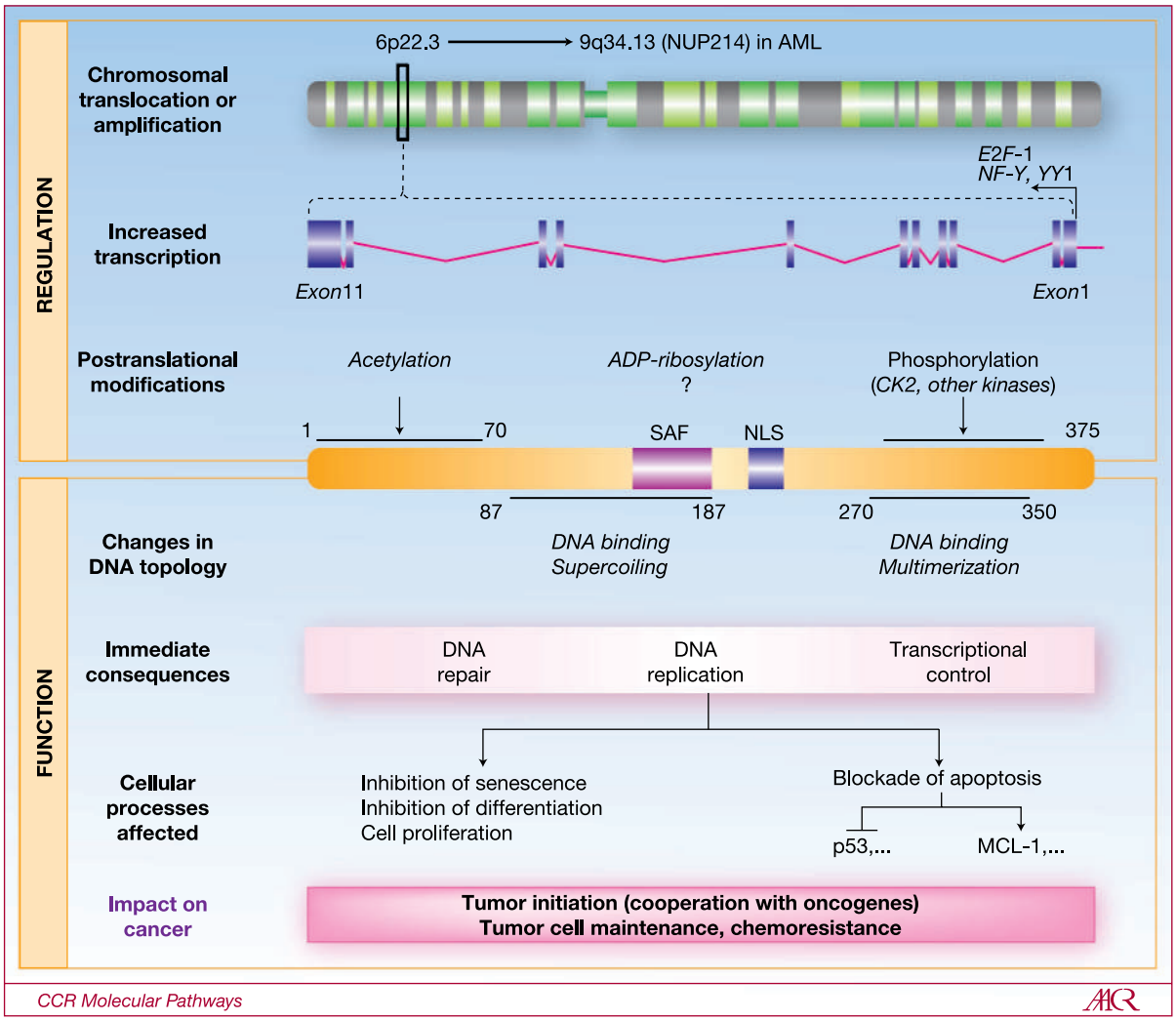

Fig. 1. Schematic summary of DEK regulation and function. DEK expression can be regulated at the DNA, RNA, and protein levels. Genomic translocations involving the 6p22.3 locus (where DEK maps) are frequent in a subset of AML. Amplifications and copy gains have been described in a variety of tumors, including retinoblastoma, bladder cancer, and melanoma. In addition, DEK mRNA transcription can be induced by various transcription factors (e.g., E2F-3, NF-Y, or YY1) whose expression and function are deregulated in multiple cancer cell types. In addition, acetylation, phosphorylation, and ADP-ribosylation can alter the affinity of DEK for chromatin and chromatin remodeling factors. By its ability to impinge on chromatin topology, DEK can influence DNA repair and DNA replication, as well as modulate the accessibility and occupancy of a still indeterminate number of promoters. Interestingly, although DEK is best known for its DNA binding features, it should be noted that DEK can also interact with RNA and components of the spliceosome. Ultimately, these functions favor tumor initiation, progression, and chemoresistance, at least in part by a concomitant blockade of senescence, differentiation, and apoptosis. By virtue of its protumorigenic roles and tumor cell–selective expression, DEK may represent a new class of drug targets and diagnostic markers.

hepatocellular carcinoma (25); melanoma (26, 27); and in an increasing list of other tumor types (20, 27–33). However, the mechanisms leading to this preferential accumulation of DEK in cancer cells are not completely understood. No mutations have been reported in the coding sequence of human *DEK*. However, a variety of other regulatory mechanisms have been identified at the DNA, RNA, and protein levels (see Fig. 1).

Genomic reorganizations-DNA amplification

As indicated above, *DEK* was discovered by the identification of the translocation t(6;9) (p23;q34) in a subset of patients with AML, and was named on the basis of the initials of the patient DK (2). The observation that this chromosomal change was associated with an accelerated tumor onset and poor prognosis prompted a series of studies that ultimately support a causative role for DEK in tumor development. Specifically, the t(6;9) translocation was found to result in an in-frame fusion between nearly the entire DEK (missing just the last 25 amino acids), and two thirds of the nucleoporin NUP214 on chromosome 9 (Fig. 1). Although NUP214 (formally known as CAN) localized at the nuclear pore, the DEK-NUP214 fusion was found in the nucleoplasm (34).

Amplifications and copy gains at the short arm of chromosome 6, encompassing the DEK gene, were also found in the absence of translocations in a variety of malignancies, particularly in bladder cancer (29) and retinoblastoma (22, 23). Melanomas can also present with gains of the chromosome 6p area (35). However, other mechanisms of regulation of DEK may exist, as this protein can accumulate to high levels in AML, melanomas, and other tumors without specific amplifications or gains of the DEK locus.

Transcriptional regulation

Analyses aimed at identifying regulatory elements within the DEK promoter revealed binding sites for NF-Y and YY1 at positions 170 and 135, respectively, from the transcriptional starting site (36). NF-Y and YY1 are transcription factors with well-documented roles in cellular proliferation and transformation (37, 38), and thus could provide a mechanistic link between DEK upregulation and tumor development. Still, it remains unclear what the upstream modulators are that activate NF-Y and YY1 in order to signal through DEK in the context of malignancies.

Additional insights about the transcriptional control of DEK emerged from studies in virally induced pathologies. Analyses of human papillomavirus (HPV)-positive cervical cancer cells indicated that DEK can be transcriptionally activated by the E7 oncogene, a classical negative regulator of the retinoblastoma (Rb) protein (39). These results were confirmed by ectopic overexpression of E7 in primary human keratinocytes, and by the observation of DEK upregulation in human cervical cancer specimens infected with HPV (40, 41). Moreover, retinoblastoma and small cell lung cancers, both associated with Rb loss, present with high DEK levels (21). Consistent with Rb deficiency favoring transcription via the E2F family of proteins (42), chromatin immunoprecipitation assays showed that the *DEK* promoter is bound by endogenous E2F-1 in tumor cell lines (27). Mutation of E2F binding sites in the DEK promoter abrogated transcriptional activation in reporter assays (27). Therefore, tumor-associated E2F-1 activation may involve a concomitant activation of DEK mRNA transcription.

Post-transcriptional modifications

Post-transcriptional modifications add an additional layer of complexity in the regulation of DEK. For example, DEK can be phosphorylated, ADP-ribosylated, or acetylated. Phosphorylation has been reported to inhibit the binding of DEK to DNA, but favor the interaction of this protein with RNA splicing factors and potentially other nuclear proteins (14, 43). Similarly, poly(ADP)ribosylation and acetylation may reduce the affinity of DEK for DNA (44), but facilitate the interaction with other proteins involved in chromatin remodeling (see below).

With regard to phosphorylation, multiple consensus sites for casein kinase 2 (CK2) have been identified within the DEK carboxy terminus (43). In actively proliferating cells, DEK remains bound to DNA in a rather constant manner throughout the cell cycle. Yet, at the G1 phase there is a peak in DEK phosphorylation (43), but it is unclear to what extent this phosphorylation affects cell division. In line with this, DEK phosphorylation was recently suggested to act as a switch to favor or inhibit the association with proteins involved in chromatin remodeling or RNA splicing. Thus, in *Drosophila*, CK2-phosphorylated DEK can affect the deposition of histone H3.3, at least in the context of the nuclear ecdysone receptor (45). In overexpression studies, human DEK can also bind CK2 and act as a histone chaperone (45). Intriguingly, the fraction of phosphorylated, non-DNA-associated DEK, was found to accumulate in apoptotic cells (44). However, it is unclear whether this is the cause or consequence of cell death, and which kinases are involved, as CK2 may not be required in this process (44).

Another modification of DEK found to increase in cells dying in response to genotoxic agents is poly(ADP-ribosyl)ation (44). It has been proposed that this modification results from the interaction of DEK with poly(ADP-ribose) polymerase 1 (PARP1), likely to aid in DNA repair. Poly(ADP ribosylated) DEK is displaced from chromatin (46) and can be released into the extracellular space, where it can generate reactive auto-antibodies (44). This consequence of DEK modification may have important clinical implications as accumulation of DEK-auto-antibodies is found in synovial fluids of patients affected by juvenile rheumatoid arthritis or juvenile idiopathic arthritis (44). Therefore, deregulation of DEK's post-translational modifications may be critical to the pathogenesis of inflammatory diseases.

The affinity of DEK for DNA can also be reduced by acetylation (8). This modification localizes DEK to nuclear speckles or interchromatin granule clusters, which are well-known for containing RNA-processing and transcription factors (47). In contrast to phosphorylation that involves mostly the C-terminus of DEK, acetylation apparently affects lysines mapping within the first 70 amino acids (8). Together, these results support domain-specific modifications that may affect DEK conformation and/or interaction with distinct partners.

In addition to the above mentioned regulation of DEK by phosphorylation, acetylation, or ADP(ribosylation), it should be mentioned that DEK-DNA interactions can be modulated by a series of other chromatin-associated factors such as histone deacetylases, methyltransferases (SET), histone variants (H2A1.1), remodeling complexes (WSTF-SNF2h), or death modulators (Daxx; refs. 45, 46, 48–50).

In summary, DEK is a very dynamic protein, which may serve as a hub to recruit histones, histone modifiers and chromatin remodeling factors, and modulate their interaction with DNA. These activities of DEK depend on various post-transcriptional modifications, which in turn may respond to specific environmental or stress-related signals. In light of the hypothesis, it has been suggested that DEK could be one of the so-called "alarmins," molecules, that in the extracellular space, signal cell and tissue damage (44).

DEK in Tumor Progression and Drug Response

DEK-NUP214

From the initial discovery of the DEK-NUP214 fusion protein in a subset of patients with AML, DEK has been associated with tumor development. Yet, the precise mechanism of action of DEK-NUP214 in leukemogenesis has remained elusive. It has been recently reported that in malignant myeloid cells DEK-NUP214 expression correlates with a general activation of protein synthesis and increased the phosphorylation of eIF4E, a key factor in translational initiation and a marker for translational activity (51). In addition, in 293T cells, the DEK-NUP214 fusion protein was found to have an impaired ability to associate with histones and to be phosphorylated by CK2α and CK2β (51). If these results applied to the situation in human tumors, they would provide a molecular support for the hypothesis that the (refs. 6, 9) (p23;q34) translocation modifies the chromatin binding and remodeling activity of DEK.

DEK as a transcriptional modulator

Although it may be intuitive that the localization and function of DEK can be affected by its fusion to the nucleoporin NUP214 in AML, it is not clear how DEK exerts its protumorigenic effects in cancers that do not exhibit translocations of the 6p22-23 locus. It is plausible that the high levels of DEK found in these tumor types result in the occupancy of promoters and enhancers, which in normal cells remain "DEK-free." As indicated above, phosphorylation, acetylation, or ADP(ribosylation) can affect the affinity of DEK for DNA, and alter the stoichiometry of DNA-binding complexes. It is likely, although it has not yet been explored in sufficient mechanistic detail, that these post-translational DEK modifications are quantitatively and qualitatively different in benign and malignant tissues. Given the intricate and dynamic nature of chromatin, a comprehensive hierarchical map of these modifications, and how specifically they impact on DEK function and cellular fate, will undoubtedly pose a challenge. In fact, DEK can act as a transcriptional inducer or inhibitor, depending on the specific gene, cell type, and microenvironmental conditions. For example, DEK has been detected in transcriptional repressor complexes binding to Daxx in U937T cells (52); as well as to P/CAF, p300, or p65/nuclear factor-κB in HeLa cells (48, 53). On the other hand, other studies also in HeLa cells, indicate that DEK is largely excluded from heterochromatin and can accumulate at promoter-enhancer regions of select actively transcribed genes (54). Other activating effects of DEK have been linked to the activation of the transcription factor AP-2a (87MG or D17 astrocytoma cells; ref. 55) or the nuclear splicing factor U2AF (HeLa; ref. 14).

Inhibition of cellular senescence by DEK

In addition to assays aimed at uncovering DEK binding partners, assessing cellular and environmental cues that affect endogenous levels of DEK provided new insights on the multiple processes in which DEK is an active player. The first hint linking DEK to the proliferative status of cells was provided by the repression of its mRNA in two conditions: (i) HPV-positive cervical cancer cell lines undergoing senescence-like cell-cycle arrest, and (ii) primary keratinocytes and fibroblasts maintained for multiple passages in culture (and thus suffering telomere attrition). Interestingly, in both settings, DEK overexpression extended cellular life span, supporting critical roles for DEK as a senescence inhibitor (39).

As senescence bypass is an obligated hallmark of tumor cells, DEK activation may represent a new class of the so-called "tumor gatekeepers" (56). Proof for this hypothesis has recently been provided by selective depletion of DEK in melanoma cells by interfering short hairpin RNAs (shRNA). In a subset of metastatic melanoma cell lines, three independent DEK shRNAs prompted a progressive abrogation of cell proliferation, accompanied by the characteristic flattening, vacuolization, and acidic β-galactosidase activity of senescent cells (26). Considering the large number of genetic and epigenetic alterations that melanoma cells accumulate during their malignant transformation (57), it is remarkable that inhibiting the expression of a single gene can drive them out of the cell cycle. It also important to note that whereas human melanoma specimens show high DEK protein expression, their benign and senescent counterparts (nevi) are virtually negative (26).

Inhibition of differentiation and facilitation of cellular transformation by DEK

The interplay between DEK and the proliferative status of cells was also shown in the context of cellular differentiation. In human promyelocytic HL-60 cells or in human foreskin keratinocytes, differentiation led to DEK downregulation (41, 58). Moreover, mature cells from peripheral blood were found to contain a 10 fold lower amount of DEK than immature CD34-positive cells (59). Conversely, when DEK is overexpressed, differentiation programs can be counteracted, favoring oncogenic transformation. Thus, in the presence of ectopic DEK, immortalized keratinocytes could shift from differentiation to a hyperproliferative state when reconstituted into artificial epidermal rafts (41). Additionally, these DEK-expressing immortalized keratinocytes had an enhanced capability to grow in soft agar and form tumors in mice when transduced with the HRAS, and HPV E6 and E7 oncogenes (40). Further proof for an active protumorigenic role of DEK was recently provided by elegant studies in mouse models. DEK deficient mice were significantly more resistant than their wild-type littermates to the induction of skin papillomas in a classical 7,12-dimethyl-benz(a)anthracene (DMBA)-12-O-tetradecanoylphorbol-13-acetate (TPA) two-step carcinogenesis protocol (40). Whether DEK knockout mice are also protected from the development of metastatic tumors is an interesting question that warrants further analysis.

Apoptosis and chemosensitization by targeted depletion of DEK

Although overexpression studies have identified a role of DEK in favoring proliferation and blocking differentiation, targeted knockdown is unraveling key functions of DEK as a survival factor. DEK depletion in HeLa resulted in the induction of apoptosis, at least in part, as a consequence of the stabilization and activation of the tumor suppressor p53 (60), and the deregulation of multiple proteins with direct or indirect roles in cell viability (61). Nevertheless, the extent to which DEK controls cell survival is likely to depend on the genetic makeup of the tumor cells. For example, DEK depletion did not lead to an overt killing of melanoma cells (26). However, these cells still paid a toll in the absence of DEK. A subset of metastatic melanoma cells showed a progressive inhibition of cell-cycle progression upon DEK shRNA transduction, to ultimately stall into a senescence-like program (26). Other melanoma lines continued to proliferate, but became highly sensitive to genotoxic agents. Interestingly, this chemosensitization by DEK shRNAs was found independent on the functional status of p53. Instead, a new function of DEK was identified in the transcriptional control of the anti-apoptotic factor MCL-1 (26). MCL-1 upregulation is a general feature of aggressive cancers, which also express high DEK levels. Therefore, it is tempting to speculate that the MCL-1 locus may be under the control of DEK in multiple tumor types.

Clinical-Translational Advances

DEK as a tumor marker

Since its discovery as the target of the t(6;9) translocation in a subset of AML patients, DEK has been recurrently associated with tumor development. In fact, this translocation has been suggested to be considered in AML patient stratification (62). Chromosomal alterations at the *DEK* locus are now known not to be a universal feature of malignancy, even in AML (20). However, the increasing list of tumor types showing high DEK protein expression that can be easily detected by commercially available antibodies raises the exciting possibility of using DEK as a tumor marker. The finding that DEK expression levels can distinguish benign nevi from malignant melanomas (26) is a prime example of a clinically relevant setting in which this protein may prove to be highly useful. Moreover, as DEK may be present at higher levels in immature cells than in their differentiated counterparts (59), it could also aid in gauging the differentiation potential of tumor cells. Whether DEK can mark stem or tumor initiating cells is an interesting question that merits further analysis.

DEK as drug target

Being an abundant and pleiotropic factor that binds large stretches of chromatin, it could perhaps have been expected that interfering with DEK functions would result in intolerable side effects in normal cells. However, the fact that DEK-deficient mice are viable whereas DEK-depleted tumor cells enter into senescence or apoptosis (40), supports a DEK-dependent "oncogenic addiction" that could be exploited for drug design. From a translational point of view, it is also interesting that intratumoral injection of DEK shRNAs can lead in the induction of apoptotic features in mouse xenografts generated by Ras/E6/E7-transformed human keratinocytes (40). The feasibility and efficacy of sustained DEK downregulation has yet to be proven in physiologically relevant tumor models or clinical settings. However, the development of new strategies for small interfering RNA (siRNA) delivery, and the observation that normal cells may be less sensitive to DEK downregulation than their hyperproliferative counterparts (40), offers a window for therapeutic intervention. The fact that DEK controls the resistance of tumor cells to genotoxic agents (26, 44) could also be used as a guide for a rational selection of compounds that may better synergize with DEK-inhibitor agents. A proof of principle for this hypothesis has been recently suggested in experimental models of melanoma (26). The observation that DEK is released from apoptotic cells and generates autoantibodies may also provide an alternative to assess drug efficacy in pharmacokinetic or pharmacodynamic studies of pro-apoptotic agents.

The understanding of regulatory elements in the DEK promoter has additional translational implications. Specifically, the transcriptional control of DEK by E2F-1 (27) may be relevant in the context of drug response. Thus, anticancer agents that affect cell-cycle proliferation may downregulate E2F-1 and, consequently, DEK expression and the corresponding DEK-dependent functions.

In summary, the DEK oncogene is overexpressed in a broad spectrum of cancers and plays an active role in tumor initiation, maintenance, and drug response. There are still many open questions about the regulation and function of this protein, which will certainly keep researchers active in multiple disciplines. From a structural point of view, it is unclear how DEK can bind chromatin in a sequence unspecific manner but act at discrete sites in the RNA [in fact the RNA-interacting domain(s) of DEK are unknown]. Which of the reported post-transcriptional modifications that might determine this differential DNA versus RNA recognition are also not well understood. The histone and chromatin modifiers, as well as the components of the spliceosome that interact with and are affected by DEK, need also to be better defined. Importantly, a thorough genome-wide analysis is required to establish a hierarchical map of DEK-dependent modulators of cell proliferation and cell viability. The crosstalk between DEK, p53, Rb, and the apoptotic machinery also deserves attention, as this information may guide the development of improved therapies. Although these questions are being investigated, the available knowledge about the tumor-selective expression and function of DEK can already be funneled into clinical practice (in the form of diagnostic markers, and as a platform for drug design). These results illustrate how a multidisciplinary characterization of

chromatin organizing factor can efficiently merge basic and translational research in oncology.

Disclosure of Potential Conflicts of Interest

The authors declare no potential conflicts of interest.

Acknowledgments

We apologize to investigators whose research was not cited or discussed because of space constraints. We thank Ferdinand Kappes, Susanne Wells, David Markovitz, and Agnieszka Checkinska for helpful suggestions and critical reading of this manuscript.

Grant Support

Work in the Soengas laboratory is supported by grants NIH R01 CA107237, CA125017; Spanish Ministry of Science and Innovation SAF2008-1950 (M.S. Soengas); and institutional grants from the Spanish Association Against Cancer and Spanish National Cancer Research Centre.

Received 02/25/2010; revised 03/24/2010; accepted 03/24/2010; published OnlineFirst 05/25/2010.

References

1. Kappes F, Burger K, Baack M, Fackelmayer FO, Gruss C. Subcellular localization of the human proto-oncogene protein DEK. J Biol Chem 2001;276:26317–23.
2. von Lindern M, Fornerod M, van Baal S, et al. The translocation (6;9), associated with a specific subtype of acute myeloid leukemia, results in the fusion of two genes, dek and can, and the expression of a chimeric, leukemia-specific dek-can mRNA. Mol Cell Biol 1992;12: 1687–97.
3. Soekarman D, von Lindern M, Daenen S, et al. The translocation (6;9) (p23;q34) shows consistent rearrangement of two genes and defines a myeloproliferative disorder with specific clinical features. Blood 1992;79:2990–7.
4. Alexiadis V, Waldmann T, Andersen J, Mann M, Knippers R, Gruss C. The protein encoded by the proto-oncogene DEK changes the topology of chromatin and reduces the efficiency of DNA replication in a chromatin-specific manner. Genes Dev 2000;14:1308–12.
5. Waldmann T, Eckerich C, Baack M, Gruss C. The ubiquitous chromatin protein DEK alters the structure of DNA by introducing positive supercoils. J Biol Chem 2002;277:24988–94.
6. Hu HG, Scholten I, Gruss C, Knippers R. The distribution of the DEK protein in mammalian chromatin. Biochem Biophys Res Commun 2007;358:1008–14.
7. Takata H, Nishijima H, Ogura S, et al. Proteome analysis of human nuclear insoluble fractions. Genes Cells 2009;14:975–90.
8. Cleary J, Sitwala KV, Khodadoust MS, et al. p300/CBP-associated factor drives DEK into interchromatin granule clusters. J Biol Chem 2005;280:31760–7.
9. Waldmann T, Baack M, Richter N, Gruss C. Structure-specific binding of the proto-oncogene protein DEK to DNA. Nucleic Acids Res 2003;31:7003–10.
10. Kappes F, Scholten I, Richter N, Gruss C, Waldmann T. Functional domains of the ubiquitous chromatin protein DEK. Mol Cell Biol 2004;24:6000–10.
11. Böhm F, Kappes F, Scholten I, et al. The SAF-box domain of chromatin protein DEK. Nucleic Acids Res 2005;33:1101–10.
12. Devany M, Kappes F, Chen KM, Markovitz DM, Matsuo H. Solution NMR structure of the N-terminal domain of the human DEK protein. Protein Sci 2008;17:205–15.
13. Kipp M, Gohring F, Ostendorp T, et al. SAF-Box, a conserved protein domain that specifically recognizes scaffold attachment region DNA. Mol Cell Biol 2000;20:7480–9.
14. Soares LM, Zanier K, Mackereth C, Sattler M, Valcarcel J. Intron removal requires proofreading of U2AF/3′ splice site recognition by DEK. Science 2006;312:1961–5.
15. McGarvey T, Rosonina E, McCracken S, et al. The acute myeloid leukemia-associated protein, DEK, forms a splicing-dependent interaction with exon-product complexes. J Cell Biol 2000;150:309–20.
16. Le Hir H, Gatfield D, Izaurralde E, Moore MJ. The exon-exon junction complex provides a binding platform for factors involved in mRNA export and nonsense-mediated mRNA decay. EMBO J 2001;20: 4987–97.
17. Mor-Vaknin N, Punturieri A, Sitwala K, et al. The DEK nuclear autoantigen is a secreted chemotactic factor. Mol Cell Biol 2006;26: 9484–96.
18. Sitwala KV, Mor-Vaknin N, Markovitz DM. Minireview: DEK and gene regulation, oncogenesis and AIDS. Anticancer Res 2003;23: 2155–8.
19. Casas S, Nagy B, Elonen E, et al. Aberrant expression of HOXA9, DEK, CBL and CSF1R in acute myeloid leukemia. Leuk Lymphoma 2003;44:1935–41.
20. Larramendy ML, Niini T, Elonen E, et al. Overexpression of translocation-associated fusion genes of FGFRI, MYC, NPMI, and DEK, but absence of the translocations in acute myeloid leukemia. A microarray analysis. Haematologica 2002;87:569–77.
21. Grasemann C, Gratias S, Stephan H, et al. Gains and overexpression identify DEK and E2F3 as targets of chromosome 6p gains in retinoblastoma. Oncogene 2005;24:6441–9.
22. Orlic M, Spencer CE, Wang L, Gallie BL. Expression analysis of 6p22 genomic gain in retinoblastoma. Genes Chromosomes Cancer 2006; 45:72–82.
23. Paderova J, Orlic-Milacic M, Yoshimoto M, da Cunha Santos G, Gallie B, Squire JA. Novel 6p rearrangements and recurrent translocation breakpoints in retinoblastoma cell lines identified by spectral karyotyping and mBAND analyses. Cancer Genet Cytogenet 2007; 179:102–11.
24. Kroes RA, Jastrow A, McLone MG, et al. The identification of novel therapeutic targets for the treatment of malignant brain tumors. Cancer Lett 2000;156:191–8.
25. Kondoh N, Wakatsuki T, Ryo A, et al. Identification and characterization of genes associated with human hepatocellular carcinogenesis. Cancer Res 1999;59:4990–6.
26. Khodadoust MS, Verhaegen M, Kappes F, et al. Melanoma proliferation and chemoresistance controlled by the DEK oncogene. Cancer Res 2009;69:6405–13.
27. Carro MS, Spiga FM, Quarto M, et al. DEK Expression is controlled by E2F and deregulated in diverse tumor types. Cell Cycle 2006;5: 1202–7.
28. Evans AJ, Gallie BL, Jewett MA, et al. Defining a 0.5-mb region of genomic gain on chromosome 6p22 in bladder cancer by quantitative-multiplex polymerase chain reaction. Am J Pathol 2004;164: 285–93.
29. Sanchez-Carbayo M, Socci ND, Lozano JJ, et al. Gene discovery in bladder cancer progression using cDNA microarrays. Am J Pathol 2003;163:505–16.
30. Han S, Xuan Y, Liu S, et al. Clinicopathological significance of DEK overexpression in serous ovarian tumors. Pathol Int 2009;59:443–7.
31. Wu Q, Li Z, Lin H, Han L, Liu S, Lin Z. DEK overexpression in uterine cervical cancers. Pathol Int 2008;58:378–82.
32. Abba MC, Sun H, Hawkins KA, et al. Breast cancer molecular signatures as determined by SAGE: correlation with lymph node status. Mol Cancer Res 2007;5:881–90.
33. Nagpal JK, Das BR. Identification of differentially expressed genes in tobacco chewing-mediated oral cancer by differential display-polymerase chain reaction. Eur J Clin Invest 2007;37:658–64.
34. Fornerod M, Boer J, van Baal S, et al. Relocation of the carboxyterminal part of CAN from the nuclear envelope to the nucleus as a result of leukemia-specific chromosome rearrangements. Oncogene 1995; 10:1739–48.

35. Santos GC, Zielenska M, Prasad M, Squire JA. Chromosome 6p amplification and cancer progression. J Clin Pathol 2007;60:1–7.
36. Sitwala KV, Adams K, Markovitz DM. YY1 and NF-Y binding sites regulate the transcriptional activity of the dek and dek-can promoter. Oncogene 2002;21:8862–70.
37. Goodarzi H, Elemento O, Tavazoie S. Revealing global regulatory perturbations across human cancers. Mol Cell 2009;36:900–11.
38. Castellano G, Torrisi E, Ligresti G, et al. The involvement of the transcription factor Yin Yang 1 in cancer development and progression. Cell Cycle 2009;8:1367–72.
39. Wise-Draper TM, Allen HV, Thobe MN, et al. The human DEK proto-oncogene is a senescence inhibitor and an upregulated target of high-risk human papillomavirus E7. J Virol 2005;79:14309–17.
40. Wise-Draper TM, Mintz-Cole RA, Morris TA, et al. I. Overexpression of the cellular DEK protein promotes epithelial transformation *in vitro* and *in vivo*. Cancer Res 2009;69:1792–9.
41. Wise-Draper TM, Morreale RJ, Morris TA, et al. DEK proto-oncogene expression interferes with the normal epithelial differentiation program. Am J Pathol 2009;174:71–81.
42. Sherr CJ, McCormick F. The RB and p53 pathways in cancer. Cancer Cell 2002;2:103–12.
43. Kappes F, Damoc C, Knippers R, Przybylski M, Pinna LA, Gruss C. Phosphorylation by protein kinase CK2 changes the DNA binding properties of the human chromatin protein DEK. Mol Cell Biol 2004;24:6011–20.
44. Kappes F, Fahrer J, Khodadoust MS, et al. DEK is a poly(ADP-ribose) acceptor in apoptosis and mediates resistance to genotoxic stress. Mol Cell Biol 2008;28:3245–57.
45. Sawatsubashi S, Murata T, Lim J, et al. A histone chaperone, DEK, transcriptionally coactivates a nuclear receptor. Genes Dev 2009;24: 159–70.
46. Gamble MJ, Fisher RP. SET and PARP1 remove DEK from chromatin to permit access by the transcription machinery. Nat Struct Mol Biol 2007;14:548–55.
47. Lamond AI, Spector DL. Nuclear speckles: a model for nuclear organelles. Nat Rev Mol Cell Biol 2003;4:605–12.
48. Ko SI, Lee IS, Kim JY, et al. Regulation of histone acetyltransferase activity of p300 and PCAF by proto-oncogene protein DEK. FEBS Lett 2006;580:3217–22.
49. Ouararhni K, Hadj-Slimane R, Ait-Si-Ali S, et al. The histone variant mH2A1.1 interferes with transcription by down-regulating PARP-1 enzymatic activity. Genes Dev 2006;20:3324–36.
50. Cavellan E, Asp P, Percipalle P, Farrants AK. The WSTF-SNF2h chromatin remodeling complex interacts with several nuclear proteins in transcription. J Biol Chem 2006;281:16264–71.
51. Ageberg M, Drott K, Olofsson T, Gullberg U, Lindmark A. Identification of a novel and myeloid specific role of the leukemia-associated fusion protein DEK-NUP214 leading to increased protein synthesis. Genes Chromosomes Cancer 2008;47:276–87.
52. Hollenbach AD, McPherson CJ, Mientjes EJ, Iyengar R, Grosveld G. Daxx and histone deacetylase II associate with chromatin through an interaction with core histones and the chromatin-associated protein Dek. J Cell Sci 2002;115:3319–30.
53. Sammons M, Wan SS, Vogel NL, Mientjes EJ, Grosveld G, Ashburner BP. Negative regulation of the RelA/p65 transactivation function by the product of the DEK proto-oncogene. J Biol Chem 2006;281: 26802–12.
54. Hu HG, Illges H, Gruss C, Knippers R. Distribution of the chromatin protein DEK distinguishes active and inactive CD21/CR2 gene in pre- and mature B lymphocytes. Int Immunol 2005;17:789–96.
55. Campillos M, Garcia MA, Valdivieso F, Vazquez J. Transcriptional activation by AP-2α is modulated by the oncogene DEK. Nucleic Acids Res 2003;31:1571–5.
56. Campisi J, d'Adda di Fagagna F. Cellular senescence: when bad things happen to good cells. Nat Rev Mol Cell Biol 2007;8: 729–40.
57. Gray-Schopfer V, Wellbrock C, Marais R. Melanoma biology and new targeted therapy. Nature 2007;445:851–7.
58. Savli H, Aalto Y, Nagy B, Knuutila S, Pakkala S. Gene expression analysis of 1,25(OH)2D3-dependent differentiation of HL-60 cells: a cDNA array study. Br J Haematol 2002;118:1065–70.
59. Ageberg M, Gullberg U, Lindmark A. The involvement of cellular proliferation status in the expression of the human proto-oncogene DEK. Haematologica 2006;91:268–9.
60. Wise-Draper TM, Allen HV, Jones EE, Habash KB, Matsuo H, Wells S. I. Apoptosis inhibition by the human DEK oncoprotein involves interference with p53 functions. Mol Cell Biol 2006;26: 7506–19.
61. Kim DW, Chae JI, Kim JY, et al. Proteomic analysis of apoptosis related proteins regulated by proto-oncogene protein DEK. J Cell Biochem 2009;106:1048–59.
62. Garcon L, Libura M, Delabesse E, et al. DEK-CAN molecular monitoring of myeloid malignancies could aid therapeutic stratification. Leukemia 2005;19:1338–44.

Melanoma Proliferation and Chemoresistance Controlled by the DEK Oncogene

Michael S. Khodadoust,[1] Monique Verhaegen,[2] Ferdinand Kappes,[3] Erica Riveiro-Falkenbach,[7] Juan C. Cigudosa,[8] David S.L. Kim,[4] Arul M. Chinnaiyan,[4,5,6] David M. Markovitz,[1,3] and María S. Soengas[2,7]

[1]Program in Immunology, Departments of [2]Dermatology, [3]Internal Medicine, Division of Infectious Diseases, [4]Department of Pathology, [5]Michigan Center for Translational Pathology, and [6]Howard Hughes Medical Institute, University of Michigan Medical Center, Ann Arbor, Michigan and [7]Melanoma Laboratory, Molecular Pathology Programme and [8]Molecular Cytogenetics Group, Centro Nacional de Investigaciones Oncológicas (Spanish National Cancer Research Centre), Madrid, Spain

Abstract

Gain of chromosome 6p is a consistent feature of advanced melanomas. However, the identity of putative oncogene(s) associated with this amplification has remained elusive. The chromatin remodeling factor *DEK* is an attractive candidate as it maps to 6p (within common melanoma-amplified loci). Moreover, DEK expression is increased in metastatic melanomas, although the functional relevance of this induction remains unclear. Importantly, in other tumor types, DEK can display various tumorigenic effects in part through its ability to promote proliferation and inhibit p53-dependent apoptosis. Here, we report a generalized up-regulation of DEK protein in aggressive melanoma cells and tumors. In addition, we provide genetic and mechanistic evidence to support a key role of DEK in the maintenance of malignant phenotypes of melanoma cells. Specifically, we show that long-term DEK down-regulation by independent short hairpin RNAs resulted in premature senescence of a variety of melanoma cell lines. Short-term abrogation of DEK expression was also functionally relevant, as it attenuated the traditional resistance of melanomas to DNA-damaging agents. Unexpectedly, DEK short hairpin RNA had no effect on p53 levels or p53-dependent apoptosis. Instead, we identified a new role for DEK in the transcriptional activation of the antiapoptotic MCL-1. Other MCL-1–related factors such as BCL-2 or BCL-x_L were unaffected by changes in the endogenous levels of DEK, indicating a selective effect of this gene on the apoptotic machinery of melanoma cells. These results provide support for DEK as a long sought-after oncogene mapping at chromosome 6, with novel functions in melanoma proliferation and chemoresistance. [Cancer Res 2009;69(16):6405–13]

Introduction

Metastatic melanomas are invariably chemoresistant and carry a grim prognosis (1). Complicating drug development, melanoma cells accumulate a plethora of changes in gene expression with the potential to unleash uncontrolled proliferation, evade senescence programs, and inhibit death pathways at multiple levels (2). A hierarchical mapping of these alterations (to distinguish central nodes in tumor cell maintenance from inconsequential byproducts of tumor development) has remained elusive. Equally unclear are the mechanisms underlying common melanoma-associated events that have been ascribed neither to mutations nor to genetic or epigenetic alterations. This is particularly relevant for the antiapoptotic members of the BCL-2 family (BCL-2, BCL-x_L, and MCL-1). These proteins are invariably overexpressed in melanoma cells and play key roles in their chemoresistance (3). BCL-2 up-regulation may be a consequence of MITF gene amplification (4). BCL-x_L and MCL-1 can be under the control of the mitogen-activated protein kinase or nuclear factor-κB signaling cascades (5). However, neither MITF, mitogen-activated protein kinase, nor nuclear factor-κB inhibition abrogates the expression of these BCL-2 family members (6–8), suggesting alternative, and yet unknown, mechanisms of regulation of the apoptotic machinery in melanoma cells.

Alteration of chromosome 6 is one of the most consistent cytogenetic changes in melanoma (9). In particular, gain of the 6p arm is prevalent in different manifestations of the disease, including cutaneous (both sun-exposed and non–sun-exposed), acral, mucosal, and uveal melanomas (10, 11). Furthermore, temporal clustering of karyotypic changes in melanoma indicates that 6p gain may represent an early event in the acquisition of chromosomal imbalances (12). Adding to the clinical relevance of chromosome 6, 6p copy gains have been associated with poor prognosis in ocular melanomas (11). Therefore, it has been long suggested that this genomic region could contain one or multiple pro-oncogenes (9, 13, 14). Although the minimal region of 6p gain has not been described in melanoma, several reports in retinoblastoma and bladder cancer have identified a narrow region of gain in 6p22-23 (15–18). This region notably contains the chromatin remodeling factor DEK.

DEK was originally discovered as the target of a chromosomal translocation event [t(6;9)(p23;q34)] in a subset of acute myeloid leukemias (19). Subsequent studies have repeatedly identified DEK as a frequently overexpressed gene in several neoplasms (16, 20–22). Furthermore, we and others have shown that DEK has effects on mRNA splicing, transcriptional control, DNA damage repair, differentiation, cell viability, and cell-to-cell signaling (23–31). Pro-oncogenic roles of DEK are supported by its ability to inhibit p53-mediated apoptosis (32), cooperate with the viral oncogenes E6 and E7 to overcome senescence (29), and promote HRAS-driven keratinocyte transformation (28). The mechanism(s) through which DEK mediates its effects, particularly in the context of cellular oncogenes, is not well understood. DEK is a structurally unique

Note: Supplementary data for this article are available at Cancer Research Online (http://cancerres.aacrjournals.org/).

Requests for reprints: María S. Soengas, Centro Nacional de Investigaciones Oncológicas, Melchor Fernández Almagro 3, Madrid 28049, Spain. Phone: 34-91-732-8000, ext. 3680; Fax: 34-91-732-8000; E-mail: msoengas@cnio.es and David M. Markovitz, Department of Internal Medicine, University of Michigan Medical Center, Ann Arbor, 1150 West Medical Center Drive, Ann Arbor, MI 48109-5640. Email: dmarkov@umich.edu.

doi:10.1158/0008-5472.CAN-09-1063

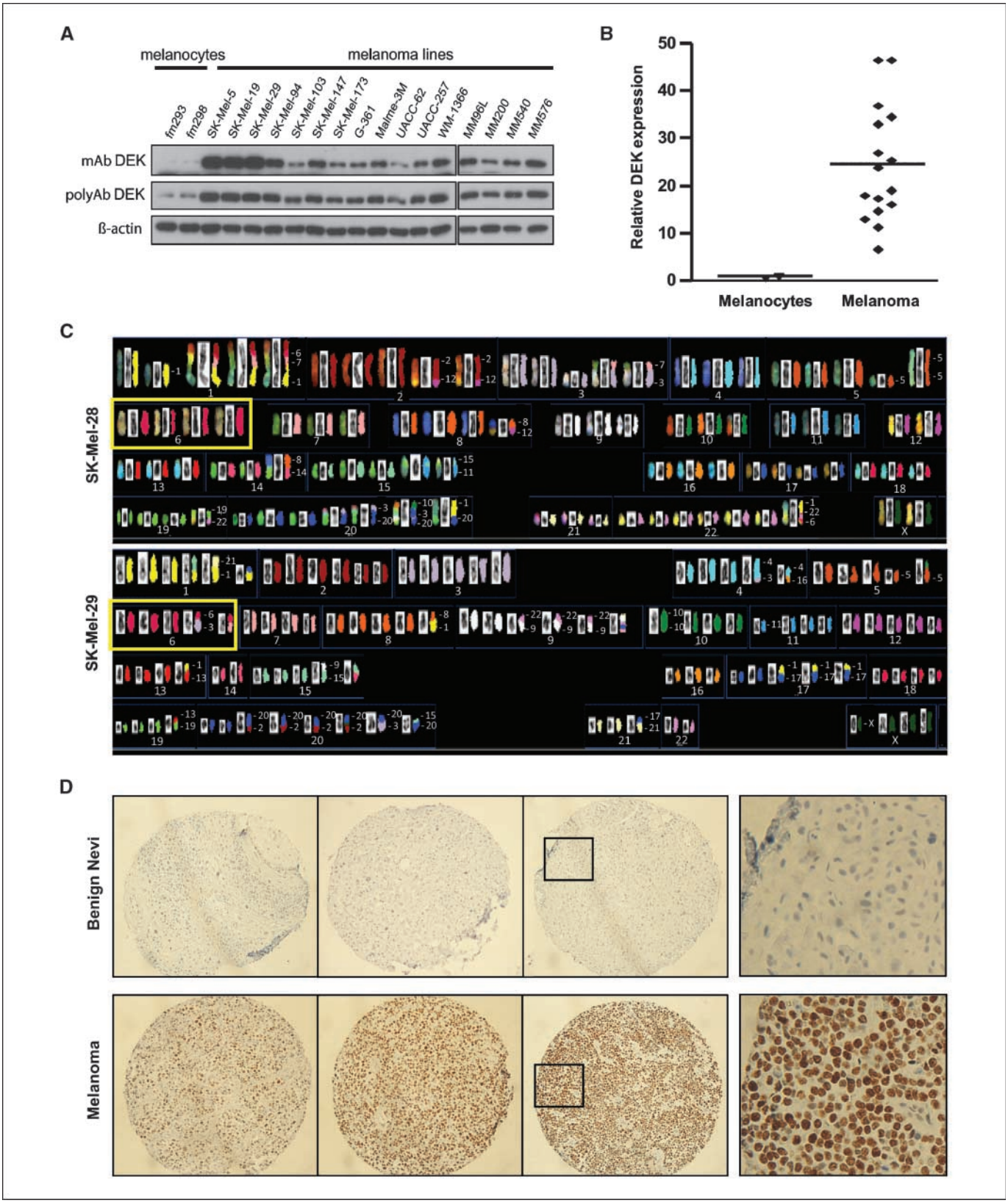

Figure 1. Overexpression of DEK in melanoma cell lines and tissue specimens. *A,* immunoblotting of a panel of metastatic melanoma lines and primary foreskin-derived melanocytes (FM293 and FM298), with monoclonal (*mAb*) and polyclonal (*polyAb*) anti-DEK antibodies. *B,* monoclonal anti-DEK band densities were quantified by densitometry, and relative DEK protein levels were normalized to FM293 melanocytes. *Horizontal line,* mean for each group. *C,* spectral karyotyping analysis showing increased copy number at chromosome 6 (*yellow boxes*) in SK-Mel-28 and SK-Mel-29, both expressing high levels of DEK (Figs. 1*A* and 2*C*). *D,* representative examples of DEK staining in benign nevi (*top*) and melanoma lesions (*bottom*) included in tissue microarrays. *Right,* higher-magnification views of the indicated areas.

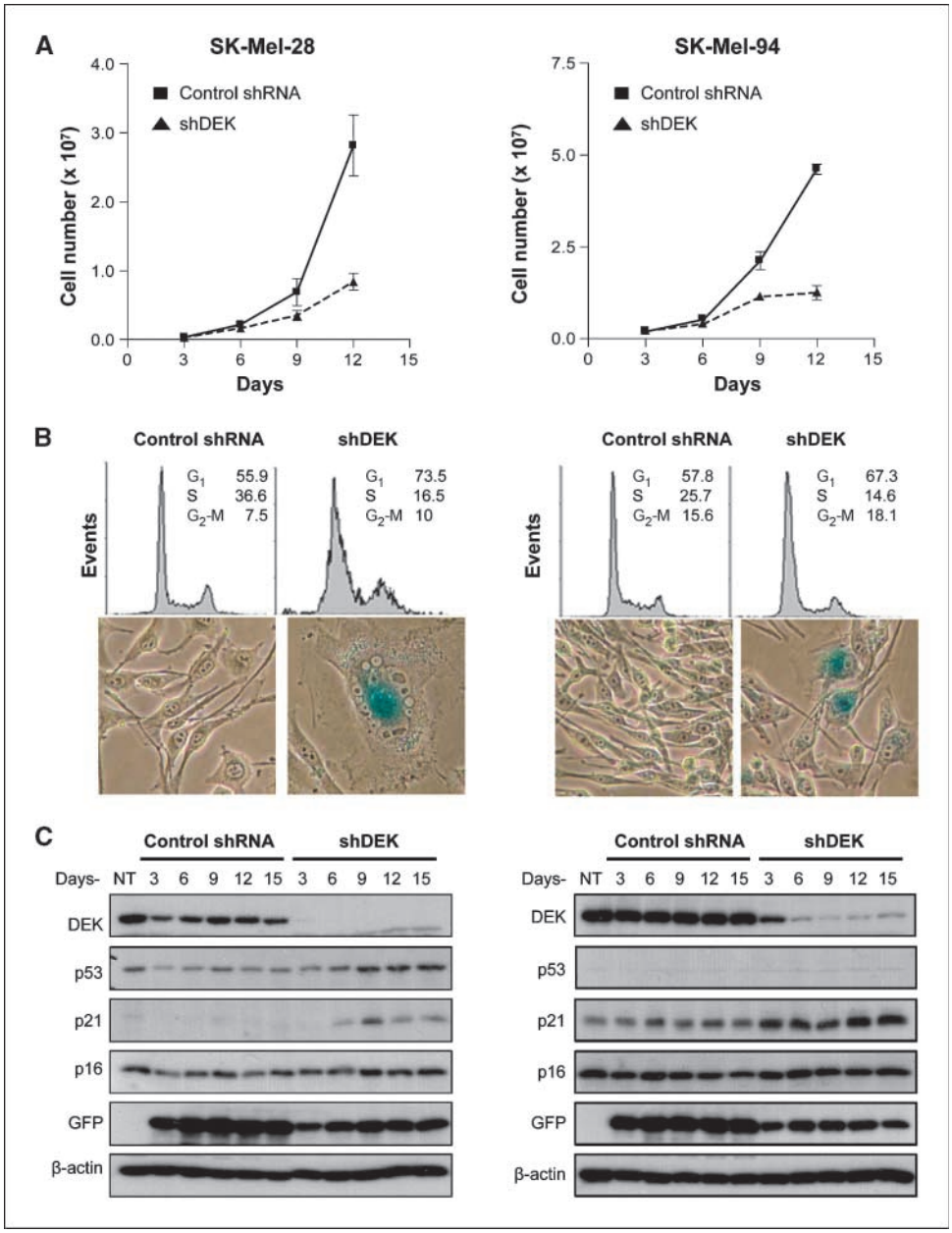

Figure 2. Induction of senescence-like cell cycle arrest by long-term down-regulation of DEK. *A,* total cell numbers estimated in SK-Mel-28 (*left*) and SK-Mel-94 (*right*) after infection with *control shRNA* or shDEK-2 (*shDEK*)–expressing lentiviruses. *Bars,* SE. *B,* melanoma cell lines were transduced as in *A*. Fifteen days after infection, cell cycle profile distribution was analyzed by flow cytometry (*top*), and senescence features were determined by senescence-associated β-galactosidase activity (*bottom, blue signal*). *C,* cells were treated as in *A*. Whole-cell lysates were processed for detection of the indicated proteins by immunoblotting. *NT,* no treatment.

protein (33) that binds preferentially to euchromatin, although it can also be found within interchromatin granule clusters (34). Consequently, it is unclear which DEK targets have a causative role in tumor development and which are passengers of global changes of chromatin architecture.

The contribution of DEK to melanoma progression and chemoresistance has yet to be analyzed. Increased DEK mRNA and protein has been reported in a small number of melanoma cell lines or tissues (21, 35). However, DEK function is highly dependent on post-translational modifications (34, 36). Therefore, it is unclear whether altered DEK expression is a generalized feature of advanced melanomas and whether this gene has a functional contribution to melanoma cell maintenance and drug response. To assess these questions, we used tissue microarrays to compare the expression of DEK among benign nevi and malignant melanoma specimens. In addition, the role of DEK was defined in a panel of aggressive melanoma cell lines that recapitulate the most frequent melanoma-associated defects. Our studies establish *DEK*, a gene mapping to the genetically unstable 6p region, as the first chromatin remodeling factor with dual and selective roles in proliferation and apoptotic resistance in melanoma, acting independently of classic tumor suppressor pathways.

Materials and Methods

Cells and reagents. Human melanocytes and melanoma lines were isolated and cultured as described previously (6, 37). Doxorubicin hydrochloride, cycloheximide, and 4′,6-diamidino-2-phenylindole (DAPI) were purchased from Sigma. Bortezomib was obtained from Millennium Pharmaceuticals. z-VAD-fmk was purchased from Calbiochem. TW-37 synthesis and validation has been described elsewhere (38).

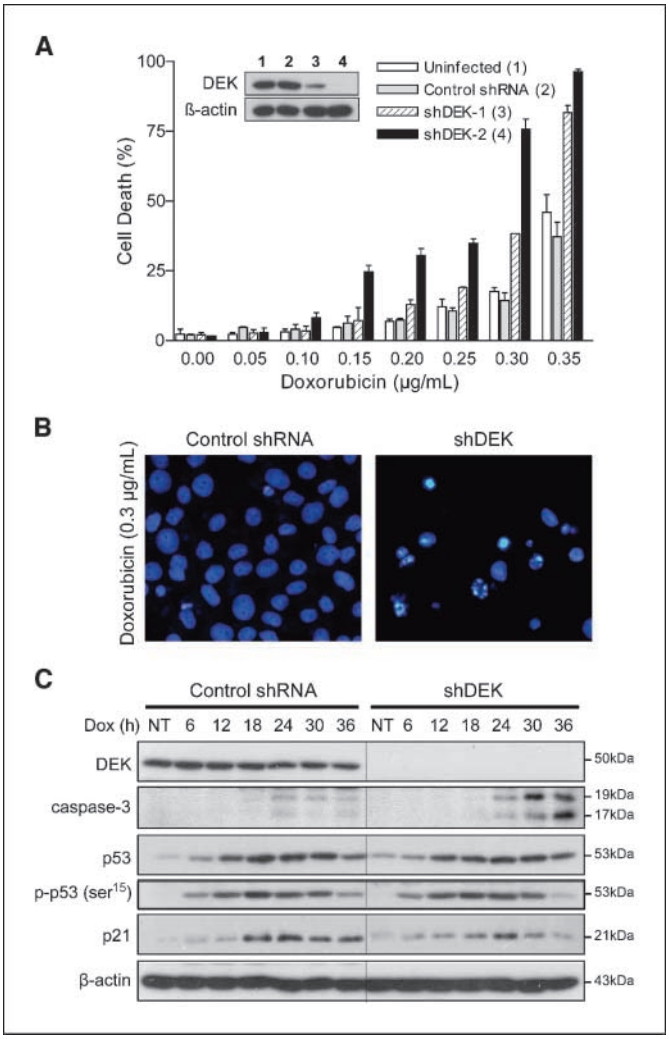

Figure 3. p53-independent induction of cell death by short-term inactivation of DEK. *A,* SK-Mel-19 cells transduced with the indicated shRNAs were treated with doxorubicin (*Dox*) for 30 h, and cell death was determined by DAPI staining and counting of condensed and fragmented nuclei. *B,* fluorescence microscopy illustrating cell nuclear morphology after treatment with 0.3 μg/mL doxorubicin for 30 h in cells transduced with a control vector (*left*) or shDEK-2 (*right*). *C,* SK-Mel-19 cells transduced as in *A* were treated with 0.2 μg/mL doxorubicin, collected at the indicated times, and analyzed by immunoblotting.

Extract preparation and gene expression analyses. Total cell lysates were obtained by Laemmli extraction, separated by SDS-PAGE, and transferred to Immobilon-P membranes (Millipore) for immunoblotting (antibodies used in this study are listed in Supplementary Materials). Protein expression was quantified using Scion image densitometry software (Scion). Lentiviral-mediated modulation of DEK, MCL-1, BCL-2, and BCL-x_L, tissue microarrays, spectral karyotyping, and comparative genomic hybridization procedures are described in Supplementary Information.

Cell proliferation and viability assays. Total cell numbers were estimated at the indicated times by manual counting, and cell death rates were determined by standard trypan blue exclusion assays (38). For flow cytometry assays, cells were fixed in 70% ethanol, digested with 0.5 mg/mL RNase A, and stained with 50 μg/mL propidium iodide before analysis in a FACSCalibur (Becton Dickinson Immunocytometry Systems). Data were fitted using ModFit software (Verity Software). Senescence-associated β-galactosidase staining was done as described previously (37). Nuclear condensation and fragmentation were assessed by fluorescence microscopy after DAPI staining using an Olympus BX-51 upright microscope.

Quantitative real-time reverse transcription-PCR. RNA purification and real-time reverse transcription-PCR using a Bio-Rad iCycler (Bio-Rad) were done essentially as described previously (37, 39) using the following primers: *mcl1* forward ATGCTTCGGAAACTGGACAT and reverse TCCTGATGCCACCTTCTAGG and *β-actin* forward CGCCCAGCACGATGAAA and reverse CCGCCGATCCACACAGA. The assay included a no-template control and a standard curve of six dilutions for both *mcl-1* and *β-actin*. Results are given as the average ± SE of three experiments, and each sample was amplified and analyzed in triplicate.

Luciferase reporter gene assays. The human *MCL-1* promoter reporter plasmid −203/+10 was a generous gift of Douglas Cress (40). Cells were transfected using Lipofectamine 2000 (Invitrogen) and the lysates were assayed for firefly and *Renilla* luciferase activity using the Dual-Luciferase Reporter Assay System (Promega). Luminescence was detected with a Tecan GENios plate reader. Data are presented as the mean ± SE of three experiments.

Statistics. Statistical analyses of cell death, quantitative real-time reverse transcription-PCR, and luciferase reporter assays were done using a paired, two-tailed Student's *t* test.

Results

DEK protein overexpression in metastatic melanoma. We hypothesized that gain of 6p in melanoma may function to promote DEK overexpression. To this end, a panel of 16 metastatic melanoma lines was selected to reflect the most common melanoma-associated alterations in oncogenes or tumor suppressors (see Supplementary Table S1). In parallel, primary human foreskin-derived melanocytes were used as controls for normal cells. Immunoblotting revealed a generalized high expression of DEK, with an average 30-fold induction over the basal levels of normal melanocytes (Fig. 1*A* and *B*).

Interestingly, spectral karyotyping confirmed that melanoma cell lines with high DEK expression (SK-Mel-28 and -29) contained, among other genetic abnormalities, an increased copy number of chromosome 6 (Fig. 1*C*). However, large-scale chromosome 6p amplifications are unlikely to be the sole mechanism underlying DEK up-regulation. Thus, lines such as SK-Mel-103 or SK-Mel-147, with moderate levels of DEK protein (Fig. 1*A*), had a normal copy number of chromosome 6 defined by spectral karyotyping (Supplementary Fig. S1*A*). Comparative genomic hybridization showed focal gains at 6p22.3 but centromeric to DEK (Supplementary Fig. S1*B*).

To validate the increased DEK protein expression found in cell lines, an extensive immunohistochemical analysis was done on two tissue microarrays, containing surgically removed melanocytic lesions, each spotted in triplicate. Specifically, these tissue microarrays included 87 primary melanomas and 115 metastatic specimens. In addition, 3 dysplastic nevi, 7 benign nevi, and 5 biopsies of normal skin were included as reference. Notably, 90% of the tumors analyzed showed clear positive DEK expression (10% being very marked and 80% with moderate DEK levels; see representative examples in Fig. 1*D, bottom*). Normal skin melanocytes and benign nevi showed no detectable DEK expression (Fig. 1*D, top*; results not shown). Therefore, these results support a broad-spectrum up-regulation of DEK during melanoma progression.

Long-term down-regulation of the endogenous DEK expression in melanoma induces premature senescence. Lentiviral vectors were used to transduce short hairpin RNAs (shRNA) and down-regulate DEK in a stable manner. To avoid complications of off-target effects, three independent shRNAs were tested (see Supplementary Fig. S2). In 6 of 12 lines analyzed (SK-Mel-28, SK-Mel-94, G-361, UACC-62, UACC-257, and MM576),

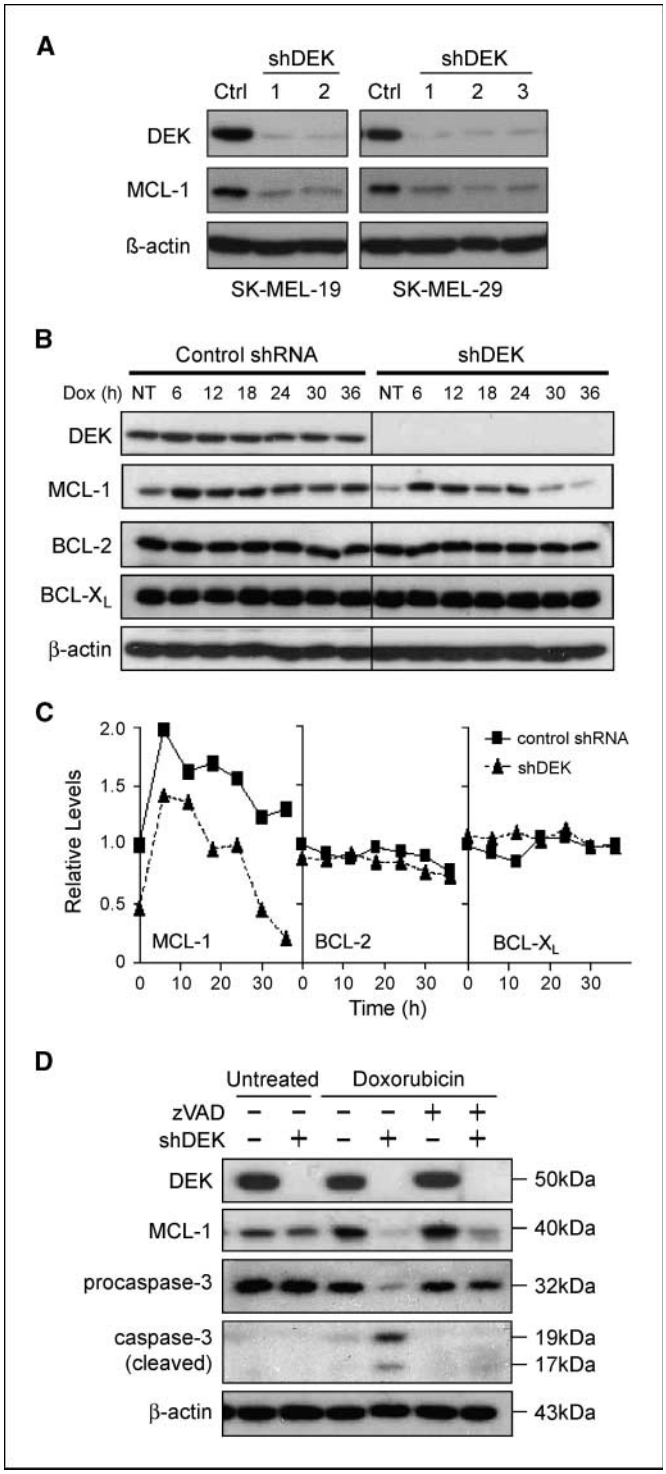

Figure 4. Caspase-independent down-regulation of MCL-1 by DEK shRNA. *A,* indicated melanoma cells were infected with either a control (*Ctrl*) lentivirus or one of three distinct vectors targeting DEK expression (*shDEK-1, shDEK-2*, and *shDEK-3*). Ninety-six hours after infection, cells were collected and their lysates were immunoblotted for DEK and MCL-1 expression. *B,* SK-Mel-19 cells transduced with the indicated shRNAs were treated with 0.2 μg/mL doxorubicin and collected for immunoblotting analyses. *C,* relative expression of MCL-1 (*left*), BCL-2 (*middle*), and BCL-x_L (*right*) following doxorubicin treatment as estimated by band densitometry. Expression is shown relative to that of untreated control-transduced cells. *D,* protein immunoblots in control and shDEK-infected SK-Mel-19 cells treated with 0.2 μg/mL doxorubicin alone or with doxorubicin in the presence of 50 μmol/L of the pan-caspase inhibitor z-VAD-fmk.

DEK depletion led to a progressive cell cycle arrest, eventually resulting in a near complete inhibition of cell proliferation as determined by total cell counting (Fig. 2*A*) and flow cytometry (Fig. 2*B, top*).

The reduction of cells in S phase of the cell cycle (Fig. 2*B, top*) was accompanied by cell enlargement, flattening, and vacuolization (Fig. 2*B, bottom*) reminiscent of classic senescent phenotypes (41). In fact, staining for senescence-associated β-galactosidase activity was positive in DEK-depleted melanoma cells (Fig. 2*B, bottom*). Interestingly, cell cycle arrest and the acquisition of senescent-like features occurred in cells expressing either wild-type p53 or mutated p53 (e.g., SK-Mel-94 or SK-Mel-28, respectively; Fig. 2*C*). Notably, DEK shRNAs did not affect the expression of $p16^{INK4A}$ (Fig. 2*C*), a senescence-associated tumor suppressor. These results show that DEK is required for the continued proliferation of metastatic melanoma cells and point to novel p53 and p16 ^{INK4A}-independent senescence programs.

Short-term down-regulation of DEK expression bypasses melanoma chemoresistance. Recently, we have shown that DEK can enhance resistance to DNA-damaging agents by promoting efficient resolution of DNA damage foci (42). Therefore, we sought to determine whether short term down-regulation of DEK (therapeutically more feasible than sustained gene inactivation) could contribute to the ability of melanoma cells to withstand genotoxic agents. The anthracycline doxorubicin is a potent antineoplastic agent in other tumor types but has only limited efficacy against metastatic melanoma (8). This drug was selected to treat cells with the highest levels of DEK, as they may be more dependent on this protein for survival (see Fig. 3 for SK-Mel-19 and Fig. 4 for SK-Mel-29; results with other cell lines are discussed next). SK-Mel-19 was infected with a control shRNA lentiviral vector, a vector expressing a single DEK-specific shRNA (shDEK-1) or a vector expressing two distinct DEK-specific shRNAs (shDEK-2). Two days after lentiviral infection, cells were treated with increasing doses of doxorubicin and cell death was estimated within 24 to 36 h after treatment. Relatively high levels of doxorubicin were required to kill melanoma cells in the presence of DEK (>0.2 μg/mL; Fig. 3*A*). However, DEK depletion resulted in a marked increase in doxorubicin-driven cell death, particularly on dual-shRNA targeting (Fig. 3*A*). Importantly, the increased response of DEK-depleted melanoma cells to doxorubicin was associated with classic apoptotic features such as chromatin condensation (Fig. 3*B*) and caspase processing (Fig. 3*C*). Therefore, although DEK may not be the sole mediator of melanoma chemoresistance, our results support a key role of this gene contributing to the malignant features of melanoma cells.

DEK does not modulate p53 levels in melanoma cells. DEK has been shown previously to mediate antiapoptotic effects through destabilization of p53 protein and inhibition of p53 activity (23, 32). However, as with the case of long-term down-regulation of DEK shown above (Fig. 2*C*), short-term expression of DEK shRNA was not found to significantly affect total p53 levels (Fig. 3*C*). Furthermore, the activation of p53 (detected by phosphorylation of its serine 15) and the induction of p53 targets, such as $p21^{CIP1}$, were similar in DEK-expressing and DEK-deficient melanoma cells (Fig. 3*C*).

DEK-knockdown cells have diminished MCL-1 expression. Overexpression of antiapoptotic BCL-2 family members has been associated with melanoma chemoresistance (3). Therefore, we tested whether DEK could control BCL-2 family members. Interestingly, DEK down-regulation with two different shRNAs led

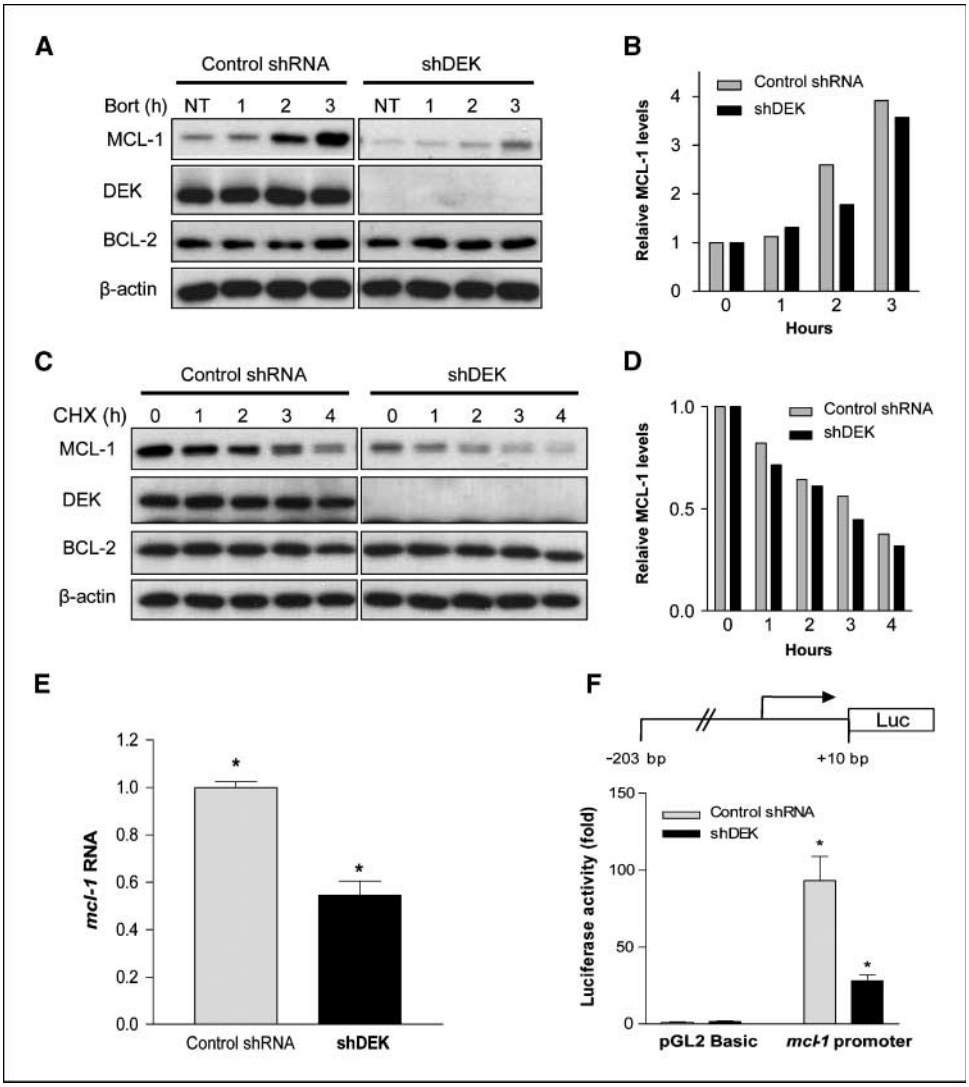

Figure 5. Transcriptional control of MCL-1 by DEK. *A,* comparative analysis of MCL-1 protein down-regulation in SK-Mel-19 cells transduced with control or DEK shRNAs and treated for the indicated times with 25 nmol/L bortezomib (*Bort*). BCL-2 and β-actin are included as examples of DEK-independent proteins and for loading control, respectively. *B,* quantification by densitometry of MCL-1 levels in *A* depicted with respect to nontreated control-infected cells. *C* and *D,* control or shRNA-transduced SK-Mel-19 cells were treated for 5 h with 25 nmol/L of the proteasome inhibitor bortezomib. Cells were then washed to remove bortezomib and incubated with cycloheximide (*CHX*) for the indicated times. Following treatment, cells were collected and processed for immunoblotting (*C*) and subsequent quantification by densitometry (*D*). *E, MCL-1* mRNA expression of control and shDEK-treated SK-Mel-19 cells determined by quantitative real-time reverse transcription-PCR. *F,* control and shDEK-transduced SK-Mel-19 cells were transfected with either the promoterless pGL2 basic plasmid or a plasmid expressing the firefly luciferase gene under the control of the human *MCL-1* promoter (*−203/+10 bp*). The average luciferase activity of three experiments is shown relative to that of control-transduced cells transfected with the pGL2 basic plasmid. *Bars,* SE. *, $P < 0.05$.

to a drastic decrease in MCL-1 expression in SK-Mel-19, SK-Mel-29, SK-Mel-5, and MM576 (Fig. 4*A*; data not shown). Notably, DEK shRNA did not alter BCL-2 or BCL-x_L levels (Fig. 4*B*), suggesting selective effects on the apoptotic machinery.

To further assess the requirement of DEK for high MCL-1 expression, DEK-depleted cells were treated with doxorubicin (which induces MCL-1 levels in melanoma cells; Fig. 4*B* and *C*). As shown in Fig. 4*B*, DEK shRNA cells ultimately expressed minimal levels of MCL-1 after doxorubicin treatment (see quantification in Fig. 4*C*). Again, the effects of DEK on the apoptotic machinery were selective, as no changes in BCL-2 or BCL-x_L levels were observed before or after doxorubicin treatment (Fig. 4*B* and *C*). Importantly, the reduction of MCL-1 expression in DEK-shRNA cells was not due to proteolytic cleavage by apoptotic caspases (43). Thus, the pan-caspase inhibitor z-VAD-fmk, although it eliminated caspase-3 cleavage, could not prevent MCL-1 down-regulation in shDEK-treated cells (Fig. 4*D*).

Decreased MCL-1 in shDEK-treated cells is not due to increased MCL-1 degradation. To determine if the decrease in MCL-1 protein in DEK-knockdown cells was due to enhanced proteasomal turnover, cells were treated with the proteasome inhibitor bortezomib. As we reported previously (39, 44), bortezomib induced a massive MCL-1 stabilization in control melanoma cells within 2 to 3 h of treatment (Fig. 5*A*). A similar rate of MCL-1 accumulation was observed in shDEK-expressing melanoma cells (Fig. 5*B*), although these cells have, as indicated above, intrinsically lower basal levels of MCL-1 (note that MCL-1 immunoblots in Fig. 5*A* were overexposed to favor the visualization of the endogenous low expression of MCL-1 in shRNA-DEK cells). Therefore, the diminished MCL-1 levels in DEK-knockdown cells were not due to increased proteosome-dependent MCL-1 degradation.

To assess the stability of MCL-1 protein in DEK-knockdown cells, cycloheximide, a translational inhibitor, was used to inhibit *de novo* MCL-1 synthesis. To better visualize the decrease in MCL-1 expression, cells were first pretreated with bortezomib to augment MCL-1 levels. Bortezomib was subsequently removed, and cells were incubated in cycloheximide and then processed for immunoblotting analysis (see Materials and Methods for additional details). As shown in Fig. 5*C* and *D*, depletion of MCL-1 occurred with similar kinetics in both control and shDEK-treated cells.

Novel role of DEK in *MCL-1* transcription. Because DEK was not affecting DEK protein stability, it could be controlling

its transcription. To this end, mRNA levels were estimated by quantitative reverse transcription-PCR. As shown in Fig. 5*E*, DEK down-regulation leads to a 50% reduction in *MCL-1* mRNA. To confirm the requirement of DEK for MCL-1 mRNA transcription, a reporter construct driving luciferase expression under the control of the proximal region of the human *MCL-1* promoter was transduced into either control or shDEK-transduced SK-Mel-19 cells (Fig. 5*F*). We found a 70% to 80% reduction in promoter activity in MCL-1 in the absence of DEK (Fig. 5*F*). These results show a new role for DEK in the transcriptional control of *MCL-1*.

Functional implication of DEK-dependent MCL-1 expression. To define the specific interplay between DEK and MCL-1 in the enhancement of melanoma chemoresistance, we generated isogenic series of melanoma cell lines with differing levels of both proteins and compared their response to doxorubicin. Additional isogenic cell lines were generated to alter (positively and negatively) the endogenous expression of BCL-x_L. BCL-x_L was chosen as an example of an antiapoptotic BCL-2 factor that is not under the control of DEK (Fig. 4*B*) but is also overexpressed in melanoma cells (3).

To alter MCL-1 expression, we used two approaches. First, we generated lentiviral vectors to drive MCl-1 from an ectopic promoter that is not sensitive to DEK. Viral titers were selected to restore MCL-1 levels to the basal conditions (Fig. 6*A, left, inset*).

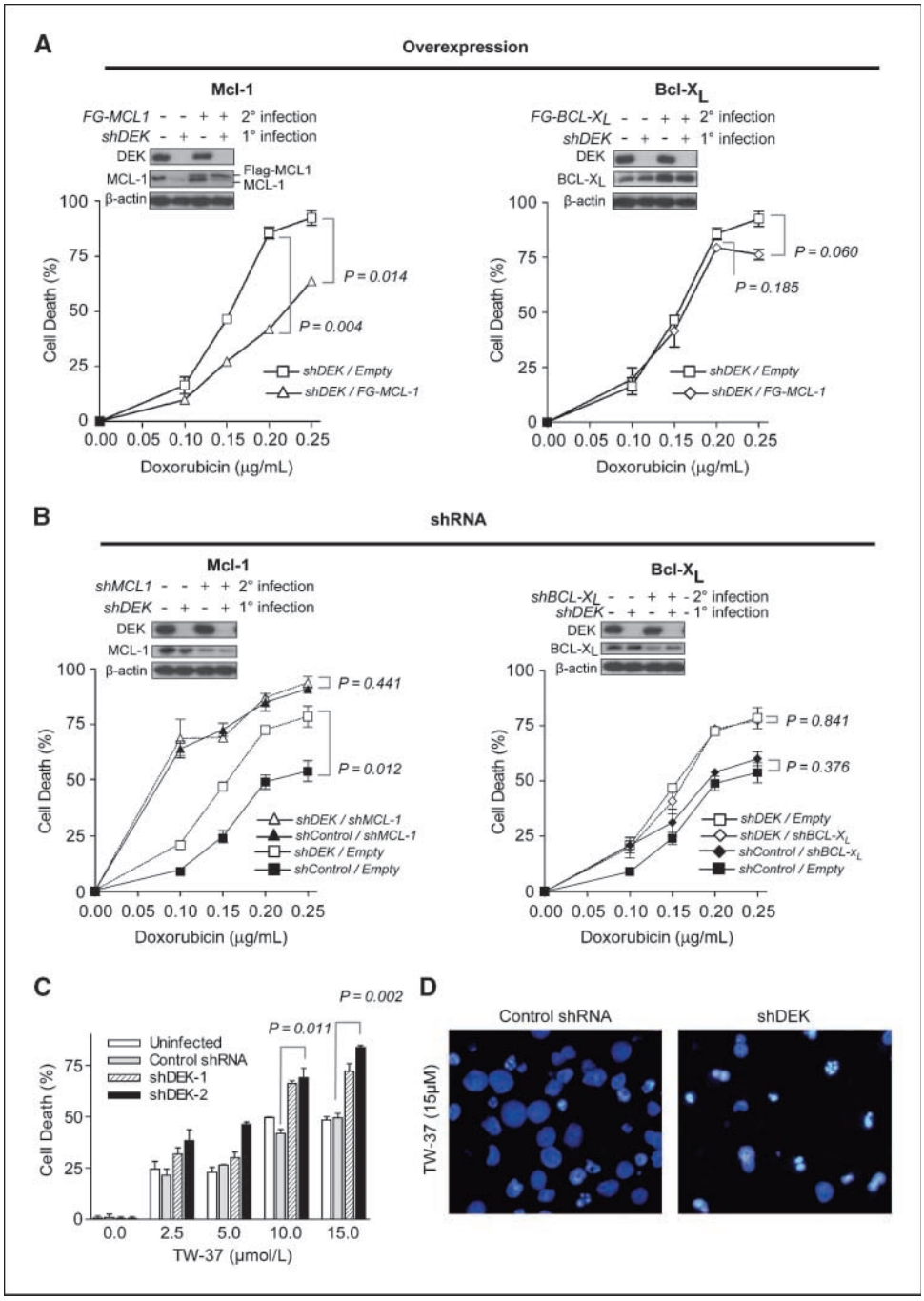

Figure 6. Functional effect of the selective regulation of BCL-2 family members by DEK. *A,* restoration of MCL-1 levels using lentiviral vectors coding for MCL-1 under an exogenous promoter that is not sensitive to DEK shRNA down-regulation (*left*). Control infections were also done with a vector expressing BCL-x_L (*right*). Seventy-two hours after infection with MCL-1 or BCL-x_L lentiviruses, cells were treated with the indicated concentration of doxorubicin for 30 h. Following treatment, cells were stained with DAPI and apoptotic cells were counted by fluorescence microscopy. *B,* inactivation of MCL-1 (*left*) or BCL-x_L (*right*) with the corresponding shRNAs. *Insets,* shRNA-mediated knockdown of DEK and either knockdown or overexpression of BCL-x_L and MCL-1 as determined by immunoblotting. *C,* SK-Mel-19 cells were transduced as in Fig. 3 and treated with the BH3 mimetic TW-37 for 48 h and then stained with trypan blue. *Bars,* SE. *D,* fluorescence microscopy by DAPI staining illustrating cell nuclear morphology after treatment with 15 μmol/L TW-37 in cells infected with a control shRNA expressing vector (*left*) or shDEK-2 (*right*). *P* values for the indicated pair-wise comparisons were determined by two-tailed Student's *t* test.

In a second set of experiments, the opposite strategy was tested (Fig. 6*B*), that is, to abrogate MCL-1 mRNA and protein expression with shRNAs that we have previously validated (6, 39, 44). Interestingly, exogenous MCL-1 significantly protected DEK-depleted melanoma cells, reducing the killing activity of doxorubicin in half (Fig. 6*A*; $P = 0.014$ for concentrations of doxorubicin of 0.25 μg/mL). On the other hand, when MCL-1 was depleted, DEK shRNA was not able to further enhance drug response (Fig. 6*B, left*; $P = 0.441$).

In contrast to MCL-1, altering BCL-x_L levels by either overexpression (Fig. 6*A, right*) or shRNAs (Fig. 6*B, right*) had no significant effect on melanoma cell viability whether in the presence or absence of DEK (see the corresponding *P* values in Fig. 6*A* and *B*).

From the data presented above, it follows that DEK shRNA may augment the therapeutic efficacy of small molecules, the antitumor activity of which depends on MCL-1 inactivation. To examine this possibility, we tested the small-molecule BH3 mimetic TW-37, which we have shown previously to act primarily by inhibiting MCL-1 (6, 38). Interestingly, DEK-depleted SK-Mel-19 cells were significantly more sensitive to TW-37 treatment than their control counterparts, showing an accelerated killing (Fig. 6*C*; $P = 0.011$-0.002) and induction of apoptotic-like features (see chromatin condensation in Fig. 6*D*). These results provide proof-of-principle for the development of rational therapies targeting DEK/MCL-1–dependent mechanisms of cell survival in melanoma.

Discussion

In this study, we identified new roles for DEK in metastatic melanoma cells. Despite the high degree of heterogeneity characteristic of this tumor type, we found that the DEK protein was invariably overexpressed in all 16 metastatic cell lines investigated independent of their genetic background. Moreover, high-throughput immunohistochemical analyses revealed a marked expression of DEK in 90% of primary and metastatic melanomas studied. In the same conditions, DEK expression in normal skin and benign nevi was nearly undetectable. Importantly, this high expression of DEK was not a simple byproduct of melanoma development. Abrogation of endogenous DEK expression resulted in the disruption of characteristic malignant features of melanomas. Thus, long-term expression of DEK shRNAs led to cell cycle arrest with features of senescence. In turn, acute down-regulation of DEK was sufficient to enhance the response to DNA damaging agents and BH3 mimetics (doxorubicin and TW-37, respectively). Our results additionally unveiled a previously undescribed role for DEK in the regulation of a critical mediator of chemoresistance, MCL-1.

The contribution of DEK to melanoma proliferation and drug resistance provides mechanistic support for the long-suspected presence of oncogene(s) mapping to the short arm of chromosome 6 (9, 13, 14). A complication in the identification of the putative onocogene(s) in this region has been its high gene density (624 genes in the 6p21-23 interval). Moreover, this area is heavily enriched in CpG islands; therefore, it can be subject to complex epigenetic regulation. Interestingly, a common area of copy gain at 6p22-p23 in ocular melanomas (11) had also been reported in bladder cancer and retinoblastoma (16–18). Of the 7 genes in this region, only DEK was found to have a correlation between copy gain and gene expression (18). Our spectral karyotyping and comparative genomic hybridization analyses revealed duplications of chromosome 6 in melanoma cell lines expressing high levels of DEK. However, other mechanisms of regulation may favor DEK up-regulation, as its expression can also be induced in cells with a normal copy number at the DEK locus.

Considering the high number of mutations and alterations in proliferative pathways that melanoma cells express, it is interesting that down-regulation of a single gene (DEK) can ultimately drive them into senescence-like cell cycle arrest. In fact, melanomas are considered to be particularly efficient at overcoming premature senescence, as this is one of the early barriers to melanocyte transformation (45). Mechanisms that circumvent premature senescence in melanomas are not well characterized. In fact, a puzzling feature of this disease is that a large fraction of acquired melanomas neither mutate nor delete p53 or $p16^{INK4a}$, two tumor suppressors with key roles in the induction of senescence programs (2). Therefore, DEK overexpression may represent an alternative mechanism to counteract the tumor suppressor activity of p53 and p16 in melanoma cells. The precise effects of DEK in promoting sustained proliferation will require further studies, but it is tempting to speculate that it may cooperate with other oncogenes mapping at chromosome 6p, such as c-MYC, which we have recently shown to control melanoma senescence (46).

Although the requirement of sustained expression of DEK to avoid premature senescence has implications for basic aspects of melanoma, the new roles of DEK shown here in the control of the apoptotic machinery are perhaps more significant from a therapeutic perspective. Although DEK has been shown previously to participate in the regulation of gene transcription (23–25, 30, 47), promotion of *MCL-1* expression is the first demonstration of a transcriptional target of DEK directly contributing to an oncogenic phenotype. The requirement of DEK for MCL-1 expression is relevant as this protein has an intrinsically short half life (5); yet, it is consistently accumulated in melanoma cells (3). In addition, MCL-1 transcription can be inhibited by p53 (48), E2F1, or E2F2 (40), all of which are expressed in melanoma cells. Therefore, the effects of DEK on MCL-1 transcription may serve to compensate for negative regulatory signals intrinsically expressed in melanoma cells. Furthermore, we and others have shown that MCL-1 is essential for long-term survival of melanoma cells, and it is a main determinant of their resistance to dacarbazine, BH3 mimetics, and inhibitors of MEK or the proteasome (6, 44, 49). MCL-1 can also control melanoma cell survival under conditions of anoikis (50). Thus, enhanced MCL-1 expression caused by DEK overexpression may represent a major mechanism of melanoma cell survival in response to chemotherapeutic agents and other stress-inducing factors.

In conclusion, our results implicate overexpression of the 6p proto-oncogene *DEK* as an extremely frequent event in metastatic melanomas. Remarkably, this single event can have a dual effect on melanoma cell proliferation and chemoresistance (preventing senescence and inducing the antiapoptotic MCL-1, respectively). Therefore, our results suggest that DEK may be a relevant target for therapeutic intervention in this aggressive disease.

Disclosure of Potential Conflicts of Interest

No potential conflicts of interest were disclosed.

Acknowledgments

Received 3/24/09; revised 6/11/09; accepted 6/18/09.

Grant support: NIH training grant T32-GM07863 and National Science Foundation and Rackham Predoctoral Fellowships (M.S. Khodadoust); William D. Robinson

Fellowship from the Arthritis Foundation/Michigan Chapter and Arthritis Foundation Postdoctoral Fellowship (F. Kappes); NIH Prostate Specialized Program of Research Excellence grant P50CA69568 and NIH grant U01 CA111275 (D.S.L. Kim and A.M. Chinnaiyan); NIH grant R01-AI062248 and Burroughs Wellcome Fund Clinical Scientist Award in Translational Research (D.M. Markovitz); NIH grant R01-CA107237, grant SAF2008-1950 from the Spanish Ministry of Innovation and Science, and Spanish Association Against Cancer development grant (M.S. Soengas); and Fundación Obra Social Caja Navarra post-residency award (E. Riveiro-Falkenbach).

The costs of publication of this article were defrayed in part by the payment of page charges. This article must therefore be hereby marked *advertisement* in accordance with 18 U.S.C. Section 1734 solely to indicate this fact.

We thank MaryBeth Riblett (University of Michigan) and Tonantzin G. Calvo (Centro Nacional de Investigaciones Oncológicas) for technical assistance, M. Carmen Martin and Bibiana I. Ferreira (Centro Nacional de Investigaciones Oncológicas) for help with spectral karyotyping and comparative genomic hybridization analyses, and Karolyn Oetjen and Colin Duckett for the BCL-x_L expression vector.

References

1. Gray-Schopfer V, Wellbrock C, Marais R. Melanoma biology and new targeted therapy. Nature 2007;445:851–7.
2. Chin L, Garraway LA, Fisher DE. Malignant melanoma: genetics and therapeutics in the genomic era. Genes Dev 2006;20:2149–82.
3. Soengas MS, Lowe SW. Apoptosis and melanoma chemoresistance. Oncogene 2003;22:3138–51.
4. McGill GG, Horstmann M, Widlund HR, et al. Bcl2 regulation by the melanocyte master regulator mitf modulates lineage survival and melanoma cell viability. Cell 2002;109:707–18.
5. Kutuk O, Letai A. Regulation of Bcl-2 family proteins by posttranslational modifications. Curr Mol Med 2008;8:102–18.
6. Verhaegen M, Bauer JA, Martin de la Vega C, et al. A novel BH3 mimetic reveals a mitogen-activated protein kinase-dependent mechanism of melanoma cell death controlled by p53 and reactive oxygen species. Cancer Res 2006;66:11348–59.
7. Ueda Y, Richmond A. NF-κB activation in melanoma. Pigment Cell Res 2006;19:112–24.
8. Gogas HJ, Kirkwood JM, Sondak VK. Chemotherapy for metastatic melanoma: time for a change? Cancer 2007;109:455–64.
9. Santos GC, Zielenska M, Prasad M, Squire JA. Chromosome 6p amplification and cancer progression. J Clin Pathol 2007;60:1–7.
10. Curtin JA, Fridlyand J, Kageshita T, et al. Distinct sets of genetic alterations in melanoma. N Engl J Med 2005;353:2135–47.
11. Namiki T, Yanagawa S, Izumo T, et al. Genomic alterations in primary cutaneous melanomas detected by metaphase comparative genomic hybridization with laser capture or manual microdissection: 6p gains may predict poor outcome. Cancer Genet Cytogenet 2005;157:1–11.
12. Hoglund M, Gisselsson D, Soller M, Hansen GB, Elfving P, Mitelman F. Dissecting karyotypic patterns in malignant melanomas: temporal clustering of losses and gains in melanoma karyotypic evolution. Int J Cancer 2004;108:57–65.
13. Balaban G, Herlyn M, Guerry D, 4th, et al. Cytogenetics of human malignant melanoma and premalignant lesions. Cancer Genet Cytogenet 1984;11:429–39.
14. Pathak S, Drwinga HL, Hsu TC. Involvement of chromosome 6 in rearrangements in human malignant melanoma cell lines. Cytogenet Cell Genet 1983;36:573–9.
15. Chen D, Gallie BL, Squire JA. Minimal regions of chromosomal imbalance in retinoblastoma detected by comparative genomic hybridization. Cancer Genet Cytogenet 2001;129:57–63.
16. Evans AJ, Gallie BL, Jewett MA, et al. Defining a 0.5-mb region of genomic gain on chromosome 6p22 in bladder cancer by quantitative-multiplex polymerase chain reaction. Am J Pathol 2004;164:285–93.
17. Grasemann C, Gratias S, Stephan H, et al. Gains and overexpression identify DEK and E2F3 as targets of chromosome 6p gains in retinoblastoma. Oncogene 2005;24:6441–9.
18. Orlic M, Spencer CE, Wang L, Gallie BL. Expression analysis of 6p22 genomic gain in retinoblastoma. Genes Chromosomes Cancer 2006;45:72–82.
19. von Lindern M, van Baal S, Wiegant J, Raap A, Hagemeijer A, Grosveld G. Can, a putative oncogene associated with myeloid leukemogenesis, may be activated by fusion of its 3′ half to different genes: characterization of the set gene. Mol Cell Biol 1992;12:3346–55.
20. Waldmann T, Scholten I, Kappes F, Hu HG, Knippers R. The DEK protein-an abundant and ubiquitous constituent of mammalian chromatin. Gene 2004;343:1–9.
21. Carro MS, Spiga FM, Quarto M, et al. DEK Expression is controlled by E2F and deregulated in diverse tumor types. Cell Cycle 2006;5:1202–7.
22. Wu Q, Li Z, Lin H, Han L, Liu S, Lin Z. DEK overexpression in uterine cervical cancers. Pathol Int 2008;58:378–82.
23. Sammons M, Wan SS, Vogel NL, Mientjes EJ, Grosveld G, Ashburner BP. Negative regulation of the RelA/p65 transactivation function by the product of the DEK proto-oncogene. J Biol Chem 2006;281:26802–12.
24. Faulkner NE, Hilfinger JM, Markovitz DM. Protein phosphatase 2A activates the HIV-2 promoter through enhancer elements that include the pets site. J Biol Chem 2001;276:25804–12.
25. Gamble MJ, Fisher RP. SET and PARP1 remove DEK from chromatin to permit access by the transcription machinery. Nat Struct Mol Biol 2007;14:548–55.
26. Kappes F, Scholten I, Richter N, Gruss C, Waldmann T. Functional domains of the ubiquitous chromatin protein DEK. Mol Cell Biol 2004;24:6000–10.
27. Mor-Vaknin N, Punturieri A, Sitwala K, et al. The DEK nuclear autoantigen is a secreted chemotactic factor. Mol Cell Biol 2006;26:9484–96.
28. Wise-Draper TM, Morreale RJ, Morris TA, et al. DEK proto-oncogene expression interferes with the normal epithelial differentiation program. Am J Pathol 2009;174:71–81.
29. Wise-Draper TM, Allen HV, Thobe MN, et al. The human DEK proto-oncogene is a senescence inhibitor and an upregulated target of high-risk human papillomavirus E7. J Virol 2005;79:14309–17.
30. Kim DW, Chae JI, Kim JY, et al. Proteomic analysis of apoptosis related proteins regulated by proto-oncogene protein DEK. J Cell Biochem 2009.
31. Sitwala KV, Mor-Vaknin N, Markovitz DM. Minireview: DEK and gene regulation, oncogenesis and AIDS. Anticancer Res 2003;23:2155–8.
32. Wise-Draper TM, Allen HV, Jones EE, Habash KB, Matsuo H, Wells SI. Apoptosis inhibition by the human DEK oncoprotein involves interference with p53 functions. Mol Cell Biol 2006;26:7506–19.
33. Devany M, Kappes F, Chen KM, Markovitz DM, Matsuo H. Solution NMR structure of the N-terminal domain of the human DEK protein. Protein Sci 2008;17:205–15.
34. Cleary J, Sitwala KV, Khodadoust MS, et al. p300/CBP-associated factor drives DEK into interchromatin granule clusters. J Biol Chem 2005;280:31760–7.
35. Grottke C, Mantwill K, Dietel M, Schadendorf D, Lage H. Identification of differentially expressed genes in human melanoma cells with acquired resistance to various antineoplastic drugs. Int J Cancer 2000;88:535–46.
36. Kappes F, Damoc C, Knippers R, Przybylski M, Pinna LA, Gruss C. Phosphorylation by protein kinase CK2 changes the DNA binding properties of the human chromatin protein DEK. Mol Cell Biol 2004;24:6011–20.
37. Denoyelle C, Abou-Rjaily G, Bezrookove V, et al. Anti-oncogenic role of the endoplasmic reticulum differentially activated by mutations in the MAPK pathway. Nat Cell Biol 2006;8:1053–63.
38. Wang G, Nikolovska-Coleska Z, Yang CY, et al. Structure-based design of potent small-molecule inhibitors of anti-apoptotic Bcl-2 proteins. J Med Chem 2006;49:6139–42.
39. Fernandez Y, Verhaegen M, Miller TP, et al. Differential regulation of noxa in normal melanocytes and melanoma cells by proteasome inhibition: therapeutic implications. Cancer Res 2005;65:6294–304.
40. Croxton R, Ma Y, Song L, Haura EB, Cress WD. Direct repression of the Mcl-1 promoter by E2F1. Oncogene 2002;21:1359–69.
41. Collado M, Blasco MA, Serrano M. Cellular senescence in cancer and aging. Cell 2007;130:223–33.
42. Kappes F, Fahrer J, Khodadoust MS, et al. DEK is a poly(ADP-ribose)-acceptor in apoptosis and mediates resistance to genotoxic stress. Mol Cell Biol 2008;28:3245–57.
43. Han J, Goldstein LA, Gastman BR, Froelich CJ, Yin XM, Rabinowich H. Degradation of Mcl-1 by granzyme B: implications for Bim-mediated mitochondrial apoptotic events. J Biol Chem 2004;279:22020–9.
44. Wolter KG, Verhaegen M, Fernandez Y, et al. Therapeutic window for melanoma treatment provided by selective effects of the proteasome on Bcl-2 proteins. Cell Death Differ 2007;14:1605–16.
45. Prieur A, Peeper DS. Cellular senescence in vivo: a barrier to tumorigenesis. Curr Opin Cell Biol 2008;20:150–5.
46. Zhuang D, Mannava S, Grachtchouk V, et al. C-MYC overexpression is required for continuous suppression of oncogene-induced senescence in melanoma cells. Oncogene 2008;27:6623–34.
47. Ko SI, Lee IS, Kim JY, et al. Regulation of histone acetyltransferase activity of p300 and PCAF by proto-oncogene protein DEK. FEBS Lett 2006;580:3217–22.
48. Pietrzak M, Puzianowska-Kuznicka M. p53-dependent repression of the human MCL-1 gene encoding an anti-apoptotic member of the BCL-2 family: the role of Sp1 and of basic transcription factor binding sites in the MCL-1 promoter. Biol Chem 2008;389:383–93.
49. Qin JZ, Xin H, Sitailo LA, Denning MF, Nickoloff BJ. Enhanced killing of melanoma cells by simultaneously targeting Mcl-1 and NOXA. Cancer Res 2006;66:9636–45.
50. Boisvert-Adamo K, Longmate W, Abel EV, Aplin AE. Mcl-1 is required for melanoma cell resistance to anoikis. Mol Cancer Res 2009;7:549–56.

Cancer Cell
Article

Targeted Activation of Innate Immunity for Therapeutic Induction of Autophagy and Apoptosis in Melanoma Cells

Damià Tormo,[1] Agnieszka Chęcińska,[1] Direna Alonso-Curbelo,[1] Eva Pérez-Guijarro,[1] Estela Cañón,[1] Erica Riveiro-Falkenbach,[1] Tonantzin G. Calvo,[1] Lionel Larribere,[1] Diego Megías,[2] Francisca Mulero,[3] Miguel A. Piris,[4] Rupesh Dash,[5] Paola M. Barral,[5] José L. Rodríguez-Peralto,[6] Pablo Ortiz-Romero,[6] Thomas Tüting,[7] Paul B. Fisher,[5] and María S. Soengas[1,*]
[1]Melanoma Laboratory, Molecular Pathology Programme
[2]Confocal Microscopy and Cytometry Unit
[3]Molecular Imaging Unit
[4]Lymphoma Laboratory
Spanish National Cancer Research Centre (CNIO), Madrid 28049, Spain
[5]Department of Human and Molecular Genetics, VCU Institute of Molecular Medicine and VCU Massey Cancer Center, Virginia Commonwealth University, School of Medicine, Richmond, VA 23298-0033, USA
[6]Hospital Universitario 12 de Octubre, Madrid 28041, Spain
[7]Laboratory of Experimental Dermatology, Department of Dermatology, University of Bonn, 53105 Bonn, Germany
*Correspondence: msoengas@cnio.es
DOI 10.1016/j.ccr.2009.07.004

SUMMARY

Inappropriate drug delivery, secondary toxicities, and persistent chemo- and immunoresistance have traditionally compromised treatment response in melanoma. Using cellular systems and genetically engineered mouse models, we show that melanoma cells retain an innate ability to recognize cytosolic double-stranded RNA (dsRNA) and mount persistent stress response programs able to block tumor growth, even in highly immunosuppressed backgrounds. The dsRNA mimic polyinosine-polycytidylic acid, coadministered with polyethyleneimine as carrier, was identified as an unanticipated inducer of autophagy downstream of an exacerbated endosomal maturation program. A concurrent activity of the dsRNA helicase MDA-5 driving the proapoptotic protein NOXA resulted in an efficient autodigestion of melanoma cells. These results reveal tractable links for therapeutic intervention among dsRNA helicases, endo/lysosomes, and apoptotic factors.

INTRODUCTION

Melanoma remains a prototype of solid cancers with increasing incidence and extremely poor prognosis at advanced stages (Jemal et al., 2008). Considerable effort has been devoted to the identification of molecular determinants underlying melanoma chemo- and immunoresistance (Chin et al., 2006; Gray-Schopfer et al., 2007). Still, the average survival of patients with inoperable disseminated metastases is less than 10 months (Tawbi and Kirkwood, 2007). High throughput histogenetic and functional studies have revealed complex mechanisms associated with treatment failure (Fecher et al., 2008). These range from increased expression of drug pumps and detoxification enzymes to a pleiotropic potentiation of key survival pathways (Fecher et al., 2008; Gray-Schopfer et al., 2007; Soengas and Lowe, 2003). In addition, apoptotic programs involving the mitochondria, the endoplasmic reticulum, or death receptors are invariably ineffective in vivo (Hersey and Zhang, 2008; Soengas and Lowe, 2003). Consequently, current anticancer drugs either do not reach their target(s) in a productive manner or have to be

SIGNIFICANCE

Melanoma cells accumulate multiple genetic and epigenetic alterations. Still, they still remain highly sensitive to dsRNA mimics, shown here for the synthetic molecule pIC. However, the delivery vehicle is critical. PEI, a polycation that favors endosomal uptake and cytosolic release, was able to shift the mode of action of pIC from a transient innocuous transcriptional program to persistent cycles of fusion events involving a sequential recruitment of Rab7 (a small GTPase), LC3 (autophagosome marker), and lysosomes. A convergent mechanism of cellular stress was found driven by MDA-5 and involving an efficient NOXA-dependent caspase activation. Selective antitumor activity of $[pIC]^{PEI}$ in vivo further supports cytosolic dsRNA sensors as viable targets for drug development in melanoma.

administered at dosing schedules that result in unbearable toxicities to normal cellular compartments (Tawbi and Kirkwood, 2007). Similarly, melanomas have an inherent ability to bypass or overcome antitumoral activities of immunomodulators (Ilkovitch and Lopez, 2008; Tormo et al., 2006; Verma et al., 2008).

Autophagy, and in particular macroautophagy, which involves the sequestration of bulk cytosolic components in autophagosomes for subsequent lysosomal degradation (Xie and Klionsky, 2007), is an understudied process in melanoma. The clinical relevance of macroautophagy (herein referred to as autophagy for simplicity) stems from its potential to protect cells against a variety of intracellular and extracellular stress signals and favor tumor development (Mathew et al., 2009; Mizushima et al., 2008). Paradoxically, autophagy has also been associated with cell death (Kroemer et al., 2009). Thus, excessive or persistent autophagy can promote cell killing by depletion of key organelles (e.g., endoplasmic reticulum or mitochondria), rewiring of survival signals, deregulation of lysosomal enzymes, and/or activation of caspase-dependent apoptotic programs (Eisenberg-Lerner et al., 2009; Hoyer-Hansen and Jaattela, 2008; Maiuri et al., 2007; Xie and Klionsky, 2007). Given these pro- and anti-apoptotic roles of autophagy, it is unclear whether this program could be a viable target for drug development (Kroemer and Levine, 2008; Rubinsztein et al., 2007; Scarlatti et al., 2009).

Autophagy genes can also have pleiotropic roles in the immune system (Virgin and Levine, 2009). Thus, autophagy can modulate antigen presentation, inhibit or potentiate interferon responses, and display critical functions in the clearance of intracellular viral and bacterial pathogens (Levine and Deretic, 2007; Sanjuan and Green, 2008). Typically, these responses are engaged to protect infected cells or the host (Virgin and Levine, 2009). The precise mechanisms underlying this immune autophagy are not well defined. Membrane-bound pattern recognition receptors of the Toll-like receptor (TLR) family (particularly TLR-3, TLR-4, and TLR-7) can favor pathogen sequestration in autophagosomes (Delgado and Deretic, 2009; Levine and Deretic, 2007). These TLRs have a restricted expression pattern, being enriched in cells of the immune system, such as macrophages and dendritic cells (Paulos et al., 2007; Wenzel et al., 2008). Whether melanoma cells have other sensors of viral pathogens that can be engaged to induce autophagy and cell death is unknown.

Here, we have assessed the interplay between autophagy and apoptosis in the context of tumor cell-selective elimination of melanoma cells.

RESULTS

Identification of Autophagosome Inducers in Melanoma Cells

Melanoma cells stably expressing the autophagosome marker LC3 fused with GFP (Klionsky et al., 2008) were used to screen for autophagy inducers among commercially available chemotherapeutic drugs and immunomodulators. To improve intracellular delivery, cationic carriers, e.g., polyethyleneimine (PEI), were added to DNA- or RNA-based agents (Bieber et al., 2002). The initial screen was performed with the SK-Mel-103 cell line. Subsequent validation studies were performed using a panel of nine human metastatic melanoma cell lines of diverse genetic background (see Table S1 available online), as well as the well-known B16 mouse melanoma cells. Primary skin melanocytes, keratinocytes, and fibroblasts were included as controls for normal cells. We also tested drug response in mouse embryonic fibroblasts (MEFs) expressing or deficient for the autophagy factor Atg5 to provide a genetically controlled model to assess classical autophagy programs (Salazar et al., 2009).

Multiple drugs were found to promote focal GFP-LC3 fluorescence emission without significantly affecting cell viability (A.C. and M.S.S., unpublished data). Among prodeath agents, the classical double-stranded RNA (dsRNA) mimic polyinosine-polycytidylic acid (pIC; Wenzel et al., 2008) complexed with PEI ($[pIC]^{PEI}$) induced a potent accumulation of GFP-LC3 foci (Figure 1A). About 50% of cells treated with low doses (0.5–1 μg/ml) of $[pIC]^{PEI}$ showed GFP-LC3 staining within 2–4 hr. These results were intriguing as pIC had been linked to autophagy in immune cells (Delgado et al., 2008), but not in the context of tumor cell death. Therefore, we focused on the identification of the cellular machinery that sensed and executed the response of melanoma cells to $[pIC]^{PEI}$.

Consistent with autophagy, $[pIC]^{PEI}$ induced electrophoretic mobility changes of the endogenous LC3, which are characteristic of lipidation of this protein during autophagy (Figure 1B). $[pIC]^{PEI}$ also lead to LC3 foci formation in oncogenically transformed MEFs, an activity that required Atg5 (Figure 1C, upper panels). In fact, inhibition of LC3 redistribution in $Atg5^{-/-}$ cells treated with $[pIC]^{PEI}$ was as prominent as with rapamycin (Figure 1C), a classical autophagy inducer (Noda and Ohsumi, 1998). However, rapamycin and $[pIC]^{PEI}$ were not equivalent. LC3 foci were transient in melanoma treated with rapamycin, but sustained with $[pIC]^{PEI}$ (Figure 1D). In addition, rapamycin, but not $[pIC]^{PEI}$, inhibited the mTOR pathway as visualized by monitoring the expression of the phosphorylated S6 kinase (Figure 1E).

Electron microscopy provided independent evidence of autophagosome/autolysosome formation driven by $[pIC]^{PEI}$. Thus, large mutivesicular structures (>500 nm diameter; Figure $1F_d$) were found following uptake of $[pIC]^{PEI}$ nanoparticles in melanoma cells (Figure $1F_b$). This uptake was probably facilitated by the known activity of PEI to coat genetic material and favor endocytosis (Boussif et al., 1995; Kopatz et al., 2004). Importantly, neither naked pIC nor PEI alone was able to induce autophagosome formation (see Figure S1 for representative examples). Together, these results suggest an mTOR-independent autophagy driven by pIC that requires an appropriate cellular delivery method.

Selective Melanoma Cell Death after $[pIC]^{PEI}$ -Driven Autophagy

Notably, in all melanoma cell lines tested in this study, the early activation of autophagy by $[pIC]^{PEI}$ was invariably followed by cell death (Figure 1G and Table S1). In contrast, melanocytes retained their viability and did not display markers of autophagy (Figures S2A–S2C). Interestingly, although complexed efficiently with PEI, dsDNA, the immunogenic variant ds-BDNA (Ishii et al., 2006), or other dsRNA molecules such as pA:U had no obvious impact on melanoma physiology (Figure S2D and data not shown). These results are consistent with the known superior immunomodulatory efficacy of pIC over other dsRNA mimics (Alexopoulou et al., 2001).

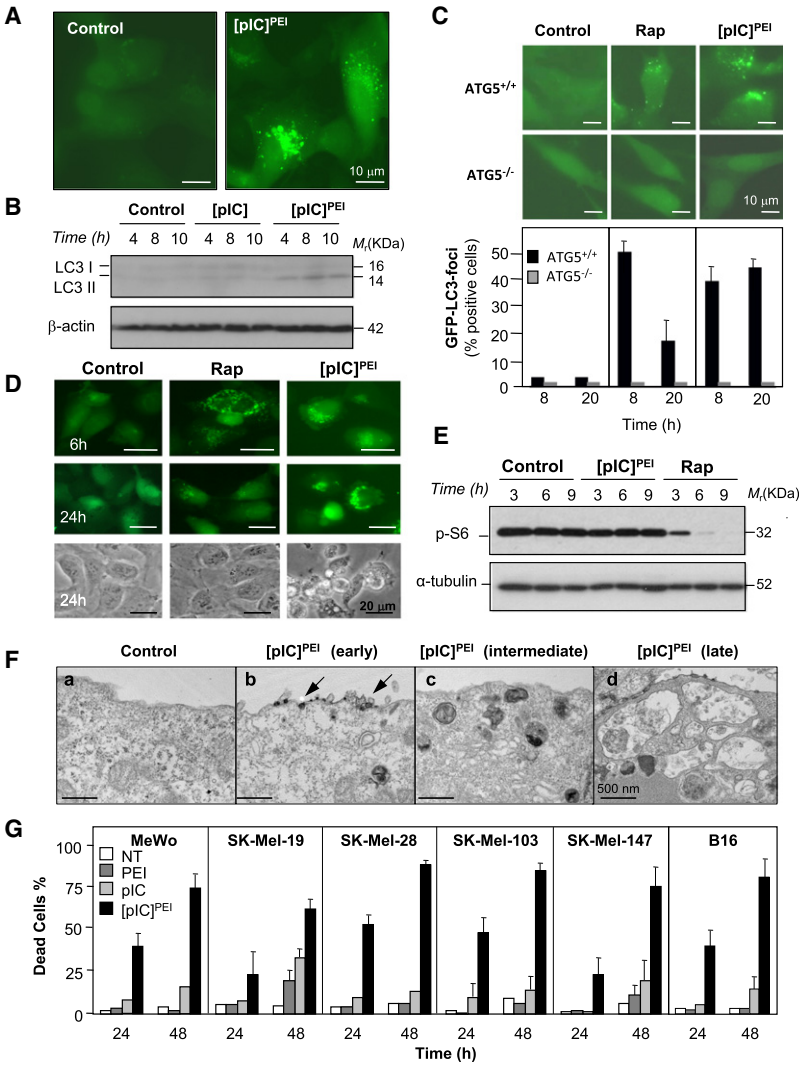

Figure 1. Induction of Autophagy by [pIC]^{PEI} Results in Melanoma Cell Death

(A) Fluorescence imaging of GFP-LC3 distribution in SK-Mel-103 melanoma cells treated for 6 hr with 1 μg/ml [pIC]^{PEI}. Cells treated with PEI as single agent are shown as reference controls.

(B) Changes in the electrophoretic mobility of the endogenous LC3 in SK-Mel-103 treated for the indicated times with pIC, [pIC]^{PEI}, or vehicle control (PEI).

(C) Visualization of eGFP-LC3 distribution in wild-type or Atg5$^{-/-}$ MEFs treated for 8 hr with 25 nM Rapamycin (Rap) or 1 μg/ml [pIC]^{PEI}. pIC-treated cells are included as controls (upper two rows). Bottom panels show quantification of the percentage of cells with focal GFP-LC3 at the indicated times after treatment. Error bars correspond to SEM of three independent experiments.

(D) Differential response of SK-Mel-103 melanoma cells to rapamycin and [pIC]^{PEI} determined by visualization of LC3-GFP fluorescence (upper two rows) and bright-field microscopy imaging (bottom row). Cells treated with vehicle were included as controls.

(E) Immunoblots of total cell extracts isolated from SK-Mel-103 cells treated as indicated and probed with antibodies specific for phospho-S6 or tubulin.

(F) Transmission electron micrographs of melanoma cells treated with [pIC]^{PEI}. Arrows point to conjugates of pIC and PEI being endocytosed into the treated cells. Note the large multivesicular structures at late time points after [pIC]^{PEI} treatment (F_d).

(G) Murine B16 melanoma cells and the indicated human melanoma cell lines compared for sensitivity to PEI and pIC as single agents or in combination. Cell death was estimated by trypan blue exclusion 24 and 48 hr after treatment and presented as means ± SEM of three independent experiments.

Inhibition of Metastatic Melanoma Dissemination by [pIC]^{PEI} in Immunocompetent and Immunosuppressed Mice

A detailed characterization of the mechanism of action of [pIC]^{PEI} would not be meaningful without significant activity in vivo. To this end, three tumor models were investigated. First, B16 melanoma cells were tested following subcutaneous or intravenous inoculation in immunocompetent mice. In a second setting, B16 or SK-Mel-103 cells expressing GFP (to allow for noninvasive imaging) were used in a surrogate model of lung metastasis in SCID beige mice (Figures 2A–2D). These animals lack functional B cells, T cells, and NK cells (Croy and Chapeau, 1990), representing severely immunocompromised backgrounds, which can be found in melanoma patients. As summarized in Figures 2A–2D and Figures S3A–S3C, [pIC]^{PEI} showed a considerably stronger antimelanoma activity than naked pIC in all the models tested, even in the highly immunosuppressed SCID beige mice, in which pIC had virtually no effect.

The third system analyzed was the *Tyr::NRAS^{Q61K}; INK4a/ARF$^{-/-}$* mice. These animals develop melanomas with key features similar to the human disease (Ackermann et al., 2005). Here, again, the antitumor activity of [pIC]^{PEI} was significantly higher than that of pIC, as determined by quantification of tumor number, tumor size, metabolic activity, and histological analyses (Figures 2E–2G and Figure S3D). Of note, [pIC]^{PEI} prolongs the progression-free survival (Figure 2E) at dosing schedules without noticeable secondary toxicities (see below). Together, these results support an efficient and tumor cell-selective antitumor activity of [pIC]^{PEI}.

Requirement of ATG5 for [pIC]^{PEI}-Mediated Cell Death

Next, we investigated the molecular basis by which [pIC]^{PEI} mediates self-killing of melanoma cells. Electronic microscopy (Figure 3A), real-time fluorescence analyses of GFP-LC3 distribution (Movies S1 and S2), and Nomarski interference contrast microscopy analyses (Movie S3) indicated that melanoma cell death invariably followed the activation of classical autophagocytic vesicles (see Figure S4 for an example). To confirm that autophagy is a key effector of [pIC]^{PEI} action (and not a byproduct of cellular stress), knockdown of key autophagy genes (Beclin1 and ATG7) was attempted in various melanoma cells. However, transient or stable knockdown of these genes induced either cellular senescence or cell death (A.C. and M.S.S., unpublished data), as described in other systems (Hoyer-Hansen and Jaattela, 2007; Mathew et al., 2009; Miller et al., 2008). This is consistent with a basal rate of autophagy that can be visualized by

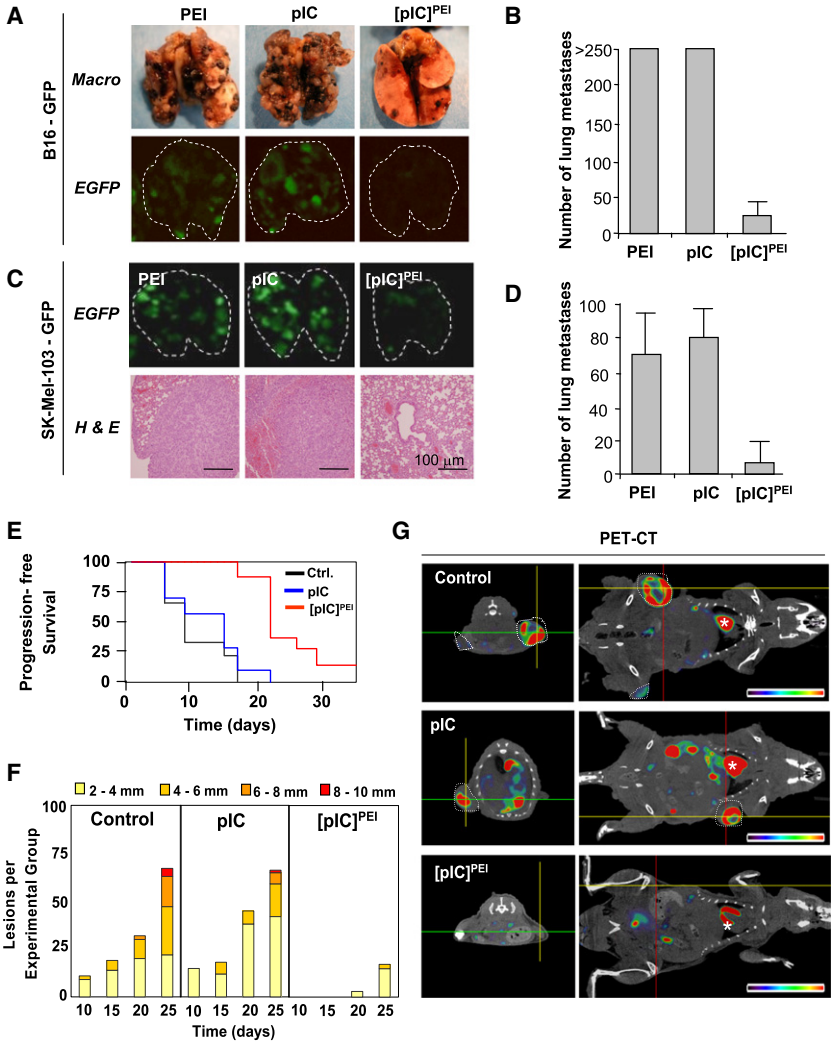

Figure 2. Antimelanoma Activity of [pIC]^{PEI} in Mice

(A)–(D) are results from SCID Beige mice; (E)–(G) are results from *Tyr::Ras*^{Q61K} × *Ink4a/Arf*$^{-/-}$ mice.

(A) Representative images of lungs of mice 14 days after intravenous inoculation of B16 melanoma cells and treatment as indicated and photographed under visible (Macro) or fluorescent (eGFP) light.

(B) Representation of the mean number of metastases (±SEM) induced by B16 as indicated in (A). *p < 0.01 between PEI or pIC and [pIC]^{PEI} treatment groups (n = 5; generalized Mann-Whitney test).

(C) Lung colonization by eGFP-SK-Mel-103 in SCID beige mice treated with the indicated agents and assessed by fluorescence imaging and histological analyses.

(D) Quantification of average number of external lung nodules (±SEM) in the indicated treatment groups shown in (C). *p < 0.01 between PEI, pIC, and [pIC]^{PEI} treatment groups (n = 5; generalized Mann-Whitney test).

(E) Cohorts of *Tyr::Ras*^{Q61K} *x Ink4a/Arf*$^{-/-}$ mice were treated topically with a single dose of 200 μg DMBA at 8 weeks of age. Upon appearance of pigmented lesions of >1 mm diameter, mice were treated as indicated. Control groups received PEI in 5% glucose. The fraction of animals with tumors of <1mm diameter (progression free survival) was represented by Kaplan-Meier graphs.

(F) Average number of cutaneous melanocytic neoplasms developing in each of the different treatment groups. Scoring was performed every 5 days and tumors were grouped by size as indicated.

(G) Representative transverse (left panels) and coronal sections (right panels) of PET /CT fused images to assess metabolic activity (^{18}F-FDG incorporation) of representative examples of mice treated as indicated. Tumors are encircled with white dashed lines. The asterisks mark animal hearts.

monitoring LC3-GFP dynamics in untreated melanoma cells (see Movie S1). Therefore, to avoid confounding results of testing drug response in cells whose proliferative capacity and viability is already severely compromised, [pIC]^{PEI}-driven cell death was determined in transformed wild-type and *Atg5*$^{-/-}$ MEFs. Although oncogenically transformed wild-type MEFs were less sensitive to [pIC]^{PEI}-mediated death than melanoma cells, they were significantly more sensitive than their *Atg5*$^{-/-}$ counterparts (Figure 3B). However, it should be noted that *Atg5*$^{-/-}$-transformed MEFs died efficiently at high doses of [pIC]^{PEI} (>1 μg/ml; not shown), perhaps reflecting the dual roles of autophagy in cell survival and cell death, as in immune cells (Virgin and Levine, 2009).

Requirement of Autophagosome-Lysosome Fusion in [pIC]^{PEI} -Mediated Cell Death

As indicated above, a defining ultrastructural feature of [pIC]^{PEI} treatment is the induction of large multivesicular structures (Figure 1F$_d$). These vesicles could result from halted autophagosomes in which lysosomes are either not recruited or dysfunctional (Amaravadi et al., 2007; Ostenfeld et al., 2008). In this scenario, autophagosomes would grow in size as a consequence of accumulation of improperly degraded material. Alternatively, these vesicles could correspond to homotypic fusions among large endosomes, subsequently recruiting multiple autophagosomes (to generate hybrid structures, also referred to as amphisomes). To assess these possibilities, we transduced melanoma cells with Cherry-GFP-LC3, which displays dual red-green fluorescence in autophagosomes but loses GFP signal in the acidic environment of autolysosomes (Tasdemir et al., 2008). We found that [pIC]^{PEI}, similar to rapamycin, induced autolysosomes in melanoma cells (see "red-only" LC3 foci in Figure 3C). Supporting a lysosomal-dependent mode of action of [pIC]^{PEI}, transient treatment with the lysosomotropic agent chloroquine protected melanoma cells against [pIC]^{PEI}-driven cell death (Figure 3D), without affecting the endosomal uptake of this dsRNA mimic (as determined by colocalization of FluoRed-labeled [pIC]^{PEI} with GFP-fused early endosomal protein Rab5; Figure 3E). Similar inhibitory effects were observed using the broad spectrum protease inhibitors E64d and pepstatin A and the vacuolar ATPase blocker bafilomycin (Figure 3D).

To independently monitor lysosomal activity during [pIC]^{PEI} treatment, we assayed cells for the ability to process DQ-BSA (a derivative of BSA whose green fluorescence is quenched

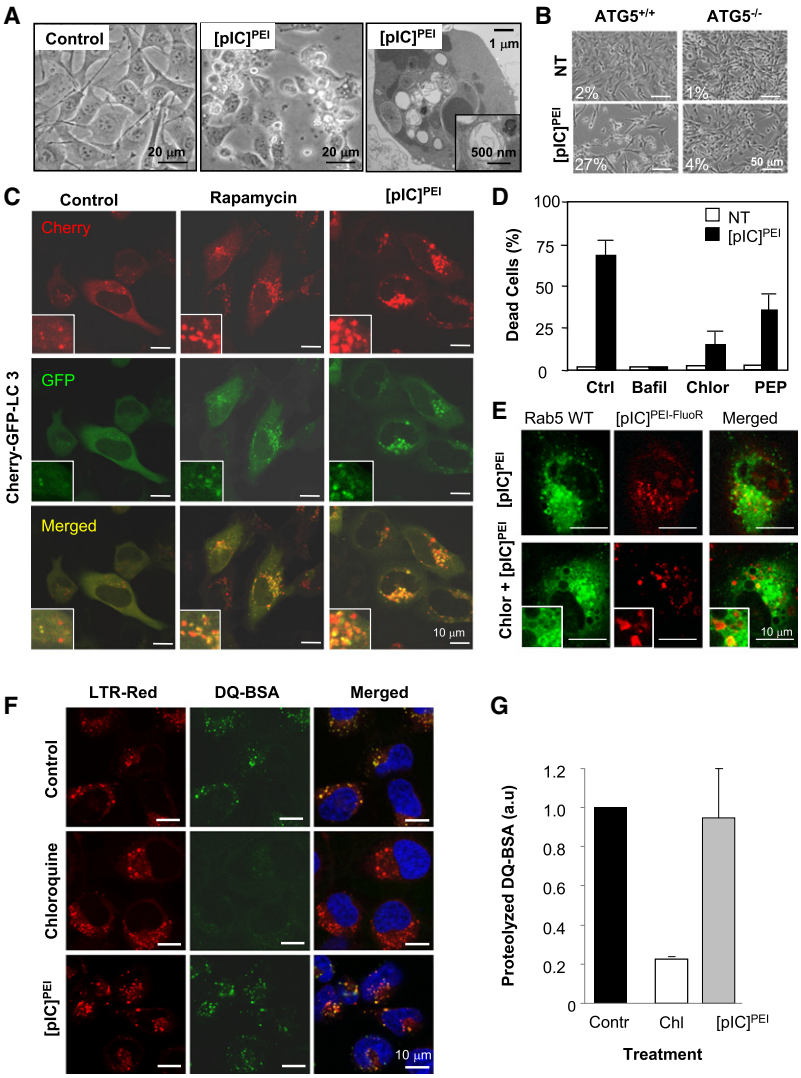

Figure 3. [pIC]^{PEI}-Triggered Melanoma Cell Death Is Driven by Autophagosome-Autolysosome Formation

(A) Representative bright field (left and middle panels) and electron microscope (right panel) micrographs of SK-Mel-103 treated as indicated (30 hr).

(B) Transformed wild-type or *Atg5*$^{-/-}$ MEFs treated with low dose (0.2 μg/ml) of [pIC]^{PEI} or control. Cell death was estimated by trypan blue exclusion 48 hr after treatment and presented as means of three independent experiments.

(C) Confocal fluorescence images of SK-Mel-103 transduced with Cherry-GFP-LC3 to detect autophagosomes (red and green foci) and autolysosomes (red-only foci) after treatment with [pIC]^{PEI}, 25 nM Rapamycin (Rap), or solvent control.

(D) Inhibitory effect of 100 μM bafilomycin (Bafil), 20 μM chloroquine (Chlor), or 10 μg/ml pepstatin (PEP) on cell death estimated by trypan blue exclusion 20 hr after treatment with vehicle (white bars) or [pIC]^{PEI} (black bars). Data are indicated as means ± SEM of three independent experiments.

(E) Confocal fluorescence images of SK-Mel-103 cells stably transfected with eGFP-Rab5 and incubated with [pIC]^{PEI} labeled with FluoRed. Shown is the internalization of [pIC]^{PEI} by the melanoma cells in the presence or absence of chloroquine.

(F) Confocal visualization of lysosomal-dependent proteolysis upon cleavage and release of the fluorescent moiety of DQ-BSA (green) in control or [pIC]^{PEI}-treated SK-Mel-103. Chloroquine is included to monitor DQ-BSA emission in cells with blocked lysosomal activity. Cells were simultaneously imaged in the presence of Lysotracker red (LTR-red) to visualize the lysosomal compartment.

(G) The DQ-BSA-Lysotracker colocalization was estimated in a minimum of 150 cells in two independent experiments, and it is expressed (as arbitrary fluorescence units) with respect to control treated cells. Error bars correspond to SEM.

unless cleaved by proteolytic enzymes). As shown in Figures 3F and 3G, DQ-BSA was efficiently cleaved in the presence of [pIC]^{PEI} (note that DQ-BSA emission was detected at the lysosomes, as indicated by colocalization with Lysotracker red).

Dynamic Endosome Mobilization by [pIC]^{PEI}

Having determined that autophagosomes fuse to active lysosomes in response to [pIC]^{PEI}, we assessed whether these organelles interacted with or were recruited to endosomes. First, endosomal dynamics were assessed in melanoma cells expressing GFP fused to the late endosomal marker Rab7 (Luzio et al., 2007). Basal endosome generation and resolution (i.e., progressive reduction in size) was detected in untreated melanoma cells (Figure S5, right panels; and Movie S4). [pIC]^{PEI} treatment markedly enhanced endosomal activity, inducing a sustained and multiwave generation of endosomes (Figure S5, left panels; and Movie S5). These endosomes were found to be filled with lysosomes, as determined by dual imaging of GFP-Rab7 and Lysotracker red (Figure 4A). Moreover, time-lapse microscopy revealed fast kinetics of multiple recruitments of lysosomes to GFP-Rab7-decorated endosomes (Movie S7; see also a sequential series of fusion events in Figure 4B). Importantly, as shown in Figure 4A (right panels), endosome-lysosome fusion was significantly inhibited if cells overexpressed Rab7-T22N, a known dominant-negative mutant of this protein (Gutierrez et al., 2004). In total, these results uncovered a dynamic mobilization of endo/lysosomal compartments in tumor cells treated with [pIC]^{PEI}.

Generation and Resolution of [pIC]^{PEI}-Driven Amphisome Formation

To determine whether and when autophagosomes are recruited to endosomes, we imaged melanoma cells simultaneously for GFP-Rab7, Cherry-LC3, and Lysotracker blue at different time points after [pIC]^{PEI} addition. As shown in Figure 4C and Figure S6A, the first event detected was generally the incorporation of Rab7 to the membrane of preexisting "empty" (early-endosome) vesicles. LC3 was recruited afterwards usually starting from an initial nucleation event, to ultimately decorate the entire Rab7-positive vesicles. Lysotracker blue incorporation into these endosome/autophagosome hybrids (amphisomes) was found to be the last to occur. At this point, the corresponding vesicle progressively diminished in size to ultimately become

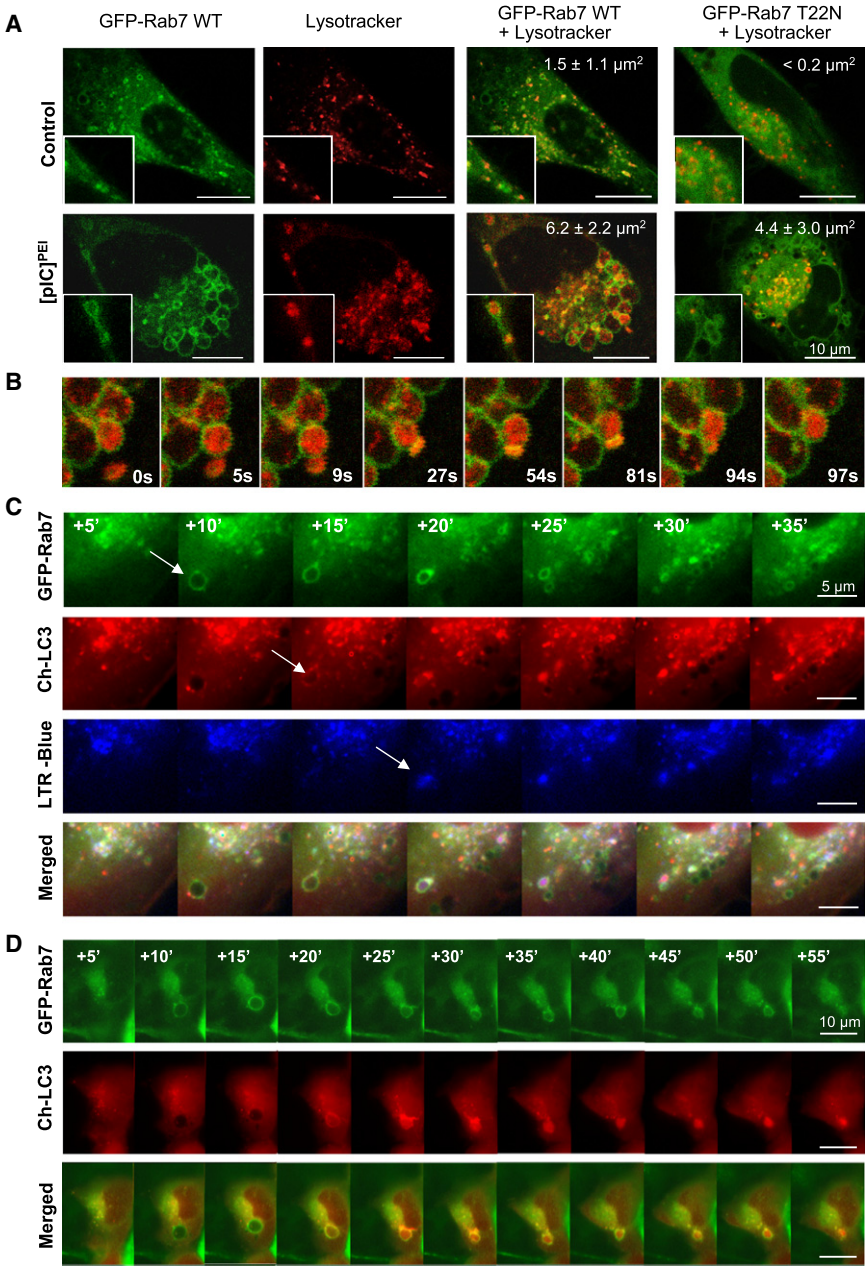

Figure 4. Generation and Resolution of Amphisomes upon [pIC]^{PEI} Treatment

(A) SK-Mel-103 cells stably transfected with eGFP-Rab7 wild-type or eGFP-Rab7 T22N were incubated with [pIC]^{PEI} for visualization of Rab7 (green fluorescence) and Lysotracker red. Microphotographs were captured by confocal microscopy 10 hr after treatment with [pIC]^{PEI}. Values in insets correspond to the average area contained in Rab7-decorated vesicles.

(B) Sequence of confocal microphotographs taken at the indicated time intervals (in seconds) to illustrate the fusion to and incorporation of lysosomes to Rab7-positive vesicles upon [pIC]^{PEI} treatment.

(C) Real-time triple-imaging fluorescence microscopy of GFP-Rab7 wild-type, Cherry-LC3, and Lysotracker blue (green, red, and blue fluorescence, respectively) in SK-Mel-103 cells treated with [pIC]^{PEI}. Images were taken at the indicated time intervals (in minutes), 1 hr after treatment initiation. Arrows mark the first sequence in which the indicated markers appear visible.

(D) Incorporation of LC3 to the surface of Rab7 endosomal vesicles prior to internalization and subsequent degradation. These endosome/LC3 hybrid structures (amphisomes) were visualized by fluorescence real-time microscopy of SK-Mel-103 cells expressing eGFP-Rab7 wild-type and Cherry-LC3.

undetectable, indicating a bona fide autodegradative process (Figure 4C and Figure S6, see arrows marking the Rab7 > LC3 > Lysotracker sequence). The presence of Lysotracker did not interfere with endosomal dynamics, as similar progressive recruitment and internalization of LC3 to Rab7 endosomes was found in its absence (Figure 4D).

[pIC]^{PEI} Links Autophagy to Apoptotic Caspases

Notably, the sequential fusion events mentioned above for a single vesicle were found to involve large numbers of endosomes and occur in a persistent manner throughout the entire cytosol of treated cells (Figure S6). This was independent of the imaging reagents used (see examples of cells imaged with Lysotracker blue in Figure S6A or Lysotracker red in Figure S6B). Still, we found a considerable delay from the starting point of endosome mobilization (2–5 hr), until final cellular collapse (24–48 hr). Thus, we hypothesized that cell demise required an additional, later event. Interestingly, cleaved regulatory and effector caspases (casp-8, 9, 7, and 3) were detected 15–20 hr after [pIC]^{PEI} treatment (Figure S7A). Accordingly, caspase inhibitors (zVAD-fmk, and to a lesser extent DEVD-CHO) reduced [pIC]^{PEI}-driven cell death (Figure S7B). Similarly, the sensitivity of MEFs to [pIC]^{PEI} was significantly reduced in cells deficient for the apoptotic factors Bax and Bak (Figure S7C, left panels). Importantly, neither caspase inactivation in melanoma cells nor BAX/BAK deficiency in MEFs prevented the generation of GFP-LC3 foci (Figures S7B and S7C). Therefore, [pIC]^{PEI} is able to induce an early but persistent autophagy and a late apoptotic program. This is in contrast to other systems where caspases are the initiating death signals and autophagy is induced to favor the clearance of partially degraded cytosolic components (Kroemer and Levine, 2008).

Differential Gene Expression Induced by Naked and PEI-Complexed pIC in Melanoma Cells

Next, we investigated the molecular sensor(s) of [pIC]^{PEI} that might link autophagy to apoptosis in a tumor cell-selective manner. Using cDNA arrays, we found melanocytes to undergo minimal changes in gene expression at early or late time points

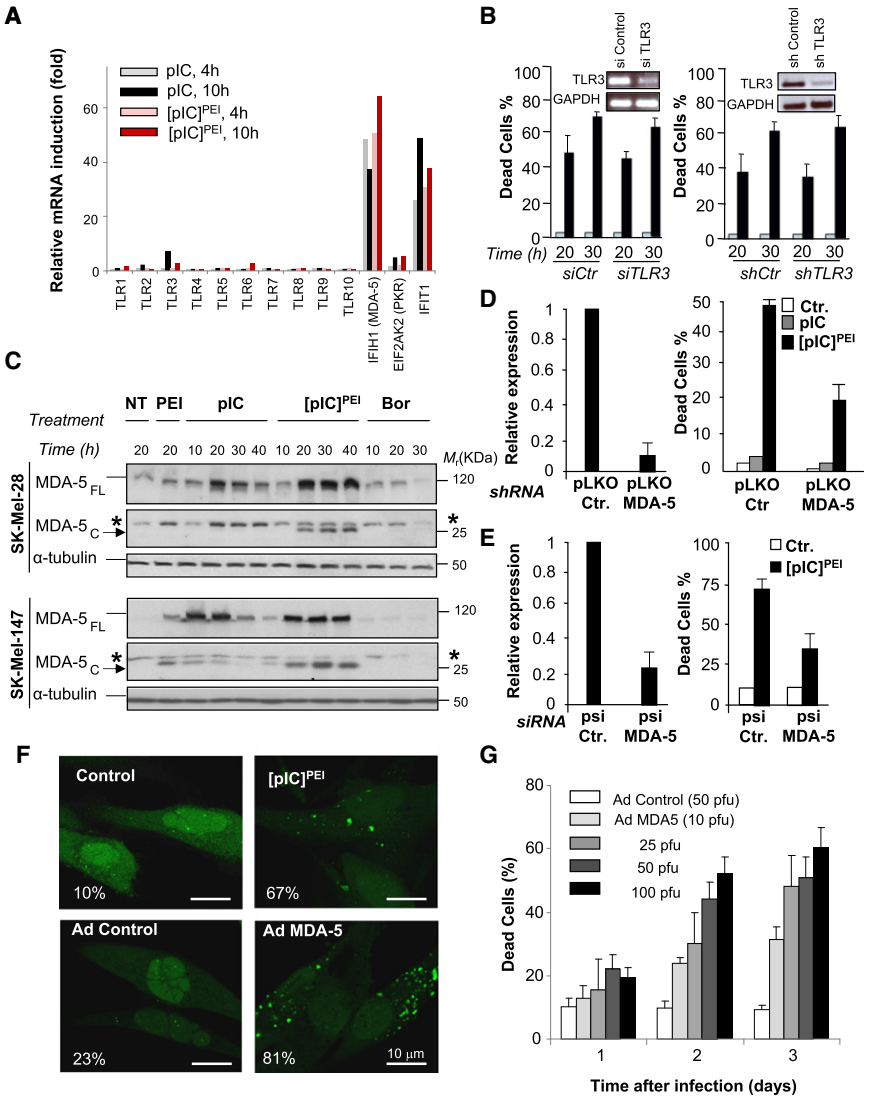

Figure 5. MDA-5 Is a Sensor and Driver of [pIC]^{PEI} Cytotoxicity in Melanoma Cells

(A) Fold induction of the transcript levels of the indicated pathogen-associated receptors relative to nontreated cells. The *IFIT-1* gene was used as a reference for a classical IFN-responsive factor.

(B) Inhibition of *TLR-3* expression by transient transduction of siRNA (left panels) or stable infection with lentivirus coding for shTLR3 (right panels). Cell death was assessed by trypan blue exclusion after treatment with vehicle (white bars) or [pIC]^{PEI} (black bars). Insets correspond to mRNA levels detected by RT-PCR. Data are shown as means ± SEM of three independent experiments.

(C) MDA-5 induction visualized by immunoblotting in SK-Mel-28 and SK-Mel-147 treated with PEI, pIC, or [pIC]^{PEI}. Bortezomib was used as a control for an effective death inducer. Full-length and cleaved MDA-5 (MDA-5_{FL} and MDA-5_{C}, respectively) are indicated with arrows. Asterisk corresponds to a nonspecific band (not blocked by MDA-5 shRNA; not shown).

(D) MDA-5 mRNA levels (left panel) and cell death (right panels) in SK-Mel-103 infected with the pLKO lentivirus expressing scrambled or MDA-5 shRNAs and treated as indicated. Data are shown as means ± SEM of three independent experiments. $p < 0.05$ between control and shMDA-5 cells in the presence of [pIC]^{PEI} (two-tailed Student's t test).

(E) Inhibition of MDA-5 expression by transient transduction of a second set of control and MDA-5 siRNAs driven by the psi-vector frame (see Experimental Procedures). Cell death in control and [pIC]^{PEI}-treated SK-Mel-103 (24 hr) was determined by trypan blue exclusion and plotted as means ± SEM of three independent experiments. In the [pIC]^{PEI} treatment group, $p < 0.05$ between control shRNA and shMDA-5-transduced cells (two-tailed Student's t test).

(F) Confocal visualization of GFP-LC3 in MeWo melanoma cells infected with adenovirus control or adenovirus MDA-5. [pIC]^{PEI} was included as a reference for autophagosome formation. Numbers represent fraction of cells with eGFP-LC3 foci.

(G) Cell death resulting from adenovirus-driven expression of MDA-5 in MeWo cells. The viral concentration (in plate forming units [pfu]) is indicated. Data correspond to means ± SEM of three independent experiments.

after treatment with pIC or [pIC]^{PEI}. In contrast, melanoma cells responded to both agents with substantial alterations of their transcriptome (Figure S8A). Interestingly, while pIC induced expected changes in interferon response genes, this response was largely transient. In contrast, the effect of [pIC]^{PEI} was sustained and extended to additional transcripts (Figures S8A and S8B). These results reveal key idiosyncratic differences between melanocytes and melanoma cells regarding the uptake and signaling to dsRNA mimics.

Qualitatively Different Activation of MDA-5 by pIC in the Absence and Presence of PEI

The best known innate programs that control the sensing of long dsRNA are (1) the Toll-like receptor 3, (2) the melanoma differentiation-associated gene-5 (MDA-5)/interferon induced with helicase C domain 1 protein (IFIH1), and (3) the dsRNA-activated protein kinase (PKR, also known as eIF2AK2) (Takeuchi and Akira, 2008). Of these genes, MDA-5 showed the strongest and most sustained induction by [pIC]^{PEI} (Figure 5A). Moreover, knockdown of TLR3 with independent siRNA or shRNA had no impact on [pIC]^{PEI}-driven cell death (Figure 5B). Therefore, we focused on MDA-5 for further analyses. Protein immunoblotting demonstrated a sustained activation of full-length MDA-5 by [pIC]^{PEI} (Figure 5C). In addition, an apoptosis-associated processing of MDA-5 (Barral et al., 2007; Kovacsovics et al., 2002) was found preferentially (and in a more sustained manner) in [pIC]^{PEI}-treated cells (Figure 5C). Of note, this induction and processing of MDA-5 was not simply a consequence of activated apoptotic programs. Treatment with bortezomib, a proteasome inhibitor that engages intrinsic apoptotic pathways in melanoma

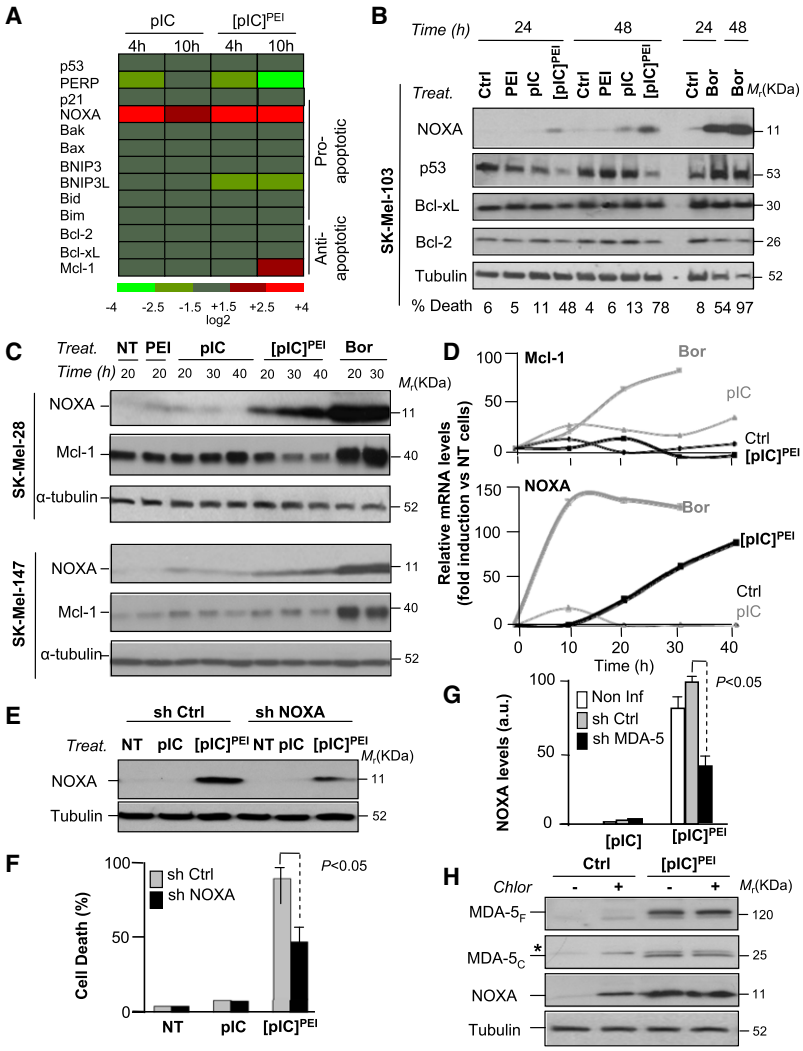

Figure 6. [pIC]^{PEI} Engages Apoptosis via NOXA Independently of the Status of p53 or without Inducing Compensatory MCL-1 Activation

(A) Heat map of log2 ratio values of the indicated genes after pIC or [pIC]^{PEI} treatment of SK-Mel-103 and calculated with respect to control (PEI)-incubated cells.

(B) Immunoblots of total cell extracts isolated from SK-Mel-103 treated for 24 and 48 hr with pIC, [pIC]^{PEI}, or Bortezomib for the relative levels of NOXA, p53, and anti-apoptotic Bcl-2 and Bcl-xL proteins.

(C) SK-Mel-28 and SK-Mel-147 (expressing p53 L145A and p53 wild-type, respectively) were treated with PEI, pIC, [pIC]^{PEI}, or 25 nM Bortezomib. Shown are the relative levels of NOXA and MCL-1 protein at different time points after treatment.

(D) Quantification of the levels of Mcl-1 and NOXA in SK-Mel-28 after each treatment and represented with respect to control untreated cells.

(E) NOXA protein expression in melanoma SK-Mel-103 treated for 24 hr with pIC or [pIC]^{PEI} 2 days after infection with a lentiviral vector expressing inactive shRNA (sh Ctrl) or shRNA for NOXA.

(F) Death rates (±SEM) of control and NOXA shRNA transduced SK-Mel-103 melanoma cells and incubated with pIC or [pIC]^{PEI} for 24 hr.

(G) Inhibitory effect of MDA-5 downregulation on NOXA induction by [pIC]^{PEI} determined in SK-Mel transduced with control or MDA5 shRNAs. Data is represented as means ± SEM of four independent experiments. Levels of NOXA were quantified by densitometry of the corresponding immunoblots and plotted with respect to untreated controls.

(H) Immunoblots of total cell extracts isolated from SK-Mel-103 treated for 24 hr with vehicle or [pIC]^{PEI} in the presence or absence of chloroquine and probed for the detection of MDA-5 (full-length and cleaved forms) and NOXA.

(Fernandez et al., 2005; Wolter et al., 2007), had no effect on MDA-5 levels or processing (Figure 5C).

Downregulation of MDA-5 expression by siRNA (Figure 5D) or shRNA (Figure 5E) reduced [pIC]^{PEI}-driven cell death by 50%–60%, providing evidence for a critical role of MDA-5 as sensor and effector of this dsRNA mimic. Interestingly, although MDA-5 needs interaction with dsRNA for full activation (Takeuchi and Akira, 2008), ectopic expression of this protein is sufficient to promote cell death in a subset of melanoma cells (e.g., MeWo [Kang et al., 2004, 2002]). In these cells, MDA-5 was also found to engage focal aggregation of LC3 (Figure 5F) prior to cell killing (Figure 5G and data not shown). These results uncover a proautophagy role of MDA-5. However, although MDA-5 may favor autophagy, it is unlikely that this is the sole contribution of this protein to [pIC]^{PEI}-mediated cell death. Thus, MDA5-shRNA or *Mda-5*$^{-/-}$ MEFs could still engage autophagosome formation after sustained treatment with [pIC]^{PEI} (data not shown).

MDA-5-Driven NOXA-Dependent Cell Death

A main known role of endogenous MDA-5 is to elicit IFN responses to blunt viral infection (Takeuchi and Akira, 2008). IFN-α was secreted in [pIC]^{PEI}-treated melanoma cells (data not shown). However, IFN-α was a poor inducer of melanoma cell death, even at doses 100 times higher than those secreted by [pIC]^{PEI} -treated cells (Figure S8C).

cDNA microarray data generated above was analyzed to identify mediators of [pIC]^{PEI}/MDA-5-driven melanoma cell death. Among known proapoptotic factors, a strong and sustained upregulation (up to 16-fold) of NOXA mRNA and protein levels was found (Figures 6A–6D). Moreover, [pIC]^{PEI}-mediated death induction was reduced by 50%–60% when the NOXA level was reduced using a shRNA (Figures 6E and 6F). Importantly, [pIC]^{PEI}-driven NOXA induction was significantly abrogated by MDA-5 shRNA (Figure 6G). Therefore, these results uncover functional links between dsRNA sensors and the apoptosis program via NOXA.

Other chemotherapeutic agents such as the proteasome inhibitor bortezomib can also upregulate NOXA and kill melanoma cells deficient for Apaf-1 or other apoptotic modulators (Fernandez et al., 2005; Qin et al., 2005). However, a main disadvantage of bortezomib is that it concomitantly induces various antiapoptotic factors, including MCL-1, a NOXA antagonist (Qin et al., 2006; Wolter et al., 2007). In contrast, no compensatory accumulation of MCL-1 protein was found in the response to [pIC]^{PEI} (Figures 6C and 6D).

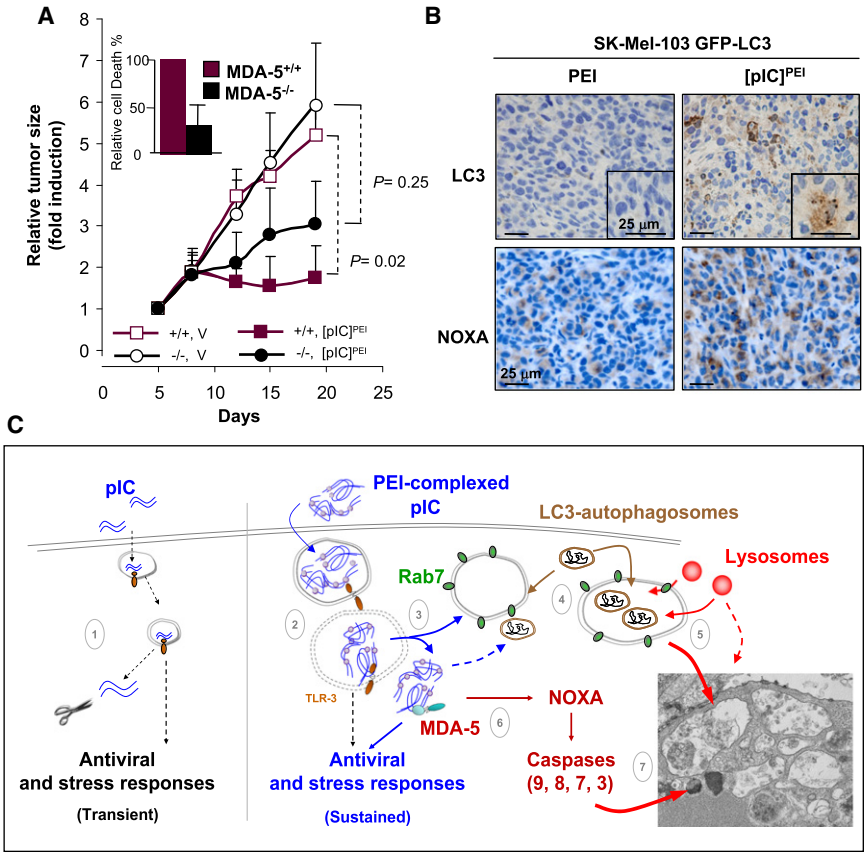

Figure 7. Defining the Mode of Action of [pIC]^{PEI} In Vivo

(A) Response of oncogenically transformed wild-type (+/+) or Mda-5$^{-/-}$ (−/−) MEFs, measured as time-dependent changes in tumor size (±SEM) upon treatment with naked pIC (V) or [pIC]^{PEI}. Shown are p values for comparative analyses between the indicated treatment groups (n = 10, generalized Mann-Whitney test). Inset bar graphs corresponds to death rates (±SEM; n = 3) of the indicated cell populations 24 hr after treatment in culture with 1 µg/ml [pIC]^{PEI}.

(B) SK-Mel-103 GFP-LC3 melanoma cells implanted subcutaneously into SCID beige mice were left to grow to 6–8 mm diameter and then treated with PEI or [pIC]^{PEI}. Paraffin-embedded sections were stained for LC3 or NOXA antibodies. For LC3, high magnification photographs are also included to show the formation of foci characteristic of autophagosomes.

(C) Model summarizing main results of this study. A transient activation of IFN and other antiviral stress response factors by naked pIC (1) can be shifted into a sustained stress program when this dsRNA mimic is delivered to cells with PEI (2). PEI packs pIC into nanoparticles and favors both its endosomal uptake and delivery to the cytosol for subsequent activation of the helicase MDA-5 (3). In addition to favor endosomal swelling, PEI has been described to favor endosome-endosome fusion. Within 2–3 hr after incubation with [pIC]^{PEI} melanoma cells undergo massive ultrastructural changes in the endosomal compartment (4). These changes involve a sustained and cyclic Rab7 > LC3 > Lysotracker sequence of fusion events, revealing an active generation and resolution of endosome-autophagosome-lysosome hybrids (5). Although MDA-5 can facilitate autophagosome formation, a main function of this protein described here is the induction of the proapoptotic factor NOXA (6). NOXA is per se a poor apoptotic inducer, but can lower the threshold for caspase processing. Sustained lysosomal-dependent degradative process together with the activation of apoptotic caspases can ultimately converge in efficient tumor cell death (7). Importantly, we demonstrate a potent anti-melanoma activity of [pIC]^{PEI} in various animal models, at concentrations with no obvious toxicity to normal cellular compartments.

Importantly, the induction of MDA-5 and NOXA by [pIC]^{PEI} was found to occur even when lysosome activity was blocked by chloroquine or by cathepsin inhibitors (Figure 6H and Figure S7D and data not shown). Thus, NOXA can be activated independently of the autophagy program. From a therapeutic perspective, it was interesting to note that cDNA arrays failed to identify changes in NOXA expression in melanocytes (data not shown). Similarly, MDA-5 and NOXA were not upregulated in skin fibroblasts (Figure S8D), which also showed increased resistance to [pIC]^{PEI} in culture (Figure S8E) and no obvious signs of toxicity in biopsies from treated animals (Figure S8F; note also lack of toxicity to other organs).

[pIC]^{PEI}-Mediated Therapeutic Effects In Vivo: MDA-5 Requirement, LC3 Foci Formation, and NOXA Induction

Next, we investigated the dependency on MDA-5 and the dual activation of autophagosome and apoptotic markers identified above by [pIC]^{PEI} in vivo. Available antibodies against MDA-5 cannot distinguish full length from processed forms of this protein. In the absence of current Mda-5-deficient mouse melanoma models, we decided to take advantage of homozygous knockout MEFs for the Mda-5 gene. As shown in Figure 7A, transformed Mda-5$^{-/-}$ MEFs were significantly more resistant to [pIC]^{PEI} than their wild-type counterparts, both in tissue culture systems and when grown as xenografts in mice.

Selective antibodies for LC3 and NOXA were used to visualize autophagosome formation and activation of NOXA by [pIC]^{PEI} in human melanoma xenografts. Although sporadic stainings for LC3 or NOXA were detected in vehicle-treated SK-Mel-103 xenografts, the total number of positive cells and the corresponding signal intensity of NOXA or LC3 per individual cell were noticeably stronger in the [pIC]^{PEI}-treated specimens (Figure 7B). The animal model used (SCID beige) is highly immunodeficient. Therefore, these results serve as the proof-of-principle for the ability of [pIC]^{PEI} to bypass the requirement for immune effectors and drive tumor cell death by a coordinated autophagy/apoptosis mechanism.

DISCUSSION

Melanomas accumulate a plethora of genetic and epigenetic alterations that contribute to the limited efficacy of current anticancer treatments (Chin et al., 2006; Soengas and Lowe, 2003). However, here we have shown that melanoma cells retain the ability to sense and respond to mimetics of viral dsRNA and that this feature can be exploited therapeutically. Specifically,

our results revealed tractable points of crosstalk between innate sensors of dsRNA, endo/lysosomal compartments, and tumor cell death.

Given the ability of melanoma cells to deactivate death programs (Gray-Schopfer et al., 2007), it is intriguing that they remain sensitive to lysosomal-dependent autodegradative mechanisms. This is particularly relevant because autophagy has been abundantly linked to cytoprotection in innate and acquired immune responses (Levine and Deretic, 2007; Sanjuan and Green, 2008; Virgin and Levine, 2009). Activation of autophagosomes by TLR3 has also been reported for naked dsRNA in macrophages, but in this case, for protection of the host at both the cellular and organismal levels (Delgado et al., 2008). In the melanoma cells studied here, however, TLR3 was found dispensable for $[pIC]^{PEI}$-driven autophagy or apoptotic induction, perhaps reflecting inherent differences in TLR3 expression between professional immune cells and melanomas.

An intriguing feature of the response of melanoma cells to $[pIC]^{PEI}$ was a considerable time lag from the detection of the first series of endosome-autophagosome-lysosome fusions (within an hour of treatment) to the final cellular collapse (24–48 hr). It is therefore conceivable that autophagy is engaged in response to $[pIC]^{PEI}$ as an initial mechanism of protection, which is later shifted into a prodeath program (see model in Figure 7C). Thus, autophagy could be engaged to resolve an exacerbated endocytosis driven by pIC complexed to PEI (Boussif et al., 1995; Kopatz et al., 2004). Endocytic recruitment of autophagosomes could initially help tumor cells to maintain a "clean" cytosol. Intraendocytic degradation would prevent leakage or the accumulation of partially degraded autophagocytic structures, and/or damaged lysosomes, which could be potentially lethal to cells (Kroemer and Jaattela, 2005). However, the physical concentration of autophagosomes and lysosomes within endocytic vesicles may also provide a point of vulnerability of melanoma cells. Recurrent cycles of endo/lysosome generation-degradation could lower the threshold for the activation of death programs (i.e., by depleting ATP and/or key proteins or organelles required for cell maintenance) as described in other systems (Eisenberg-Lerner et al., 2009). In fact, a main difference between $[pIC]^{PEI}$ (which kills melanoma cells) and rapamycin (innocuous to melanoma cells) is the sustainability of the endolysosome-autophagosome fusion events. An additional defining feature of $[pIC]^{PEI}$ not shared by rapamycin or by other chemotherapeutic agents is the ability to engage a potent wave of proapoptotic events driven, at least in part, by the MDA-5 dsRNA sensor (see Figure 7C).

MDA-5, a helicase now considered as a first line of defense against viral dsRNA (Kato et al., 2006), was first described as a melanoma differentiation-associated gene (Kang et al., 2002). It was noted that MDA-5 had proapoptotic activities when expressed ectopically at high levels (Kang et al., 2004; Kovacsovics et al., 2002). However, even forced expression of MDA-5 was rather inefficient in tumor cells with hyperactivated RAS/MEK/ERK pathway (Lin et al., 2006), as is the case of melanomas (Gray-Schopfer et al., 2007). Therefore, it was unclear how to drive a sustained activation of the endogenous MDA-5 protein. Moreover, the identity of death-inducing targets of MDA-5 remains unclear (Takeuchi and Akira, 2008). We showed that endogenous MDA-5 can in fact be induced to kill melanoma cells (with pIC delivered appropriately to the cytosol). Further, we uncovered roles of MDA-5 beyond the activation of IFN-driven immune responses. Specifically, we showed the ability of MDA-5 to drive autophagosome formation and NOXA activation. Still, our data also suggest that additional death inducers activated by $[pIC]^{PEI}$ are likely to act in parallel or in concert with MDA-5 and NOXA (i.e., depletion of these proteins do not completely abrogate the antitumoral activity of $[pIC]^{PEI}$). In this context, the cDNA arrays performed here indicate that $[pIC]^{PEI}$ can selectively induce a variety of stress kinases with proautophagic and proapoptotic activity (D.T. and M.S.S., unpublished data).

From a therapeutic perspective, perhaps one the most unexpected findings in this study is the cell-autonomous anti-tumoral activity of $[pIC]^{PEI}$. pIC has been used for more than four decades as a synthetic dsRNA mimic to boost the immune system in an IFN-dependent manner (Field et al., 1967). Unfortunately, clinical trials with naked pIC showed poor pIC stability and IFN induction and no detectable antitumor effect in melanoma (Robinson et al., 1976). Complexes with low molecular weight poly-L-lysine, carboxymethylcellulose, liposomes, or PEI have been reported to favor pIC's therapeutic activity via IFN-dependent immune responses (Fujimura et al., 2006; Levine et al., 1979). Our results show that PEI significantly enhances the ability of pIC to induce melanoma cells to express classical IFN-α targets. However, we also show that IFN, per se, does not recapitulate the anti-melanoma activity of $[pIC]^{PEI}$ in cultured cells. Moreover, $[pIC]^{PEI}$ can display an efficient anti-melanoma activity in animals with defective NK, T, or B cell signaling, a condition common of melanoma patients (Kirkwood et al., 2008; Wenzel et al., 2008). In addition to the xenografts in immunosuppressed and immunodeficient mice, our results in two additional in vivo models (MDA-5-deficient cells and autochthonous cutaneous melanomas generated in the *Tyr::NRAS*^{Q61K}*; INK4a/ARF*$^{-/-}$ mice) further emphasized the physiological relevance of our data. Altogether, our results provide the proof of principle for dsRNA sensors as therapeutic targets to overcome the inherent resistance of melanoma cells to current anticancer treatments.

EXPERIMENTAL PROCEDURES

Treatment, Imaging, and Expression Analyses in Cultured Cells

The human and mouse metastatic melanoma cell lines used in this study are described in the Supplemental Experimental Procedures. Normal human melanocytes and fibroblasts were isolated from anonymous discarded foreskins as previously reported (Wolter et al., 2007), using protocols approved by the University of Michigan and the Instituto Carlos III-CNIO ethics committees. Wild-type and *Atg5*- or *Bax/Bak*-deficient MEFs have been described before (Kuma et al., 2004; Lindsten et al., 2000). Oncogenically transformed derivatives of these cells, expressing $HRAS^{G12V}$ and the SV40 large T antigen, were a kind gift of G. Velasco (Universidad Complutense, Madrid, Spain). Information on PEI-complexed pIC, pharmacological inhibitors of apoptosis and autophagy, and other reagents and techniques used here to assess cell death and cell viability are described in the Supplemental Experimental Procedures. Details on transmission electron microscopy, confocal and fluorescence microscopy, protein immunoblotting, lentiviral mediated RNA interference, and cDNA microarray expression profiling are also described in the Supplemental Experimental Procedures. Full data sets corresponding to the cDNA arrays reported in this study in melanocytes and SK-Mel-103 cells were deposited to the Gene Expression Omnibus database (with accession numbers GSE16337 and GSE14445, respectively).

Treatment Response In Vivo

All experiments in mouse models were performed in accordance with institutionally approved protocols by the University of Michigan Unit for Laboratory Animal Medicine Committee and the Instituto Carlos III-CNIO ethics committee. Generation and treatment of autochthonous melanomas in the *Tyr::N-Ras*$^{Q61K/+}$*; Ink4a/Arf*$^{-/-}$ mice and the analysis of melanoma xenografts in *C57BL*/6 and in the immunosuppressed SCID beige mice are summarized in the Supplemental Experimental Procedures.

Histopathological and Immunohistochemical Analyses

Tumors or tissue sections from the indicated treatment groups were fixed in 10% buffered formalin, embedded in paraffin, and routinely stained with hematoxylin and eosin. Alternatively, tumors were immunostained with the NOXA antibody (Calbiochem) and LC3 antibody (Cell Signaling). Slides were digitalized with Dotslide (Olympus).

Statistical Analyses

Viability data are expressed as means ± SEM and statistical analysis of the differences was determined by the two-tailed Student's t test. For statistical evaluation of tumor growth and metastasis in vivo, the generalized Mann-Whitney test was used to compare the values of continuous variables between two groups. p values of < -0.05 were considered significant.

SUPPLEMENTAL DATA

Supplemental Data include Supplemental Experimental Procedures, eight figures, one table, and seven movies and can be found with this article online at http://www.cell.com/cancer-cell/supplemental/S1535-6108(09)00217-7.

ACKNOWLEDGMENTS

This study was initiated at the University of Michigan Department of Dermatology and the authors thank all of our colleagues there, particularly Monique Verhaegen, MaryBeth Ribblet, Keith Wolter, and Anj Dlugosz for their help and support. We also thank José Esteban (Center for Molecular Biology, Spain) for critical reading of this manuscript and Gabriel Núñez (University of Michigan), Marino Zerial (Max Planck Institute, Germany), and Terje Johansen (University of Tromso, Norway) for eGFP-LC3, eGFP-Rab7 (WT and T22N), and Cherry-GFP-LC3, respectively. We also thank Friedrich Beermann (ISREC, Switzerland) for the *Tyr::NRAS*^{Q61K} mice and Guillermo Velasco (Universidad Complutense, Spain) and Patricia Boya (CIB, Spain) for Bax/Bak- and Atg5-deficient MEFs. This work was supported by grants NIH R01 CA107237 and Spanish Ministry of Science and Innovation SAF2008-1950 (M.S.S.), R01 GM068448 (P.B.F.), and Tu90-6/1 and DKH 10741 (T.T.); and institutional grants from the Asociación Española Contra el Cáncer and Spanish National Cancer Research Centre (M.S.S.). P.B.F. holds the Thelma Newmeyer Corman Chair in Cancer Research at the Virginia Commonwealth University Massey Cancer Center. D.T. and D.A.-C. are recipients of a Juan de la Cierva Postdoctoral Fellowship and a Scientists in Training Predoctoral Fellowship, respectively, from the Spanish Ministry of Science and Innovation. E.R.-F. is the recipient of a post-residency training program from "Obra Social de Caja Navarra."

Received: January 5, 2009
Revised: May 26, 2009
Accepted: July 8, 2009
Published: August 3, 2009

REFERENCES

Ackermann, J., Frutschi, M., Kaloulis, K., McKee, T., Trumpp, A., and Beermann, F. (2005). Metastasizing melanoma formation caused by expression of activated N-RasQ61K on an INK4a-deficient background. Cancer Res. *65*, 4005–4011.

Alexopoulou, L., Holt, A.C., Medzhitov, R., and Flavell, R.A. (2001). Recognition of double-stranded RNA and activation of NF-kappaB by Toll-like receptor 3. Nature *413*, 732–738.

Amaravadi, R.K., Yu, D., Lum, J.J., Bui, T., Christophorou, M.A., Evan, G.I., Thomas-Tikhonenko, A., and Thompson, C.B. (2007). Autophagy inhibition enhances therapy-induced apoptosis in a Myc-induced model of lymphoma. J. Clin. Invest. *117*, 326–336.

Barral, P.M., Morrison, J.M., Drahos, J., Gupta, P., Sarkar, D., Fisher, P.B., and Racaniello, V.R. (2007). MDA-5 is cleaved in poliovirus-infected cells. J. Virol. *81*, 3677–3684.

Bieber, T., Meissner, W., Kostin, S., Niemann, A., and Elsasser, H.P. (2002). Intracellular route and transcriptional competence of polyethylenimine-DNA complexes. J. Control. Release *82*, 441–454.

Boussif, O., Lezoualc'h, F., Zanta, M.A., Mergny, M.D., Scherman, D., Demeneix, B., and Behr, J.P. (1995). A versatile vector for gene and oligonucleotide transfer into cells in culture and in vivo: polyethylenimine. Proc. Natl. Acad. Sci. USA *92*, 7297–7301.

Chin, L., Garraway, L.A., and Fisher, D.E. (2006). Malignant melanoma: genetics and therapeutics in the genomic era. Genes Dev. *20*, 2149–2182.

Croy, B.A., and Chapeau, C. (1990). Evaluation of the pregnancy immunotrophism hypothesis by assessment of the reproductive performance of young adult mice of genotype scid/scid.bg/bg. J. Reprod. Fertil. *88*, 231–239.

Delgado, M.A., and Deretic, V. (2009). Toll-like receptors in control of immunological autophagy. Cell Death Differ. *16*, 976–983.

Delgado, M.A., Elmaoued, R.A., Davis, A.S., Kyei, G., and Deretic, V. (2008). Toll-like receptors control autophagy. EMBO J. *27*, 1110–1121.

Eisenberg-Lerner, A., Bialik, S., Simon, H.U., and Kimchi, A. (2009). Life and death partners: apoptosis, autophagy and the cross-talk between them. Cell Death Differ. *16*, 966–975.

Fecher, L.A., Amaravadi, R.K., and Flaherty, K.T. (2008). The MAPK pathway in melanoma. Curr. Opin. Oncol. *20*, 183–189.

Fernandez, Y., Verhaegen, M., Miller, T.P., Rush, J.L., Steiner, P., Opipari, A.W., Jr., Lowe, S.W., and Soengas, M.S. (2005). Differential regulation of noxa in normal melanocytes and melanoma cells by proteasome inhibition: therapeutic implications. Cancer Res. *65*, 6294–6304.

Field, A.K., Tytell, A.A., Lampson, G.P., and Hilleman, M.R. (1967). Inducers of interferon and host resistance. II. Multistranded synthetic polynucleotide complexes. Proc. Natl. Acad. Sci. USA *58*, 1004–1010.

Fujimura, T., Nakagawa, S., Ohtani, T., Ito, Y., and Aiba, S. (2006). Inhibitory effect of the polyinosinic-polycytidylic acid/cationic liposome on the progression of murine B16F10 melanoma. Eur. J. Immunol. *36*, 3371–3380.

Gray-Schopfer, V., Wellbrock, C., and Marais, R. (2007). Melanoma biology and new targeted therapy. Nature *445*, 851–857.

Gutierrez, M.G., Munafo, D.B., Beron, W., and Colombo, M.I. (2004). Rab7 is required for the normal progression of the autophagic pathway in mammalian cells. J. Cell Sci. *117*, 2687–2697.

Hersey, P., and Zhang, X.D. (2008). Adaptation to ER stress as a driver of malignancy and resistance to therapy in human melanoma. Pigment Cell Melanoma Res. *21*, 358–367.

Hoyer-Hansen, M., and Jaattela, M. (2007). Connecting endoplasmic reticulum stress to autophagy by unfolded protein response and calcium. Cell Death Differ. *14*, 1576–1582.

Hoyer-Hansen, M., and Jaattela, M. (2008). Autophagy: an emerging target for cancer therapy. Autophagy *4*, 574–580.

Ishii, K.J., Coban, C., Kato, H., Takahashi, K., Torii, Y., Takeshita, F., Ludwig, H., Sutter, G., Suzuki, K., Hemmi, H., et al. (2006). A Toll-like receptor-independent antiviral response induced by double-stranded B-form DNA. Nat. Immunol. *7*, 40–48.

Ilkovitch, D., and Lopez, D.M. (2008). Immune modulation by melanoma-derived factors. Exp. Dermatol. *17*, 977–985.

Jemal, A., Siegel, R., Ward, E., Hao, Y., Xu, J., Murray, T., and Thun, M.J. (2008). Cancer statistics, 2008. CA Cancer J. Clin. *58*, 71–96.

Kang, D.C., Gopalkrishnan, R.V., Wu, Q., Jankowsky, E., Pyle, A.M., and Fisher, P.B. (2002). mda-5: an interferon-inducible putative RNA helicase with double-stranded RNA-dependent ATPase activity and melanoma growth-suppressive properties. Proc. Natl. Acad. Sci. USA *99*, 637–642.

Kang, D.C., Gopalkrishnan, R.V., Lin, L., Randolph, A., Valerie, K., Pestka, S., and Fisher, P.B. (2004). Expression analysis and genomic characterization of human melanoma differentiation associated gene-5, mda-5: a novel type I interferon-responsive apoptosis-inducing gene. Oncogene *23*, 1789–1800.

Kato, H., Takeuchi, O., Sato, S., Yoneyama, M., Yamamoto, M., Matsui, K., Uematsu, S., Jung, A., Kawai, T., Ishii, K.J., et al. (2006). Differential roles of MDA5 and RIG-I helicases in the recognition of RNA viruses. Nature *441*, 101–105.

Kirkwood, J.M., Tarhini, A.A., Panelli, M.C., Moschos, S.J., Zarour, H.M., Butterfield, L.H., and Gogas, H.J. (2008). Next generation of immunotherapy for melanoma. J. Clin. Oncol. *26*, 3445–3455.

Klionsky, D.J., Abeliovich, H., Agostinis, P., Agrawal, D.K., Aliev, G., Askew, D.S., Baba, M., Baehrecke, E.H., Bahr, B.A., Ballabio, A., et al. (2008). Guidelines for the use and interpretation of assays for monitoring autophagy in higher eukaryotes. Autophagy *4*, 151–175.

Kopatz, I., Remy, J.S., and Behr, J.P. (2004). A model for non-viral gene delivery: through syndecan adhesion molecules and powered by actin. J. Gene Med. *6*, 769–776.

Kovacsovics, M., Martinon, F., Micheau, O., Bodmer, J.L., Hofmann, K., and Tschopp, J. (2002). Overexpression of Helicard, a CARD-containing helicase cleaved during apoptosis, accelerates DNA degradation. Curr. Biol. *12*, 838–843.

Kroemer, G., and Jaattela, M. (2005). Lysosomes and autophagy in cell death control. Nat. Rev. Cancer *5*, 886–897.

Kroemer, G., and Levine, B. (2008). Autophagic cell death: the story of a misnomer. Nat. Rev. Mol. Cell Biol. *9*, 1004–1010.

Kroemer, G., Galluzzi, L., Vandenabeele, P., Abrams, J., Alnemri, E.S., Baehrecke, E.H., Blagosklonny, M.V., El-Deiry, W.S., Golstein, P., Green, D.R., et al. (2009). Classification of cell death: recommendations of the Nomenclature Committee on Cell Death 2009. Cell Death Differ. *16*, 3–11.

Kuma, A., Hatano, M., Matsui, M., Yamamoto, A., Nakaya, H., Yoshimori, T., Ohsumi, Y., Tokuhisa, T., and Mizushima, N. (2004). The role of autophagy during the early neonatal starvation period. Nature *432*, 1032–1036.

Levine, A.S., Sivulich, M., Wiernik, P.H., and Levy, H.B. (1979). Initial clinical trials in cancer patients of polyriboinosinic-polyribocytidylic acid stabilized with poly-L-lysine, in carboxymethylcellulose [poly(ICLC)], a highly effective interferon inducer. Cancer Res. *39*, 1645–1650.

Levine, B., and Deretic, V. (2007). Unveiling the roles of autophagy in innate and adaptive immunity. Nat. Rev. Immunol. *7*, 767–777.

Lin, L., Su, Z., Lebedeva, I.V., Gupta, P., Boukerche, H., Rai, T., Barber, G.N., Dent, P., Sarkar, D., and Fisher, P.B. (2006). Activation of Ras/Raf protects cells from melanoma differentiation-associated gene-5-induced apoptosis. Cell Death Differ. *13*, 1982–1993.

Lindsten, T., Ross, A.J., King, A., Zong, W.X., Rathmell, J.C., Shiels, H.A., Ulrich, E., Waymire, K.G., Mahar, P., Frauwirth, K., et al. (2000). The combined functions of proapoptotic Bcl-2 family members bak and bax are essential for normal development of multiple tissues. Mol. Cell *6*, 1389–1399.

Luzio, J.P., Pryor, P.R., and Bright, N.A. (2007). Lysosomes: fusion and function. Nat. Rev. Mol. Cell Biol. *8*, 622–632.

Maiuri, M.C., Zalckvar, E., Kimchi, A., and Kroemer, G. (2007). Self-eating and self-killing: crosstalk between autophagy and apoptosis. Nat. Rev. Mol. Cell Biol. *8*, 741–752.

Mathew, R., Karp, C.M., Beaudoin, B., Vuong, N., Chen, G., Chen, H.Y., Bray, K., Reddy, A., Bhanot, G., Gelinas, C., et al. (2009). Autophagy suppresses tumorigenesis through elimination of p62. Cell *137*, 1062–1075.

Miller, B.C., Zhao, Z., Stephenson, L.M., Cadwell, K., Pua, H.H., Lee, H.K., Mizushima, N.N., Iwasaki, A., He, Y.W., Swat, W., and Virgin, H.W. (2008). The autophagy gene ATG5 plays an essential role in B lymphocyte development. Autophagy *4*, 309–314.

Mizushima, N., Levine, B., Cuervo, A.M., and Klionsky, D.J. (2008). Autophagy fights disease through cellular self-digestion. Nature *451*, 1069–1075.

Noda, T., and Ohsumi, Y. (1998). Tor, a phosphatidylinositol kinase homologue, controls autophagy in yeast. J. Biol. Chem. *273*, 3963–3966.

Ostenfeld, M.S., Hoyer-Hansen, M., Bastholm, L., Fehrenbacher, N., Olsen, O.D., Groth-Pedersen, L., Puustinen, P., Kirkegaard-Sorensen, T., Nylandsted, J., Farkas, T., and Jaattela, M. (2008). Anti-cancer agent siramesine is a lysosomotropic detergent that induces cytoprotective autophagosome accumulation. Autophagy *4*, 487–499.

Paulos, C.M., Kaiser, A., Wrzesinski, C., Hinrichs, C.S., Cassard, L., Boni, A., Muranski, P., Sanchez-Perez, L., Palmer, D.C., Yu, Z., et al. (2007). Toll-like receptors in tumor immunotherapy. Clin. Cancer Res. *13*, 5280–5289.

Qin, J.Z., Ziffra, J., Stennett, L., Bodner, B., Bonish, B.K., Chaturvedi, V., Bennett, F., Pollock, P.M., Trent, J.M., Hendrix, M.J., et al. (2005). Proteasome inhibitors trigger NOXA-mediated apoptosis in melanoma and myeloma cells. Cancer Res. *65*, 6282–6293.

Qin, J.Z., Xin, H., Sitailo, L.A., Denning, M.F., and Nickoloff, B.J. (2006). Enhanced killing of melanoma cells by simultaneously targeting Mcl-1 and NOXA. Cancer Res. *66*, 9636–9645.

Robinson, R.A., DeVita, V.T., Levy, H.B., Baron, S., Hubbard, S.P., and Levine, A.S. (1976). A phase I-II trial of multiple-dose polyriboinosic-polyribocytidylic acid in patieonts with leukemia or solid tumors. J. Natl. Cancer Inst. *57*, 599–602.

Rubinsztein, D.C., Gestwicki, J.E., Murphy, L.O., and Klionsky, D.J. (2007). Potential therapeutic applications of autophagy. Nat. Rev. Drug Discov. *6*, 304–312.

Salazar, M., Carracedo, A., Salanueva, I.J., Hernandez-Tiedra, S., Lorente, M., Egia, A., Vazquez, P., Blazquez, C., Torres, S., Garcia, S., et al. (2009). Cannabinoid action induces autophagymediated cell death through stimulation of ER stress in human glioma cells. J. Clin. Invest. *119*, 1359–1372.

Sanjuan, M.A., and Green, D.R. (2008). Eating for good health: linking autophagy and phagocytosis in host defense. Autophagy *4*, 607–611.

Scarlatti, F., Granata, R., Meijer, A.J., and Codogno, P. (2009). Does autophagy have a license to kill mammalian cells? Cell Death Differ. *16*, 12–20.

Soengas, M.S., and Lowe, S.W. (2003). Apoptosis and melanoma chemoresistance. Oncogene *22*, 3138–3151.

Takeuchi, O., and Akira, S. (2008). MDA5/RIG-I and virus recognition. Curr. Opin. Immunol. *20*, 17–22.

Tasdemir, E., Galluzzi, L., Maiuri, M.C., Criollo, A., Vitale, I., Hangen, E., Modjtahedi, N., and Kroemer, G. (2008). Methods for assessing autophagy and autophagic cell death. Methods Mol. Biol. *445*, 29–76.

Tawbi, H.A., and Kirkwood, J.M. (2007). Management of metastatic melanoma. Semin. Oncol. *34*, 532–545.

Tormo, D., Ferrer, A., Bosch, P., Gaffal, E., Basner-Tschakarjan, E., Wenzel, J., and Tuting, T. (2006). Therapeutic efficacy of antigen-specific vaccination and toll-like receptor stimulation against established transplanted and autochthonous melanoma in mice. Cancer Res. *66*, 5427–5435.

Verma, S., Petrella, T., Hamm, C., Bak, K., and Charette, M. (2008). Biochemotherapy for the treatment of metastatic malignant melanoma: a clinical practice guideline. Curr. Oncol. *15*, 85–89.

Virgin, H.W., and Levine, B. (2009). Autophagy genes in immunity. Nat. Immunol. *10*, 461–470.

Wenzel, J., Tormo, D., and Tuting, T. (2008). Toll-like receptor-agonists in the treatment of skin cancer: history, current developments and future prospects. Handb. Exp. Pharmacol. *183*, 201–220.

Wolter, K.G., Verhaegen, M., Fernandez, Y., Nikolovska-Coleska, Z., Riblett, M., de la Vega, C.M., Wang, S., and Soengas, M.S. (2007). Therapeutic window for melanoma treatment provided by selective effects of the proteasome on Bcl-2 proteins. Cell Death Differ. *14*, 1605–1616.

Xie, Z., and Klionsky, D.J. (2007). Autophagosome formation: core machinery and adaptations. Nat. Cell Biol. *9*, 1102–1109.